US Army Corps
of Engineers
Waterways Experiment
Station

Miscellaneous Paper GL-93-7
July 1993

2

Ground Motion and Air Overpressure Study at the Naval Surface Warfare Center, Crane, Indiana

by *Michael K. Sharp, Janet Simms*
Geotechnical Laboratory

Cary Cox, Jim Pickens
Instrumentation Services Division

WES

Prepared for Crane Army Ammunition Activity

Miscellaneous Paper GL-93-7
July 1993

Ground Motion and Air Overpressure Study at the Naval Surface Warfare Center, Crane, Indiana

by Michael K. Sharp, Janet Simms
Geotechnical Laboratory

Cary Cox, Jim Pickens

Instrumentation Services Division

U.S. Army Corps of Engineers
Waterways Experiment Station
3909 Halls Ferry Road
Vicksburg, MS 39180-6199

Final report

Prepared for Crane Army Ammunition Activity
Naval Surface Warfare Center
Crane, IN 47522-5099

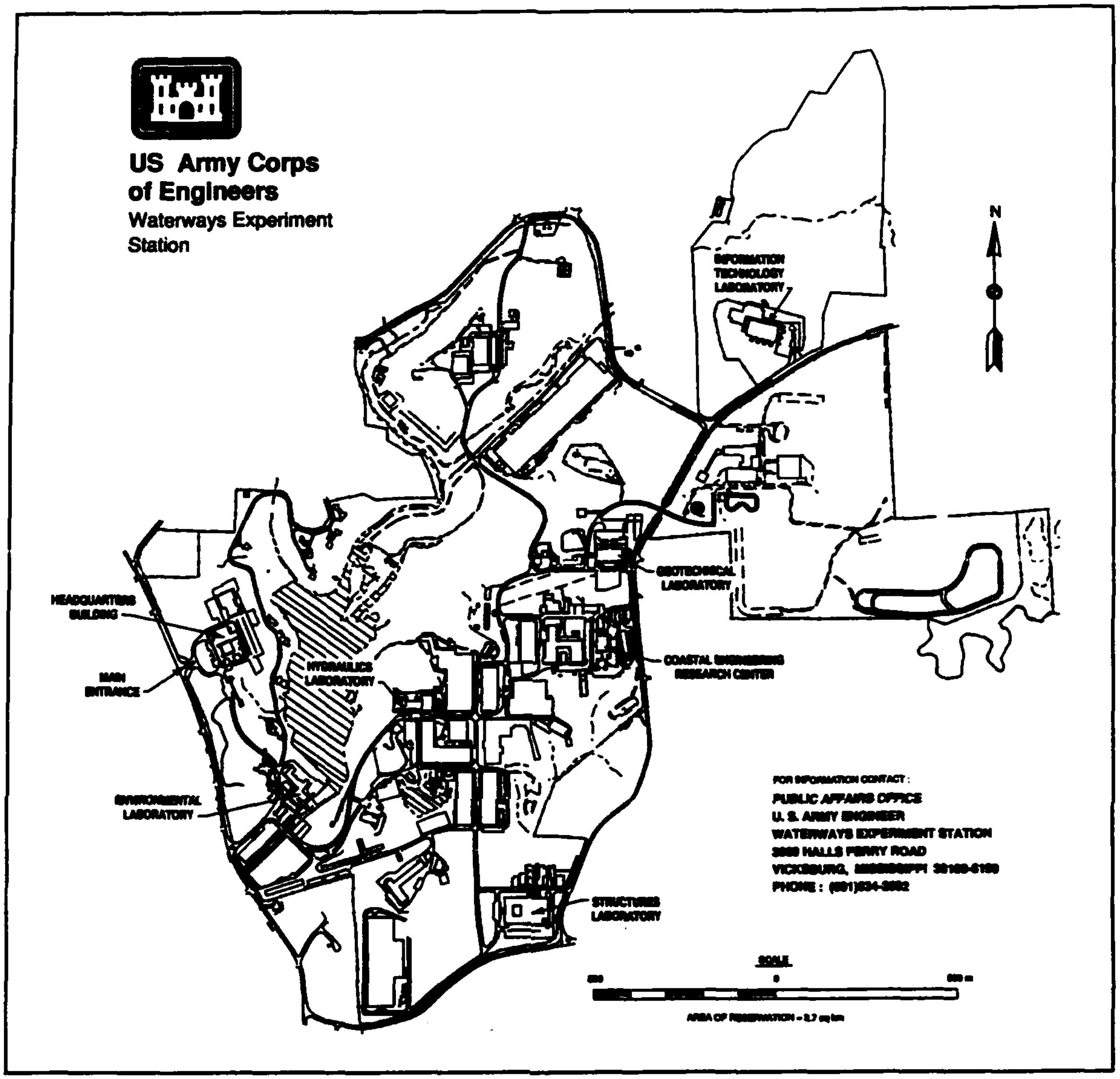

Waterways Experiment Station Cataloging-in-Publication Data

Ground motion and air overpressure study at the Naval Surface Warfare Center, Crane, Indiana / by Michael K. Sharp ... [et al.]; prepared for Crane Army Ammunition Activity.
195 p.: ill.; 28 cm. -- (Miscellaneous paper; GL-93-7)
Includes bibliographical references.
1. Ordnance disposal units -- Indiana -- Crane. 2. Explosive ordnance disposal -- Environmental aspects. 3. Seismic waves -- Damping -- Testing. 4. Aerodynamic load. I. Sharp, Michael K. II. United States. Crane Army Ammunition Activity. III. U.S. Army Engineer Waterways Experiment Station. IV. Series: Miscellaneous paper (U.S. Army Engineer Waterways Experiment Station) ; GL-93-7.

Contents

Preface

A seismic attenuation and air overpressure study was conducted by the Earthquake Engineering and Geosciences Division (EEGD), Geotechnical Laboratory (GL), U. S. Army Engineer Waterways Experiment Station (WES), during the period 24 August through 5 September 1992. The study was sponsored by the Crane Army Ammunition Activity (CAAA), of the Naval Surface Warfare Center (NSWC) in Crane, Indiana, under MIPR No. RMB 92-749. The CAAA Technical Monitor was Mr. Larry Leonard. The project was coordinated with personnel from the Structures Laboratory, WES, before field testing began.

Field tests were conducted by Mr. Michael Sharp and Ms. Janet Simms of GL, with the assistance of Messrs. Jim Pickens and David Goodin of the Instrumentation Services Division, WES. Mr. Pickens and Mr. Goodin were responsible for the field electronic instrumentation and data recovery. Data processing was by Dr. Cary Cox, ISD. Analysis of the data and preparation of the report was accomplished by Mr. Sharp and Mr. Simms. Dr. Niki Deliman of GL was instrumental in providing technical guidance for the statistical analysis, and Mr. Bill Murphy of GL provided technical guidance for the geologic interpretation. The work was performed under the direct supervision of Mr. J. R. Curro, Chief, Engineering Geophysics Branch, EEGD, GL, and under the general supervision of Dr. A. G. Franklin, Chief, EEGD, GL, and Dr. W. F. Marcuson III, Director, GL. The report was reviewed by Dr. Paul F. Hadala and Messrs. Joseph R. Curro II and Donald E. Yule.

At the time of publication of this report, Director of WES was Dr. Robert W. Whalin. Commander was COL Bruce K. Howard, EN.

Conversion Factors, Non-SI to SI Units of Measurement

Non-SI units of measurement used in this report can be converted to SI units as follows.

Multiply	By	To Obtain
Fahrenheit degrees	5/9	Celsius degrees or Kelvins[1]
feet	0.3048	meters
inches	2.54	centimeters
miles (US statute)	1.609347	kilometers
pounds (force)	4.448222	newtons
pounds (force) per square inch	6.894757	kilopascals

[1]To obtain Celsius (C) temperature readings from Fahrenheit (F) readings, use the following formula: C = (5/9)(F-32). To obtain Kelvin (K) readings, use: K = (5/9)(F-32) + 273.15.

1 Introduction

Background

The U. S. Army Engineer Waterways Experiment Station (WES) was requested by the U. S. Army Engineer District, Louisville and the Crane Army Ammunition Activity (CAAA) of the Naval Surface Warfare Center (NSWC), Crane, Indiana (Figure 1) to conduct a blast effects study. The CAAA has as a mission the responsibility for disposing of ammunition, explosives and other dangerous articles by detonation. This activity is conducted at a site on the NSWC facility termed the demolition grounds. Personnel at the demolition grounds detonate this material on a daily basis as site conditions (weather, safety, etc.) dictate. The total amount of material disposed of on a typical day is approximately 15,000 pounds, detonated in several pits each containing less than 500 lbs. There have been at least two claims by private individuals that their property was damaged by explosions originating at the NSWC. The CAAA, having responsibility for these explosions, was interested in determining the potential for ground motions or air blasts to produce damage to structures located off-base. A limited, small scale study (four recording stations located at the North, South, East, and West boundaries) was performed in November of 1971 by Vibration Measurement Engineers, Inc. The CAAA was interested in having a more detailed analysis performed, therefore WES was asked to assist in determining the potential for sonic or seismic energy to produce damage to structures outside the boundary of the NSWC.

Purpose

The purpose of the study was twofold; determine the attenuation of explosion induced ground motions and air overpressures as a function of distance from subsurface detonated charges, and to develop parameters to predict ground particle velocities and air overpressures at distances beyond the base boundary. The development of these predicting parameters would then allow the CAAA to determine the particle velocities and air overpressures that could be expected at any distance from a particular explosion. These data would also allow the determination of damage potential to structures located on or off base from either seismic or sonic motions.

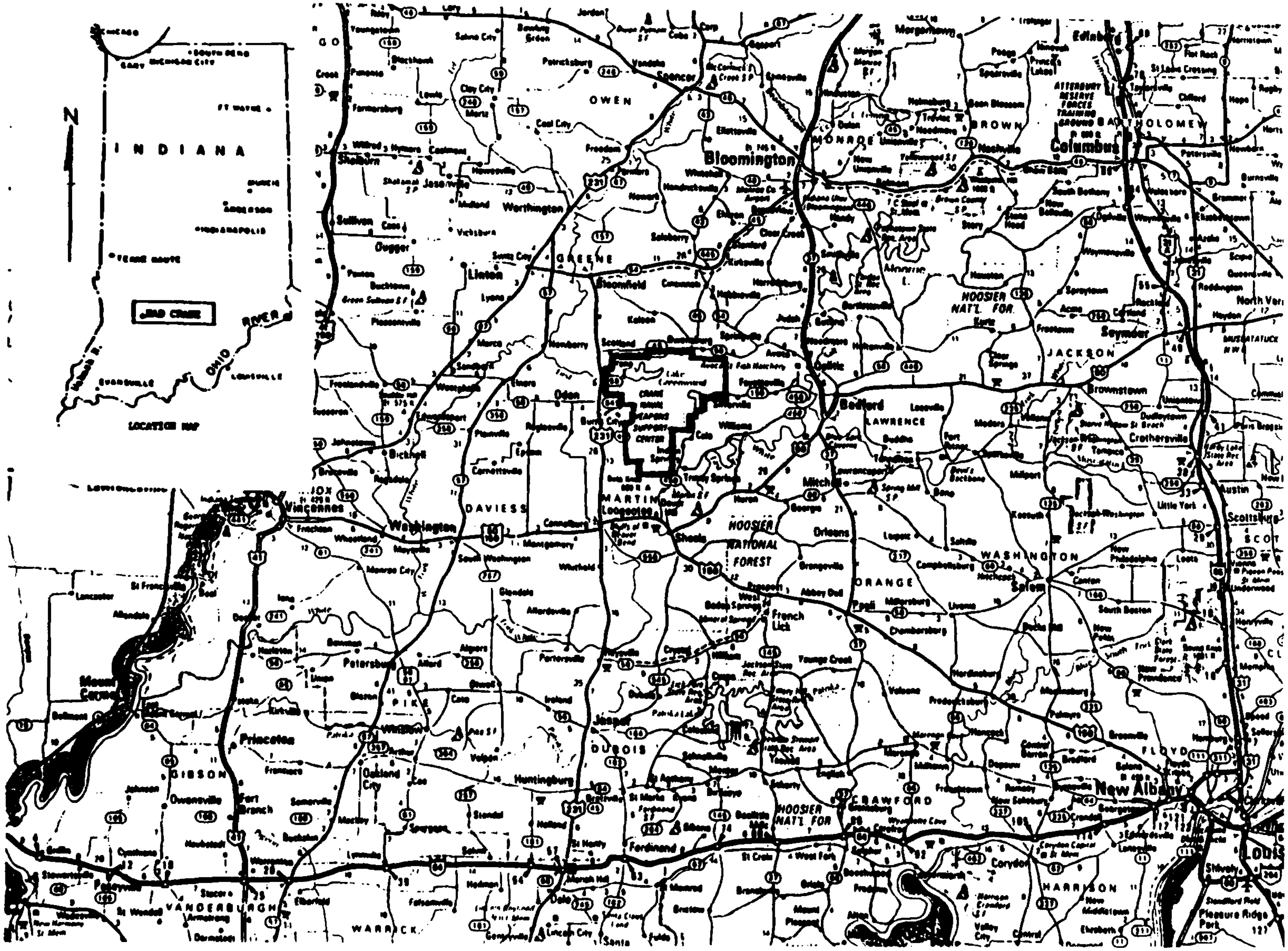

Figure 1. Site map showing the location of the NSWC Crane, Indiana

2 Site Descriptions and Source Characteristics

Regional Geology

The Indiana Department of Natural Resources (DNR) prepared a report describing the Pennsylvanian and Mississippian sedimentology of the NSWC, Crane (DNR, 1992). The discussion of the geology at Crane is excerpted from this report. The NSWC is located in Martin, Greene, Daviess, and Lawrence Counties, in the southwestern part of the state. Martin county has a total area of 217,888 acres, or about 340 square miles. The county lies in the hilly part of Indiana almost entirely within the Crawford Upland, the most rugged and highly dissected part of Indiana. The streams flow southwesterly in narrow, deeply entrenched, meandering channels. The East Fork of the White River, flowing about 250 feet below the general level of the hilltops and containing Wisconsin-age outwash, drains practically all of the county. Land elevation in the county ranges from about 425 to 860 feet above sea level.

The NSWC is located in the southeastern portion of the Illinois Basin, which is a large cratonic basin that began forming during Cambrian time (Klein and Hsui, 1988). It is filled by a sequence of Paleozoic sediments of which the youngest preserved are of Pennsylvanian age (320 to 286 Ma). The Pennsylvanian section is most complete in the southern portion of the basin where it reaches a maximum thickness of approximately 3,000 feet in western Kentucky (Wanless, 1975). From there the Pennsylvanian section thins to the northeast into Indiana. Crane is located at the very eastern edge of Pennsylvanian sediments.

The stratigraphic section exposed at Crane consists of both Mississippian and Pennsylvanian sediments. The Mississippian units exposed are Chesterian in age and consist of interbedded shales, limestones and sandstones of the Blue River, West Baden, Stephensport, and Buffalo Wallow Groups. The top of the Mississippian is a major unconformity surface throughout the Illinois Basin (Schloss, 1963). At Crane, Mississippian rocks form a low-angle angular unconformity wherein successively younger Chesterian rocks outcrop along drainages or subcrop beneath Pennsylvanian cover moving from east to west across the Activity. Local relief across the unconformity at Crane is highly

variable but rarely exceeds 100 ft. The Pennsylvanian section at Crane consists almost exclusively of interbedded sandstones, siltstones, shales, coals, and underclays of the Mansfield Formation, although a small interval of the Brazil Formation may be present in the northwestern portion of the center. On the Activity, Pennsylvanian sediments range from zero up to 300 ft in thickness. Thickness variations are controlled by regional dip, local relief on the Mississippian surface, and erosion. Sandstones, siltstones, and coals of the Mansfield Formation tend to be thin and stratigraphically discontinuous. Although some sandstones within the formation can be correlated laterally for up to several miles, most units can be correlated only a few thousand feet and many units can be correlated only a few hundred feet before pinching-out into other facies. The majority of the shaley intervals are also discontinuous.

A series of approximately 60 coreholes containing anywhere from 13 to 246 ft of Pennsylvanian section were obtained by WES during several coring programs conducted over the last eight years. The three sites where cores were taken consist of the Rockeye, Ammunition Burning Ground (ABG), and Demolition Area sites. Three regional cross sections were constructed to stratigraphically tie the Rockeye, Demolition Area, and ABG sites together. The cross sections show lateral and vertical lithostratigraphic facies relationships. In addition to the WES core taken, seven additional wells (Indiana Geological Survey wells) were cored connecting these three sites during the fall of 1991. Figure 2 shows the location of the three cross sections and the wells used in constructing them. Figure 3 is a legend showing the symbols used in the construction of the vertical columnar profiles from which the cross sections were generated. Cross section A-A' (Figure 4) is a northeast to southwest trending cross section that links the Rockeye area to the Demolition area. Cross section B-B' (Figure 5) is a north to south trending cross section that links Rockeye to the ABG, and the C-C' cross section (Figure 6) is an east to west trending section linking the ABG to the Demolition area.

The three sections, which cover most of the northern and eastern portions of the NSWC, reveal a great deal of information about the regional geology of the base. The overburden tends to be relatively shallow, ranging from approximately 10 to 20 ft. The remainder of the sections reveal intermittent layers of sandstones, siltstones, shales, and coal. Therefore, over the distances where ground motions were recorded (up to 22,000 ft) the waves will be travelling through the deeper rock layers.

Demolition Area

The location of the Demolition Area at the NSWC is shown in Figure 7. Four Demolition Area cores with Pennsylvanian section were available for examination but only two cores contained a significant Pennsylvanian section. However, these cores along with several shallow cores were used to develop a cross section for the Demolition Area. Figure 8 shows a section across the Demolition Area looking north to south (the section runs west to east). The section shows that the thickness of overburden overlying the Pennsylvanian

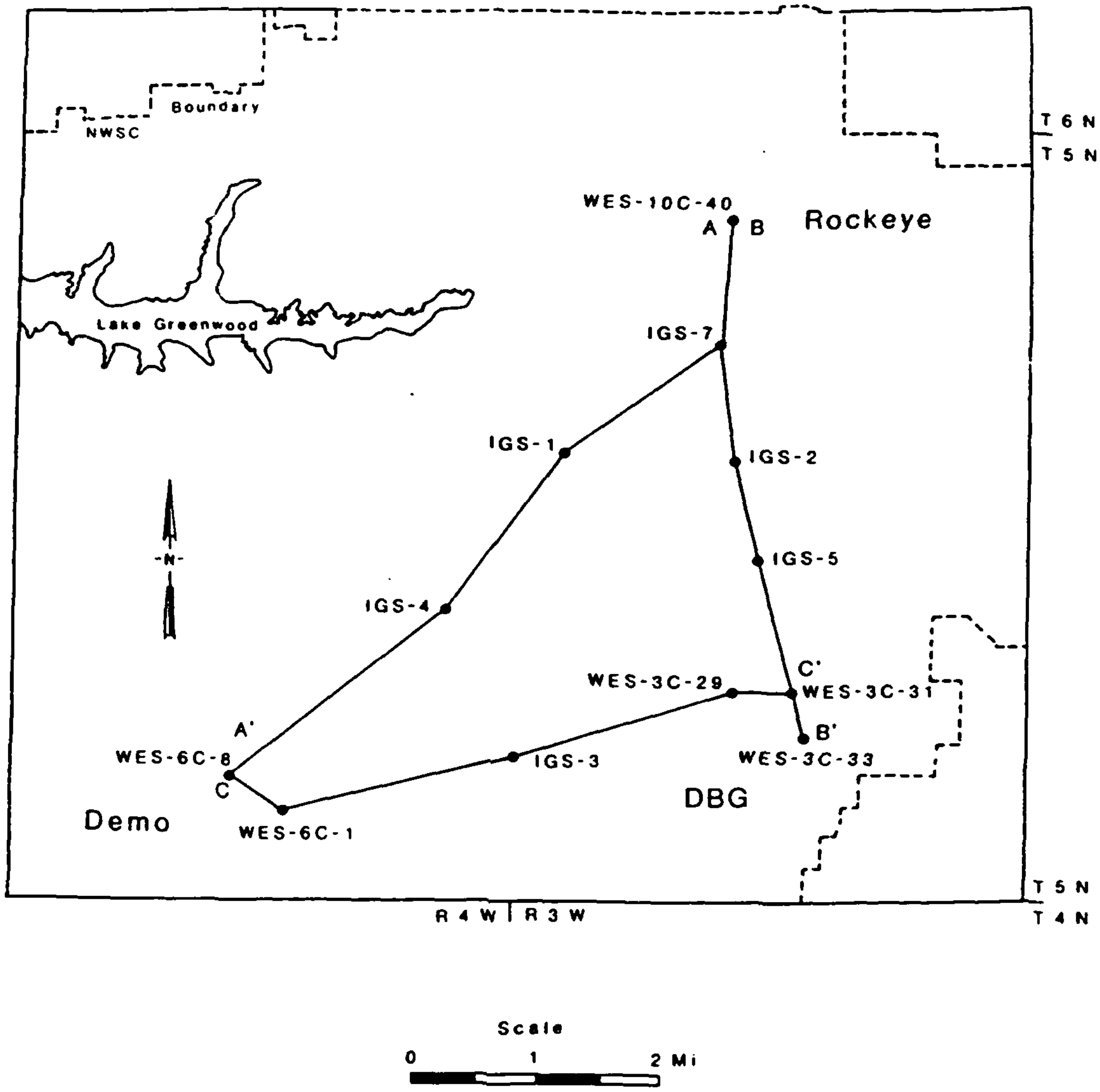

Figure 2. Location of cross sections and cores used to construct cross sections (DNR, 1992)

LEGEND

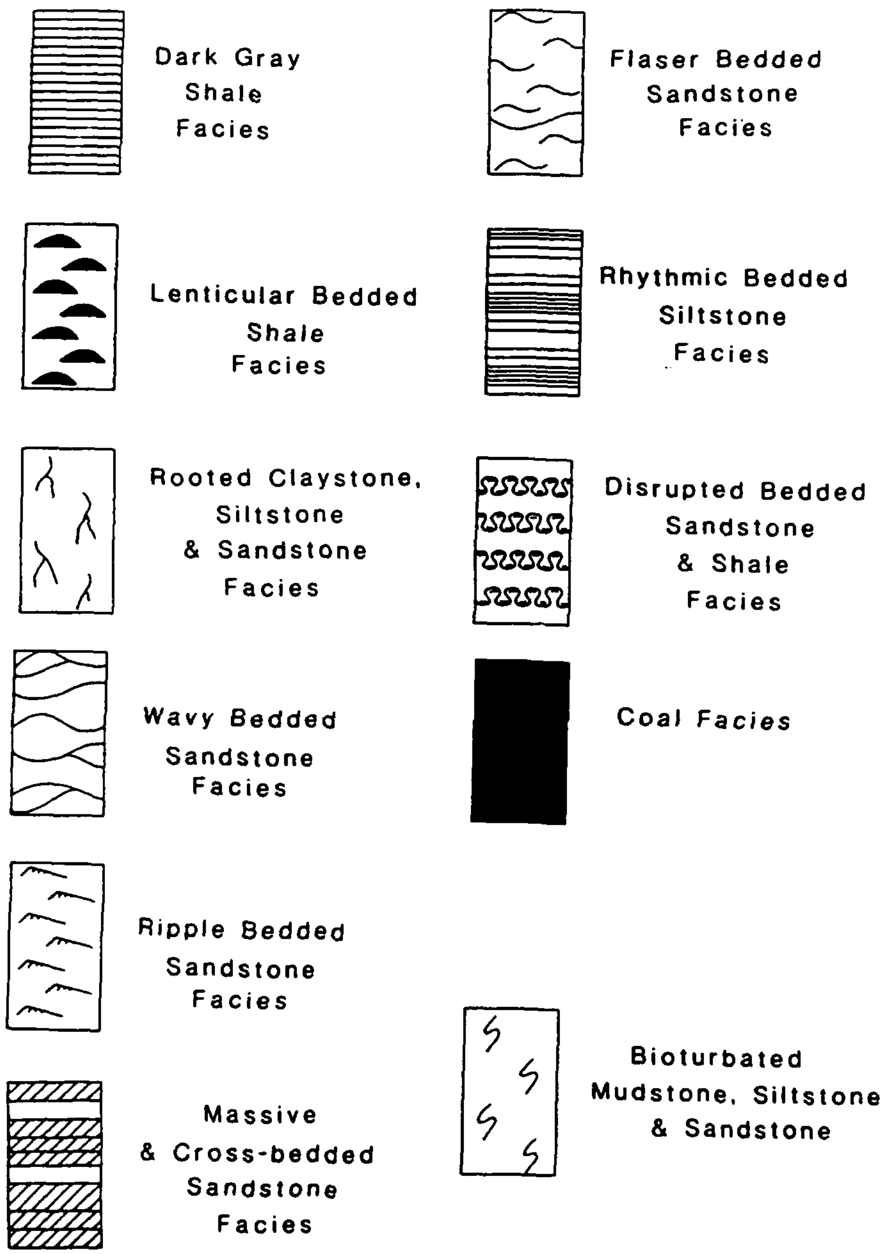

Figure 3. Legend showing the symbols used in the construction of the vertical columnar profiles on the cross sections (DNR, 1992)

A'

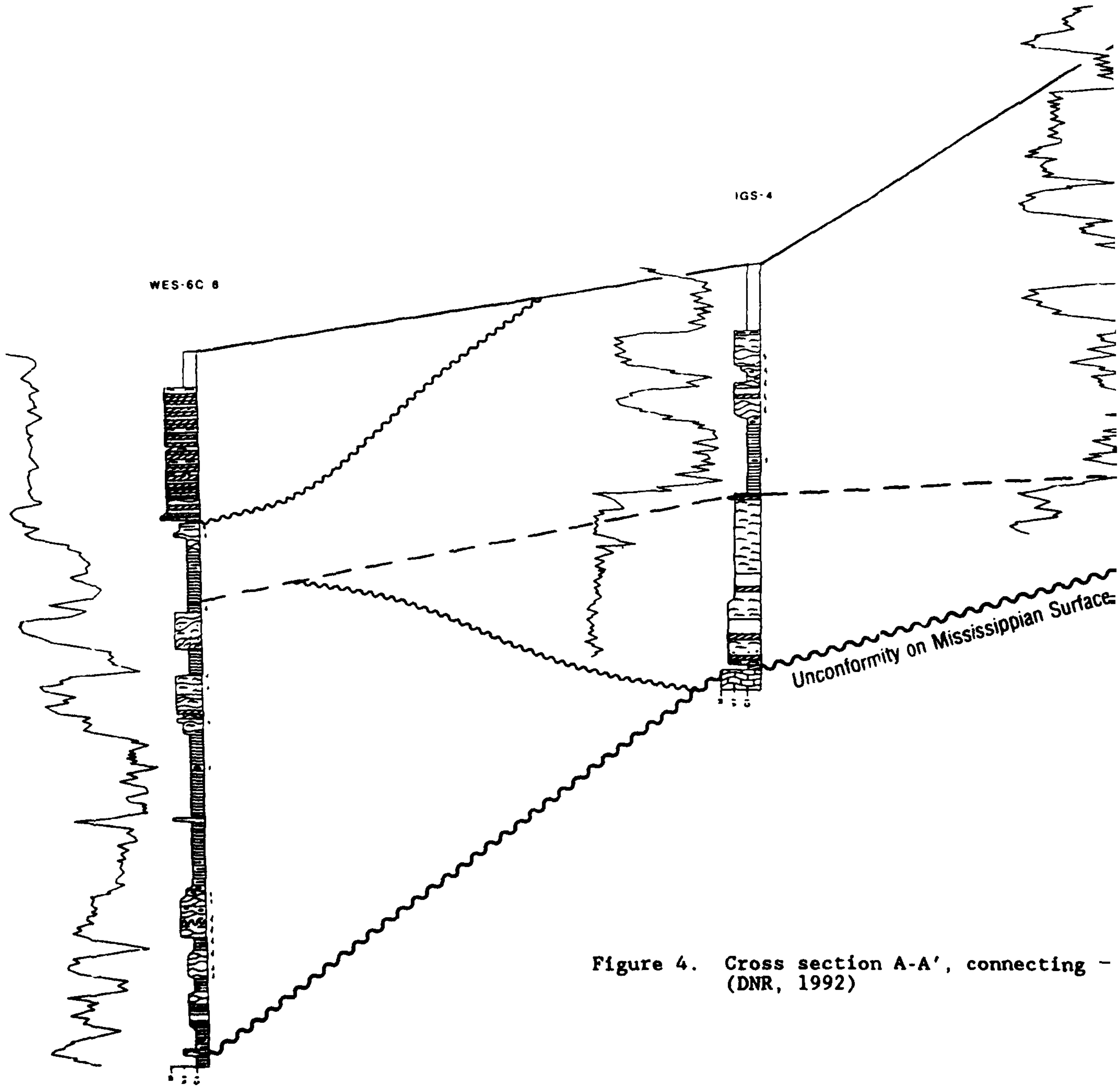

Figure 4. Cross section A-A', connecting -
(DNR, 1992)

(1)

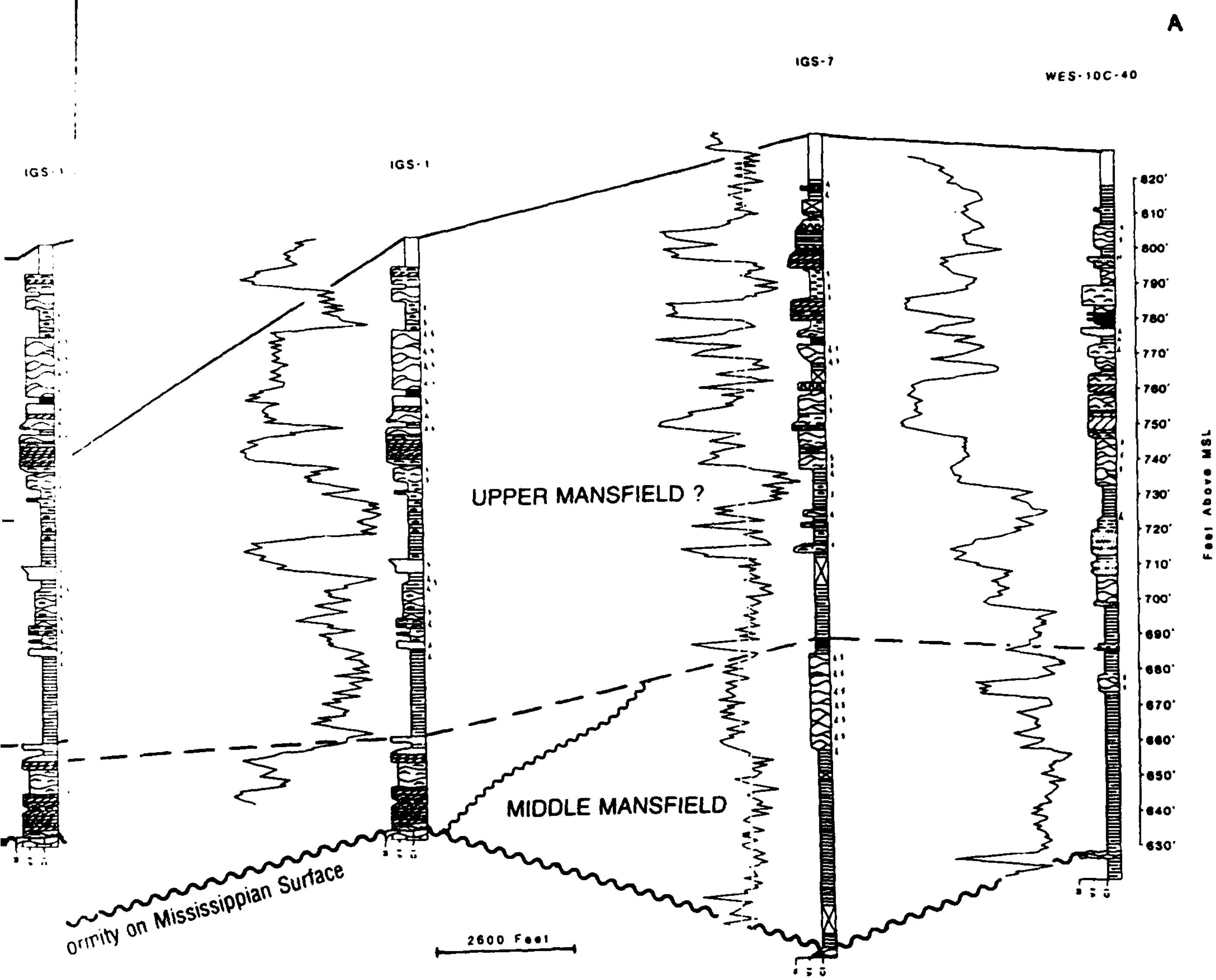

Rock ion A-A', connecting the Rockeye and Demolition Area
)

(2)

B'

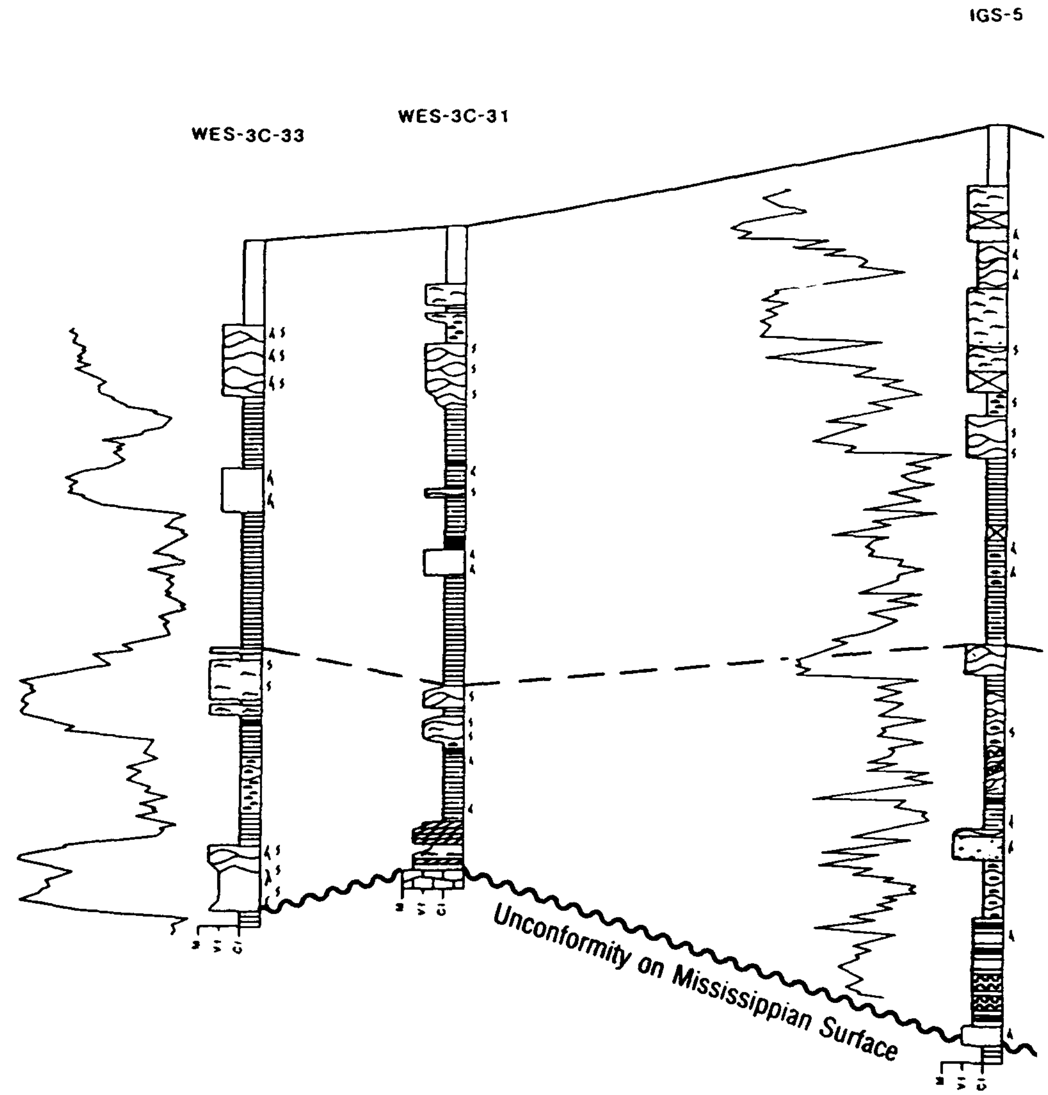

Figure 5. Cross sect

(1)

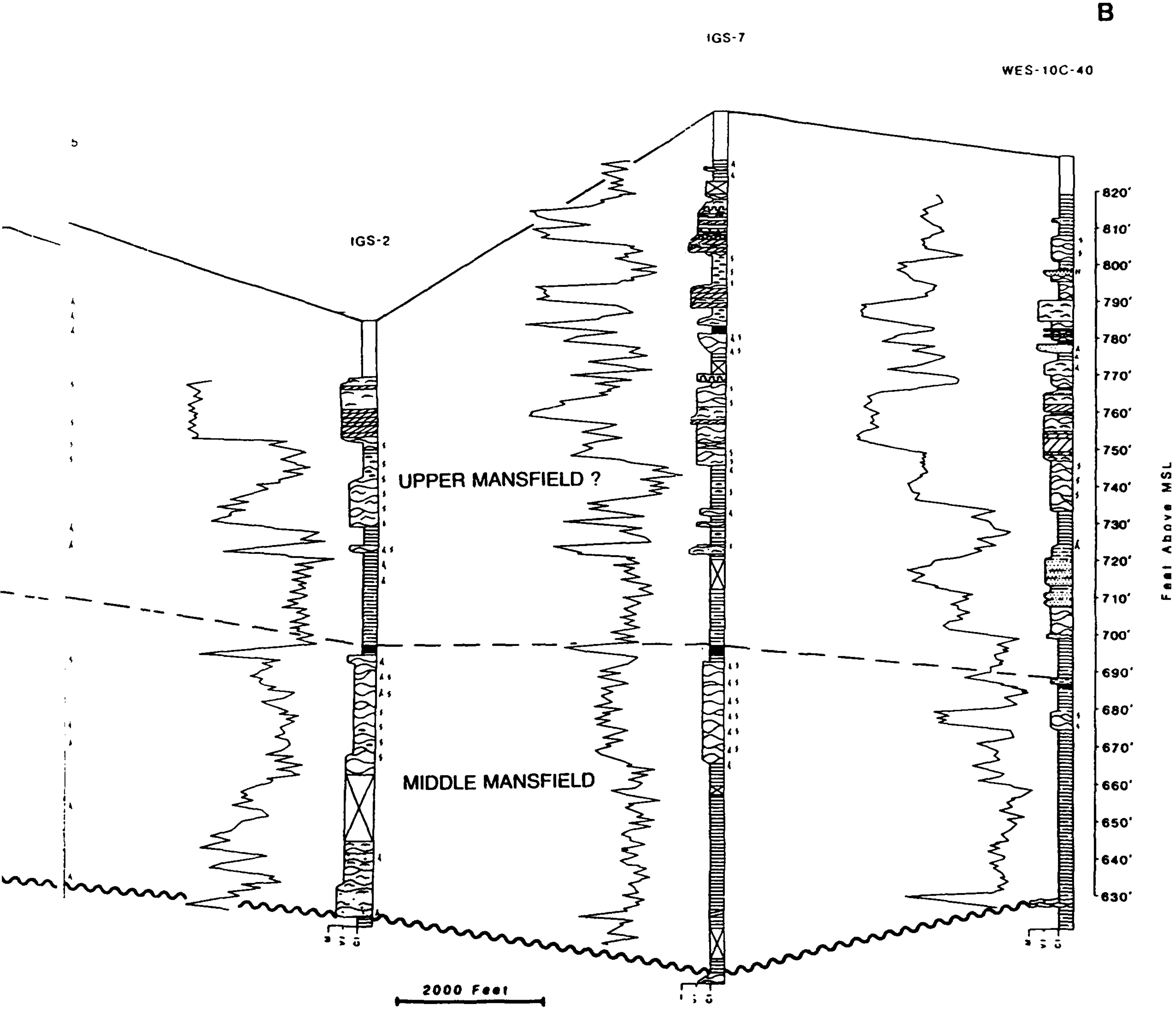

B-B' :ction B-B', connecting the Rockeye and ABG sites (DNR, 1992)

(2)

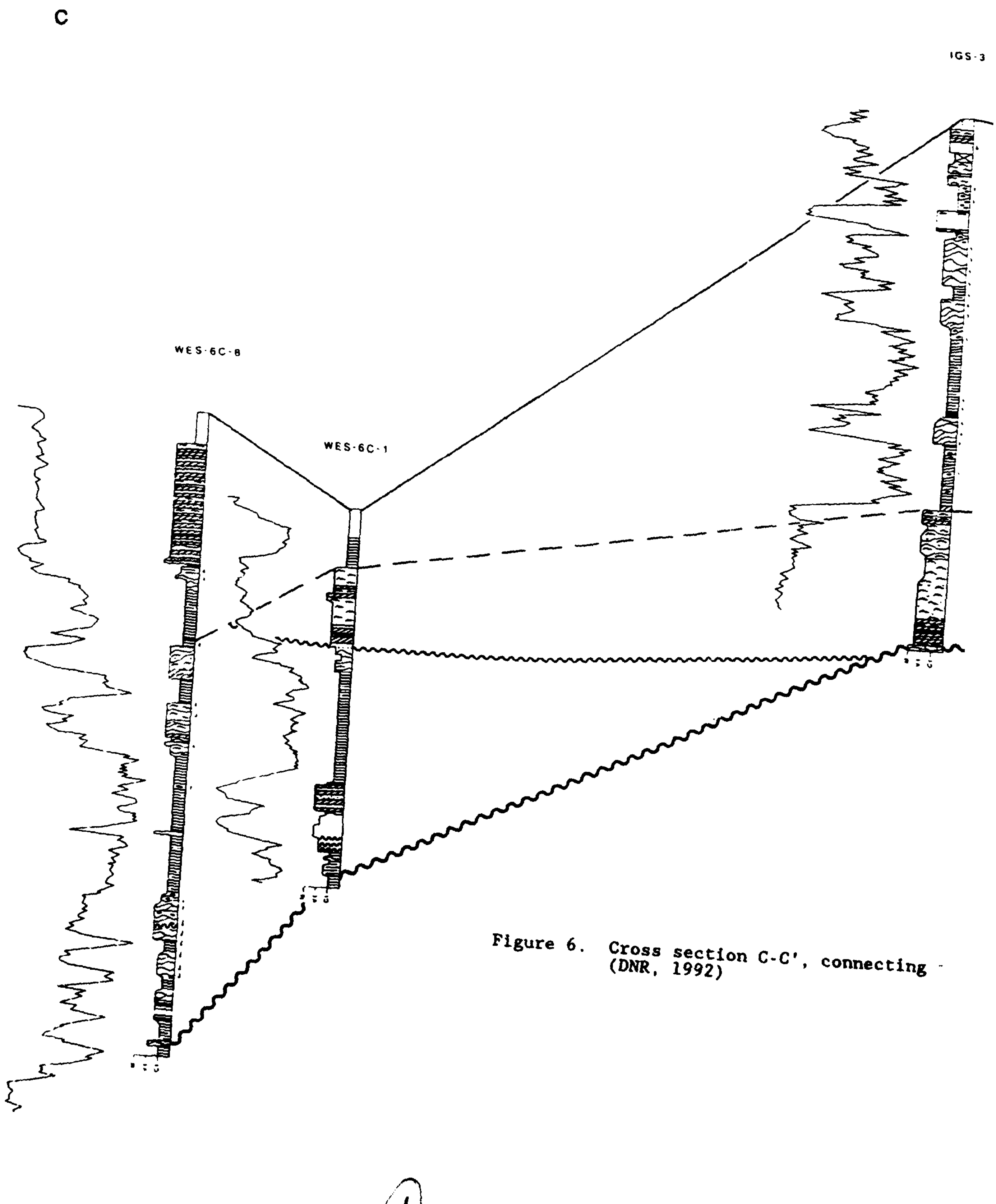

Figure 6. Cross section C-C', connecting -
(*DNR*, 1992)

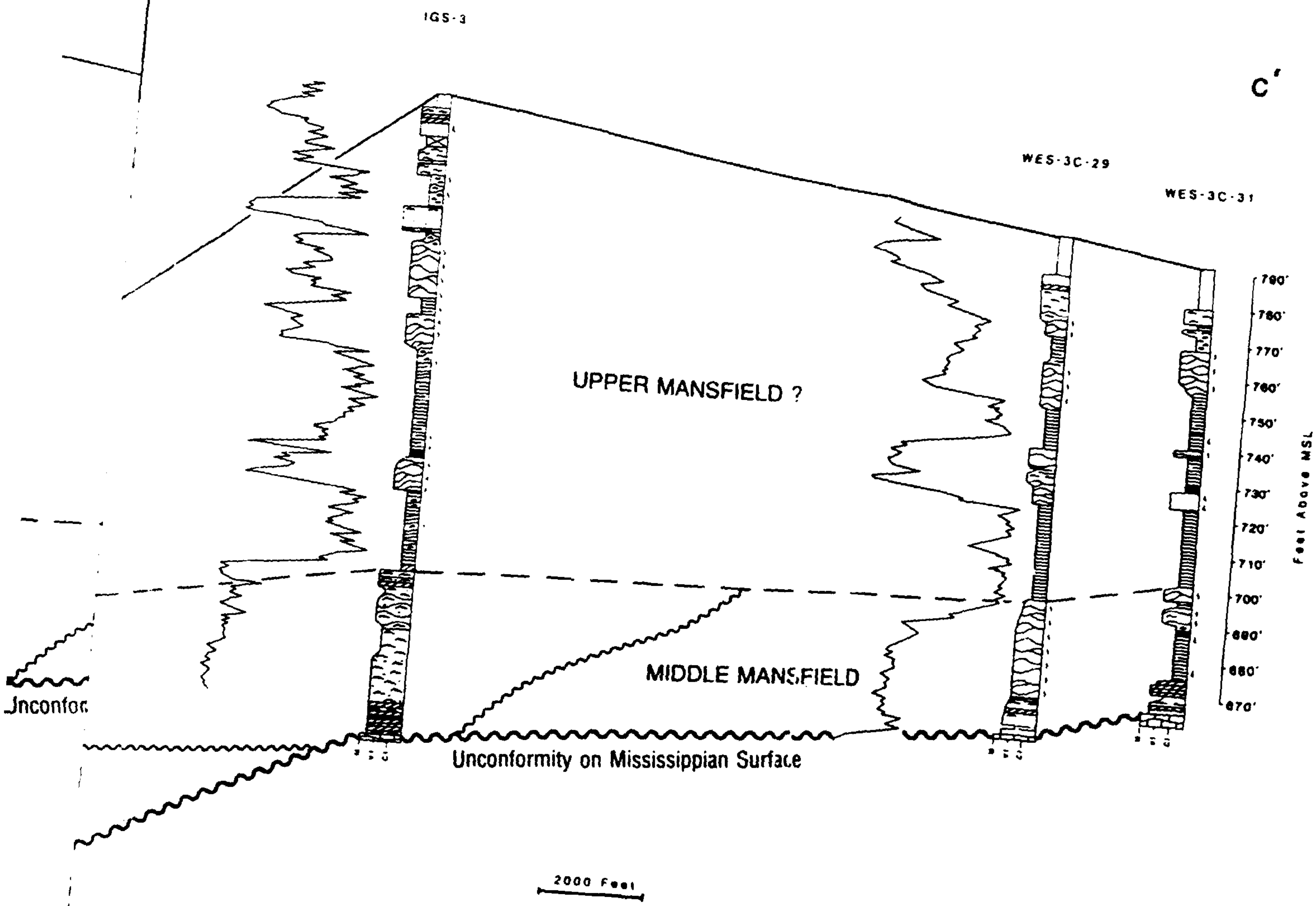

ABG a

section C-C', connecting the ABG and the Demolition Area
1992)

2

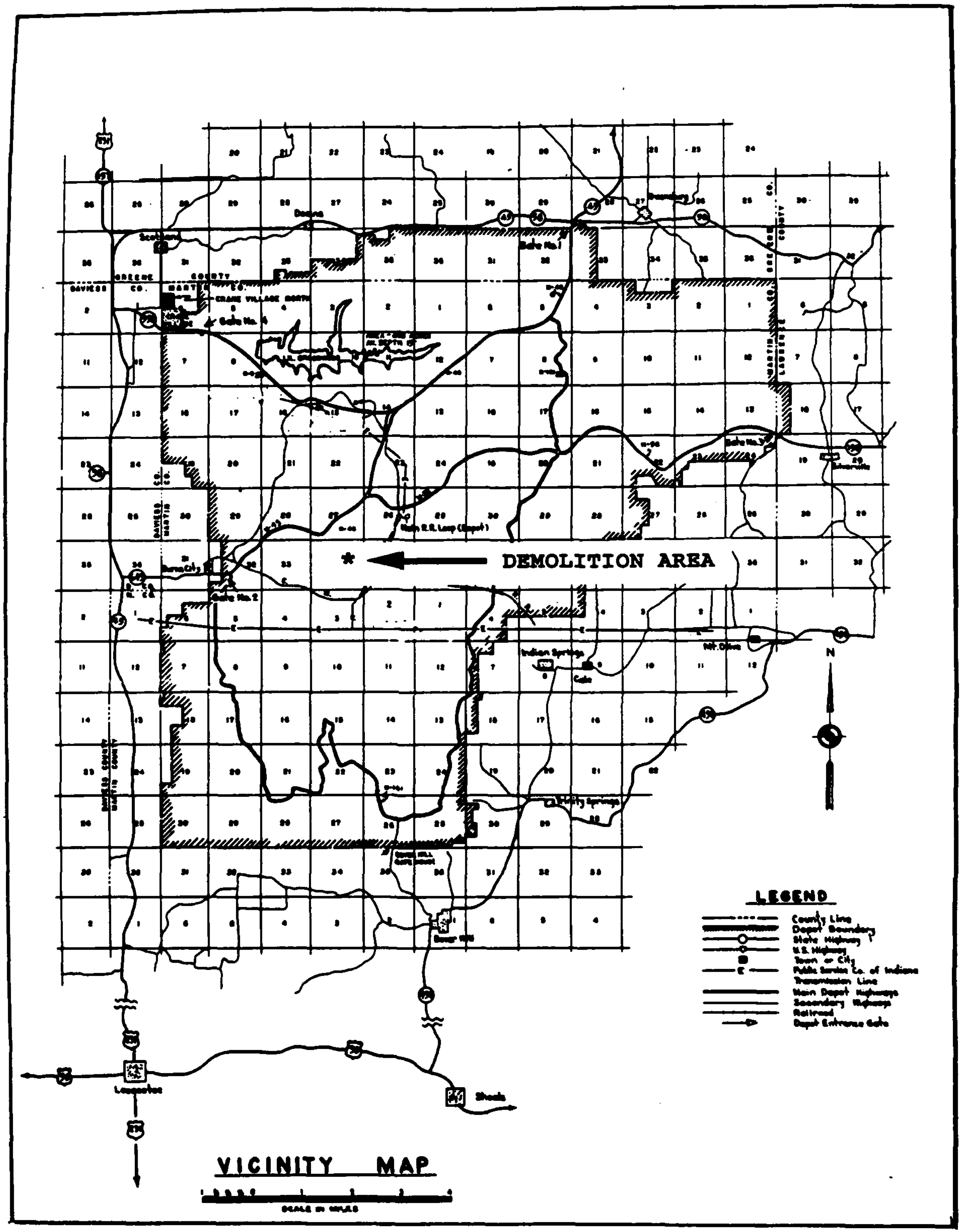

Figure 7. Vicinity map showing the location of the Demolition area at the NSWC

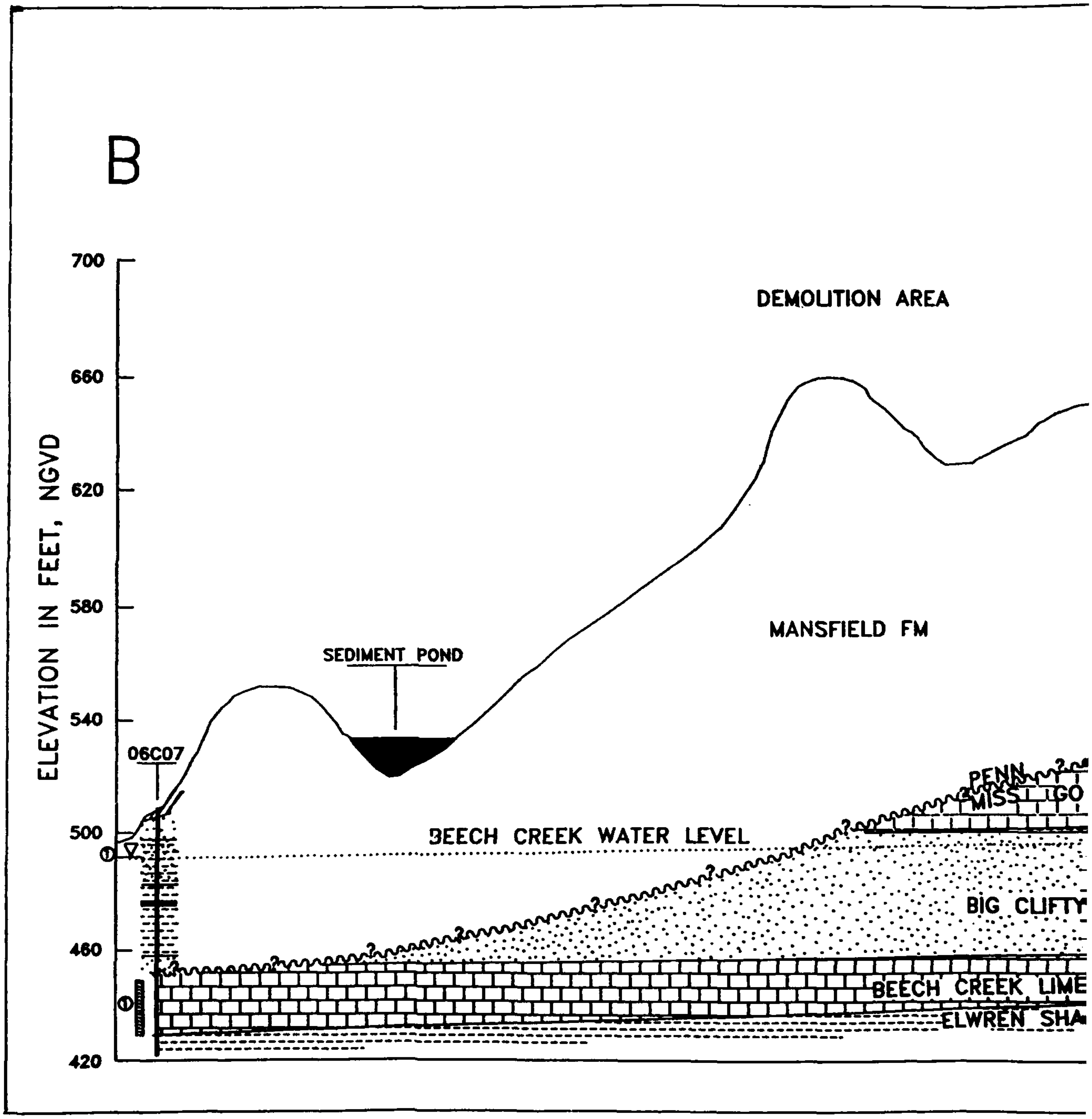

Figure 8. Cross section of the Demol

1

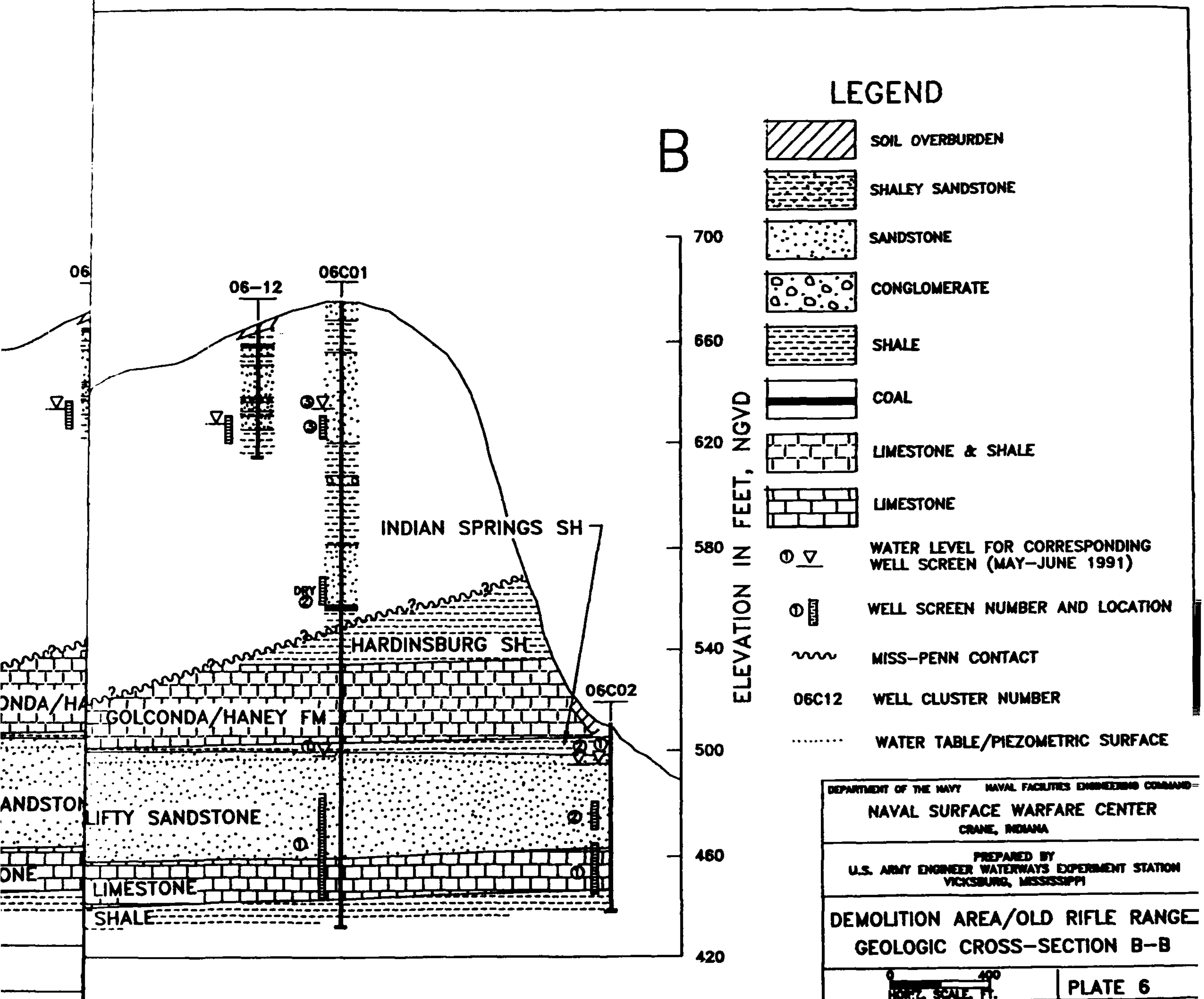

n Area - Demolition Area (DNR, 1992)

(2)

rock ranges from zero to only a few feet. The actual explosive area encompasses approximately 17 acres, with a 500 ft radius cleared of grass and brush. The site is located on a ridge with the area where detonation occurs lying on the north and south slopes. Demolition can also be performed on the east slope of the ridge. The demolition occurs in pits that are aligned in rows on each slope of the ridge (Figure 9). The north slope has three rows of ten pits each and the south slope has one row of ten pits and two rows of five pits.

Blast Source Characteristics

The demolition range disposes of many different types of material that are subject to change during the blasting season (the range disposes of material 8-9 months of the year, closing down during the winter). In addition to the material being disposed of, each pit has some type of initiator to insure a complete explosion. Complete information concerning the type of explosive material in each pit is recorded for each sequence of shots. For the period of this investigation, the primary material being disposed of consisted of fuzes, 106 mm shells, H-6 bombs, 20 mm shells, 8 inch and 5 inch projectiles, and 5 inch propellant charges. The primary initiators were TNT, C3, C4, and H-6. The total charge reported per pit is given as the net explosive weight (NEW), which includes the explosive material being disposed of and the initiator. Table 1 gives a listing of the type and amount of charge detonated each day.

Table 1
Type and Amount of Material Detonated Each Day

Recording Date and Radial	Material Detonated	Net Explosive Weight, lbs/Pit
28 August, N40°E	34 pits fuzes & TNT	370
	8 pits 106 mm & C3	440
	3 pits H-6 bombs & C4	445
29 August, N40°E	29 pits fuzes & TNT	370
	14 pits 106 mm & C3	440
	1 pit 5 inch projectiles & TNT	300
	1 pit 20 mm & TNT	460
31 August, N40°E	30 pits fuzes & TNT	370
1 Sept, S40°W	31 pits fuzes & TNT	370
	1 pit fuzes & H-6	422
	13 pits 106 mm & C3	440

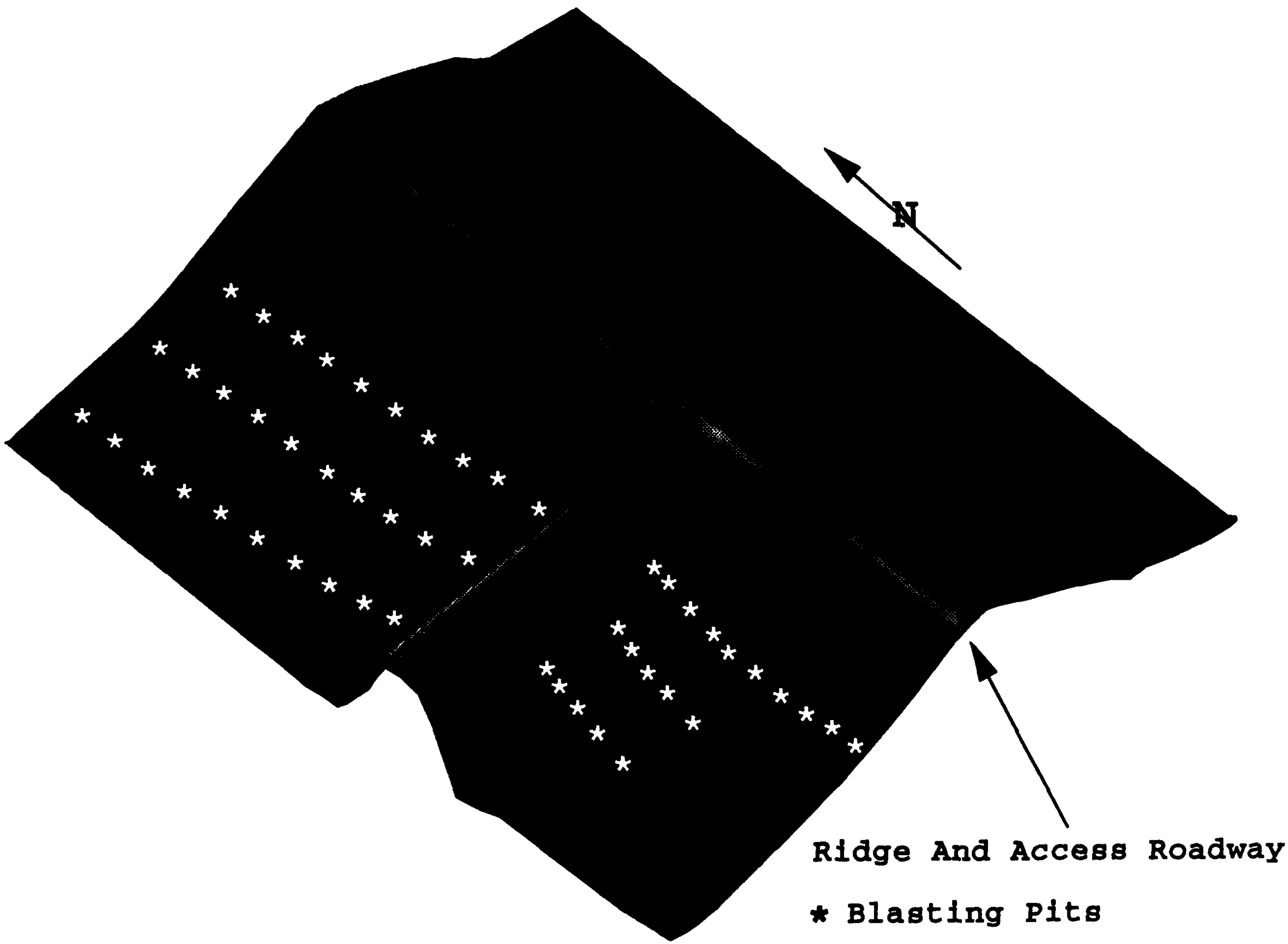

Figure 9. Idealized view of the Demolition area showing the locations of the blasting pits

Table 1
Type and Amount of Material Detonated Each Day

Recording Date and Radial	Material Detonated	Net Explosive Weight, lbs/Pit
3 Sept, S40°W	33 pits fuzes & TNT	370
	1 pit fuzes & H-6	422
	1 pit 8 inch propellants & C3	441
	2 pits 5 inch propellants & TNT	480
	1 pit 8 inch projectiles & C3	445
	7 pits 106 mm & C3	440

The blasting operations consist of digging pits, unpacking the demolition material, repacking into appropriate containers, adding initiating explosives, setting up the firing system, detonating the material, inspecting the demo range, and repeating the sequence for the next set of shots. The pits are typically dug to a depth of 8-10 ft and backfilled 5-6 ft above the ground surface before detonation. Each pit is allowed a maximum quantity of explosives of 500 lbs, and the total explosive weight permitted on the demolition grounds is 35,000 lbs.

3 Test Methodology

General

Explosion generated waves can be divided into three main categories; compressive (P), shear (S), and surface as shown in Figure 10. These three main wave types can be divided into two varieties; body waves which propagate through the body of the rock and soil, and surface waves which are transmitted along a surface (usually the ground surface). Body waves are the sound-like P waves and the distortional S waves, while the most important surface waves are the Rayleigh (R) waves. Explosions produce predominantly body waves at small distances which propagate outward in a spherical manner until they intersect a boundary such as another rock layer, soil, or the ground surface. At this intersection, shear and surface waves are produced. At larger transmission distances, the R waves become important. All three wave types arrive together at small distances but begin to separate at larger distances as shown in Figure 10. The three wave types produce radically different patterns of motion in soil and rock particles as they pass. The P wave produces particle motions in the same direction as it is propagating, the S wave produces motions perpendicular to its direction of propagation, and the R wave produces motions both in the vertical direction and parallel to its direction of propagation. To define the motion, three mutually perpendicular components are measured (vertical, radial, and transverse). No one of these perpendicular components always dominates in blasting, and the peak component varies with each blasting sequence.

A typical velocity time history is shown in Figure 11. The most important parameters that describe the time history are peak amplitude, principal period (1/principal frequency), and duration of the vibration. All these parameters are dependent on the blast and the transmission medium.

Scaling of distance is necessary to predict peak particle velocities when both the charge weight (W), and the distance or range (R), vary. The two most popular approaches are square root, $R/W^{1/2}$, scaling and cube root, $R/W^{1/3}$, scaling. Square root scaling, plotting peak particle velocity or air overpressure as a function of the distance divided by the square root of the charge weight, is more traditional than cube root scaling. Typically, for close-in measurements (closer than 6 meters) cube root scaling is more conservative, and for far-out measurements (beyond 31 meters) square root

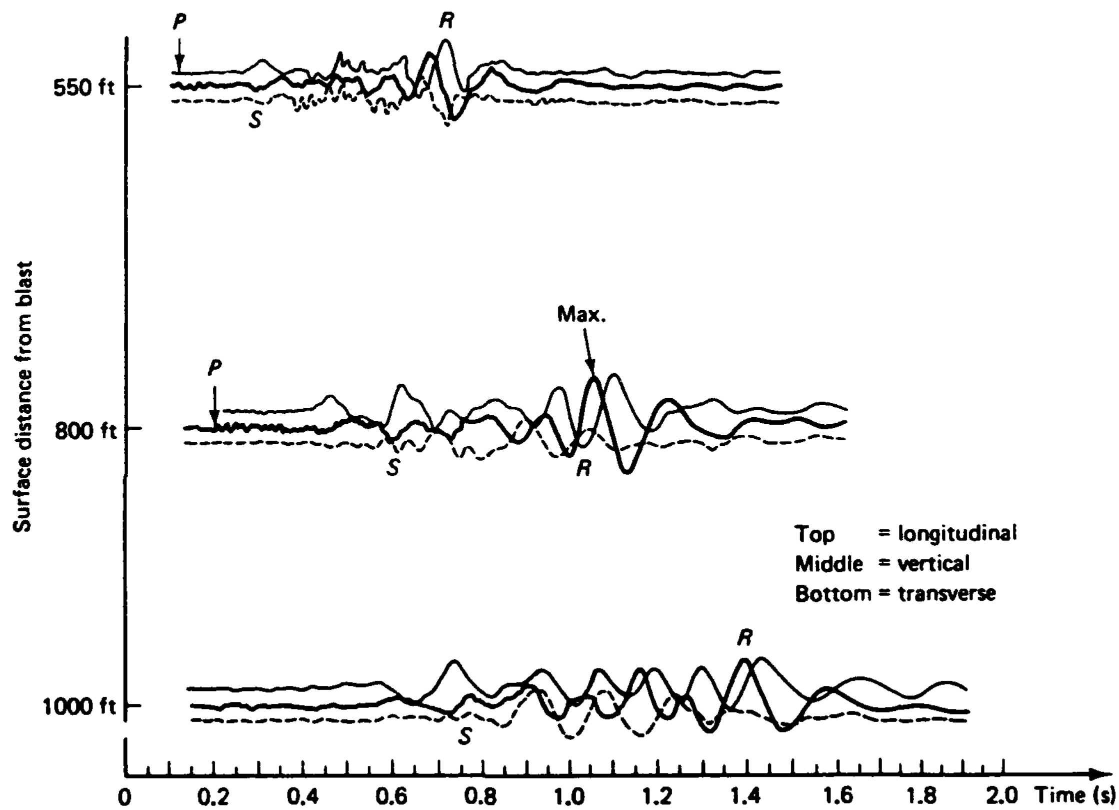

Figure 10. Generalized time histories showing compressive (P), shear (S), and surface (Rayleigh (R)) waves as a function of time (Dowding, 1985)

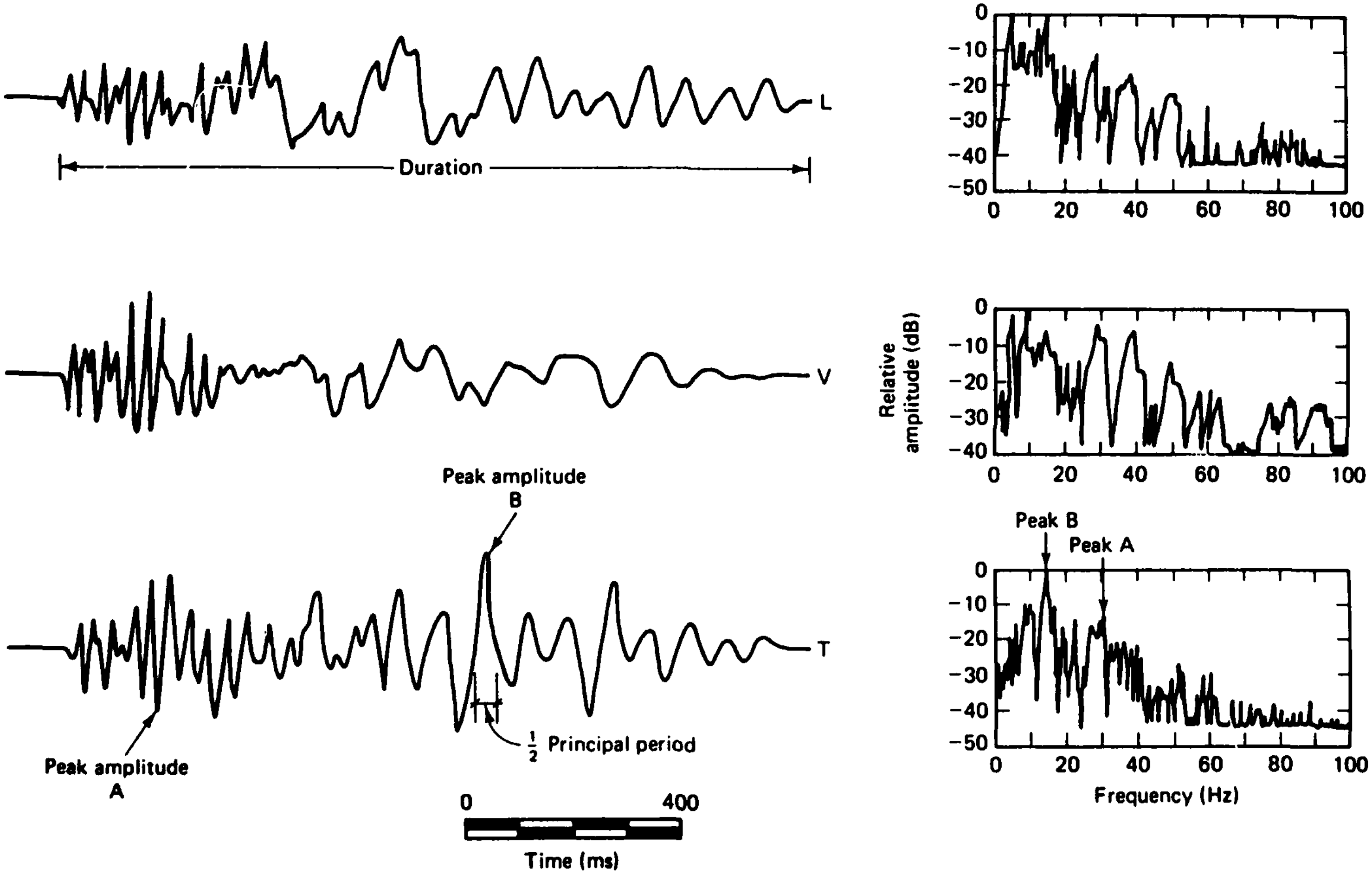

Figure 11. Typical time histories showing peak amplitude, principal period, and duration (Dowding, 1985)

scaling is more conservative. Also, scaling relationships are the most accurate when they are derived from similar W and R values and not similar ratios of R/W^a.

Air blasts are the air pressure waves generated by explosions. Just as with ground vibrations, these pressure waves can be described with time histories where the amplitude is air pressure instead of particle velocity. The higher-frequency portion of the pressure wave is audible and is the sound that accompanies a blast; the lower-frequency portion is not audible but excites structures and in turn causes a secondary and audible rattle within a structure. Air blasts are of interest for three reasons. First, by themselves or in combination with ground motions, they can produce structural motions that create cracks. Second they may crack windows, although the air blast would have to be unusually high (0.1 psi or 150 Db). The third reason being that most humans have adverse reactions to loud noises, and perceive that damage is resulting. Sound is reported in two different units of measurement, pressure (psi) or decibels (dB). When pressure units are reported they are often called overpressures to indicate that the measured pressure is that above atmosphere.

Instrumentation

Each measurement station consisted of four data channels; three seismic monitoring channels and one air overpressure monitoring channel. The measurement stations were a triaxial array of calibrated L4-3D geophones (velocity transducers manufactured by Mark Products Inc., Houston, Tx) oriented to detect the vertical, radial, and transverse components of the ground motion (Figure 12) and a microbarograph (air pressure transducer) to detect air overpressure. The microbarographs are composed of pressure cell transducers (manufactured by Valydine) and WES built amplifiers. The geophones had a natural frequency of 1.0 Hz and sensitivities of 3.07-4.55 volts/in/sec (v/ips) depending on the particular geophone. The microbarographs had a frequency response from 0 to 1000 Hz and a sensitivity of 10.0 - 45.0 volts/lb/in^2 (v/psi). Instrument sensitivities and frequency responses are given in Table 2 for each station. All geophones and microbarographs were calibrated before being utilized in the field. The geophones were calibrated on a shaker table to determine the frequency response. The microbarographs were tested using a standard water column calibration scheme. The data acquisition instrumentation consisted of multi-channel FM tape recorders (TEAC R41 and R71), oscillograph, and WES developed amplifiers, all of which were battery operated. All data were recorded on tape and an immediate data playback was obtained from the oscillograph to insure data quality and enable determination of recorded signal levels.

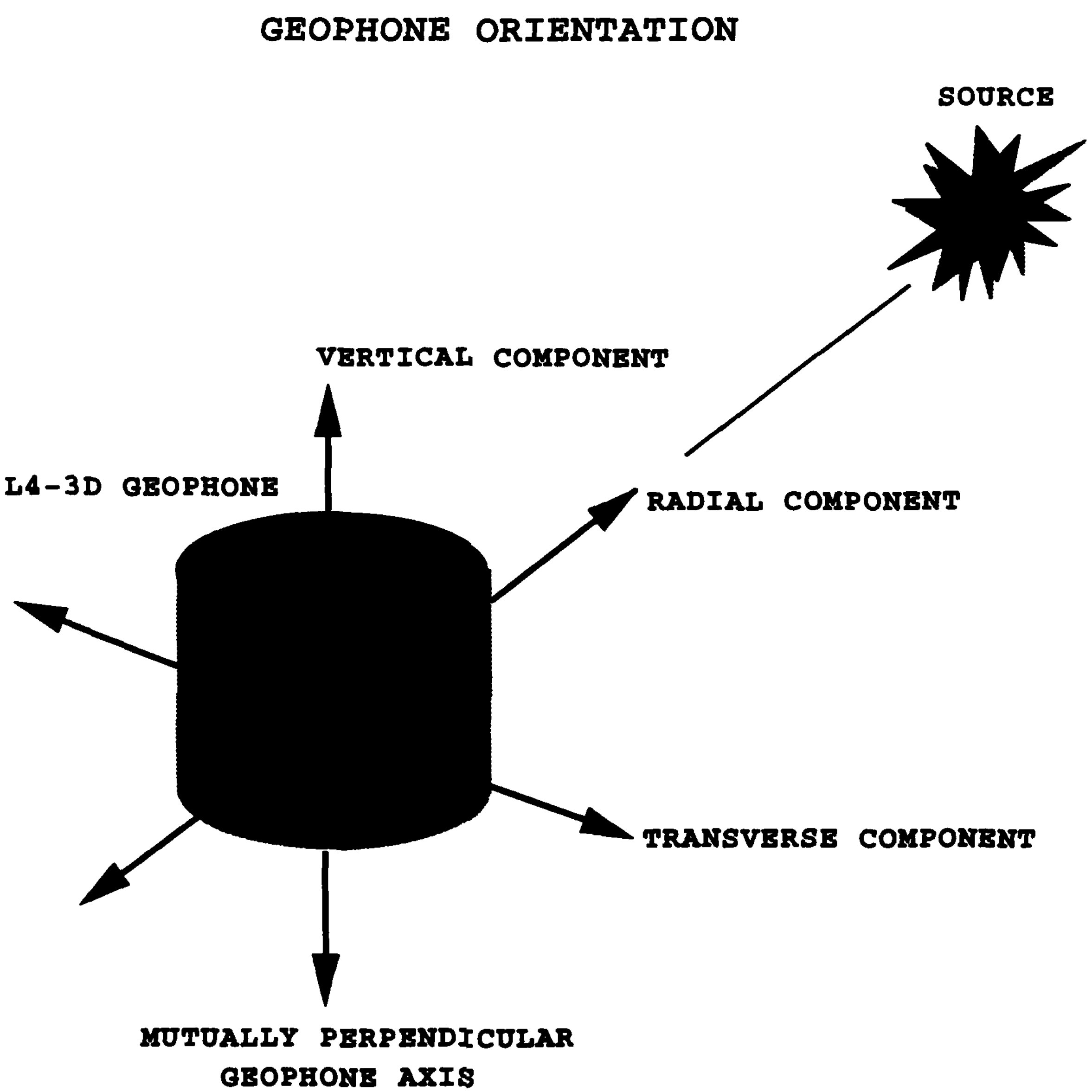

Figure 12. Diagram of geophone showing vertical, radial, and transverse recording directions

Table 2 Transducer and Microbarograph Characteristics			
Sensor		Sensitivity	Frequency Response, Hz
Geophone #507	Vertical	3.510 v/ips	1.0 natural
	Radial	3.822 v/ips	1.0 natural
	Transverse	3.851 v/ips	1.0 natural
Geophone #508	Vertical	3.455 v/ips	1.0 natural
	Radial	3.826 v/ips	1.0 natural
	Transverse	3.937 v/ips	1.0 natural
Geophone #511	Vertical	4.552 v/ips	1.0 natural
	Radial	4.243 v/ips	1.0 natural
	Transverse	4.128 v/ips	1.0 natural
Geophone #517	Vertical	3.046 v/ips	1.0 natural
	Radial	4.070 v/ips	1.0 natural
	Transverse	4.220 v/ips	1.0 natural
Geophone #518	Vertical	2.799 v/ips	1.0 natural
	Radial	2.708 v/ips	1.0 natural
	Transverse	2.716 v/ips	1.0 natural
Microbarograph #48321		39.612 v/psi	0 - 1000
Microbarograph #48322		40.328 v/psi	0 - 1000
Microbarograph #72383		9.861 v/psi	0 - 1000
Microbarograph #72384		46.115 v/psi	0 - 1000
Microbarograph #72388		39.721 v/psi	0 - 1000

Test Layout and Procedure

The actual test program consisted of recording data on consecutive days under varying blasting and weather conditions, and along two separate radials (Figure 13). The recording days were from 26 August through 3 September 1992. The data recorded on 26 August served to calibrate the instrumentation for the conditions at the site and is therefore not presented in the results. No data was recorded on 27 August or 2 September due to poor weather conditions (rain), postponing any blasting activity. Also, no data are presented for 30 August due to damaged equipment and equipment failure. The two radials selected were based on conversations with CAAA personnel,

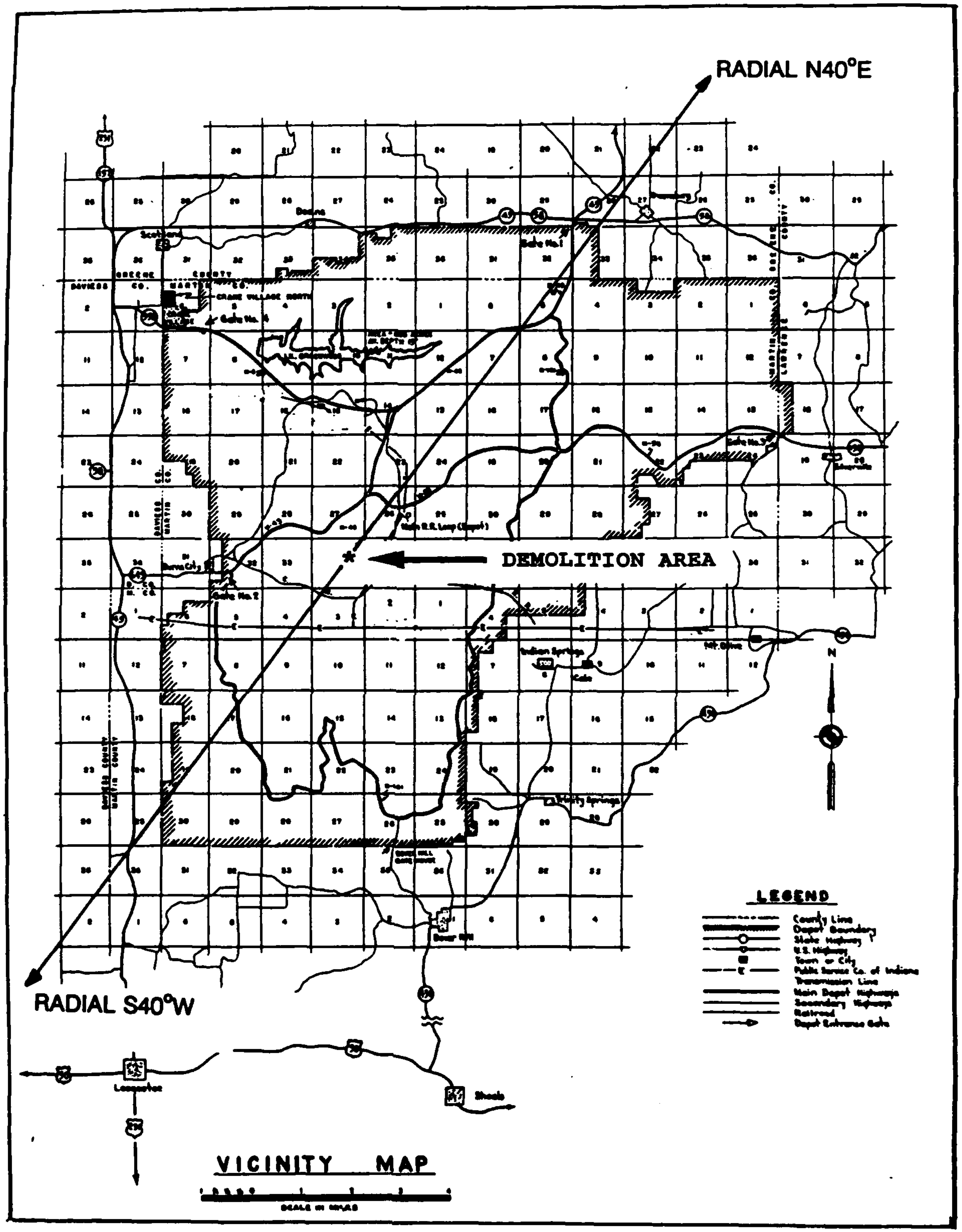

Figure 13. Vicinity map showing the two radial directions in which data were recorded

and have bearings N40°E and S40°W. Each day's recording consisted of either four or five stations placed at varying distances from the blast source. Table 3 contains information about the number of recording stations, locations for each days testing, and the pertinent weather information. The locations listed in Table 3 are nominal distances from the blasting area to the recording stations, the exact distances from each blasting pit to each recording station are presented in Appendix A.

Table 3
Nominal Locations of Recording Stations and Weather Information for Each Day

Recording Date and Radial	Nominal Station Locations, ft	Weather Information
28 August, N40°E	500	Temp 69° Humidity 63% Wind N 9 mph Barometer 29.98 Partly Cloudy Ceiling 2500 ft
	5800	
	10,000	
29 August, N40°E	500	Temp 73° Humidity 57% Wind S 9 mph Barometer 30.11 Clear Ceiling Unlimited
	1000	
	5800	
31 August, N40°E	500	Temp 71° Humidity 57% Wind W 5 mph Barometer 30.20 Partly Cloudy Ceiling 3000 ft
	750	
	1000	
	1450	
	5800	
1 Sept, S40°W	500	Temp 73° Humidity 62% Wind SE 7 mph Barometer 30.20 Hazy Ceiling 5000 ft
	2900	
	5800	
	10,800	
	22,000	
3 Sept, S40°W	250	Temp 77° Humidity 74% Wind W 6 mph Barometer 30.08 Partly Cloudy Ceiling 1500 ft
	500	
	750	
	2900	

To record the data, each day the instrumentation was first checked to verify that it was functioning properly, then each station was set up at the selected location to record the vertical, radial, and transverse ground motions in addition to the air overpressure. The geophones were buried flush with the ground surface to reduce the amount of extraneous noise. The microbarographs were placed on a flat stable surface approximately 1 ft above the ground surface. The instrumentation was zeroed, calibrated, and readied for the blasting sequence. One person was left at each station to initiate the recording, and monitor any unusual occurrences that might occur. The recorders lying outside a 3000 ft radius (safe distance secured before each shot) were typically started 2-3 minutes before the blasting began, and would record approximately 20 minutes worth of data. The recorders lying inside a 3000 ft radius were typically started 12-15 minutes before blasting began. After the shots were completed, all instrumentation was picked up and returned to a central point for data verification, and to ready for the next days activity. A log was made of each days shots which records the type and amount of material in each pit, start and completion time of blasting, and pertinent weather information. The weather information includes temperature, ceiling, wind speed and direction, humidity, and barometric pressure.

4 Results and Analysis

Data Processing and Presentation

The calibrated field data were recorded analog and unfiltered. A gain was employed on the far stations (5000 ft and greater) to enhance the signal detection. The data were then digitized (512 samples/second), stored in files on a computer, and processed using a program that allows data inspection and calculation. The calculations determine maximum peak particle velocities (PPV) and peak air overpressures (PAO) for each seismic and acoustic data set. The data were then displayed in the form of amplitude versus time plots (time histories). Due to the large amounts of data obtained (3,084 time histories), it is not possible to show a time history plot for every piece of data collected. Rather, a representative sample of the data has been selected and the time histories are presented. Appendix B contains the representative time histories for data collected at the NSWC.

Development of Attenuation Relationships

The maximum unfiltered peak particle velocity detected by each geophone at each station from each test is shown in Appendix A. These velocities were plotted versus scaled range, both square and cubic. This type of plot is the conventional way of representing the attenuation of ground motions from surface or sub-surface charges. These sets of data were then statistically analyzed using simple regression to determine the best fit ground motion attenuation curves. These curves represent the average expected value predictions, but do not account for data scatter. The assumed mathematical model is:

$$PPV = C_1(R/W^{C2})^{C3} \qquad \text{EQN 1}$$

PPV - peak particle velocity, ips
C2 - scaling constant equal to 1/2 or 1/3
R - distance from source in feet
W - charge size in pounds
C1 & C3 - constants determined from regression analysis

The results of the regression analysis along with the plotted data are presented in Appendix C. The plots consist of square and cubic scaling of:
- vertical motions for each day
- radial motions for each day
- transverse motions for each day
- air overpressures for each day
- vertical motions for radial N40°E, days 28, 29, 31 August combined
- radial motions for radial N40°E, days 28, 29, 31 August combined
- transverse motions for radial N40°E, days 28, 29, 31 August combined
- vertical motions for radial S40°W, days 1, 3 September combined
- radial motions for radial S40°W, days 1, 3 September combined
- transverse motions for radial S40°W, days 1, 3 September combined.

The results of the air overpressure measurements detected by each microbarograph at each station for each test are shown in Appendix A, with representative time histories shown in Appendix B. These set of data were also statistically analyzed using simple regression to determine the best fit curves, which represent the average expected values but do not account for data scatter. The plots are shown in Appendix C, with air overpressures versus cubic scaling, (air overpressure plots are generally not shown as a function of square scaling). The assumed mathematical model is:

$$PAO = C1(R/W^{C2})^{C3} \qquad \text{EQN 2}$$

PAO - peak air overpressure, psi
C2 - scaling constant equal to 1/3
R - distance from source in feet
W - charge size in pounds
C1 & C3 - constants determined from regression analysis

Analysis of Data Variance

Collection of scaled distance for determination of attenuation relationships for particle velocity will result in a good deal of scatter about the mean line (median line for log-log relationships). Because of this scatter, most regulations require that blasts be designed on the basis of maximum probable velocities rather than average values. Many factors are responsible for the variation of particle velocities at a given scaled distance. They include changes of geological conditions, differences between types of explosives, different wave types, differences in the geometry of the explosions, as well as errors in blast timing and measurement. The same factors, with the exception of geology, are responsible for the variation of air overpressure. Since overpressures are transmitted through air, weather conditions replace geology as a principal variable. Therefore, for the final analysis the data were also fitted with an equation representing the bound below which fall 95% of the data.

The data plots and corresponding average (50%) predictive equations as presented in Appendix C, have been evaluated and grouped into a final set of

plots and equations to help characterize the entire site. The average or 50% lines were determined from regression analysis (Power method) of the log normally distributed data. Also shown on these plots are the 95% non-exceedance equations. These equations were determined by converting the data into logarithmic (base 10) values and running regression analysis (linear) of the transformed data. From the regression analysis, the standard error of the y estimate is obtained which can be used to determine the values on the 95% non-exceedance line. These values are determined by the following formula: $y_{95\%} = y_{50\%} * 1.645 * 10^{\text{standard error of the y estimate}}$. The 95% non-exceedance line is presented so that predictions of ground motions or air overpressures can be made with a 95% confidence that the values will not be exceeded. This also implies however, that 5% of the time the predicted values will be exceeded.

Monitoring Results

The predominant motions at the site were recorded by the vertical and radial components of the geophones. Therefore, the data recorded by the transverse component is not considered in this analysis. Also, the air overpressures recorded were small and will be discussed separately. The final analysis plots are presented in Figures 14-20.

Vertical Motions

Figures 14 and 15 are the vertical motions from all the data recorded at the NSWC regardless of line direction (N40°E or S40°W) or the day (28, 29, 31 August, 1, 3 September). Figure 14 is the square scaled range, and Figure 15 is the cubic scaled range data. In general, the data are well behaved except for that located at an approximate scaled range of 1000 ft in Figure 14 and 3000 ft in Figure 15. The PPV's recorded at this location appear to be slightly less than would be predicted by the best fit line (all the points fall below the line). This could be a result of the station recording different wave forms (traveling at a slower velocity) than the wave forms being recorded by the closer stations. It could also be an indication that the particular area where the station was located has a larger attenuation thereby reducing the amount of energy reaching the geophone. Lastly, the slower PPV's could be due to the frequency content of the motions, since the frequency tends to lower as the distance from source increases.

Radial Motions

Figures 16 and 17 (square and cubic scaling respectively) are the radial motions from all the data recorded at the NSWC regardless of line direction or the day recorded. Here again, the data located at 1000 ft in Figure 16 and 3000 ft in Figure 17 appears to be lower than expected. The reasons for this would be the same as discussed in the above paragraph.

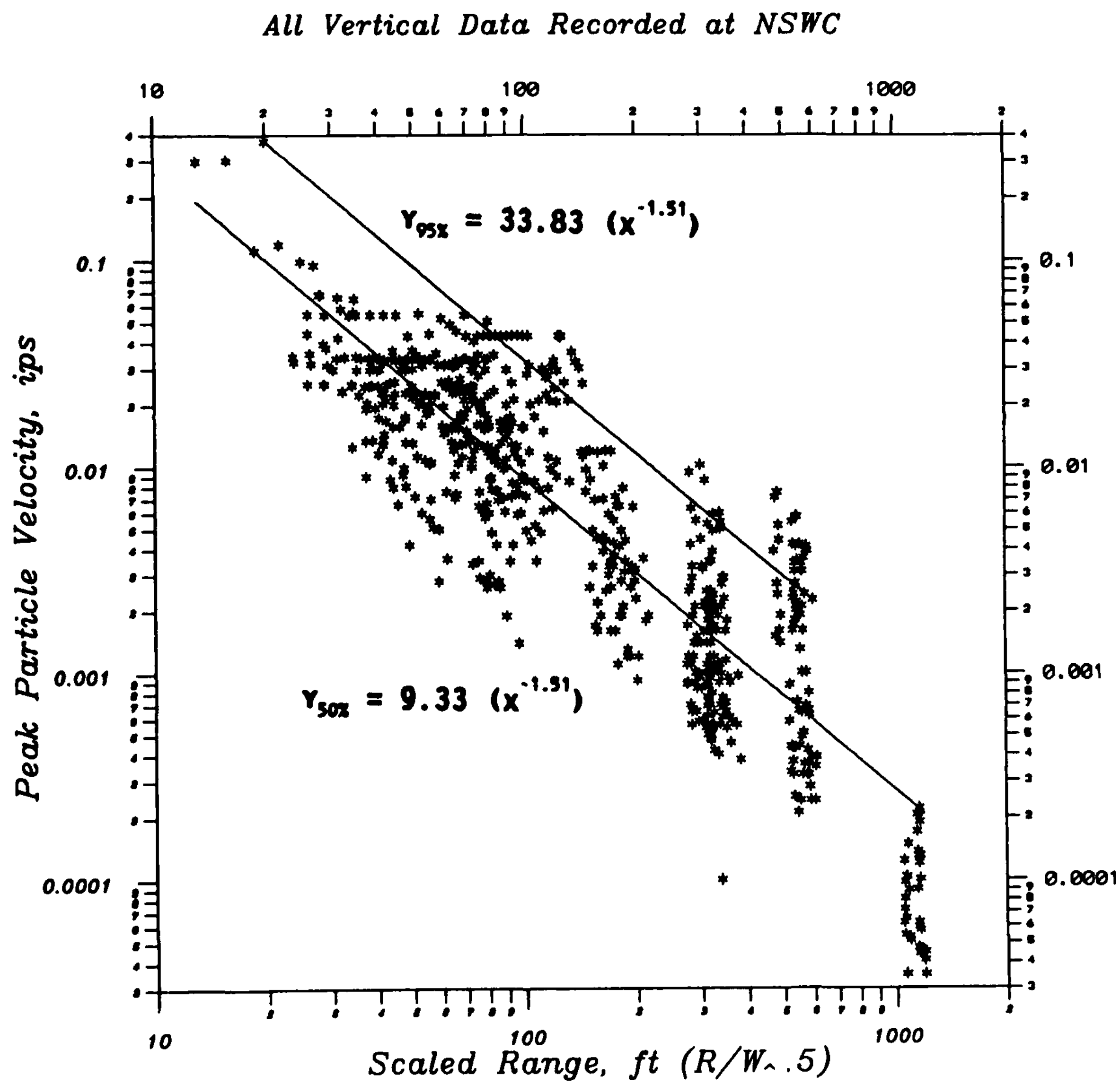

Figure 14. All data recorded in the vertical direction from source at the NSWC, versus square root scaling

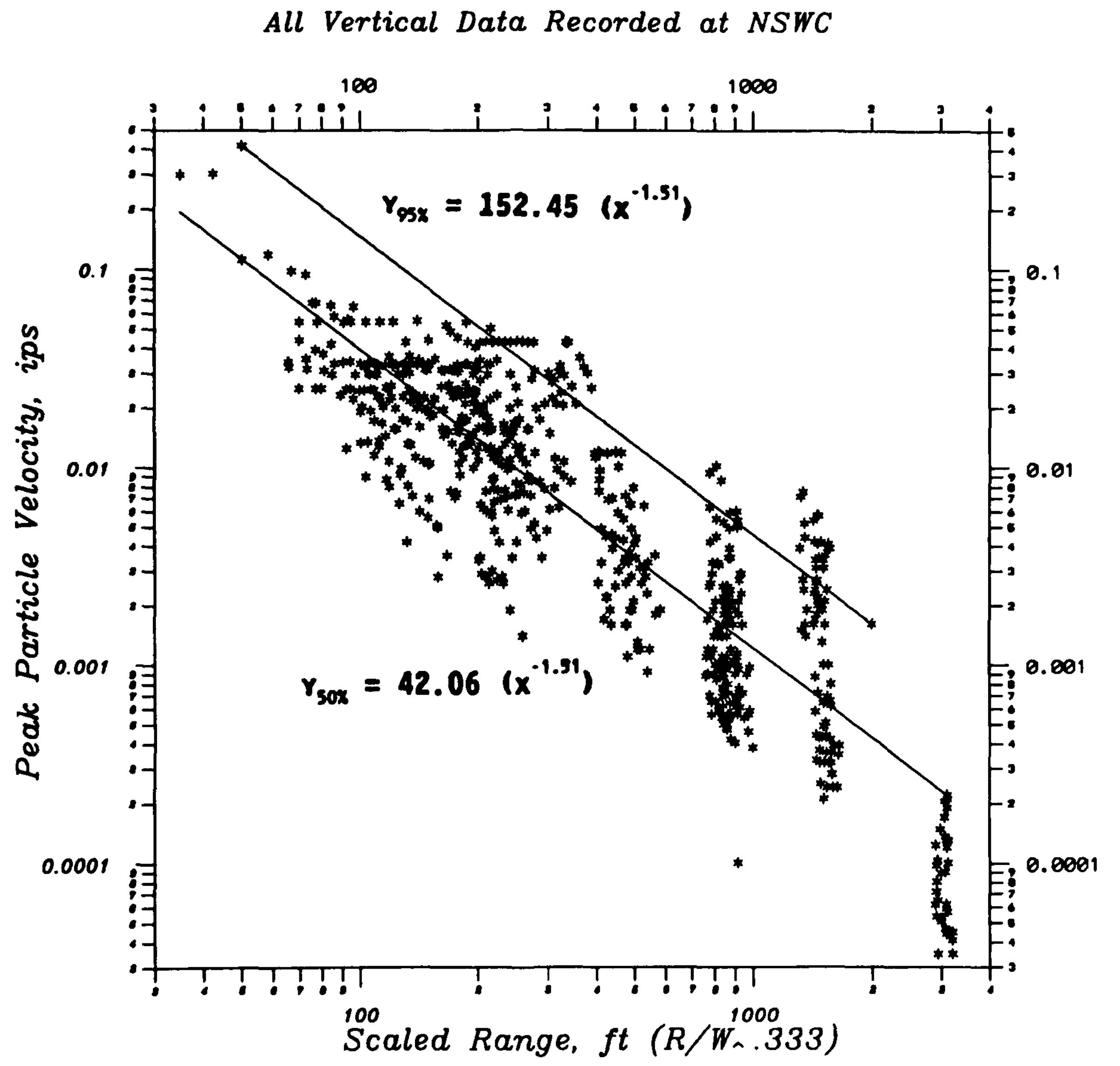

Figure 15. All data recorded in the vertical direction from source at the NSWC, versus cube root scaling

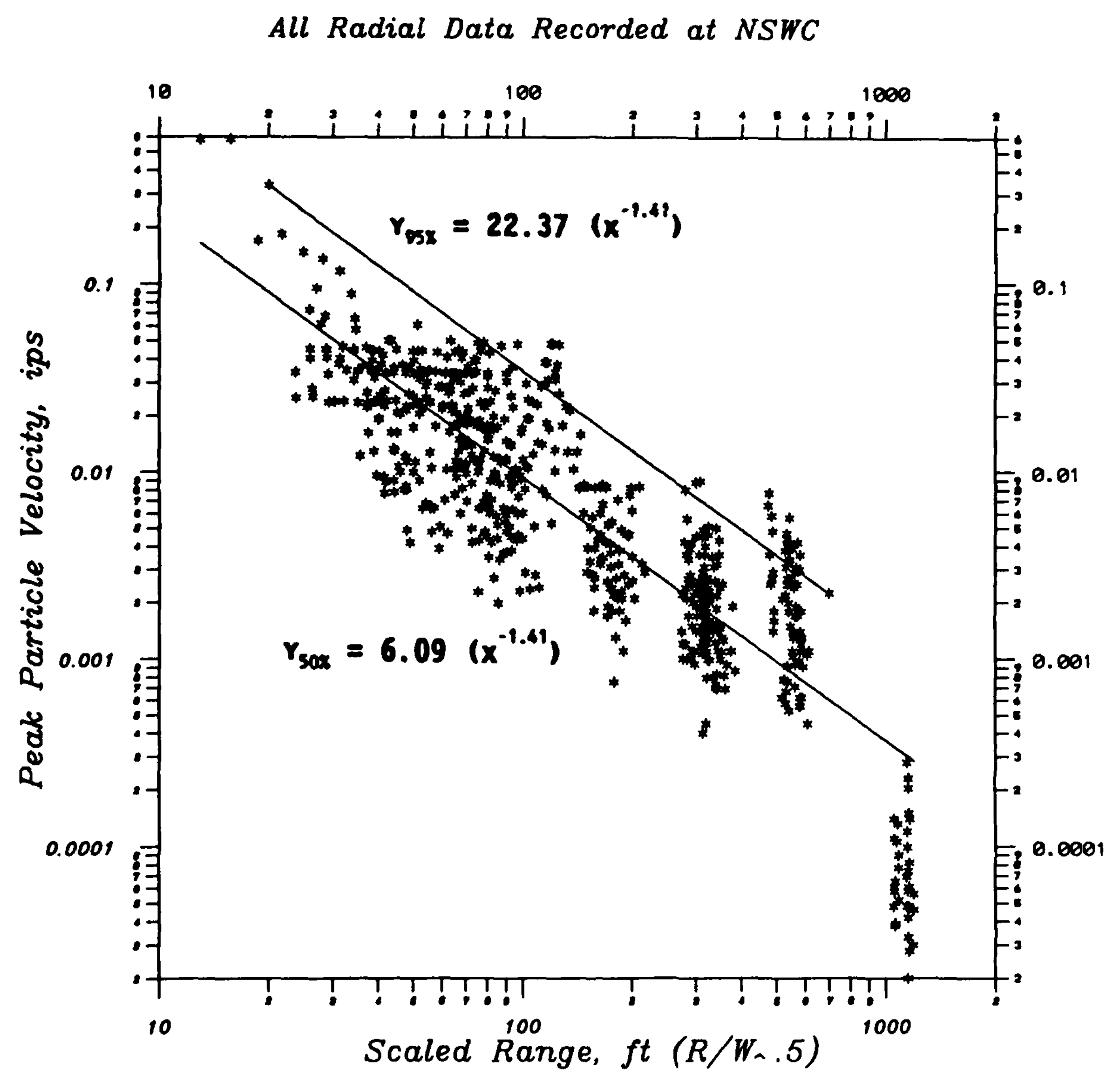

Figure 16. All data recorded in the radial direction from source at the NSWC, versus square root scaling

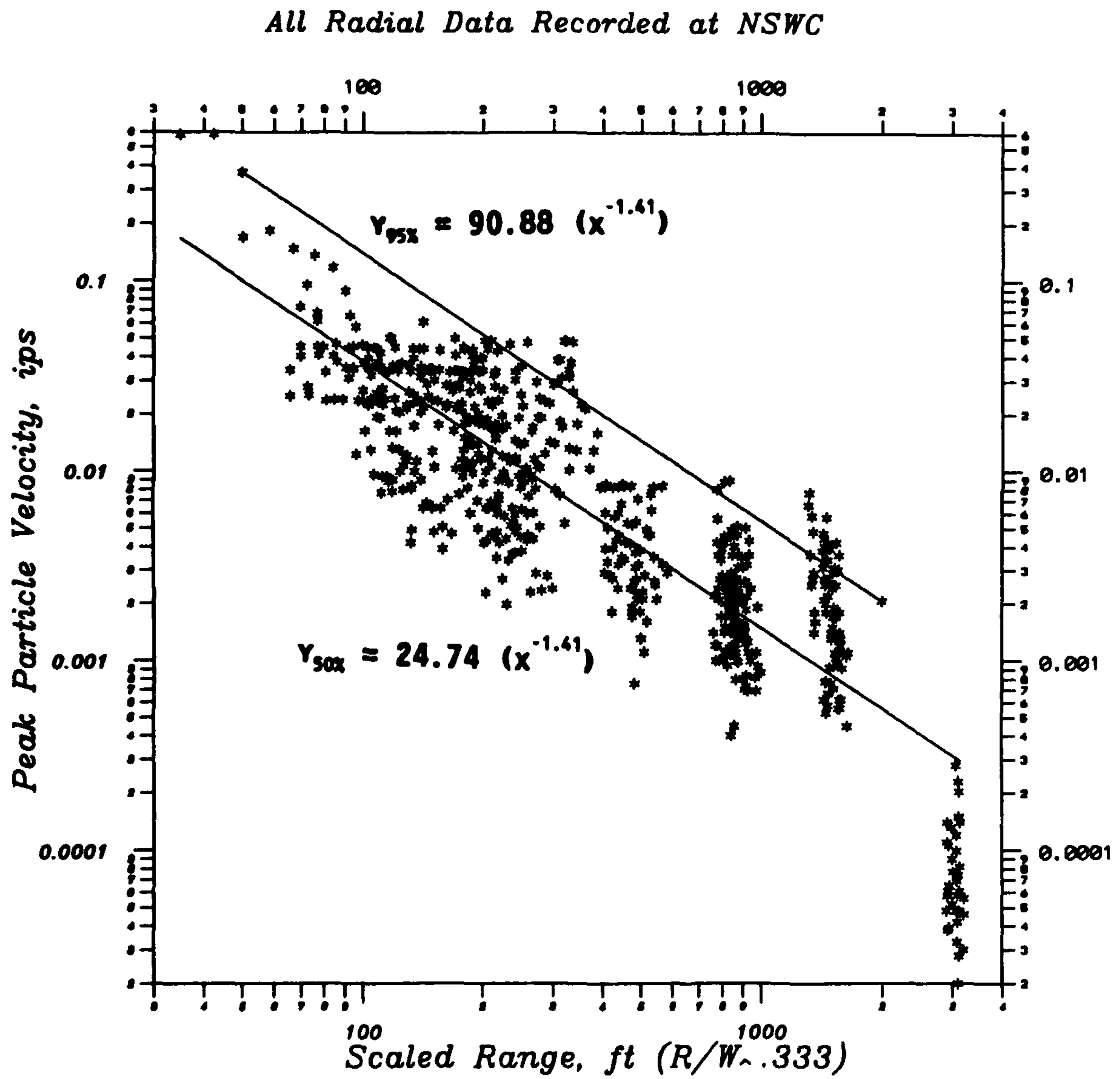

Figure 17. All data recorded in the radial direction from source at the NSWC, versus cube root scaling

Air Overpressures

Figure 18 shows the air overpressures recorded at the NSWC regardless of line direction or day recorded. On this plot, two sets of data located at an approximate scaled range of 1500 ft appear to be inconsistent with the other data. Since the air overpressure data is influenced by weather rather than geology, this must be having an influence on the results at this station. The data having the high values (0.001 to 0.01 ips) were recorded when the ceiling was 2500 ft and the skies were partly cloudy. The data having the low values (0.00001 to 0.0001) were recorded when the ceiling was 5000 ft and the skies were clear. The low ceiling and cloudy conditions could account for the increased PAO's recorded for that particular day.

Maximum Motions

Since both the vertical and radial motions are predominating at the site, Figures 19 and 20 were prepared by plotting the maximum of the two (for every shot, every day) versus scaled range. Figure 19 shows the square scaled range, and Figure 20 the cubic scaled range. The regression analysis from this plot produces a predictive equation based on the maximum peak particle velocities recorded at the site. As shown in Figures 14 through 17, the values at the largest scaled range appear to be inconsistent with the other data, this has been explained previously.

Extrapolation of Motions Off-Site

Since no data were actually recorded off-site, it is necessary to perform an extrapolation of the recorded data to make an estimate of PPV and PAO levels at locations off-site. The predominant factors that would effect utilizing the equations obtained from the regression analysis for off-site predictions would be the geology, and the weather. From the discussion of the regional geology, there does not appear to be any dramatic changes in the material in which the ground motions will be travelling across the site. Also, there is no indication that the motions are being amplified, rather the contrary, as they travel across the site. The weather conditions at the time of blasting can have a profound effect on the resulting air overpressures. The amount of cloud cover, location of the ceiling, wind velocity, and wind direction all have a large effect on recorded motions. However, since data were recorded under a variety of weather conditions this factor should be accounted for in the predictive equations determined. Therefore, the following equations are presented to predict motions off-site.

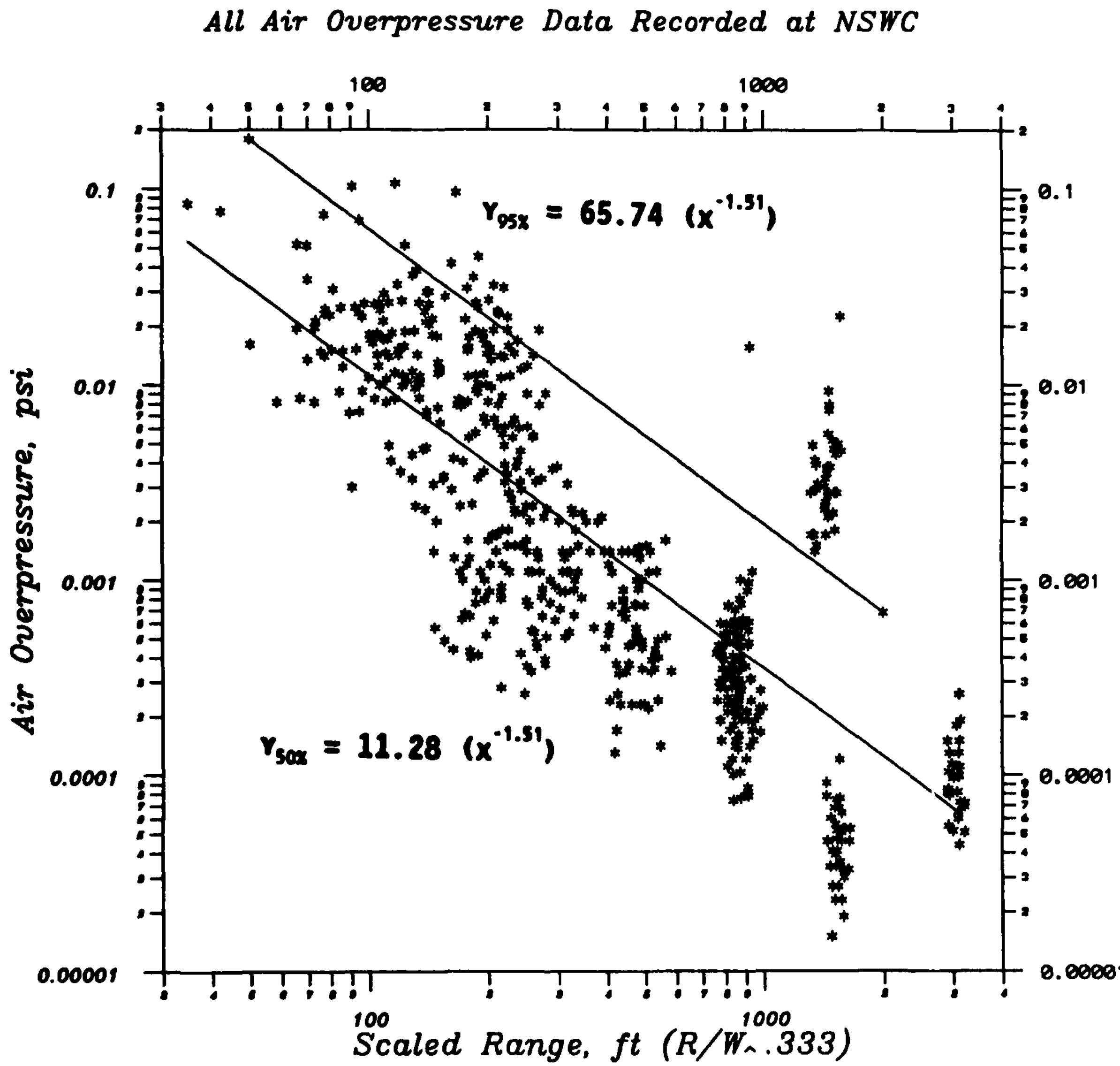

Figure 18. All air overpressure data recorded at the NSWC, versus cube root scaling

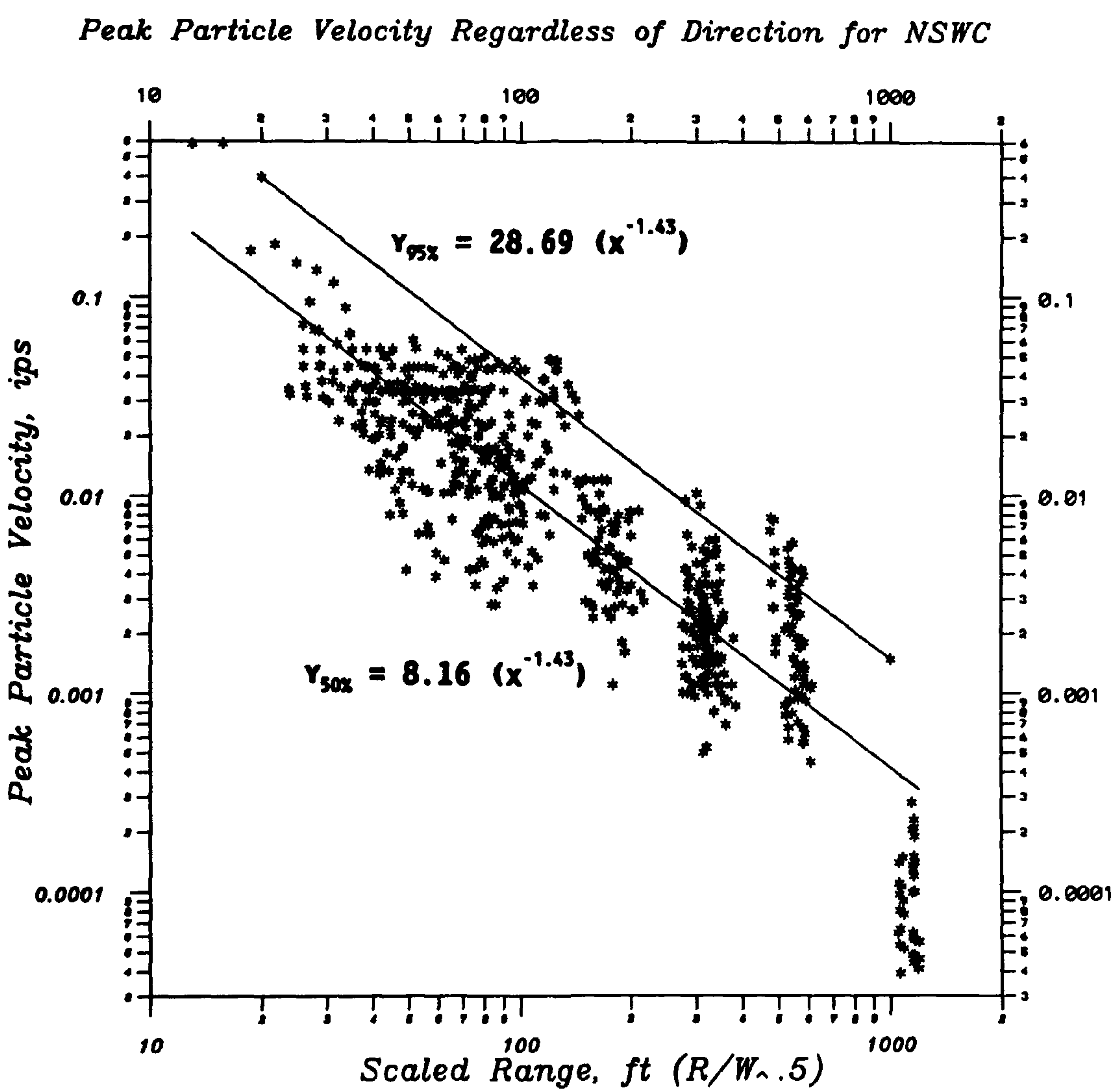

Figure 19. Maximum velocities recorded, regardless of orientation, versus square root scaling

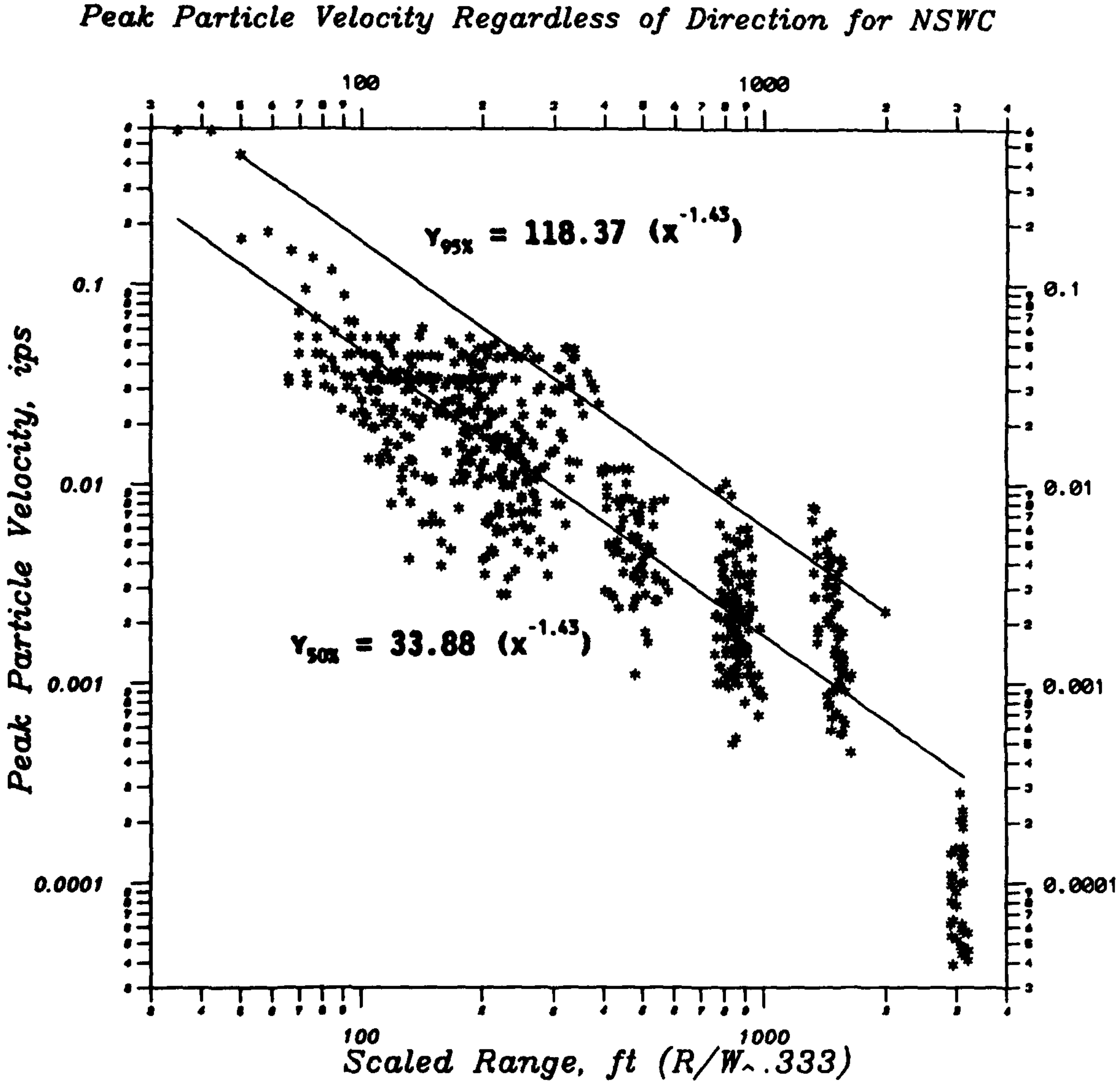

Figure 20. Maximum velocities recorded, regardless of orientation, versus cube root scaling

Ground motion predictions:

Average

$y_{50\%} = 33.88\ (x^{-1.43})$ less conservative EQN 3

$y_{50\%} = 8.16\ (x^{-1.43})$ most conservative EQN 4

y - peak particle velocity, ips
x - scaled range, ft
distance from shot divided by square root of shot weight for 4
distance from shot divided by cubic root of shot weight for 3

95% Non-exceedance

$y_{95\%} = 118.37\ (x^{-1.43})$ less conservative EQN 5

$y_{95\%} = 28.69\ (x^{-1.43})$ most conservative EQN 6

y - peak particle velocity, ips
x - scaled range, ft
distance from shot divided by square root of shot weight for 6
distance from shot divided by cubic root of shot weight for 5

Air overpressure predictions:

Average

$y_{50\%} = 11.28\ (x^{-1.51})$ EQN 7

y - peak air overpressure, psi
x - scaled range, ft
distance from shot divided by cubic root of shot weight

95% Non-exceedance

$y_{95\%} = 65.74\ (x^{-1.51})$ EQN 8

y - peak particle velocity, ips
x - scaled range, ft
distance from shot divided by cubic root of shot weight

For the ground motion equations, the reference to being more or less conservative refers to how large a motion the equation predicts (larger motions in this case are more conservative). Equations based on a square scaled range will predict larger ground motions than equations based on a cubic scaled range. In all cases, equations 6 and 8 should be used to predict ground motions and air overpressures respectively. These equations will give the most conservative predictions, and have 95% confidence that the predictions will not exceed the limiting criteria. Equation 6 for ground motion

predictions is also shown in Figure 21. This Figure is an isodiametric plot with concentric circles representing distances from the explosive source and 95% non exceedance predicted PPV's. The PPV's were determined from equation 6 by holding the shot weight constant in all cases. This value was set at 500 lbs since this is the maximum charge weight permitted per blasting pit, and would therefore constitute a worse case condition. However, the values for PPV's reported on this Figure will change if a different shot weight is selected for the corresponding distances. Equation 6 should be consulted for the proper PPV associated with any given distance and shot weight.

Blast Safety Criteria and Analysis

The next phase in the analysis is to compare the velocities and air overpressures obtained at the site to the safe limiting criteria established. The first criteria checked was established for structures located between 300 and 5000 ft from a blast by the U. S. Department of Interior Office of Surface Mines Reclamation and Enforcement 30 CFR Part 715, effective April 7, 1992 (see Figures 22 and 23). These criteria allow for peak particle velocities of 1.0 ips (allowable vibration limits) and peak air overpressures of 0.015 psi (allowable air blast limit). These criteria are based on open coal mine blasting which utilizes very large shots and many delays. From Figure 24, it is clear that most of the energy of a coal mine blast is in the low frequency range of 5 - 25 Hz. Quarry blasting is in the range of 10 - 35 Hz, and construction blasting in the range of 15 - 60 Hz. The safe limiting criteria are based on surface coal mine blasting because the lower frequency motions produce much more structural damage than do the higher frequency motions. The blasting that occurs at the NSWC is very similar to quarry or construction blasting which utilizes smaller shots and produces more high frequency motions. Therefore, the predictions of safety based on coal mine blasting criteria would be even more safe for quarry or construction type blasting. All of the data recorded at the site, are well below these criteria.

A second method to establish safe limiting criteria has been developed by the Department of the Interior, Office of Surface Mining (OSM) Reclamation and Enforcement. These rules and regulations are established in 30 CFR Parts 715, 780, 816, and 817. The new alternative blasting criteria is based on the particle velocity in ips versus the frequency in Hz as shown in Figure 25. Once the time history from a ground vibration monitoring station has been recorded, the spectral content can be found by calculating power spectral densities (PSD) from which peak frequencies can be determined. These peak frequencies are used in Figure 25 to determine safe particle velocities. For frequencies up to 4 Hz, a constant maximum displacement amplitude of 0.30 inch will be allowed. Over this frequency range the maximum allowable particle velocity increases from 0.19 ips to 0.75 ips. At frequencies of 4 through 11 Hz a constant allowable particle velocity of 0.75 ips is set. The fundamental modes of most one story residential buildings lie in this range. Over the frequency range of 11 through 30 Hz, a constant amplitude of 0.0107 inch is allowed. This correlates to maximum particle velocities of 0.75 ips to 2.0 ips. Above 30 Hz, a constant peak particle velocity of 2.0 ips

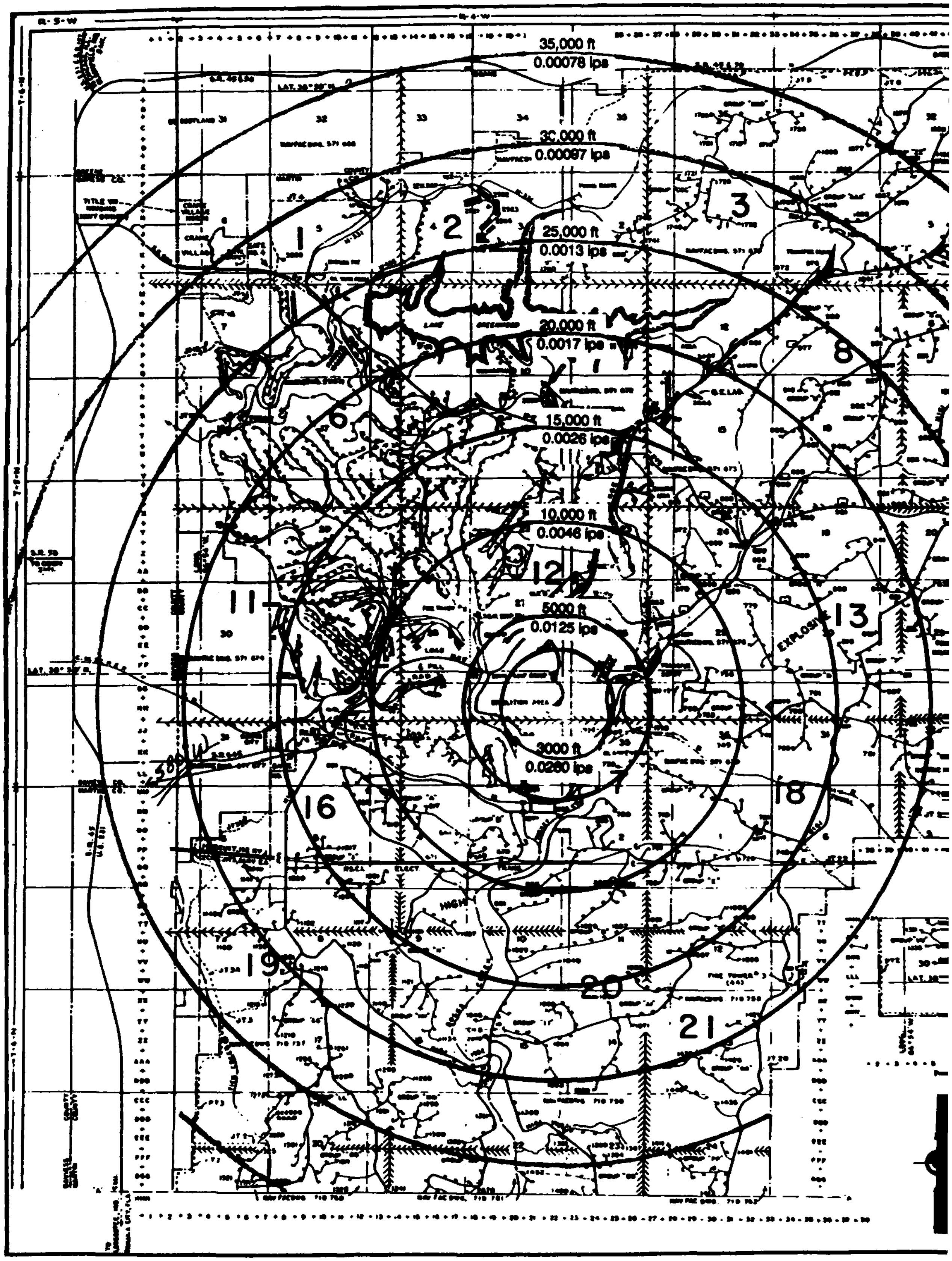

Figure 21. Isodiametric plot of PPV's
distances and a constant s

1

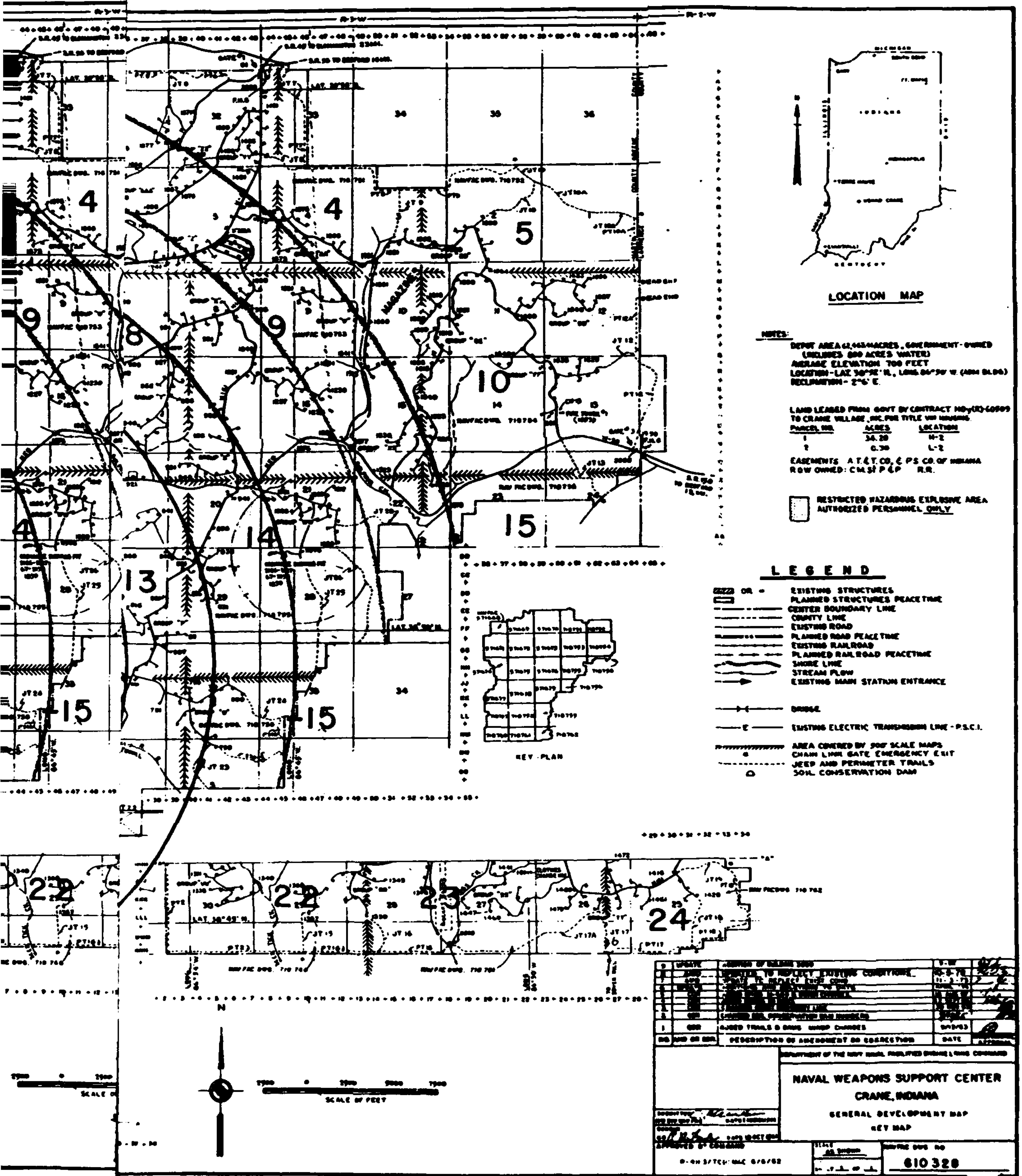

om equation … weight of

of PPV's from equation based on selected constant shot weight of 500 lbs

2

DAMAGE LEVELS FROM GROUND VIBRATIONS

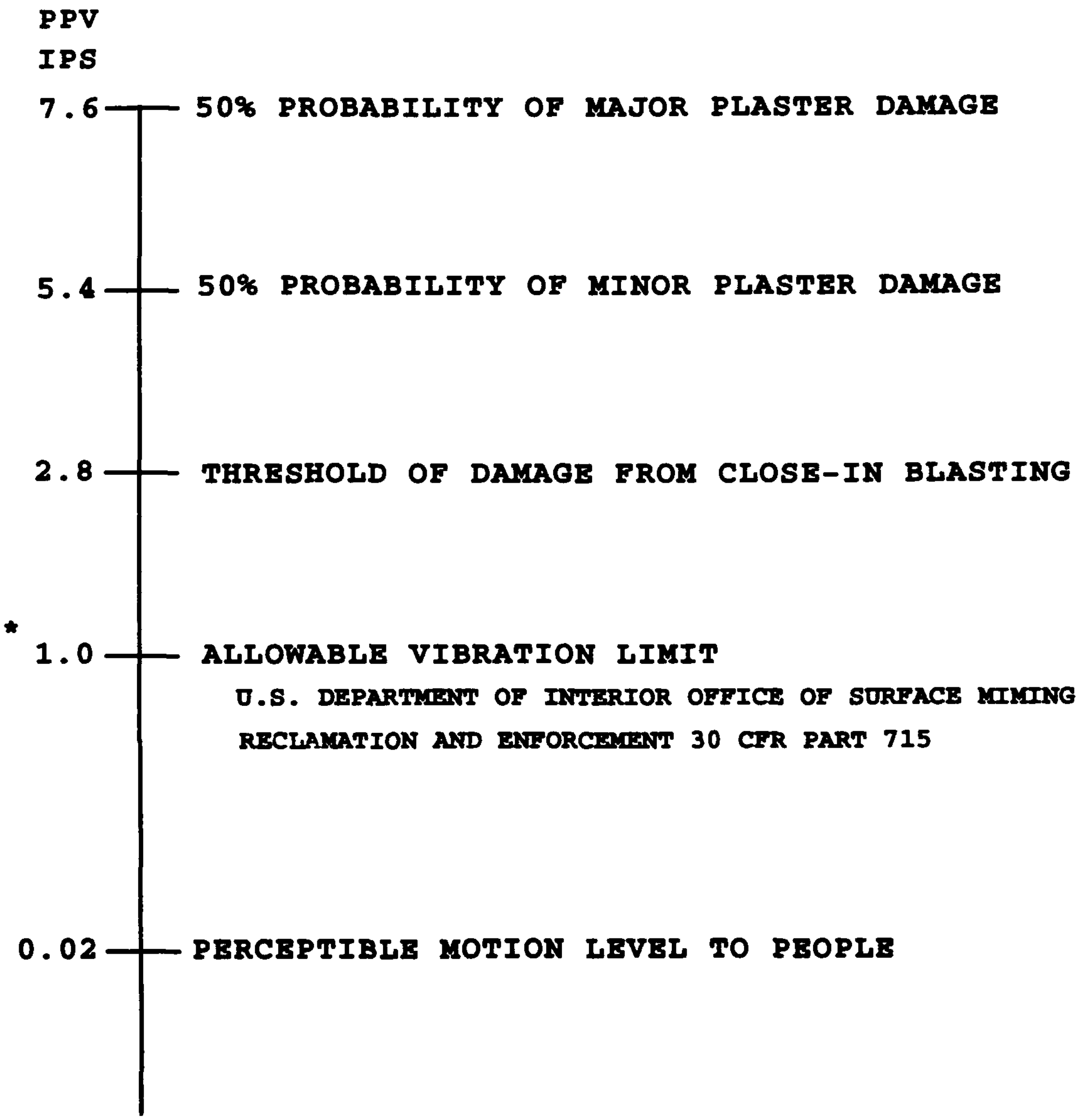

CHART FROM DUPONT BLASTER'S HANDBOOK, 16TH ED., 1977
* FEDERAL REGISTER VOL 48 NO. 46 MARCH 8, 1983

Figure 22. Chart of various damage levels produced from ground vibrations

AIR BLAST EFFECTS

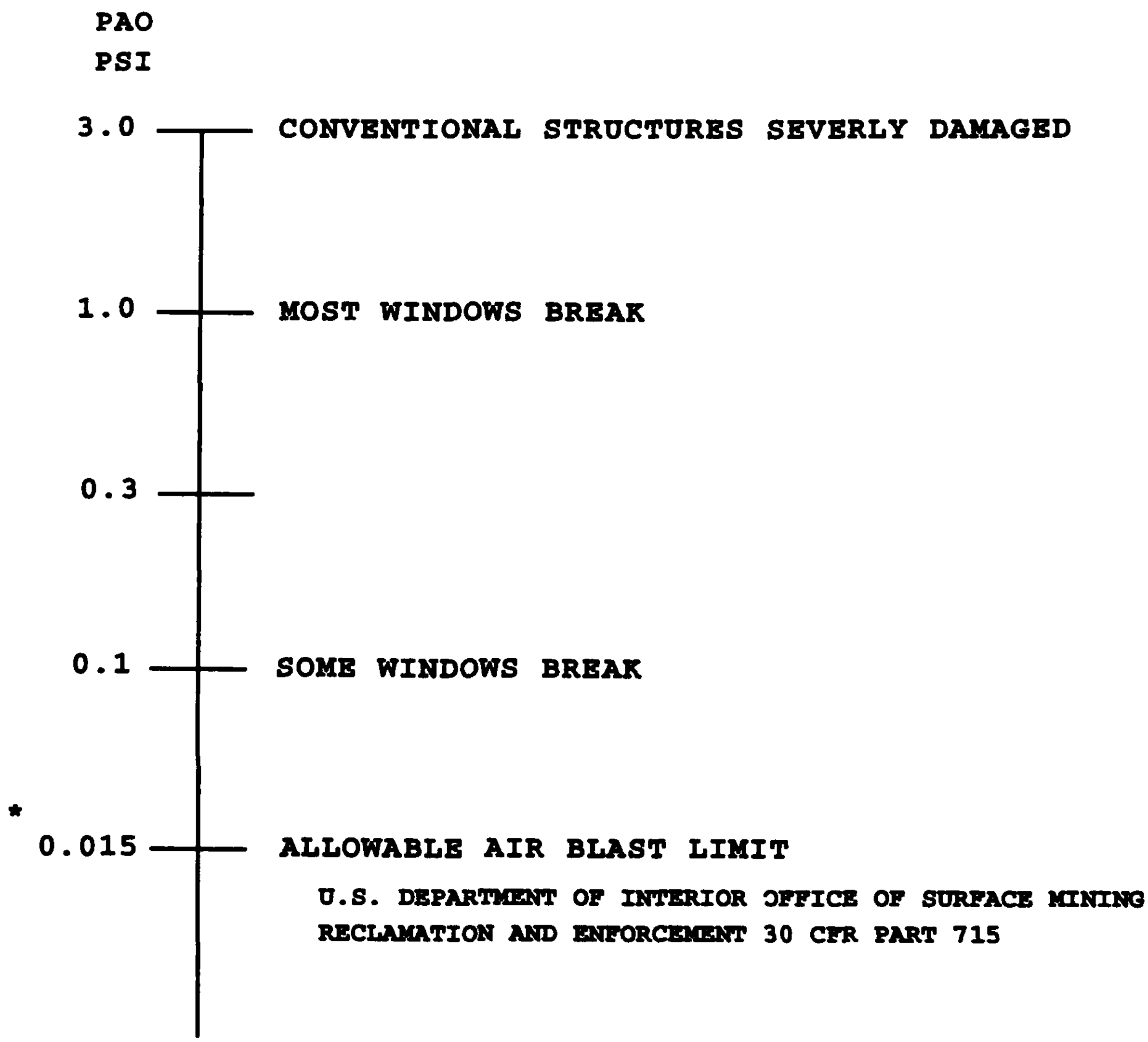

CHART FROM DUPONT BLASTER'S HANDBOOK, 16TH ED., 1977
* FEDERAL REGISTER VOL 48 NO. 46 MARCH 8, 1983

Figure 23. Chart of various damage levels produced from air blast

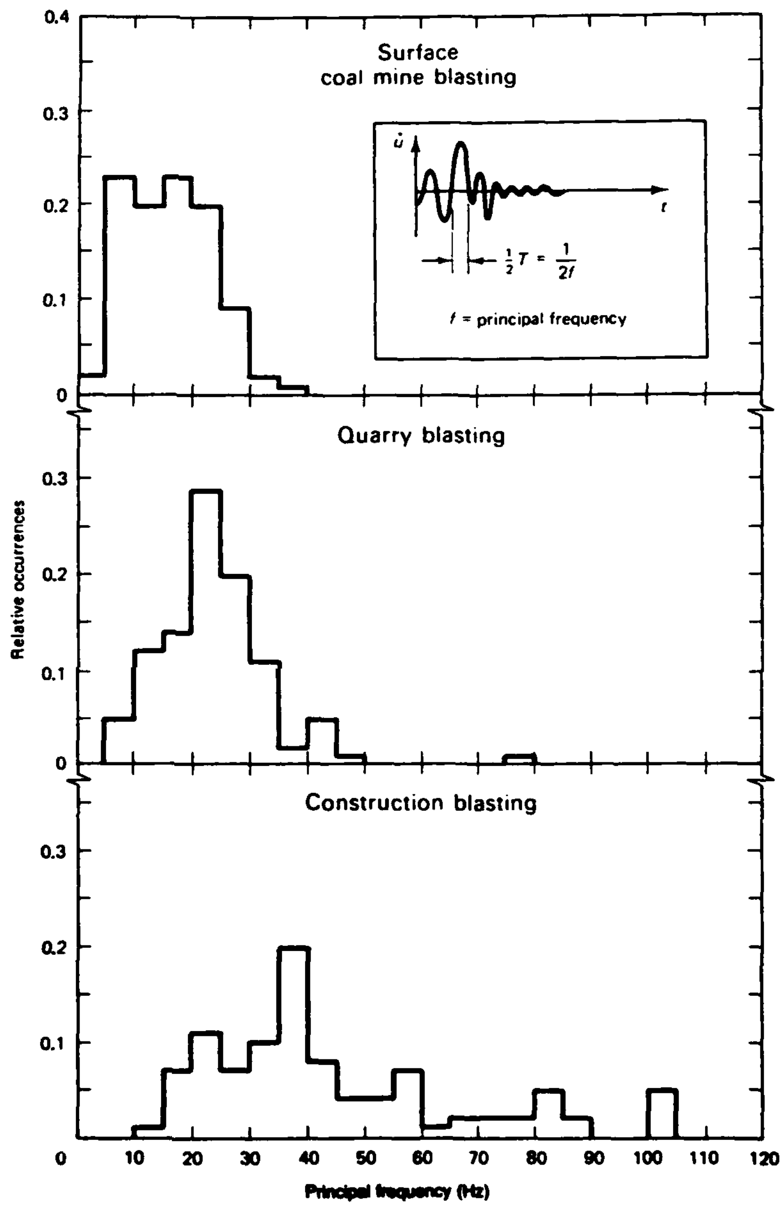

Figure 24. Predominant frequency histograms at structures of concern (Dowding, 1985)

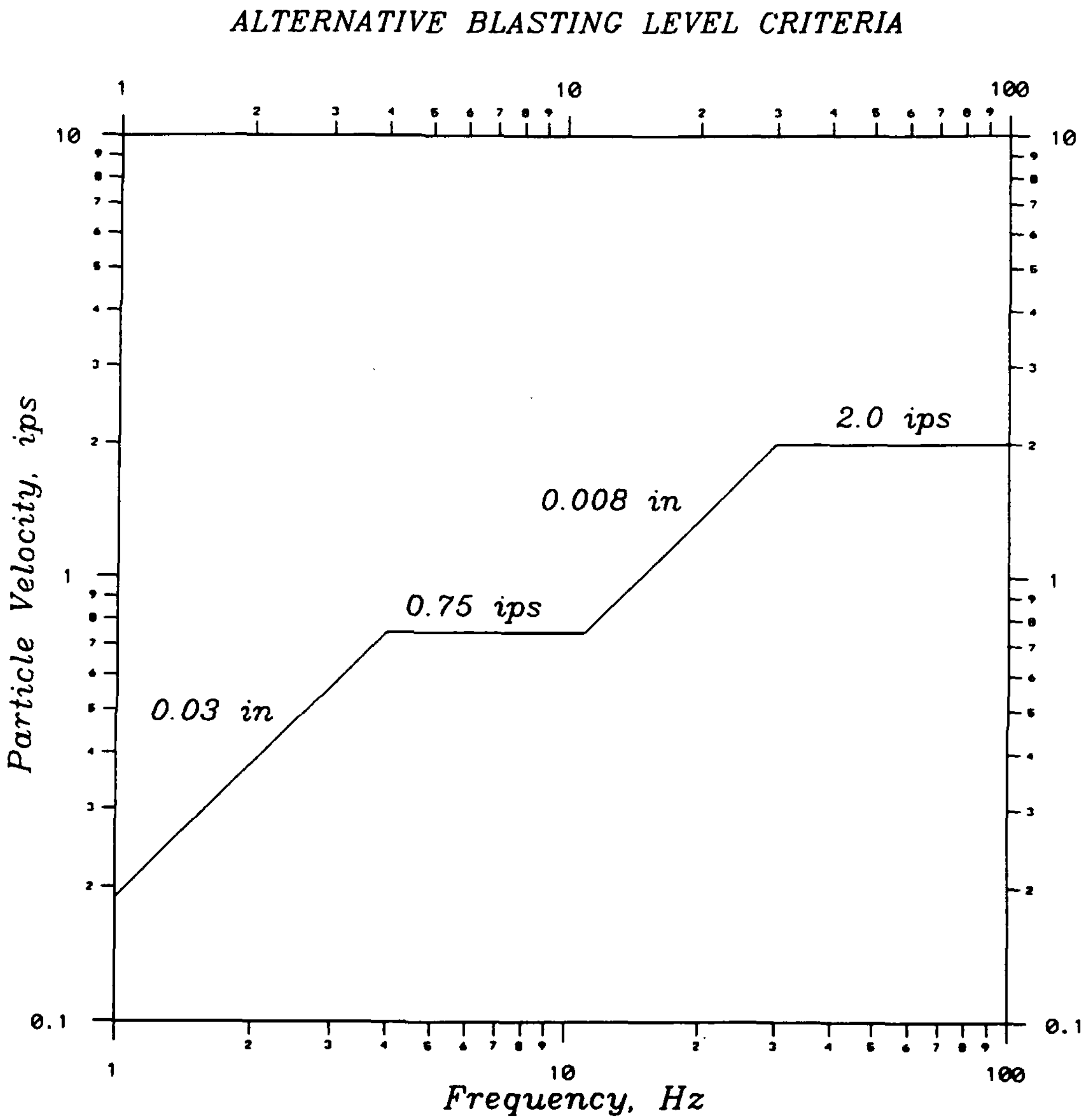

Figure 25. Determination of allowable ground vibration limits using the alternative blasting criteria (source: USBM RI-8507)

will be allowed. The OSM has established the following peak particle velocities to prevent the occurrence of threshold damage and has set such as a standard; 1.25 ips for 0-300 ft from source, 1.0 ips for distances of 301 to 5,000 ft from the source, and 0.75 ips for 5,001 ft and beyond from the source.

The data collected at the NSWC was analyzed to produce PSD's from which the peak frequency associated with the various blasts could be determined. A selected sample of the PSD's are presented in Appendix D. These types of plots are normally presented as a function of the velocity squared divided by the frequency versus the frequency. From the plots, the peak frequency ranges from 10 to 40 Hz, with the predominant frequency being approximately 20 Hz (more like quarry or construction blasting). Comparing this value with the data on Figure 25, reveals that the motions are well below the safe limiting criteria. Ground motions having a frequency content of 20 Hz could produce peak particle velocities of 1.3 ips and still be considered safe.

5 Conclusion

An investigation to determine the attenuation of explosion induced ground motions and air overpressures as a function of distance from subsurface detonated charges, and to develop parameters to predict motions at distances beyond the base boundary was successfully completed. A total of 255 shots were monitored producing 3048 time histories of ground motions recorded in the vertical, radial, and transverse directions, in addition to recording air overpressures. The data were analyzed for peak particle velocities and peak air overpressures, then plotted versus scaled range. A best fit line was put through the data to give average and 95% non-exceedance predictive equations for the site and locations off-site. As a result of the analysis, the following equations are recommended for use in predicting ground motions and air overpressures.

Ground motion predictions

$y_{95\%} = 28.69\ (x^{-1.43})$ EQN 6

y - peak particle velocity, ips
x - scaled range, ft
distance from shot divided by square root of shot weight

Air overpressure predictions

$y_{95\%} = 65.74\ (x^{-1.51})$ EQN 8

y - peak air overpressure, psi
x - scaled range, ft
distance from shot divided by cubic root of shot weight

In addition to the analysis as described above, the data were also compared to the alternative blasting source criteria utilizing the frequency content of the motions. This analysis also revealed that the ground motions recorded at the site are well below the safe limiting criteria.

References

Benjamin J. R. and Cornell C. A. (1970). *Probability, Statistics, and Decision for Civil Engineers*. McGraw-Hill, New York.

Curro, J. R., Hadala, P. F., and Landers, G. B. (1978). "Seismic Attenuation Tests At The Portsmouth, Ohio, Gaseous Diffusion Add-On Site", Miscellaneous Paper S-78-4, U.S. Army Engineer Waterways Experiment Station, Vicksburg, Ms.

Dowding C. H. (1985). *Blast Vibration Monitoring and Control*. William J. Hall, ed., Prentice-Hall, New Jersey.

Dupont (1977). *Blasters' Handbook*. 16th ed., Dupont, Delaware.

Federal Register 30 CFR Parts 715, 780, 816, and 817. (1992). "Surface Coal Mining and Reclamation Operations; Initial and Permanent Regulatory Programs; Use of Explosives", Department of the Interior, Washington, DC.

Geological Survey. (1992). "Subsurface Sedimentology of the Pennsylvanian (Mansfield) Rocks; Naval Surface Warfare Center Crane, Indiana; Rockeye, Dye Burial Ground and Demolition Area Sites", State of Indiana Department of Natural Resources, Bloomington, Indiana.

Klein, G. deV., and Hsui, A. T. (1987). "Origin of Cratonic Basins", *Geology*, v. 15, p. 1094-1098.

Miller I. and Freund J. E. (1985). *Probability and Statistics for Engineers*. 3rd ed., Prentice-Hall, New Jersey.

Schloss, L. L. (1963). "Sequences in the Cratonic Interior of North America", *Geological Society of America Bulletin*, v. 74, p. 93-114.

Vibration Measurement Engineers, Inc. (1971). "Naval Ammunition Depot Crane, Indiana", Evanston, Illinois.

Wanless, H. (1975). "Paleotectonic Investigations of the Pennsylvanian Systems in the Eastern United States", *U.S. Geological Survey*, paper 853-E, p. 71-95.

Yule, D. E., Sydow, N. J., and Pickens, J. L. (1989). "Blast Effects Monitoring Study at Hazardous Waste Site Cleanup Meddybemps, Maine", Miscellaneous Paper GL-89-29, U.S. Army Engineer Waterways Experiment Station, Vicksburg, Ms.

Appendix A: Table of Distances, Peak Particle Velocities, and Air Overpressures for Each Days Blasting

	A	B	C	D	E	F	G	H
1	Naval Surface Warfare Center (NSWC)							
2	Crane Army Ammunition Activity (CAAA)							
3	Ground Motion and Air Overpressure Study							
4								
5								
6			Scaled Range	Scaled Range	Ground Motion	Ground Motion	Ground Motion	Air Overpressu
7			R/W^.5	R/W^.333	Vertical	Radial	Transverse	psi
8			ft	ft	ips	ips	ips	
9	28 August N40E							
10	500 ft station	row 1	24	66	0.0343	0.034	0.0225	0.0194
11			26	73	0.0355	0.0276	0.0204	0.0197
12			29	81	0.0377	0.0332	0.0223	0.0151
13			35	95	0.0344	0.0344	0.0232	0.0073
14			38	103	0.0322	0.0344	0.0226	0.0085
15			42	112	0.0322	0.0337	0.0225	0.014
16			45	122	0.0328	0.01619	0.006967	0.009927
17			49	131	0.03355	0.0362	0.02296	0.009677
18			52	140	0.0333	0.02049	0.00877	0.00739
19			56	150	0.03353	0.02388	0.02247	0.007649
20			70	189	0.03344	0.03343	0.02241	0.003328
21			74	197	0.03331	0.03398	0.02155	0.006392
22			77	206	0.02084	0.0233	0.01983	0.01902
23			80	215	0.03347	0.03348	0.02249	0.000867
24			83	224	0.0234	0.01964	0.01729	0.01906
25		row 2	31	86	0.0335	0.0376	0.0236	0.0149
26			33	91	0.0341	0.0349	0.0246	0.003
27			36	100	0.0336	0.0365	0.023	0.0181
28			38	106	0.0339	0.0351	0.023	0.0125

	A	B	C	D	E	F	G	H
29			40	111	0.0334	0.0356	0.0233	0.0107
30			42	116	0.03327	0.03368	0.02212	0.01154
31			44	122	0.03351	0.03563	0.02238	0.01122
32			50	135	0.03309	0.02535	0.01053	0.0102
33			52	141	0.03313	0.02333	0.022	0.007
34			66	177	0.03318	0.03126	0.02257	0.01493
35			69	186	0.03335	0.02613	0.02015	0.005683
36			72	194	0.02972	0.03352	0.02182	0.006808
37			76	203	0.003519	0.002285	0.002757	
38		row 3	39	105	0.0336	0.0319	0.0168	0.0143
39			41	109	0.0338	0.0378	0.0239	0.0171
40			42	114	0.0168	0.0334	0.0227	
41			44	119	0.0365	0.0358	0.0234	0.0143
42			46	124	0.0333	0.0204	0.0204	0.0187
43			48	129	0.0332	0.0121	0.0046	0.0044
44			50	134	0.03675	0.03938	0.02326	0.0086
45			52	140	0.03388	0.03556	0.02304	0.00476
46			54	145	0.0332	0.02886	0.01292	0.01799
47			56	151	0.03325	0.01047	0.01121	0.01177
48	5800 ft station	row 1	275	761	0.00088	0.0014	0.00059	0.00042
49			278	768	0.0017	0.0012	0.00098	0.00043
50			280	776	0.0025	0.0042	0.0041	0.00028
51			310	832	0.00099	0.0021	0.0019	0.00028
52			313	840	0.0025	0.0045	0.0037	0.00048
53			316	848	0.0018	0.0018	0.00069	0.00039
54			319	856	0.0023	0.0016	0.0012	0.00039
55			322	864	0.0025	0.0018	0.0015	0.00023
56			325	872	0.0024	0.0024	0.0017	0.0008
57			328	880	0.0017	0.00098	0.0006	

	A	B	C	D	E	F	G	H
58			340	913	0.005	0.0026	0.0014	0.00046
59			343	920	0.0021	0.00083	0.00056	0.0156
60			346	928	0.0029	0.00069	0.00054	
61			348	935	0.0029	0.0036	0.0015	0.0011
62			351	943	0.0016	0.0024	0.001	
63		row 2	283	782	0.0042	0.0036	0.0015	
64			285	787	0.00056	0.001	0.00048	0.00043
65			286	791	0.0033	0.0036	0.0036	0.00031
66			288	796	0.0012	0.0017	0.0017	0.00039
67			290	800	0.0014	0.0039	0.0033	0.00028
68			291	805	0.0021	0.001	0.00099	0.00033
69			293	809	0.001	0.0011	0.001	0.00023
70			295	814	0.0015	0.0015	0.0012	0.00033
71			323	867	0.0035	0.0027	0.0019	0.00048
72			325	872	0.0039	0.0051	0.002	0.001
73			336	903	0.0009	0.0015	0.001	
74			339	909	0.006	0.0026	0.0015	0.00088
75			341	916	0.0054	0.005	0.0036	0.00097
76			344	923	0.0027	0.0032	0.0027	
77		row 3	313	840	0.0022	0.0014	0.00084	0.00018
78			314	844	0.0018	0.0025	0.0023	0.00024
79			316	848	0.0019	0.0017	0.0015	0.00021
80			318	853	0.0019	0.0012	0.00094	0.00025
81			319	857	0.0025	0.004	0.0035	0.00053
82			321	861	0.0014	0.0015	0.0014	0.00034
83			323	866	0.0016	0.00079	0.00067	0.00031
84			324	870	0.0023	0.0016	0.0012	
85			326	875	0.0059	0.0023	0.0013	0.00045
86			328	879	0.002	0.0016	0.0013	0.00075

	A	B	C	D	E	F	G	H
87	10000 ft statio	row 1	474	1312	0.0039	0.0066	0.0015	0.0028
88			477	1320	0.0071	0.0077	0.0023	0.0017
89			479	1327	0.0015	0.0036	0.0008	0.0049
90			528	1419	0.0054	0.0038	0.0015	0.003
91			531	1426	0.0016	0.0031	0.00082	0.0023
92			534	1434	0.0024	0.0027	0.0013	0.0025
93			537	1442	0.0026	0.004	0.0016	0.0035
94			540	1450	0.0027	0.0038	0.0016	0.0056
95			543	1457	0.0041	0.0057	0.0019	0.0074
96			546	1465	0.0035	0.0042	0.0012	0.0038
97			558	1497	0.0019	0.0013	0.00075	0.0047
98			560	1505	0.0034	0.0029	0.0015	
99			563	1512	0.0031	0.0017	0.0012	0.0018
100			566	1519	0.0016	0.0019	0.0012	0.0049
101			569	1527	0.0036	0.0031	0.0012	0.0028
102			571	1534	0.0024	0.0025	0.0012	0.005
103			574	1541	0.0039	0.0042	0.002	
104			577	1549	0.0041	0.003	0.0014	
105			580	1556	0.0039	0.003	0.0015	0.0224
106			582	1563	0.0039	0.0036	0.0013	0.0046
107		row 2	483	1335	0.0027	0.0025	0.0014	
108			485	1340	0.0075	0.0058	0.0039	0.0017
109			486	1344	0.0024	0.0027	0.001	0.0041
110			488	1349	0.0052	0.0048	0.0018	0.0014
111			490	1353	0.0044	0.0029	0.0013	0.0039
112			491	1358	0.0016	0.0014	0.0008	0.0029
113			493	1362	0.0014	0.0018	0.0006	0.0015
114			495	1367	0.0019	0.0016	0.0013	0.0031
115			541	1453	0.0057	0.0034	0.0018	0.0021

	A	B	C	D	E	F	G	H
116			543	1458	0.00072	0.00053	0.00079	
117			554	1488	0.0042	0.0039	0.0015	0.0052
118			557	1494	0.0013	0.0014	0.00054	0.0022
119			559	1501	0.0031	0.0025	0.00065	
120			562	1508	0.001	0.0029	0.00046	0.0028
121			564	1515	0.0021	0.0025	0.00067	0.0044
122		row 3	531	1425	0.0023	0.0031	0.0006	0.0024
123			533	1430	0.0042	0.0047	0.0018	0.0033
124			534	1434	0.0017	0.0044	0.0012	0.0017
125			536	1438	0.0034	0.0033	0.00094	0.0037
126			537	1443	0.0031	0.0025	0.00054	0.0038
127			539	1447	0.0018	0.002	0.00067	0.0027
128			541	1452	0.0021	0.0018	0.0006	0.0093
129			542	1456	0.002	0.0027	0.0008	0.0028
130			544	1460	0.0022	0.0018	0.0011	0.0079
131			546	1465	0.0057	0.0034	0.0018	0.0095
132								
133	29 August N40E							
134	500 ft station	row 1	24	66	0.0323	0.0248	0.0233	0.0521
135			27	73	0.0317	0.0251	0.0232	0.0213
136			29	81	0.0311	0.0235	0.0221	0.0309
137			32	89	0.0233	0.0238	0.0219	0.0072
138			35	98	0.0296	0.0234	0.0216	0.026
139			38	106	0.0296	0.023	0.0196	0.0263
140			42	115	0.0203	0.0094	0.0096	0.0185
141			45	123	0.02	0.013	0.008	0.0158
142			48	132	0.0171	0.0084	0.008	0.0384
143			56	150	0.0104	0.0064	0.0039	0.013
144			70	189	0.013	0.0112	0.0055	0.0091

	A	B	C	D	E	F	G	H
145			67	186	0.013	0.006	0.0049	0.0112
146			70	195	0.015	0.007	0.005	0.0185
147			80	215	0.0223	0.0178	0.0095	0.0109
148			83	224	0.0118	0.009	0.0041	0.0015
149			87	233	0.0166	0.0087	0.006	0.0067
150			90	242	0.011	0.0048	0.0053	0.0046
151			93	251	0.0084	0.0038	0.0028	0.0125
152			107	278	0.0052	0.0051	0.0025	0.009
153			100	269	0.0089	0.0044	0.0041	0.0079
154		row 2	30	85	0.0297	0.0237	0.0218	0.0249
155			36	96	0.0223	0.0122	0.0123	0.0223
156			38	101	0.0204	0.0162	0.0127	0.017
157			40	106	0.0194	0.0096	0.0105	0.01
158			42	112	0.0137	0.0077	0.0058	0.0172
159			40	111	0.0295	0.0191	0.0105	0.0146
160			42	116	0.0145	0.0088	0.0089	0.0085
161			48	129	0.0176	0.0113	0.0063	0.0117
162			50	135	0.0131	0.01	0.005	0.0111
163			48	133	0.0132	0.0049	0.0039	0.0107
164			66	177	0.016	0.0094	0.0067	0.0153
165			69	186	0.0174	0.015	0.0082	0.0189
166			72	194	0.01	0.005	0.003	0.0114
167			76	203	0.013	0.01	0.008	0.0134
168			79	212	0.0181	0.0221	0.0085	0.0079
169		row 3	39	105	0.03	0.024	0.022	0.0183
170			41	109	0.0298	0.0234	0.0219	0.0292
171			42	114	0.021	0.024	0.022	0.0041
172			44	119	0.022	0.009	0.016	0.0152
173			46	124	0.0157	0.01	0.0106	0.0516

	A	B	C	D	E	F	G	H
174			48	129	0.0295	0.0214	0.0145	0.0364
175			50	134	0.0301	0.0228	0.0209	0.0263
176			52	140	0.02	0.009	0.007	0.021
177			54	145	0.0108	0.0068	0.0046	0.0218
178			56	151	0.0106	0.0048	0.0042	0.0121
179	1000 ft statio	row 1	48	132	0.0311	0.0337	0.0231	0.0024
180			50	139	0.0233	0.0333	0.0202	0.0023
181			53	147	0.0315	0.0337	0.0236	0.0014
182			56	154	0.0186	0.0234	0.0117	0.0033
183			59	162	0.0313	0.0284	0.0232	0.0029
184			62	170	0.0316	0.0339	0.0234	0.0024
185			65	178	0.0305	0.0313	0.0162	0.0016
186			68	187	0.0268	0.0301	0.0188	0.00087
187			71	195	0.0242	0.0201	0.0156	0.0036
188			80	216	0.0118	0.0149	0.0071	0.0008
189			94	253	0.0213	0.0221	0.0151	0.0011
190			89	247	0.0169	0.0191	0.005	0.00026
191			92	255	0.0176	0.0141	0.0115	0.002
192			104	279	0.0309	0.0243	0.0238	0.00037
193			107	287	0.0175	0.0234	0.0173	0.001
194			110	296	0.021	0.0228	0.0079	0.00093
195			113	305	0.0149	0.014	0.0092	0.00088
196			117	313	0.0111	0.0182	0.0028	0.00087
197			133	345	0.0085	0.0128	0.0035	0.00081
198			123	331	0.0107	0.0101	0.0068	0.00089
199		row 2	53	149	0.0312	0.0337	0.0229	0.002
200			61	165	0.031	0.0334	0.0229	0.0013
201			63	170	0.0246	0.0335	0.0148	0.0011
202			65	175	0.0236	0.0335	0.0192	0.00067

	A	B	C	D	E	F	G	H
203			67	180	0.0316	0.0335	0.0239	0.0013
204			63	175	0.0316	0.0289	0.0239	
205			65	180	0.0162	0.0179	0.0185	0.00065
206			73	196	0.0224	0.0279	0.0104	0.00079
207			75	201	0.016	0.0175	0.0047	0.00087
208			71	195	0.0192	0.0179	0.0077	0.0008
209			90	242	0.0297	0.0336	0.0158	0.0015
210			93	250	0.0256	0.0254	0.0235	0.0016
211			96	258	0.0127	0.0104	0.0039	0.0011
212			99	266	0.0156	0.0163	0.0075	0.0014
213			102	275	0.0281	0.0296	0.024	0.0009
214		row 3	64	172	0.0312	0.0337	0.0231	0.001
215			66	177	0.023	0.0334	0.0093	0.0012
216			68	181	0.0168	0.033	0.023	0.0004
217			69	186	0.0212	0.0339	0.0101	0.00076
218			71	191	0.0137	0.0219	0.0064	0.0011
219			73	196	0.031	0.0337	0.0236	0.001
220			75	201	0.0315	0.0341	0.0239	0.0016
221			77	206	0.0186	0.0188	0.0197	0.0017
222			79	211	0.0152	0.0129	0.0071	0.0017
223			81	216	0.0155	0.0159	0.0084	0.00092
224	5800 ft station	row 1	277	764	0.0011	0.0022	0.0014	0.00024
225			279	771	0.0012	0.0022	0.0018	0.0003
226			282	779	0.0007	0.0012	0.001	0.0006
227			284	786	0.0011	0.0021	0.001	0.0004
228			287	793	0.0019	0.0034	0.0018	0.00053
229			290	801	0.0009	0.0028	0.0017	0.00049
230			292	808	0.00065	0.001	0.00086	0.00047
231			295	815	0.0014	0.002	0.0015	0.00073

	A	B	C	D	E	F	G	H
232			298	823	0.00058	0.0011	0.00062	0.00031
233			328	880	0.0012	0.0023	0.0012	0.00029
234			340	913	0.0011	0.0007	0.001	0.00046
235			314	869	0.00072	0.0014	0.00084	0.00035
236			317	876	0.002	0.0031	0.0019	0.00045
237			348	935	0.0023	0.0043	0.0023	0.00017
238		row 2	277	771	0.0009	0.001	0.0006	0.00046
239			310	833	0.0009	0.0024	0.0014	0.0001
240			312	838	0.0011	0.002	0.0011	
241			314	843	0.0014	0.0029	0.0015	0.00035
242			316	848	0.0018	0.0026	0.0018	0.0007
243			291	805	0.001	0.0026	0.0013	0.0005
244			293	809	0.00084	0.0025	0.0014	0.00025
245			321	862	0.0005	0.00045	0.00053	
246			323	867	0.00053	0.0011	0.0008	0.0002
247			298	823	0.001	0.0022	0.0016	0.00054
248			336	903	0.0019	0.0031	0.0018	0.00036
249			339	909	0.0007	0.0015	0.00093	0.00021
250			341	916	0.0001	0.00073	0.0015	0.00055
251		row 3	313	840	0.0016	0.0027	0.0017	0.00031
252			314	844	0.0005		0.0004	
253			316	848	0.00086	0.0012	0.0009	0.0002
254			318	853	0.0007	0.0012	0.0008	0.0003
255			319	857	0.0019	0.004	0.0024	0.00025
256			321	861	0.0011	0.0017	0.001	0.00016
257			323	866	0.0008	0.0016	0.00081	0.00022
258			324	870	0.00054	0.00099	0.0006	0.0002
259			326	875	0.00064	0.0014	0.00096	
260			328	879	0.001	0.0022	0.0016	0.00014

	A	B	C	D	E	F	G	H
261								
262	31 August N40E							
263	500 ft station	row 1	26	70	0.0547	0.0402	0.0381	0.0346
264			29	78	0.0544	0.0408	0.0385	0.0244
265			32	86	0.0582	0.0464	0.0288	0.0124
266			35	95	0.0545	0.0348	0.0383	0.02318
267			38	103	0.0545	0.0394	0.0382	0.0258
268			42	112	0.0545	0.0273	0.0377	0.0264
269			45	122	0.0545	0.0208	0.022	0.0269
270			49	131	0.0432	0.0262	0.0212	0.0189
271			52	140	0.0554	0.0314	0.0297	0.0298
272			56	150	0.0442	0.0127	0.0224	0.0115
273			70	189	0.0431	0.0098	0.00909	0.0249
274			74	197	0.0408	0.0118	0.0143	0.0161
275			77	206	0.0203	0.0117	0.0127	0.0322
276			80	215	0.0507	0.028	0.0194	0.014
277			83	224	0.035	0.012	0.0176	0.0222
278			87	233	0.0165	0.0118	0.0142	0.0145
279			90	242	0.02	0.0146	0.0149	0.012
280			93	251	0.0164	0.0082	0.0119	0.009
281			97	260	0.01107	0.00595	0.00834	0.01417
282			100	269	0.0156	0.00606	0.00786	0.01906
283		row 2	66	177	0.0455	0.0104	0.0133	0.01106
284			69	186	0.0232	0.0103	0.0109	0.00939
285			72	194	0.0249	0.0186	0.0179	0.0171
286			76	203	0.0277	0.0179	0.0176	0.0147
287			79	212	0.0297	0.0233	0.0178	0.0233
288		row 3	69	186	0.0544	0.0104	0.0132	0.0262
289			73	195	0.0296	0.0139	0.0155	0.0114

	A	B	C	D	E	F	G	H
290			76	203	0.035	0.0185	0.017	0.0154
291			79	211	0.0334	0.0167	0.0178	0.0238
292			82	220	0.0434	0.0237	0.0186	0.0139
293								
294	750 ft station	row 1	39	105				
295			42	112	0.0229	0.0225	0.023	0.0049
296			45	121	0.0227	0.0241	0.0231	0.0036
297			48	129	0.0229	0.0224	0.023	0.0033
298			51	137	0.0228	0.024	0.026	0.0047
299			54	146	0.0228	0.025	0.024	0.0031
300			58	155	0.0226	0.0176	0.0169	0.0034
301			61	164	0.0146	0.0071	0.0076	0.0042
302			64	173	0.0229	0.0224	0.0221	0.00405
303			68	182	0.0181	0.0112	0.0072	0.00245
304			82	220	0.0078	0.0042	0.0052	0.00317
305			85	229	0.0069	0.0044	0.0101	0.0026
306			89	238	0.0071	0.00367	0.0054	0.0041
307			92	246	0.0151	0.0095	0.0129	0.0022
308			95	255	0.0125	0.0088	0.0056	0.0036
309			98	264	0.006	0.0023	0.0035	0.0032
310			102	273	0.0072	0.0029	0.0045	0.0033
311			105	282	0.0044	0.00235	0.0031	0.0023
312			108	290	0.0035	0.0028	0.0029	0.0037
313			111	299	0.0048	0.0024	0.0035	0.0038
314		row 2	78	209	0.0125	0.017	0.0101	0.0017
315			81	217	0.0087	0.0172	0.0048	0.0018
316			84	226	0.0122	0.0095	0.0081	0.0028
317			87	234	0.0132	0.0112	0.0137	0.0022
318			90	243	0.0154	0.0118	0.0088	0.0029

	A	B	C	D	E	F	G	H
319		row 3	81	217	0.0159	0.0064	0.00434	0.0056
320			84	225	0.0077	0.0098	0.0075	0.0018
321			87	233	0.0152	0.01169	0.0129	0.0023
322			90	242	0.0141	0.0059	0.0054	0.0032
323			93	250	0.0072	0.0045	0.0061	0.0024
324								
325	1000 ft station	row 1	55	147	0.0194	0.0347	0.0107	0.00057
326			58	155	0.0222	0.0342	0.0152	0.00049
327			61	163	0.0197	0.0225	0.0159	0.00044
328			64	172	0.0133	0.0213	0.0105	0.00063
329			67	180	0.0234	0.018	0.0128	0.00043
330			70	189	0.0145	0.0138	0.0047	0.00041
331			74	198	0.0121	0.0115	0.0043	0.00052
332			77	207	0.0189	0.0234	0.0069	0.00062
333			80	216	0.0127	0.0148	0.0033	0.00028
334			94	253	0.0117	0.0098	0.0047	0.00074
335			97	262	0.0074	0.00737	0.00515	0.00054
336			101	270	0.0086	0.0116	0.0024	0.0011
337			104	279	0.01189	0.01047	0.0066	0.00039
338			107	287	0.0085	0.0124	0.0036	0.00076
339			110	296	0.0078	0.0143	0.0021	0.00062
340			113	305	0.00613	0.00798	0.00336	0.00071
341			117	313	0.0079	0.0075	0.003	0.00051
342			120	322	0.0063	0.0053	0.002	0.00054
343			123	331	0.00903	0.0131	0.0035	0.00066
344		row 2	90	242	0.01002	0.0114	0.0064	0.00042
345			93	250	0.0073	0.0087	0.0032	0.00036
346			96	258	0.0082	0.0101	0.0058	0.00055
347			99	266	0.0091	0.0091	0.0052	0.00045

	A	B	C	D	E	F	G	H
348			102	275	0.0086	0.0107	0.0038	0.00065
349		row 3	93	249	0.0129	0.0138	0.0035	0.00078
350			96	257	0.0075	0.0103	0.0051	0.00034
351			99	265	0.0105	0.0096	0.0071	0.00048
352			102	273	0.0049	0.0081	0.0023	0.00082
353			105	281	0.02	0.0192	0.0024	0.00051
354								
355								
356	1450 ft station	row 1	75	202	0.043	0.0487	0.027	0.0012
357			78	210	0.0435	0.049	0.0434	0.0014
358			81	218	0.0433	0.043	0.037	0.0012
359			84	226	0.0435	0.0269	0.0237	0.0011
360			87	234	0.0432	0.0469	0.0239	0.0015
361			90	242	0.0431	0.0304	0.0141	0.0015
362			93	251	0.0433	0.036	0.0145	0.0014
363			97	259	0.0433	0.0478	0.0153	0.0024
364			100	268	0.043	0.0171	0.0107	0.0013
365			103	277	0.043	0.0192	0.0108	0.0021
366			117	313	0.0279	0.0384	0.0152	0.0013
367			120	321	0.0304	0.0483	0.0247	0.0011
368			123	330	0.0207	0.034	0.013	0.0022
369			126	338	0.0427	0.0475	0.0273	0.0011
370			129	346	0.0257	0.0177	0.0179	0.0022
371			132	355	0.021	0.0223	0.009	0.002
372			135	363	0.036	0.0213	0.0094	0.0014
373			138	372	0.0322	0.0103	0.0072	0.00057
374			142	380	0.0302	0.0128	0.0097	0.002
375			145	389	0.0253	0.0158	0.012	0.0021
376		row 2	112	302	0.03	0.0283	0.0125	0.002

	A	B	C	D	E	F	G	H
377			115	310	0.0225	0.0295	0.0143	0.0014
378			118	318	0.0098	0.017	0.0136	0.0031
379			121	326	0.0239	0.0478	0.0208	0.0023
380			124	334	0.0431	0.0372	0.0183	0.0018
381		row 3	115	309	0.0271	0.0382	0.0135	0.0011
382			118	316	0.021	0.0308	0.012	0.0011
383			121	324	0.0327	0.0483	0.0163	0.0014
384			123	331	0.0293	0.031	0.0138	0.001
385			126	339	0.043	0.0261	0.0162	0.0015
386								
387	5800 ft station	row 1	301.53	809.5	0.00084	0.0014	0.00086	0.00033
388			304.36	817.12	0.00059	0.0017	0.00086	0.00035
389			307.22	824.78	0.00158	0.00262	0.00131	0.00059
390			284.36	785.82	0.00065	0.001	0.00121	0.00035
391			312.98	840.25	0.00077	0.00106	0.00084	0.00059
392			350.81	909.4	0.00065	0.00145	0.000578	0.000086
393			318.81	855.9	0.00048	0.0014	0.00067	0.0005
394			321.75	863.79	0.00056	0.0026	0.0014	0.00024
395			324.7	871.72	0.00056	0.00157	0.000969	0.000103
396			327.67	879.69	0.00056	0.00146	0.00082	0.00039
397			339.95	912.64	0.00056	0.00122	0.00077	0.00019
398			342.73	920.11	0.00099	0.00185	0.00111	0.000475
399			345.52	927.6	0.00071	0.0011	0.00081	0.00031
400			319.41	882.7	0.0012	0.0021	0.0015	0.00057
401			351.13	942.68	0.00072	0.00099	0.00073	0.00015
402			353.96	950.26	0.00054	0.00109	0.00058	0.00019
403			327.18	904.16	0.00104	0.00205	0.00116	0.000213
404			359.63	965.49	0.000897	0.000813	0.00058	0.000193
405			362.48	973.14	0.000458	0.00069	0.000416	0.00021

	A	B	C	D	E	F	G	H
406			365.34	980.82	0.000585	0.000925	0.000577	0.000165
407								
408		row 2	310.37	833.23	0.00054	0.00117	0.00071	0.00023
409			312.15	838.01	0.00069	0.0015	0.00081	0.00041
410			313.94	842.81	0.00062	0.0014	0.0006	
411			315.73	847.64	0.00075	0.00185	0.00099	0.00059
412			317.54	852.5	0.00106	0.00185	0.001	0.00015
413			354.67	919.39	0.0018	0.0013	0.0023	0.00061
414			321.19	862.28	0.00047	0.00121	0.00059	0.000136
415			358.73	929.93	0.00061	0.00125	0.00086	0.00024
416			324.87	872.16	0.00055	0.0016	0.00091	0.00035
417			336.19	902.55	0.000403	0.0008	0.00068	0.00021
418			376.22	975.26	0.00056	0.0011	0.00068	0.00022
419			379.1	982.72	0.00097	0.0019	0.0013	0.00027
420			343.96	923.43	0.00076	0.00217	0.00109	0.00031
421			384.9	997.76	0.00038	0.00086	0.00048	0.00022
422								
423		row 3	314.31	843.83	0.00076	0.0018	0.00099	0.00048
424			315.94	848.18	0.001	0.0023	0.0013	0.00015
425			352.68	914.23	0.00115	0.00151	0.00064	0.000078
426			319.21	856.98	0.00094	0.0017	0.0012	0.00059
427			356.34	923.73	0.00095	0.0025	0.0012	0.00014
428			322.53	865.89	0.00101	0.00272	0.00153	0.00026
429			343.3	904.19	0.00061	0.00154	0.00059	0.000079
430			345.08	908.9	0.00068	0.0014	0.00085	0.00021
431			327.59	879.48	0.00042	0.00128	0.00057	0.00051
432								
433	1 September S40W							
434	500 ft station	row 1	26	70	0.0252	0.0449	0.0226	0.0514

	A	B	C	D	E	F	G	H
435			29	77	0.0252	0.0451	0.0225	0.0739
436			29	80	0.0252	0.0448	0.0129	0.0228
437			34	92	0.0249	0.0444	0.022	0.0249
438			34	95	0.0251	0.0448	0.0224	0.0691
439			40	109	0.0247	0.0442	0.0144	0.0175
440			44	117	0.0256	0.0502	0.0228	0.1065
441			43	118	0.0251	0.0503	0.0229	0.0326
442			50	134	0.0247	0.0441		
443			53	142	0.0211	0.0442		0.0204
444			62	171	0.0245	0.0409		0.0078
445			65	180	0.0246	0.0438		0.0175
446			68	189	0.0246	0.0437		0.0451
447			72	198	0.0242	0.0269		0.0144
448			82	220	0.0089	0.0174		0.0049
449			86	230	0.0103	0.0174		0.0063
450			89	239	0.0061	0.0054		0.006
451			85	235	0.0077	0.0052		0.0038
452			96	259	0.0059	0.0043		0.0054
453		row 2	66	177	0.0246	0.0207		0.0312
454			68	184	0.0112	0.0082		0.0354
455			65	180	0.0121	0.0333		0.0175
456			73	197	0.0246	0.0397		0.01
457			76	204	0.0065	0.0064		0.0097
458			78	210	0.006	0.0069		0.0061
459			81	217	0.006	0.0035		0.0087
460			83	224	0.0117	0.0167		0.0035
461			86	230	0.0028	0.00198		0.0054
462		row 3	38	103	0.0247	0.0447	0.0107	0.0164
463			39	107	0.0249	0.0444	0.022	0.0242

	A	B	C	D	E	F	G	H
464			45	121	0.026	0.045		
465			44	122	0.0157	0.0338		
466			52	139	0.0113	0.0441		0.0237
467			67	179	0.0248	0.0448		0.0156
468			63	175	0.0245	0.0274		0.0216
469			72	192	0.0133	0.0191		0.0178
470			68	188	0.0175	0.0405		0.0102
471			77	206	0.0161	0.0441		
472			73	200	0.0109	0.0087		0.0271
473			82	219	0.0112	0.009		0.0313
474			84	226	0.0107	0.0099		0.0158
475	2900 ft station	row 1	151	405	0.012	0.0083	0.0083	0.0012
476			153	412	0.0049	0.0033	0.0041	0.00074
477			143	395	0.0118	0.0082	0.0083	0.0014
478			159	426	0.0118	0.0082	0.0083	
479			148	409	0.0119	0.0083	0.0084	0.0014
480			164	440	0.007	0.0046	0.0077	0.0008
481			167	448	0.012	0.0085	0.0084	0.00071
482			155	430	0.0069	0.0057	0.0083	0.00033
483			172	463	0.0119	0.0053	0.0082	0.00023
484			175	470	0.0055	0.0024	0.0029	0.00048
485			172	476	0.0035	0.0017	0.0022	0.001
486			175	484	0.0037	0.0031	0.0032	0.0014
487			178	492	0.0065	0.0022	0.0035	0.001
488			181	500	0.0041	0.0013	0.0023	
489		row 2	183	492	0.0049	0.0021	0.0027	0.00035
490			185	498	0.0079	0.0018	0.0019	0.00023
491			172	476	0.0034	0.0019	0.0022	0.00052
492		row 3	152	407	0.0087	0.0039	0.0028	0.00058

	A	B	C	D	E	F	G	H
493			145	397	0.0113	0.0083	0.0083	0.00045
494			157	423	0.0045	0.0018	0.0024	0.00037
495			147	407	0.0076	0.006	0.0063	0.00024
496			163	439	0.0046	0.0032	0.0023	0.0014
497			177	475	0.0072	0.0018	0.0018	0.00057
498			164	454	0.0101	0.0034	0.0046	0.00046
499			181	487	0.0065	0.0022	0.0035	0.001
500								
501	5800 ft station	row 1	302	810	0.00447	0.00452	0.00024	0.00011
502			304	816	0.0033	0.0023	0.00039	0.00074
503			281	777	0.0094	0.008	0.00047	0.00019
504			309	831	0.0086	0.0089	0.00044	0.00037
505			286	791	0.0029	0.0027	0.0002	0.00031
506			315	845	0.0053	0.0049	0.00043	0.00062
507			317	852	0.0021	0.0022	0.00029	0.00021
508			293	811	0.0055	0.0042	0.00068	0.00021
509			323	866	0.002	0.0023	0.00024	0.00016
510			325	874	0.0049	0.0046	0.00026	0.000076
511			310	856	0.0022	0.0023	0.00019	0.00015
512			312	863	0.0022	0.0022	0.00021	0.00015
513			315	871	0.0018	0.0013	0.0003	0.0004
514			318	879	0.0035	0.0036	0.00029	0.00027
515		row 2	330	887	0.0021	0.0021	0.00037	0.00063
516			332	893	0.0016	0.0035	0.00023	
517			307	848	0.0021	0.0036	0.00022	0.00014
518			337	903	0.0011	0.0014	0.0005	0.00012
519		row 3	301	808	0.0102	0.0088	0.00063	0.00059
520			284	780	0.0063	0.0056	0.00028	0.00019
521			306	822	0.0032	0.0025	0.00047	0.00017

	A	B	C	D	E	F	G	H
522			283	782	0.0026	0.0024	0.00018	0.00015
523			311	836	0.0021	0.0024	0.000338	0.000074
524			323	868	0.0017	0.0014	0.00015	0.00025
525			298	824	0.00096	0.00094	0.00013	0.00017
526			327	879	0.0024	0.002	0.00025	0.00019
527			302	835	0.0014	0.0019	0.00015	0.00012
528								
529	10800 ft statio	row 1	561	1507	0.00049	0.0014	0.00067	0.000023
530			564	1514	0.00032	0.00093	0.00027	0.000039
531			520	1436	0.00058	0.0021	0.00072	0.000078
532			569	1528	0.00036	0.0013	0.00037	0.000047
533			524	1449	0.00033	0.00078	0.00051	0.000046
534			575	1542	0.00069	0.0017	0.00089	0.000068
535			577	1549	0.001	0.0018	0.0011	0.00012
536			532	1469	0.00037	0.00058	0.00047	0.00006
537			582	1564	0.00042	0.0011	0.00038	0.000023
538			585	1571	0.00062	0.0018	0.00081	0.000046
539			547	1513	0.00021	0.0015	0.00024	0.000056
540			550	1520	0.00065	0.0025	0.0011	0.000075
541			553	1528	0.00044	0.0011	0.0012	0.000041
542			556	1535	0.00024	0.00103	0.00024	0.000027
543			609	1635	0.00024	0.00105	0.00026	0.000033
544			612	1643	0.00035	0.00045	0.00017	0.000046
545			615	1651	0.00039	0.0011	0.00022	0.000053
546		row 2	585	1569	0.0008	0.0014	0.00084	0.000051
547			586	1573	0.00032	0.00056	0.00032	0.000033
548			539	1489	0.00043	0.00076	0.00091	0.000041
549			589	1582	0.00028	0.0013	0.00027	0.000019
550			591	1586	0.00028	0.00062	0.00021	0.00003

	A	B	C	D	E	F	G	H
551			592	1590	0.00024	0.00091	0.00019	0.000032
552			594	1594	0.00039	0.0011	0.00022	0.000053
553		row 3	560	1504	0.00064	0.0024	0.00087	0.000068
554			526	1444	0.00044	0.00077	0.00042	0.000046
555			564	1514	0.00032	0.00071	0.00041	0.000034
556			519	1434	0.00087	0.00062	0.00037	0.000091
557			568	1525	0.00051	0.0017	0.00084	0.000052
558			577	1549	0.00065	0.00097	0.00037	0.000076
559			531	1466	0.00043	0.0022	0.00049	0.000034
560			580	1557	0.00032	0.00056	0.00037	0.000036
561			533	1474	0.00032	0.00067	0.00039	0.000015
562			583	1566	0.00066	0.00062	0.00023	0.000064
563			536	1482	0.00025	0.00092	0.00016	0.000027
564			586	1574	0.00036	0.0012	0.00027	0.000053
565								
566	22000 ft statio	row 1	1144	3071	0.000205	0.000069		
567			1146	3077	0.00009	0.000099	0.000089	0.00011
568			1054	2912	0.000123	0.00014	0.00012	0.00015
569			1152	3091	0.00013	0.000058	0.000057	0.000098
570			1058	2925	0.0000808	0.0000577	0.000061	0.000104
571			1157	3105	0.00012	0.000074	0.000065	0.00026
572			1159	3112	0.00021	0.000204	0.00017	0.00015
573			1066	2945	0.000065	0.000065	0.000054	0.00013
574			1165	3126	0.0001	0.000082	0.000068	
575			1167	3134	0.00013	0.00014	0.000126	0.00019
576			1081	2988	0.000148	0.000132	0.000085	0.000114
577			1084	2995	0.000089	0.00009	0.00005	0.0001
578			1086	3002	0.000051	0.000052	0.000038	0.000097
579			1089	3010	0.000053	0.000077	0.000061	0.000052

	A	B	C	D	E	F	G	H
580			1191	3196	0.000041	0.00003		0.000069
581			1193	3204	0.000035	0.000046		0.000072
582			1196	3212	0.000045	0.000056		0.000051
583		row 2	1158	3108	0.00022	0.00023	0.00015	0.00013
584			1158	3109	0.00013	0.00015	0.0001	
585			1063	2937	0.000035	0.000039	0.000037	0.000079
586			1160	3113	0.000045	0.000048	0.000044	0.000044
587			1160	3115	0.000046	0.000028		0.000073
588			1161	3117	0.000057	0.000028		0.00011
589			1162	3119	0.000189	0.000061	0.00011	0.00026
590		row 3	1142	3066	0.00017	0.00028	0.00017	0.00018
591			1070	2937	0.000103	0.000106	0.000056	0.00013
592			1144	3071	0.000047	0.000048	0.000036	0.000082
593			1050	2901	0.000062	0.000048	0.000036	0.000082
594			1146	3076	0.000136	0.00012	0.0000954	0.00011
595			1150	3087	0.000044	0.000042	0.000031	0.00006
596			1055	2915	0.000072	0.00011	0.000075	0.000085
597			1151	3090	0.000059	0.000033	0.000041	0.000065
598			1056	2919	0.000054	0.000038		0.000081
599			1153	3094	0.000062	0.00002		0.0001
600			1058	2923	0.000097	0.000061		0.000055
601								
602	3 September S40W							
603	250 ft station	row 1	13	35	0.2994	0.5813	0.2135	0.0836
604			16	42	0.3025	0.5849	0.2174	0.077
605			19	50	0.1119	0.1692	0.0569	0.0162
606			22	58	0.1189	0.1829	0.0705	0.0082
607			25	67	0.0984	0.1472	0.0538	0.0086
608			28	76	0.0682	0.1357	0.0572	0.0148

	A	B	C	D	E	F	G	H
609			31	84	0.0661	0.1173	0.0593	0.0093
610			35	93	0.0561	0.0655	0.0342	0.0152
611			35	96	0.0651	0.0573	0.0544	0.0093
612			41	111	0.0229	0.0421	0.0125	0.0082
613			51	142	0.035	0.0608	0.0409	0.03
614			55	151	0.0182	0.0302	0.0137	0.0064
615			63	170	0.0488	0.0501	0.0475	0.0083
616			67	180	0.0152	0.015	0.0143	
617			71	190	0.0239	0.0364	0.0167	
618			74	200	0.0204	0.0393	0.0264	0.0082
619			80	213	0.0172	0.0323	0.0067	0.0229
620		row 2	27	73	0.0944	0.0947	0.0603	0.0082
621			28	77	0.0681	0.0617	0.0401	0.0231
622			34	91	0.0542	0.0882	0.025	0.1031
623			37	100	0.0245	0.0459	0.0111	0.0109
624			41	109	0.0173	0.0258	0.0115	0.0212
625			56	149	0.0198	0.0346	0.0117	0.0177
626			58	156	0.0356	0.0436	0.0244	0.0283
627			61	163	0.0159	0.0224	0.0085	
628			63	169	0.0264		0.0164	0.0239
629			60	166	0.0524	0.0285	0.0303	0.0958
630			70	186	0.0231	0.0184	0.0121	0.0259
631		row 3	60	162	0.0258	0.0217	0.0135	0.0416
632			63	168	0.0153	0.0264	0.0065	0.0084
633			65	175	0.031		0.0076	
634			68	182	0.0175	0.0196	0.0041	
635			64	178	0.0153	0.0229	0.0047	0.0082
636			73	195	0.0211		0.0124	0.0479
637	500 ft station	row 1	26	70	0.0442	0.0727	0.0296	0.0135

	A	B	C	D	E	F	G	H
638			29	77	0.0395	0.0674	0.0319	0.0141
639			31	84	0.0421	0.0403	0.0265	
640			34	92	0.0125	0.0308	0.0142	
641			37	100	0.0134	0.0265	0.0148	
642			40	109	0.0116	0.0193	0.0111	
643			44	117	0.0087	0.0163	0.0075	
644			47	125	0.03	0.0371	0.0157	0.0105
645			46	126	0.0066	0.0107	0.0048	
646			53	142	0.0161	0.0216	0.0093	0.0259
647			62	171	0.0076	0.0103	0.0064	
648			65	180	0.0092	0.0104	0.0046	
649		row 2	37	100	0.0192	0.0233	0.0077	
650			37	103	0.009	0.0221	0.0081	
651			44	118	0.0108	0.0133	0.0072	
652			47	128	0.0099	0.012	0.0093	
653			51	137	0.0072	0.0113	0.0064	
654			66	177	0.0074	0.0115	0.0054	
655			68	184	0.0129	0.0136	0.0074	
656		row 3	67	179	0.0105	0.0129	0.0054	0.0054
657	750 ft station	row 1	39	105	0.0135	0.0129	0.0118	
658			42	112	0.0128	0.0094	0.0081	
659			44	119	0.008	0.0078	0.0063	
660			47	127	0.0092	0.008	0.005	
661			50	135	0.0217	0.0173	0.0162	
662			53	142	0.006	0.0064	0.0062	
663			56	151	0.007	0.0065	0.0038	
664			59	159	0.005	0.0051	0.003	
665			57	158	0.0051	0.0064	0.0053	
666			65	175	0.0071	0.0076	0.004	

	A	B	C	D	E	F	G	H
667			73	201	0.0034	0.0042	0.0029	
668			76	210	0.0076	0.0107	0.0055	
669			86	232	0.0026	0.0034	0.0027	
670			90	242	0.0019	0.0037	0.0024	
671			94	251	0.0042	0.0063	0.0043	0.0061
672			97	261	0.0014	0.0046	0.0019	0.0055
673		row 2	49	132	0.0042	0.0042	0.0031	
674			48	133	0.0081	0.0081	0.0046	0.0143
675			56	149	0.0056	0.0064	0.0046	
676			59	158	0.0028	0.0039	0.0031	
677			62	167	0.0036	0.0047	0.0031	0.0079
678			77	207	0.0062	0.0064	0.0043	0.0067
679			80	214	0.0026	0.0045	0.0025	
680			82	220	0.0048	0.0071	0.0036	0.0039
681			85	227	0.0042	0.0058	0.0042	0.0111
682			80	220	0.0067	0.0075	0.0051	0.0061
683			92	245	0.0035	0.0051	0.0032	
684		row 3	76	204	0.0029	0.0043	0.0032	
685			79	211	0.0028	0.0047	0.0023	
686			81	217	0.003	0.006	0.0035	
687			83	224	0.0027	0.0027	0.0028	
688			79	218	0.0057	0.0048	0.0043	
689			88	237	0.0098	0.0064	0.0059	0.0168
690	2900 ft station	row 1	151	405	0.0026	0.0029	0.0029	0.00055
691			153	412	0.0033	0.005	0.0038	0.0011
692			156	419	0.0017	0.0028	0.0026	0.00013
693			159	426	0.0022	0.0039	0.0049	0.00026
694			161	433	0.0019	0.0043	0.0052	0.00023
695			164	440	0.0039	0.0083	0.0058	0.00078

	A	B	C	D	E	F	G	H
696			167	448	0.0025	0.0035	0.0036	0.00034
697			170	455	0.0059	0.0083	0.0086	0.0014
698			158	437	0.0016	0.0024	0.0018	0.00068
699			175	470	0.0043	0.0041	0.0031	0.0014
700			172	476	0.0026	0.0052	0.0033	0.00054
701			175	484	0.0033	0.0037	0.0033	0.00147
702			194	522	0.0026	0.0046	0.0018	0.00039
703			197	530	0.0064	0.0075	0.0035	0.00041
704			201	539	0.0023	0.0035	0.0018	0.00024
705			204	547	0.0012	0.0021	0.0026	0.00014
706			213	567	0.0018	0.0032	0.0018	0.00051
707			210	565	0.0036	0.0083	0.0041	0.0016
708			196	542	0.0033	0.0025	0.002	0.0004
709			217	583	0.0019	0.0029	0.002	0.00034
710		row 2	158	424	0.0022	0.0027	0.0025	0.00017
711			147	408	0.0097	0.0085	0.0085	
712			164	440	0.0039	0.006	0.0035	0.00089
713			167	448	0.0044	0.0067	0.003	0.00064
714			170	456	0.003	0.0042	0.0023	0.00037
715			183	492	0.0028	0.0071	0.0027	0.00049
716			185	498	0.0021	0.0038	0.0016	0.00074
717			188	504	0.0035	0.0023	0.0032	0.0015
718			190	510	0.0012	0.0011	0.0018	0.00022
719			176	487	0.0037	0.0054	0.0032	0.0013
720			200	532	0.0032	0.0062	0.0035	0.00044
721			197	528	0.0031	0.0046	0.0027	0.00035
722			199	535	0.0028	0.0082	0.0036	0.0011
723			201	541	0.00092	0.0026	0.0016	0.00049
724			187	516	0.0031	0.0049	0.0029	0.0014

	A	B	C	D	E	F	G	H
725		row 3	177	475	0.0016	0.0024	0.0012	0.00074
726			179	481	0.0011	0.00075	0.00079	0.0009
727			181	487	0.0019	0.0027	0.0017	0.00023
728			184	493	0.0019	0.0032	0.0016	0.00045
729			170	471	0.0033	0.0083	0.0042	0.00075
730			188	505	0.0044	0.0021	0.0027	0.0015
731			191	512	0.0013	0.0028	0.0011	0.0011
732			193	518	0.0012	0.0016	0.0011	0.00034
733			171	480	0.0016	0.0026	0.0014	0.00029

Appendix B: Selected Particle Velocity Versus Time Records and Air Overpressure Versus Time Records for Stations Monitored at the NSWC

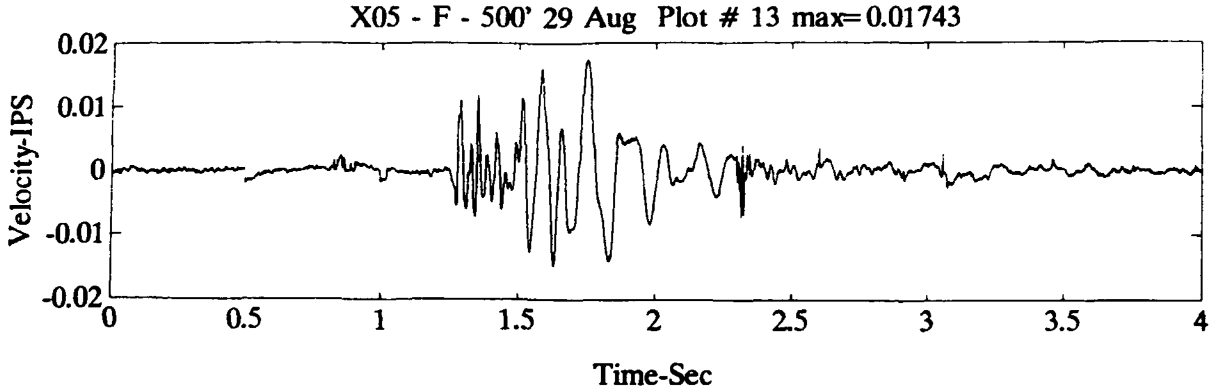
X05 - F - 500' 29 Aug Plot # 13 max=0.01743
Velocity-IPS
0.02
0.01
0
-0.01
-0.02
0
0.5
1
1.5
2
2.5
3
3.5
4
Time-Sec

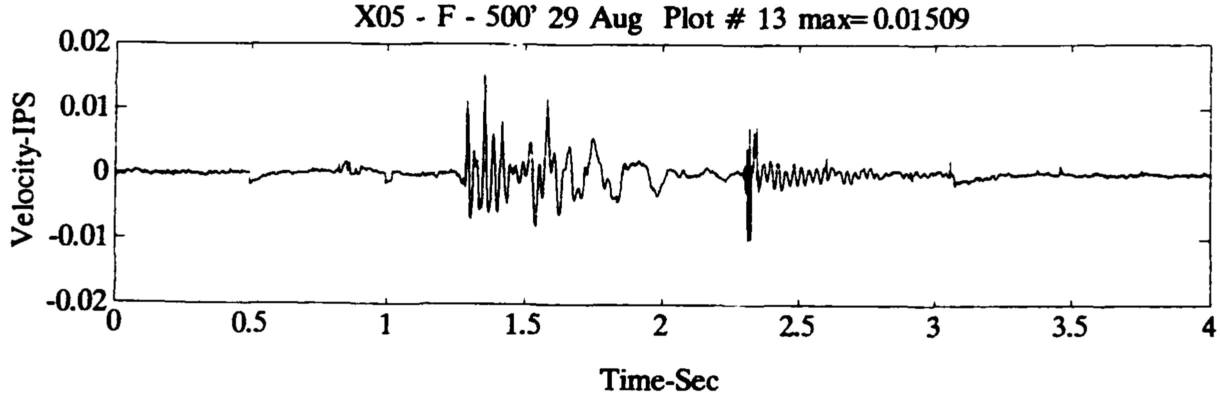
X05 - F - 500' 29 Aug Plot # 13 max=0.01509
Velocity-IPS
0.02
0.01
0
-0.01
-0.02
0
0.5
1
1.5
2
2.5
3
3.5
4
Time-Sec

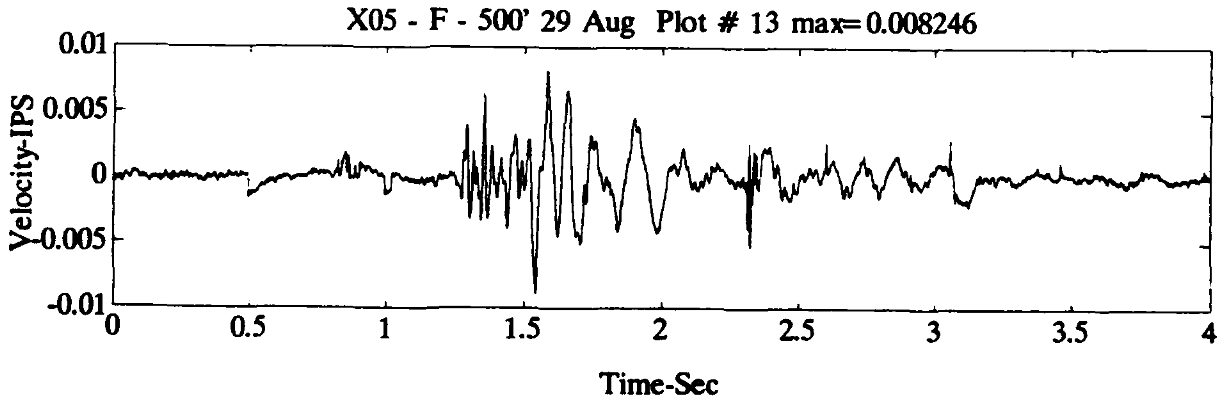
X05 - F - 500' 29 Aug Plot # 13 max=0.008246
Velocity-IPS
0.01
0.005
0
-0.005
-0.01
0
0.5
1
1.5
2
2.5
3
3.5
4
Time-Sec

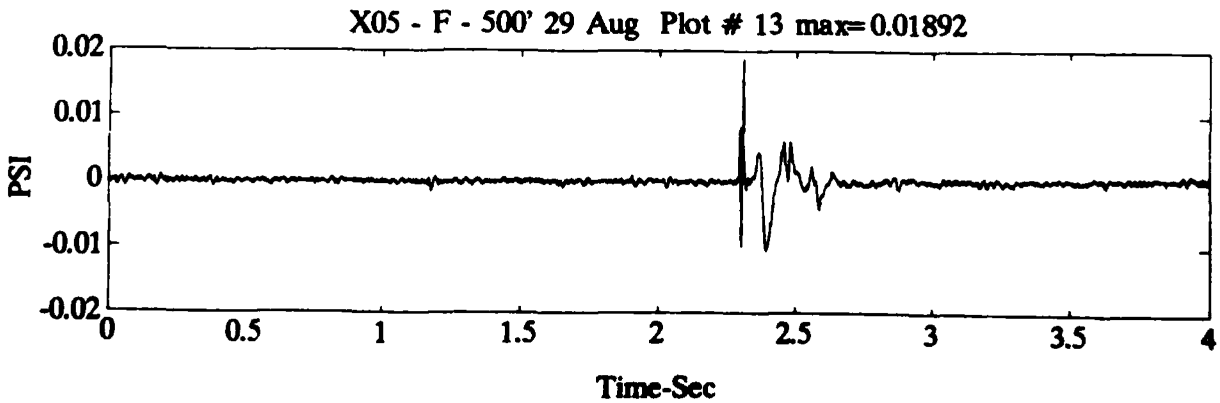
X05 - F - 500' 29 Aug Plot # 13 max=0.01892
PSI
0.02
0.01
0
-0.01
-0.02
0
0.5
1
1.5
2
2.5
3
3.5
4
Time-Sec

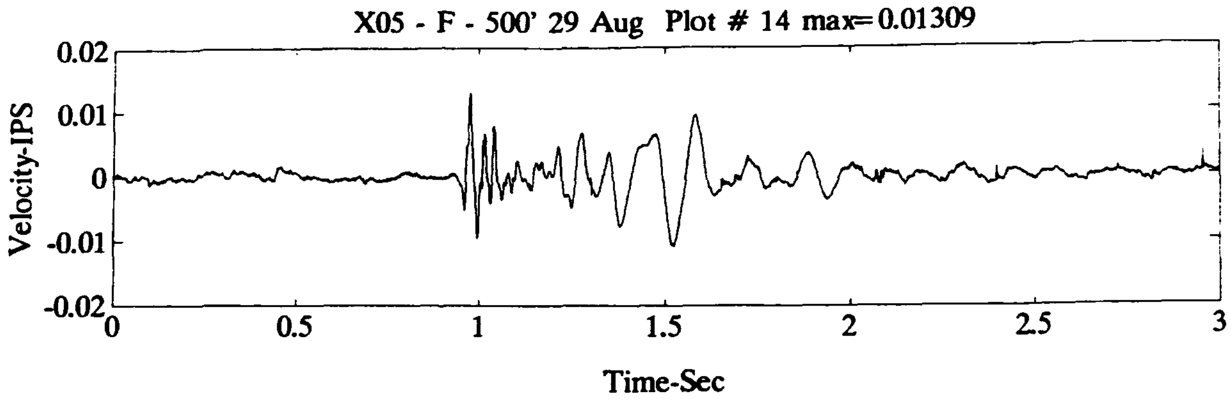
X05 - F - 500' 29 Aug Plot # 14 max= 0.01309
Velocity-IPS
Time-Sec

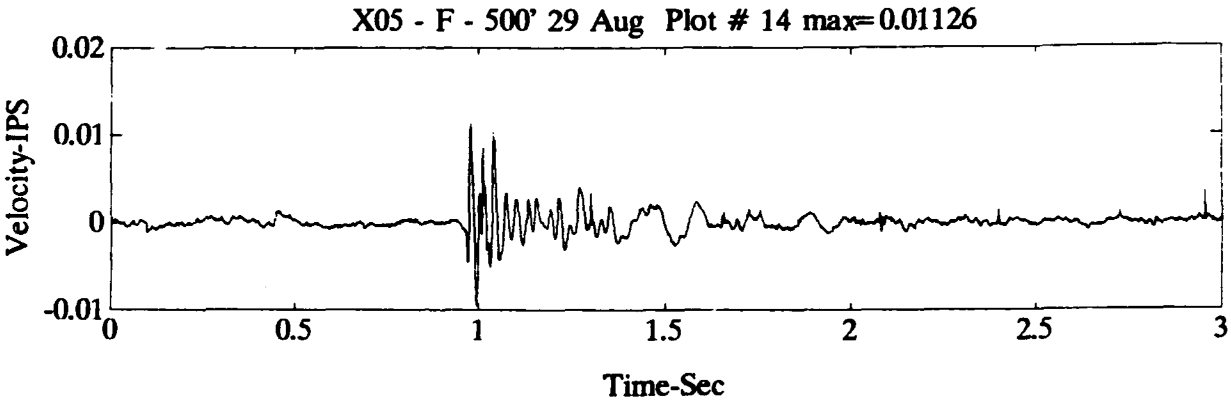
X05 - F - 500' 29 Aug Plot # 14 max= 0.01126
Velocity-IPS
Time-Sec

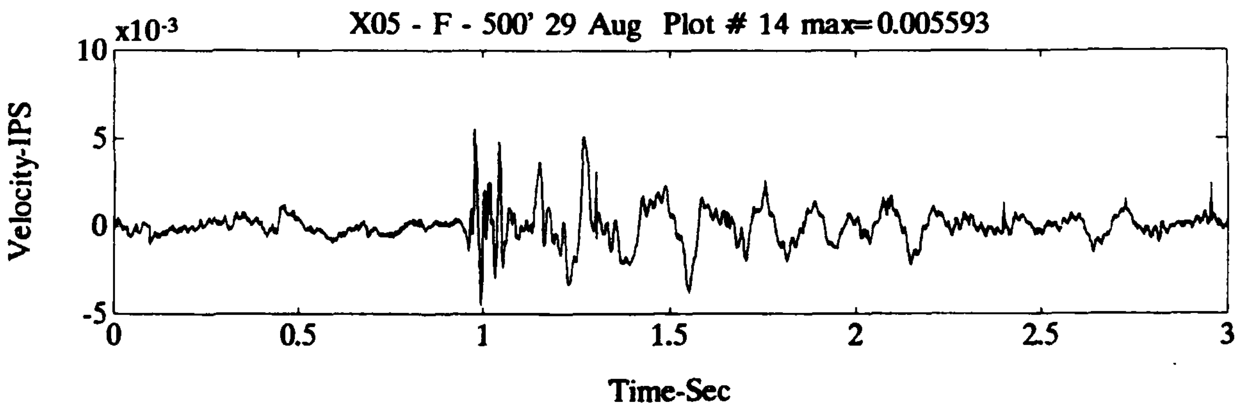
X05 - F - 500' 29 Aug Plot # 14 max= 0.005593
x10-3
Velocity-IPS
Time-Sec

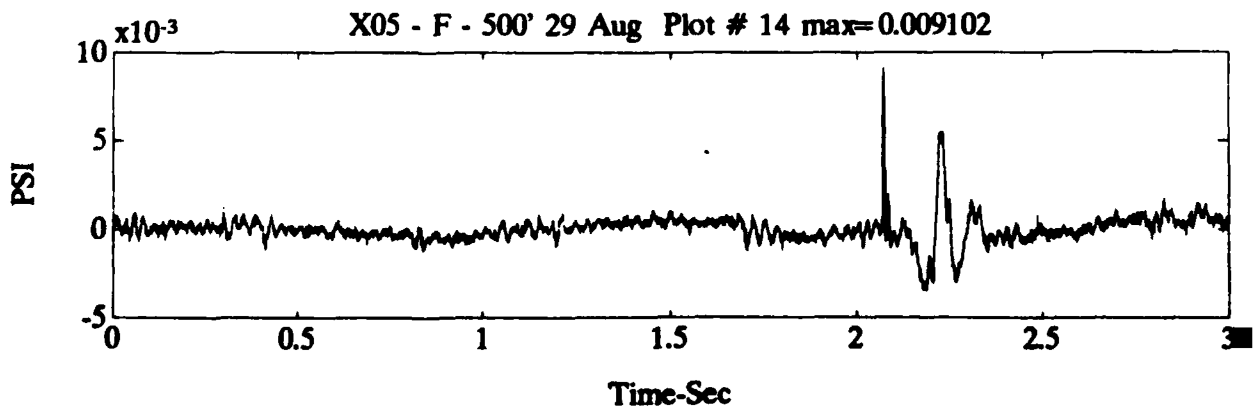
X05 - F - 500' 29 Aug Plot # 14 max= 0.009102
x10-3
PSI
Time-Sec

X05 - F - 500' 29 Aug Plot # 15 max= 0.01606

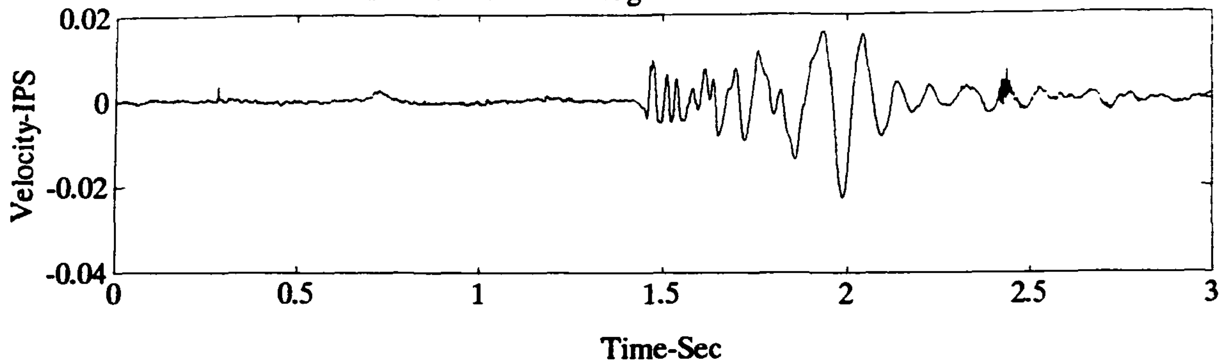

X05 - F - 500' 29 Aug Plot # 15 max= 0.009465

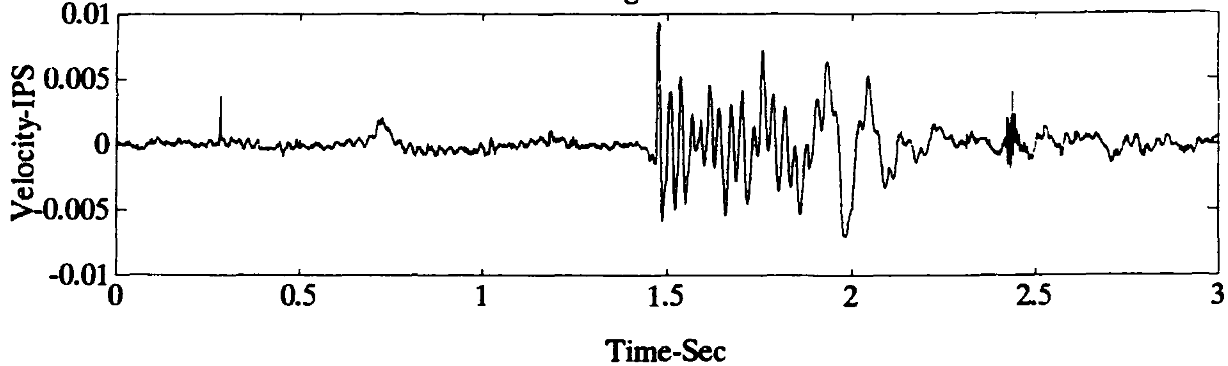

X05 - F - 500' 29 Aug Plot # 15 max= 0.006754

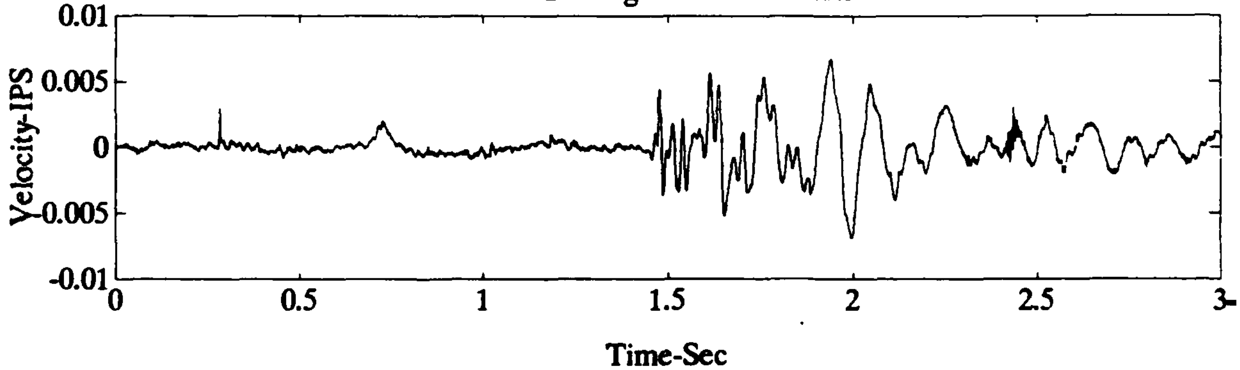

X05 - F - 500' 29 Aug Plot # 15 max= 0.01531

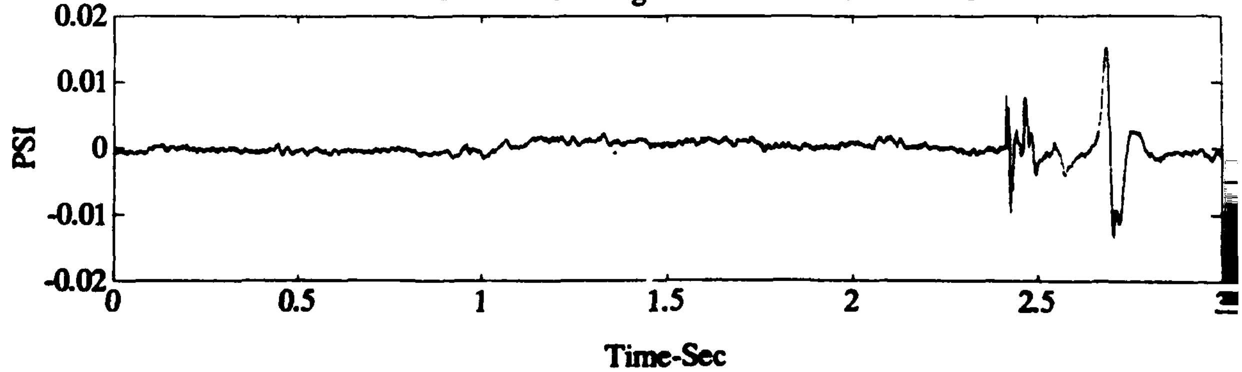

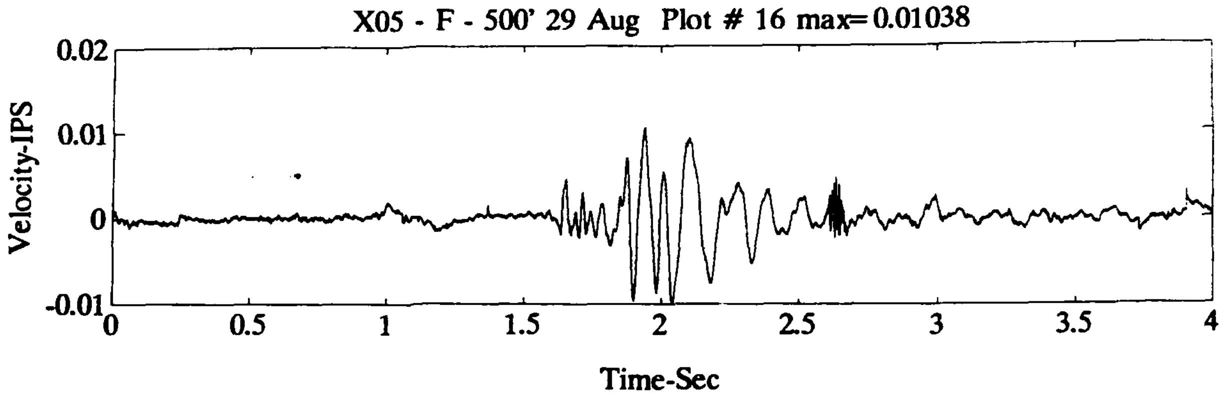
X05 - F - 500' 29 Aug Plot # 16 max=0.01038
Velocity-IPS
Time-Sec
0.02
0.01
0
-0.01
0
0.5
1
1.5
2
2.5
3
3.5
4

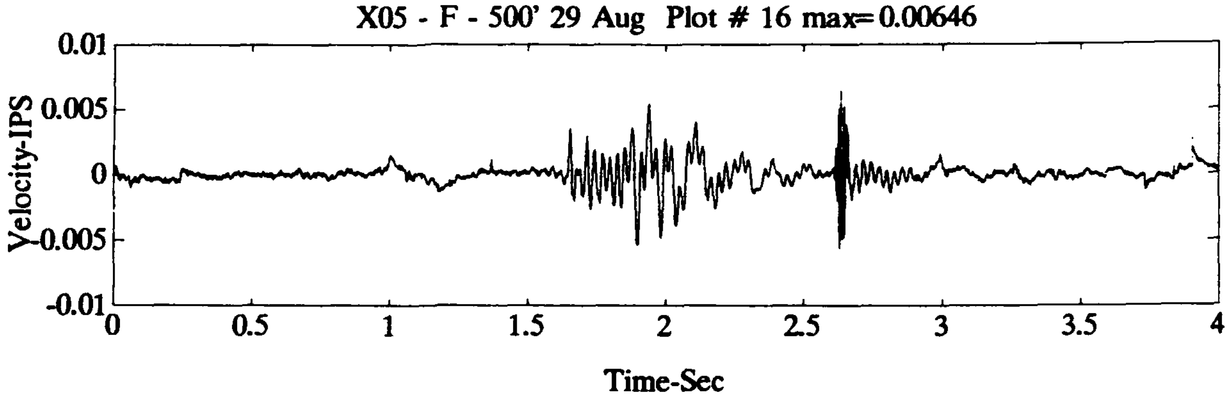
X05 - F - 500' 29 Aug Plot # 16 max=0.00646
Velocity-IPS
Time-Sec
0.01
0.005
0
-0.005
-0.01
0
0.5
1
1.5
2
2.5
3
3.5
4

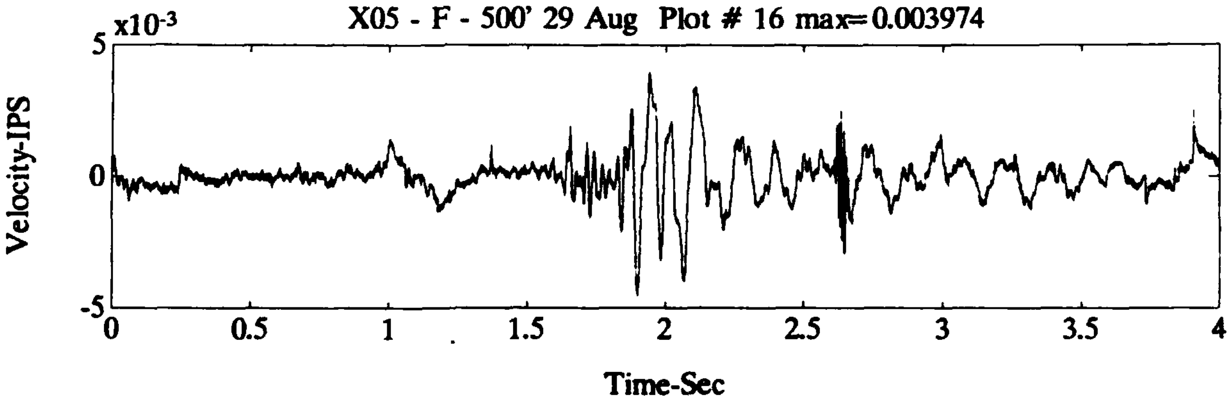
X05 - F - 500' 29 Aug Plot # 16 max=0.003974
x10-3
Velocity-IPS
Time-Sec
5
0
-5
0
0.5
1
1.5
2
2.5
3
3.5
4

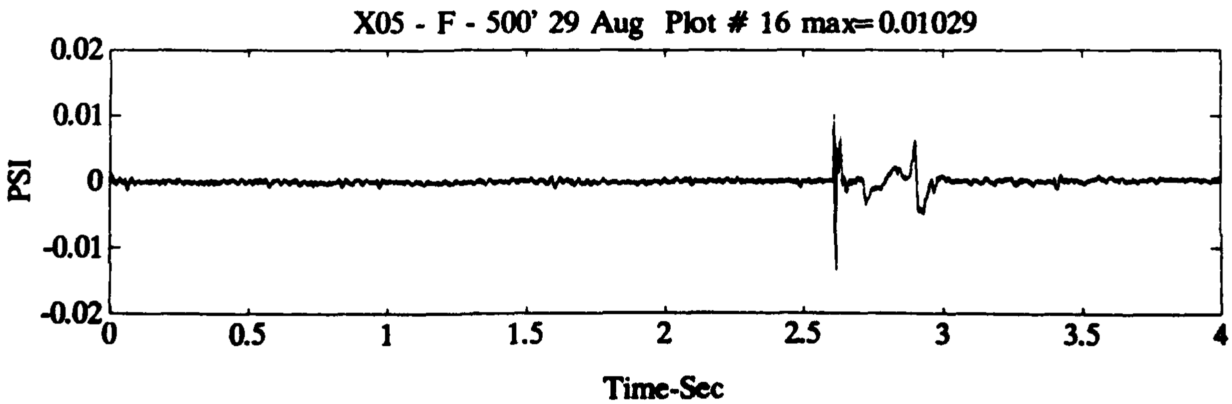
X05 - F - 500' 29 Aug Plot # 16 max=0.01029
PSI
Time-Sec
0.02
0.01
0
-0.01
-0.02
0
0.5
1
1.5
2
2.5
3
3.5
4

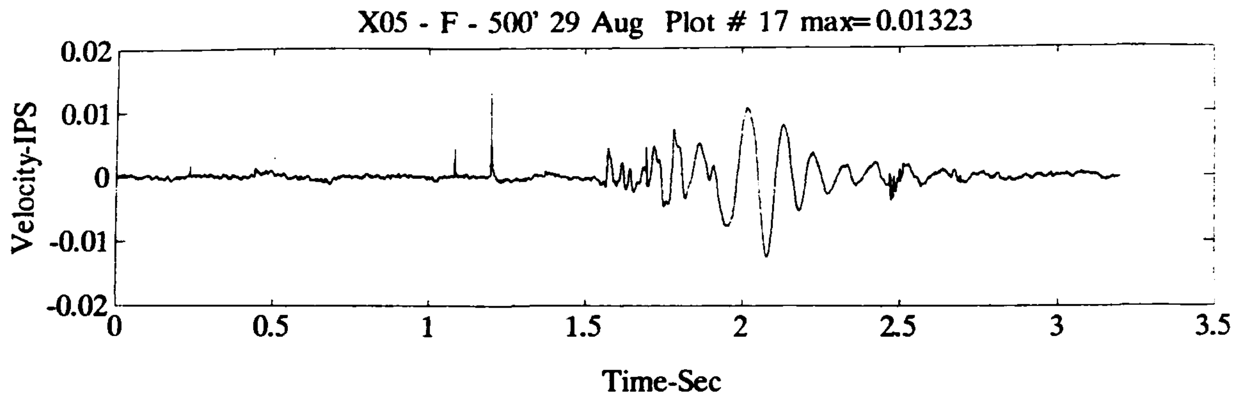
X05 - F - 500' 29 Aug Plot # 17 max=0.01323
Velocity-IPS
0.02
0.01
0
-0.01
-0.02
0
0.5
1
1.5
2
2.5
3
3.5
Time-Sec

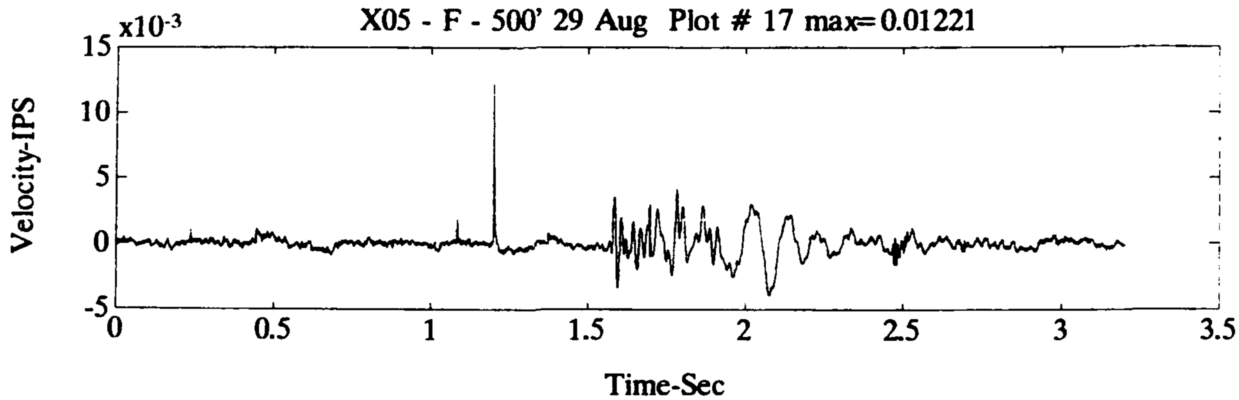
X05 - F - 500' 29 Aug Plot # 17 max=0.01221
x10-3
Velocity-IPS
15
10
5
0
-5
0
0.5
1
1.5
2
2.5
3
3.5
Time-Sec

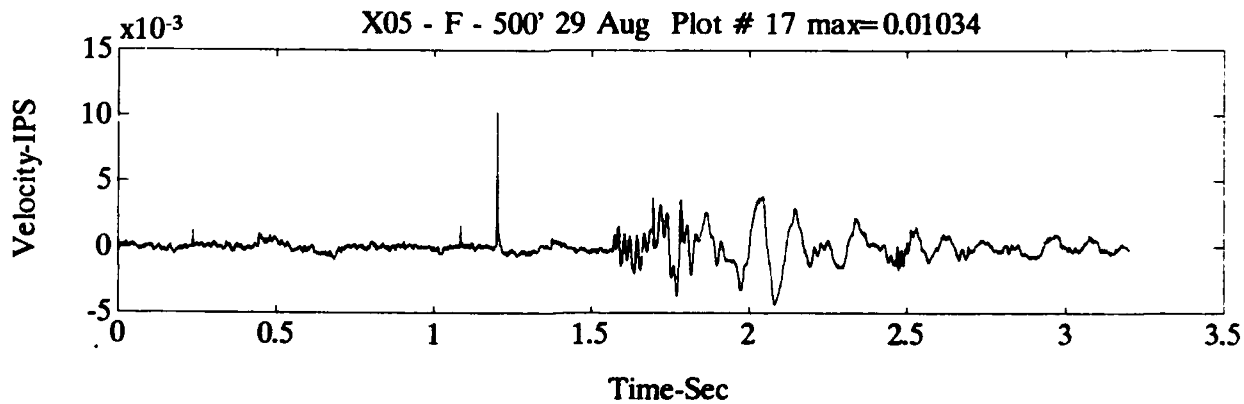
X05 - F - 500' 29 Aug Plot # 17 max=0.01034
x10-3
Velocity-IPS
15
10
5
0
-5
0
0.5
1
1.5
2
2.5
3
3.5
Time-Sec

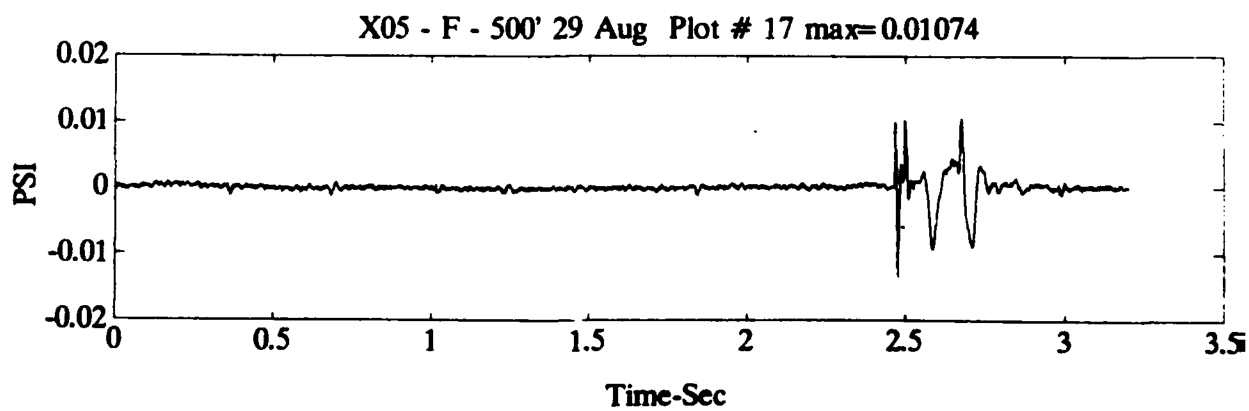
X05 - F - 500' 29 Aug Plot # 17 max=0.01074
PSI
0.02
0.01
0
-0.01
-0.02
0
0.5
1
1.5
2
2.5
3
3.5
Time-Sec

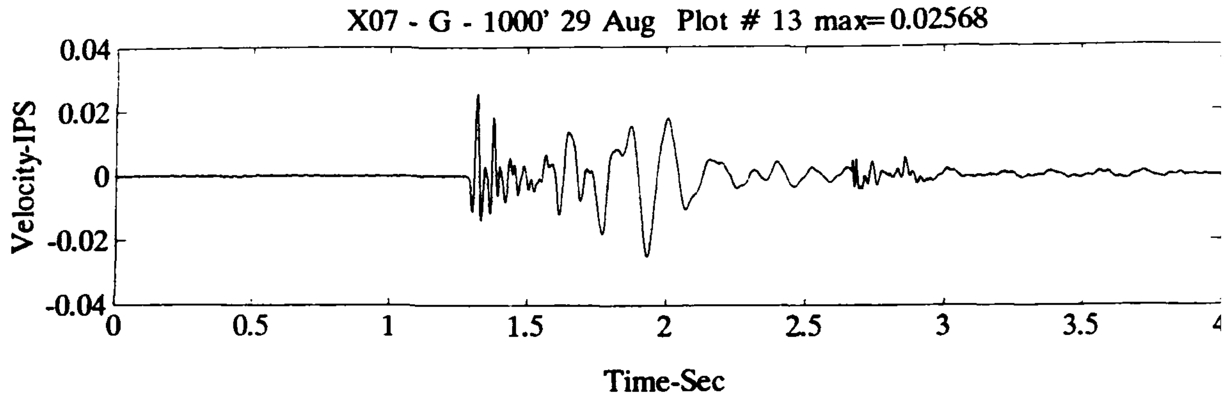
X07 - G - 1000' 29 Aug Plot # 13 max=0.02568
Velocity-IPS
0.04
0.02
0
-0.02
-0.04
0
0.5
1
1.5
2
2.5
3
3.5
Time-Sec

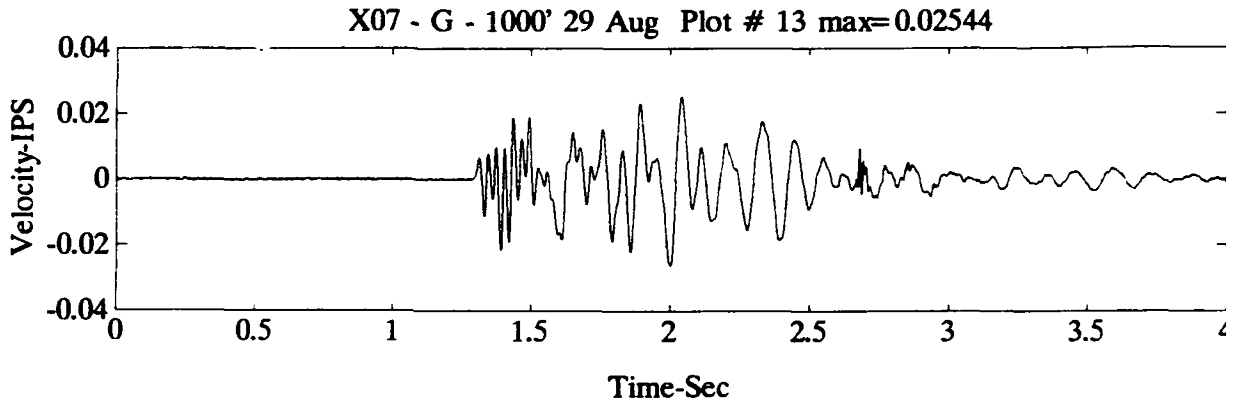
X07 - G - 1000' 29 Aug Plot # 13 max=0.02544
Velocity-IPS
0.04
0.02
0
-0.02
-0.04
0
0.5
1
1.5
2
2.5
3
3.5
Time-Sec

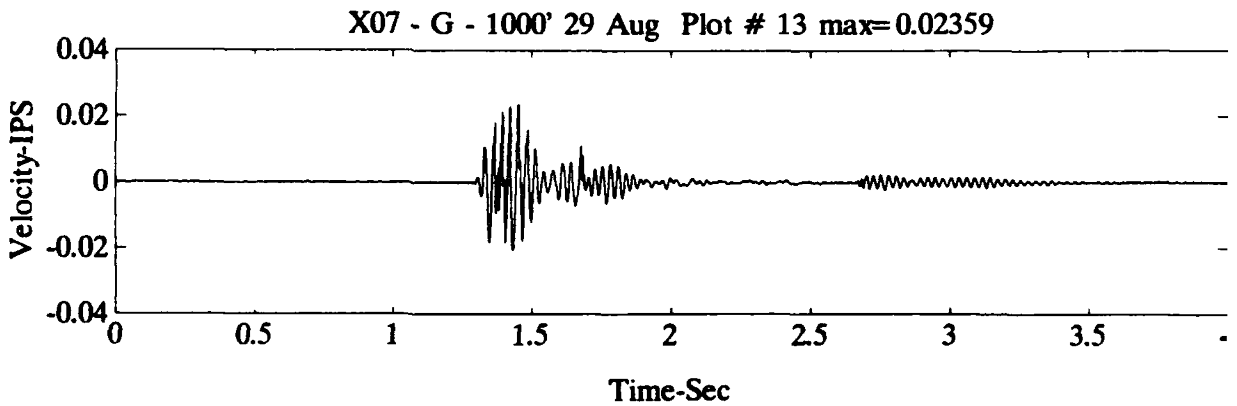
X07 - G - 1000' 29 Aug Plot # 13 max=0.02359
Velocity-IPS
0.04
0.02
0
-0.02
-0.04
0
0.5
1
1.5
2
2.5
3
3.5
Time-Sec

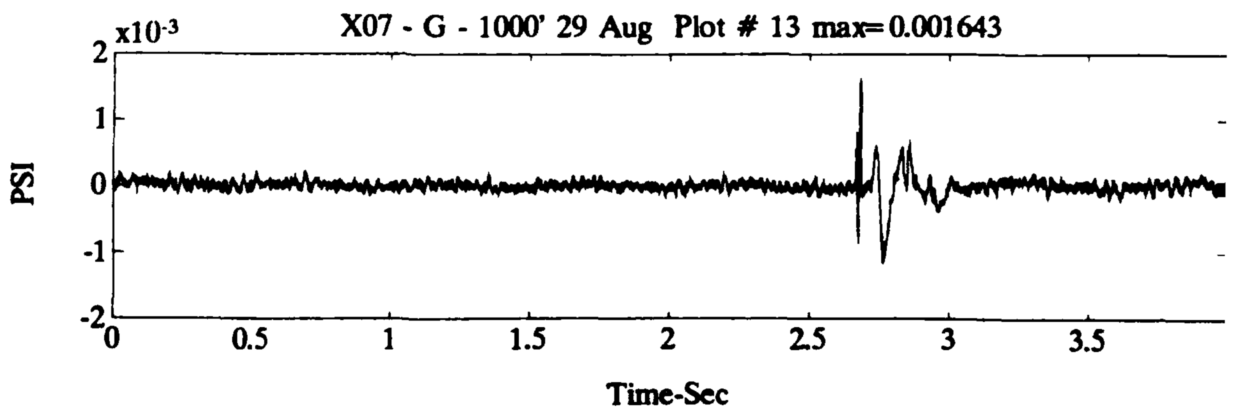
x10-3
X07 - G - 1000' 29 Aug Plot # 13 max=0.001643
PSI
2
1
0
-1
-2
0
0.5
1
1.5
2
2.5
3
3.5
Time-Sec

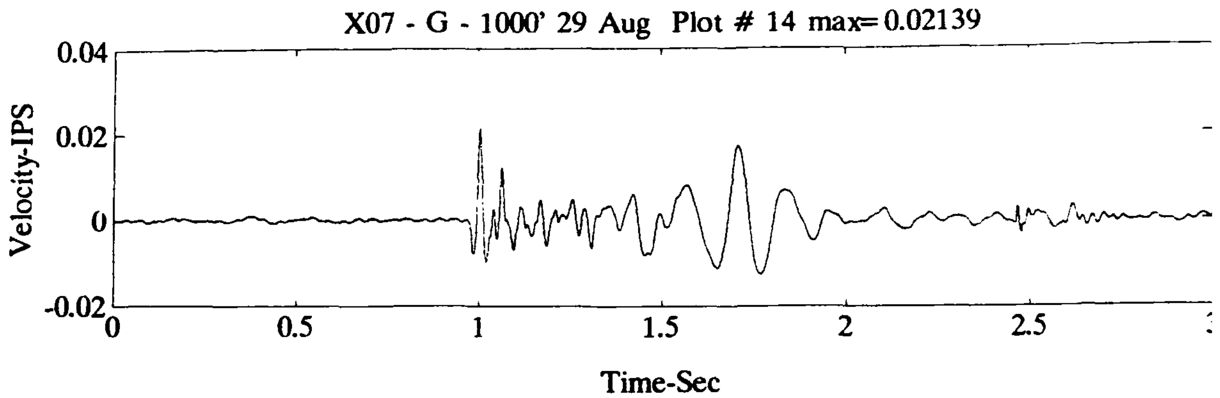
X07 - G - 1000' 29 Aug Plot # 14 max=0.02139
Velocity-IPS
Time-Sec

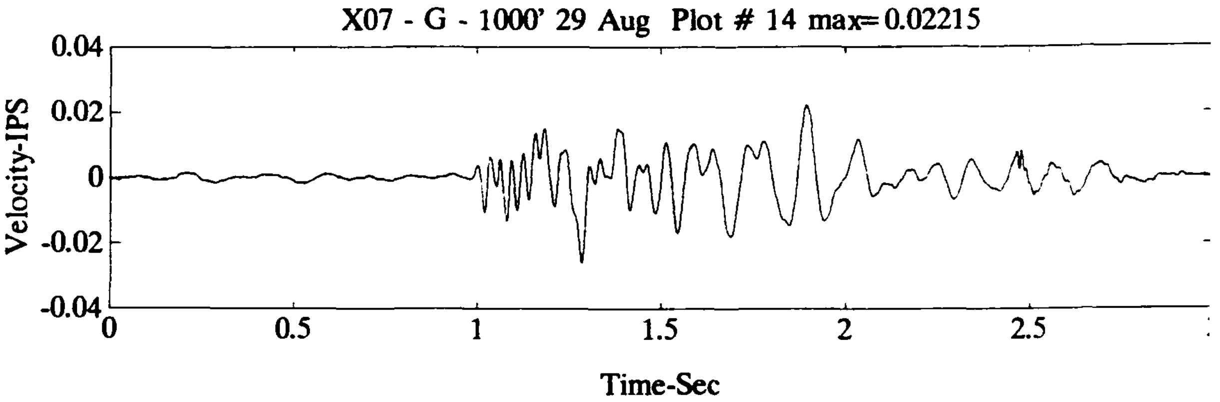
X07 - G - 1000' 29 Aug Plot # 14 max=0.02215
Velocity-IPS
Time-Sec

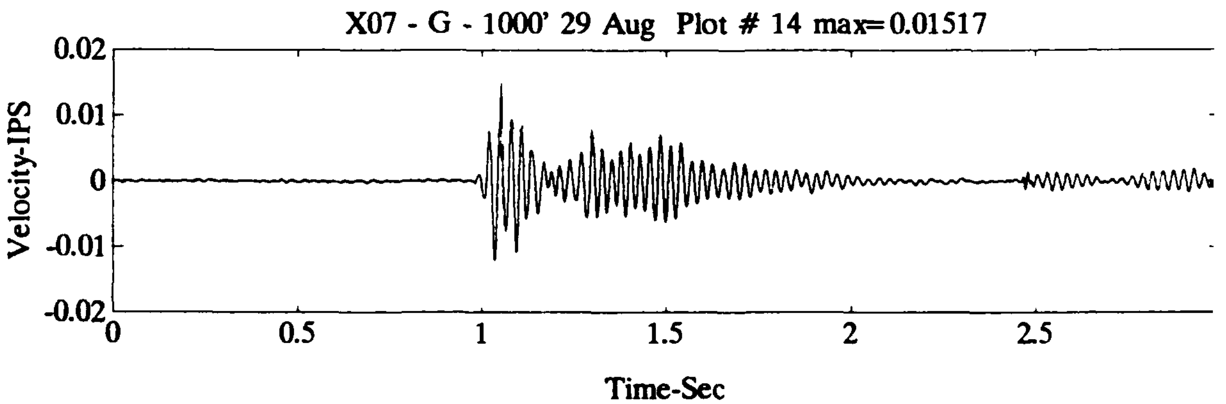
X07 - G - 1000' 29 Aug Plot # 14 max=0.01517
Velocity-IPS
Time-Sec

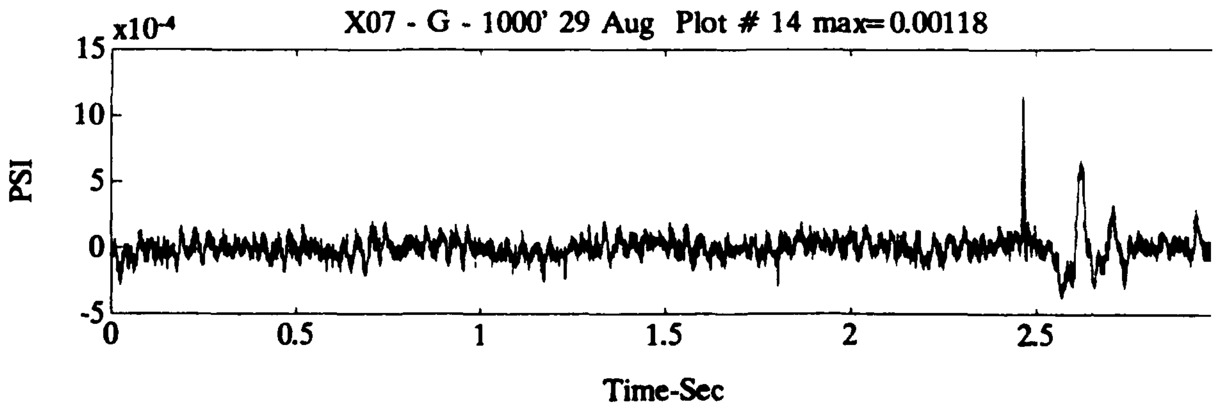
X07 - G - 1000' 29 Aug Plot # 14 max=0.00118
x10-4
PSI
Time-Sec

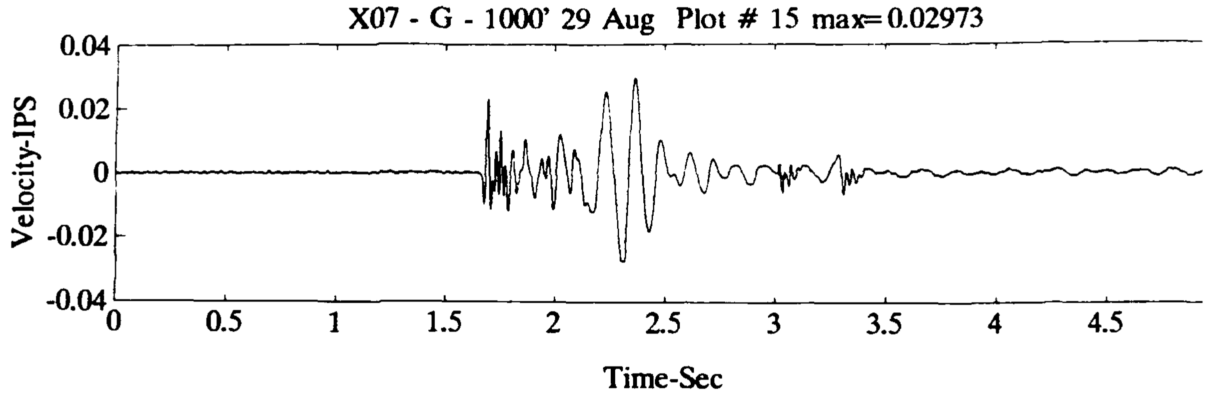
X07 - G - 1000' 29 Aug Plot # 15 max=0.02973
Velocity-IPS
Time-Sec

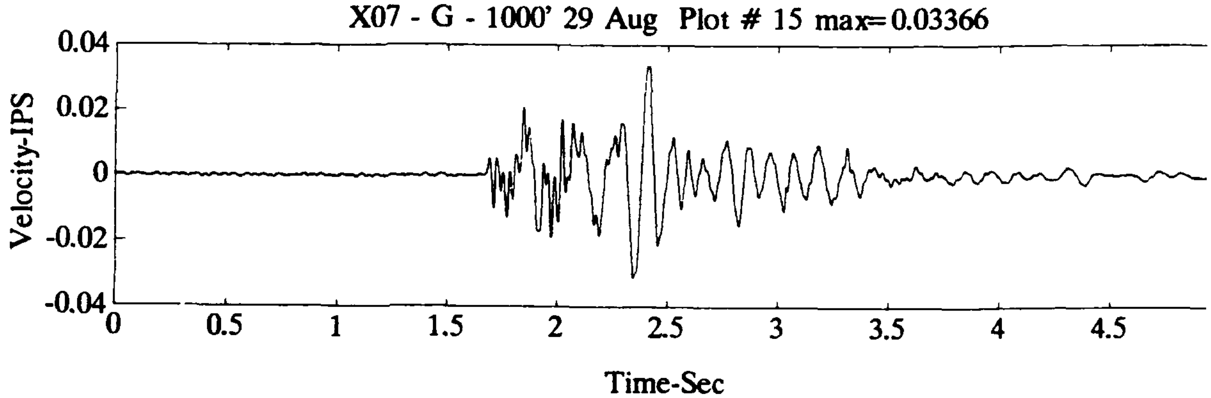
X07 - G - 1000' 29 Aug Plot # 15 max=0.03366
Velocity-IPS
Time-Sec

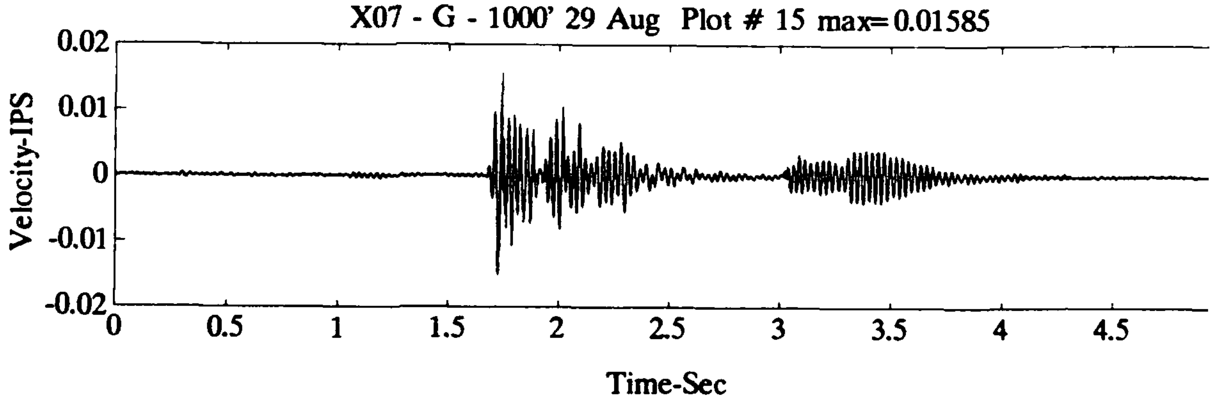
X07 - G - 1000' 29 Aug Plot # 15 max=0.01585
Velocity-IPS
Time-Sec

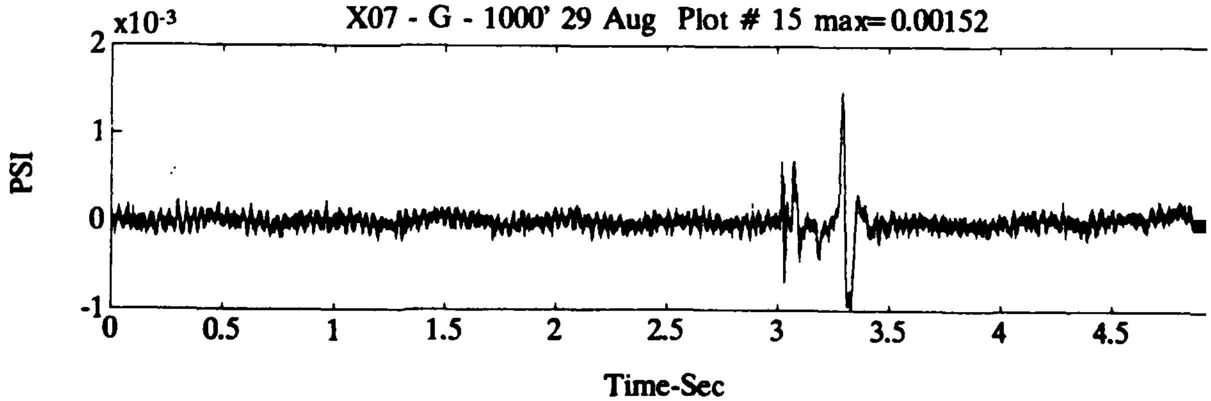
X07 - G - 1000' 29 Aug Plot # 15 max=0.00152
x10-3
PSI
Time-Sec

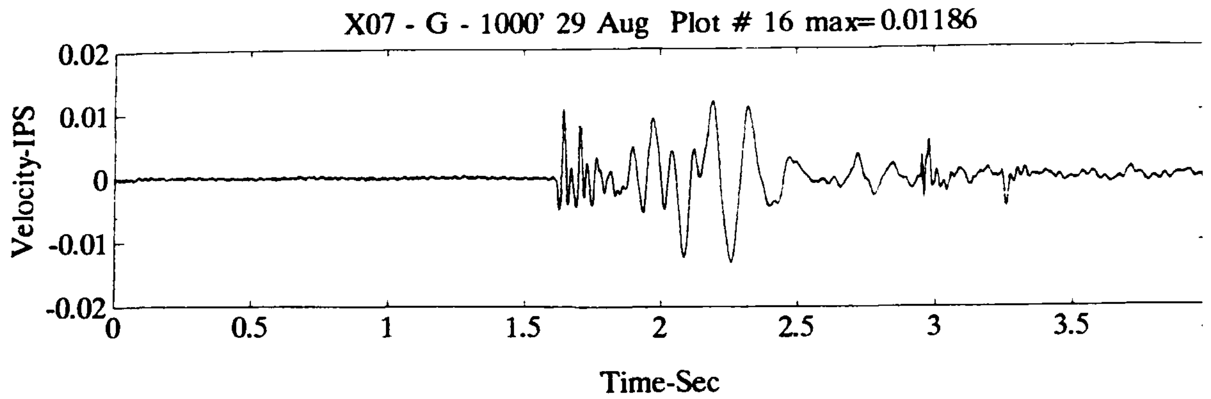
X07 - G - 1000' 29 Aug Plot # 16 max=0.01186
Velocity-IPS
Time-Sec

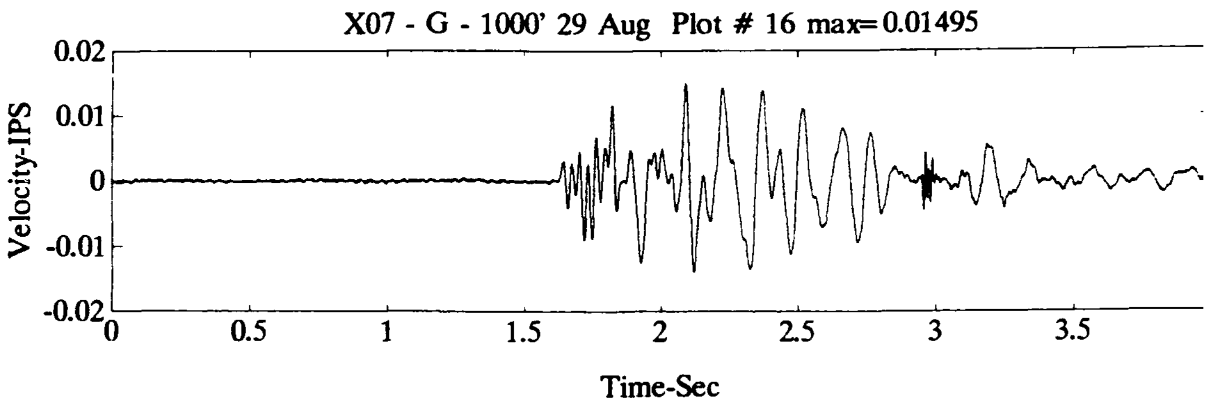
X07 - G - 1000' 29 Aug Plot # 16 max=0.01495
Velocity-IPS
Time-Sec

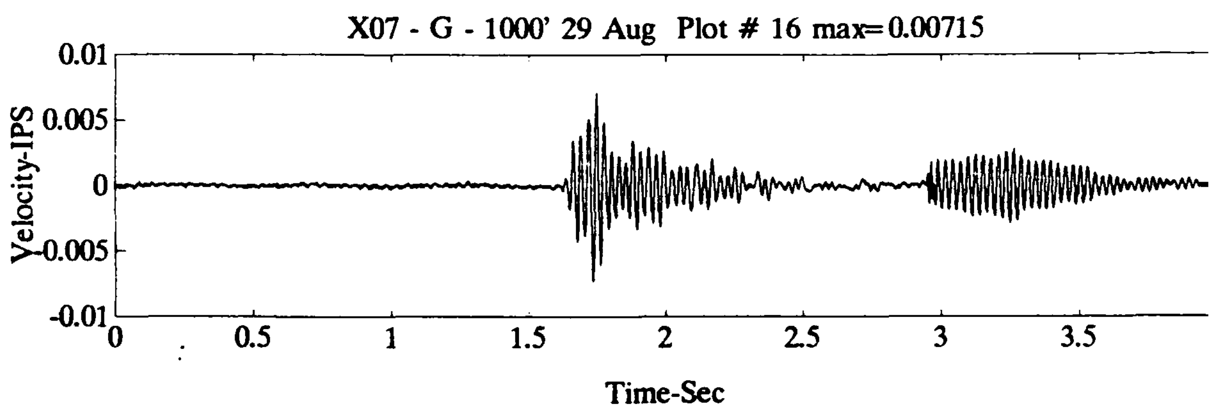
X07 - G - 1000' 29 Aug Plot # 16 max=0.00715
Velocity-IPS
Time-Sec

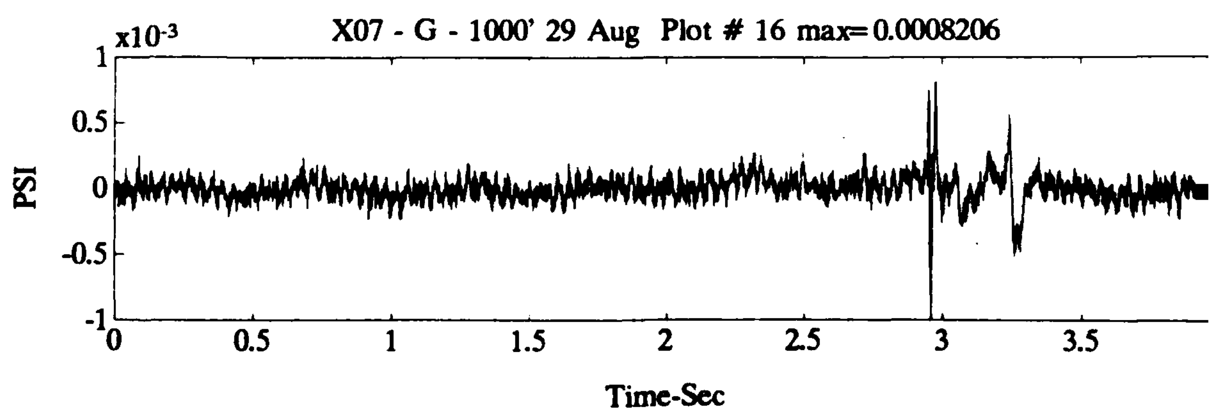
x10-3
X07 - G - 1000' 29 Aug Plot # 16 max=0.0008206
PSI
Time-Sec

X07 - G - 1000' 29 Aug Plot # 17 max= 0.01929

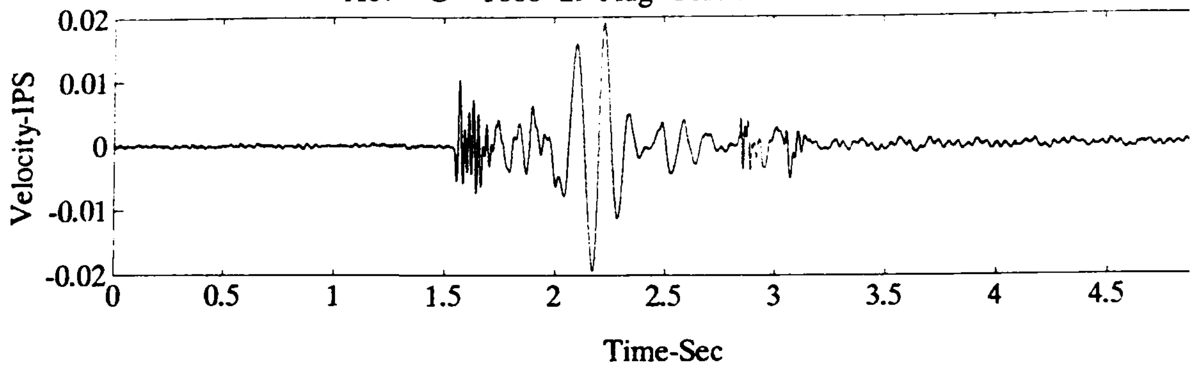

X07 - G - 1000' 29 Aug Plot # 17 max= 0.0179

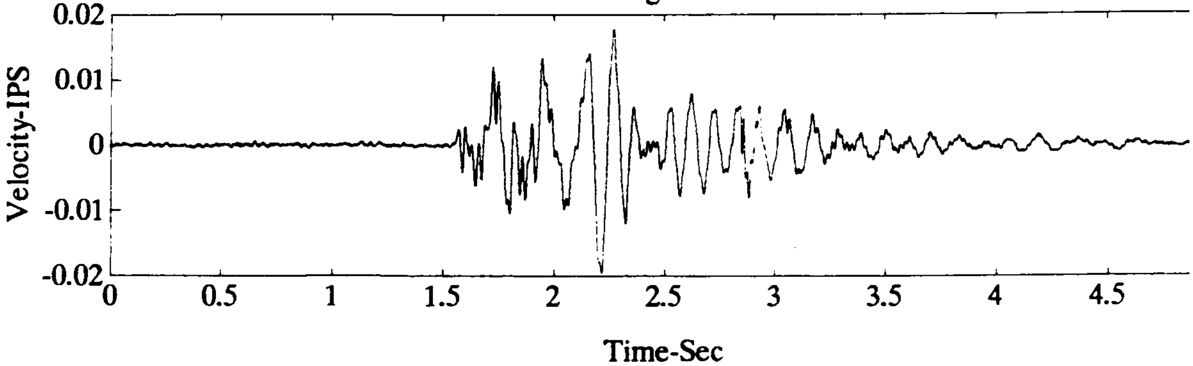

X07 - G - 1000' 29 Aug Plot # 17 max= 0.007762

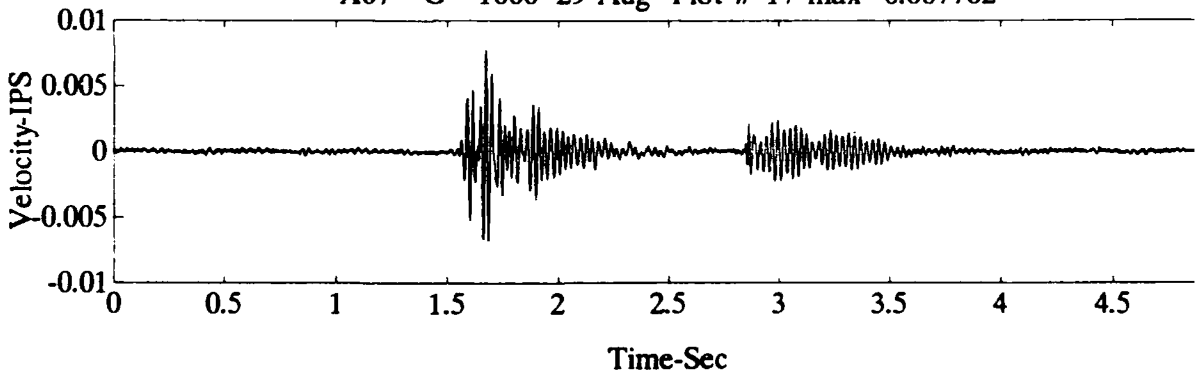

X07 - G - 1000' 29 Aug Plot # 17 max= 0.0008006

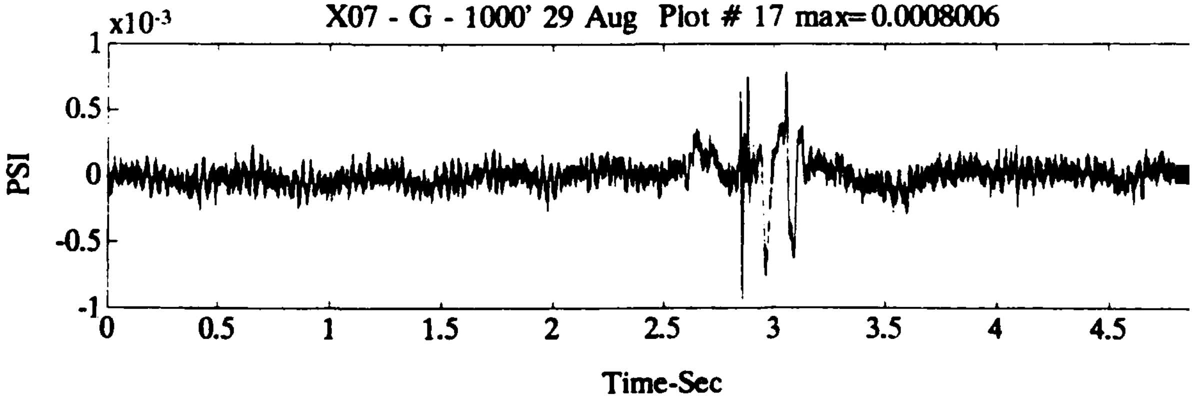

X07 - G - 1000' 29 Aug Plot # 18 max=0.01556

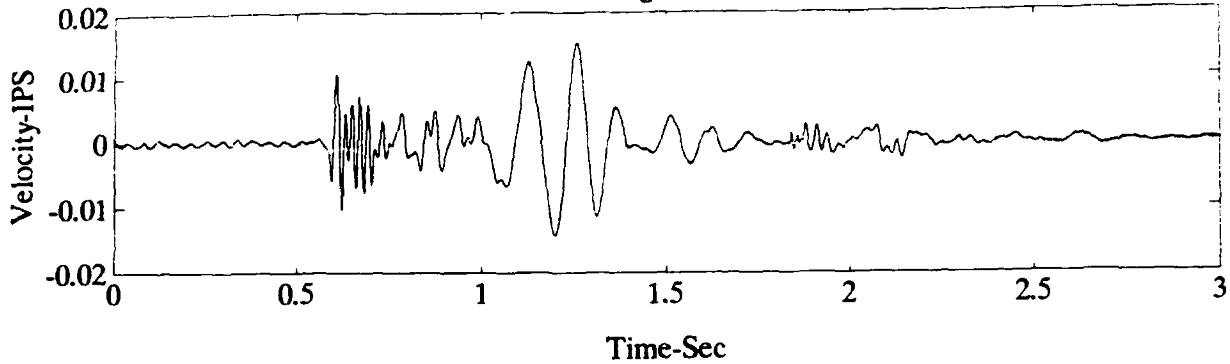

X07 - G - 1000' 29 Aug Plot # 18 max=0.01594

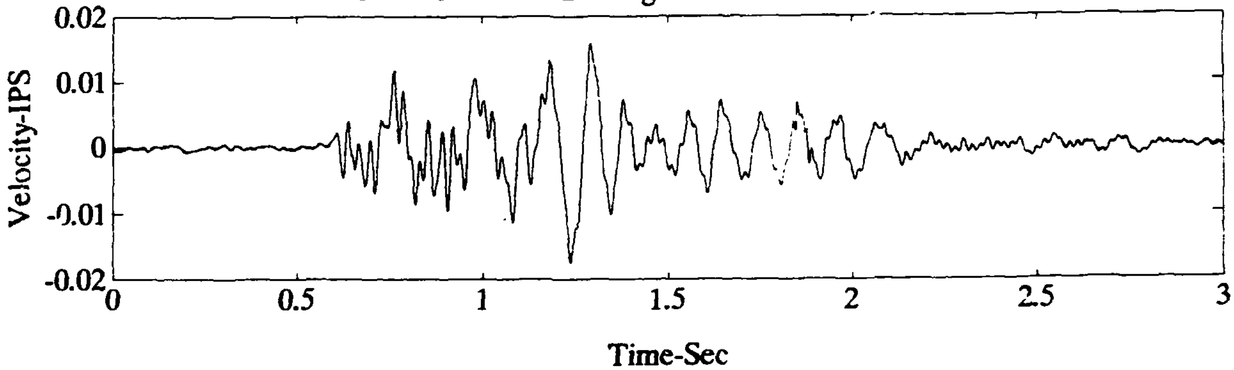

X07 - G - 1000' 29 Aug Plot # 18 max=0.008479

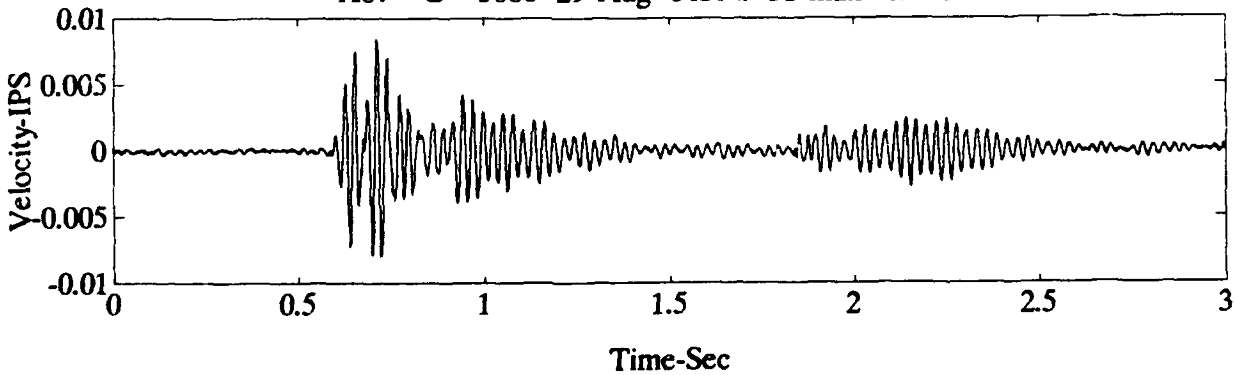

X07 - G - 1000' 29 Aug Plot # 18 max=0.0009295

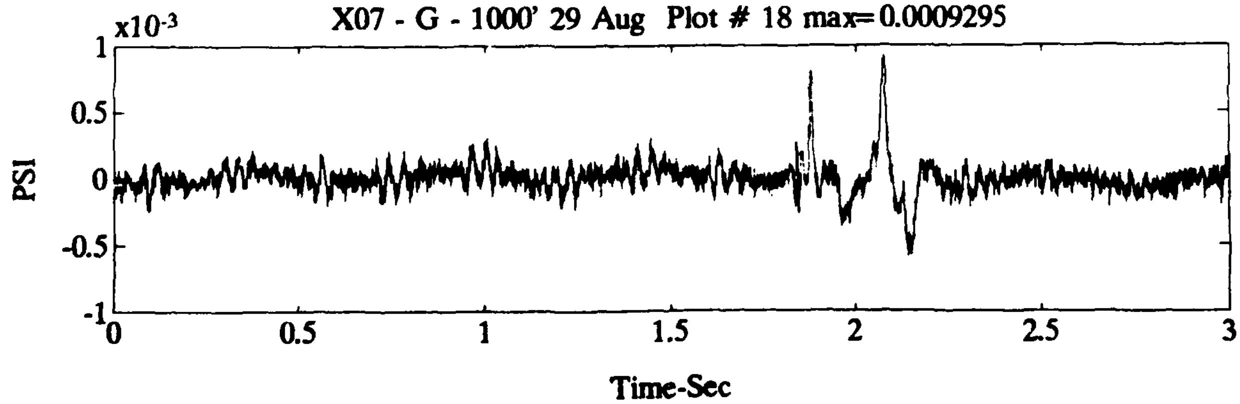

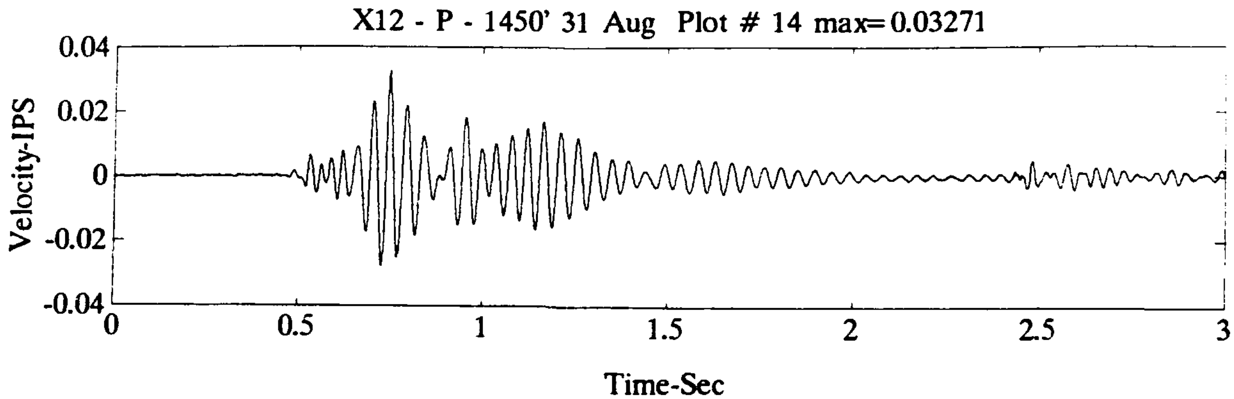
X12 - P - 1450' 31 Aug Plot # 14 max=0.03271
Velocity-IPS
Time-Sec

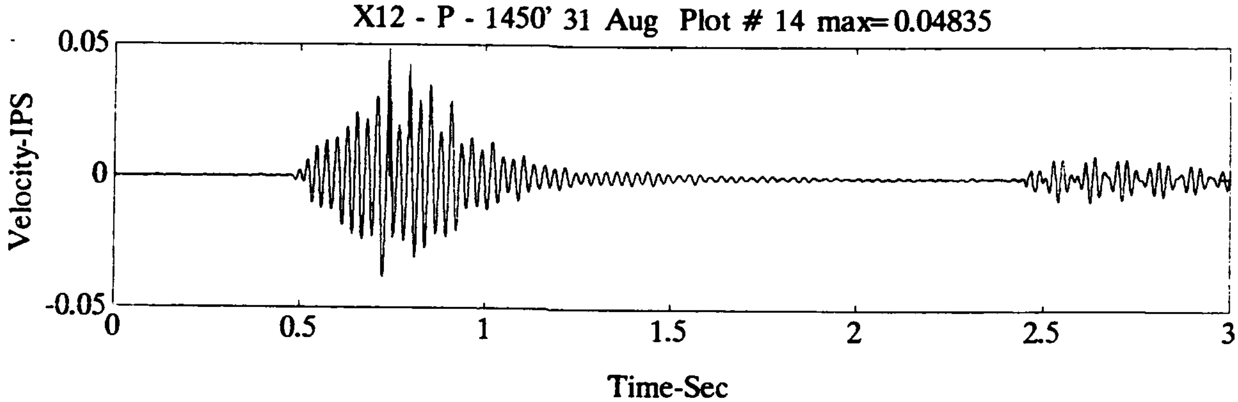
X12 - P - 1450' 31 Aug Plot # 14 max=0.04835
Velocity-IPS
Time-Sec

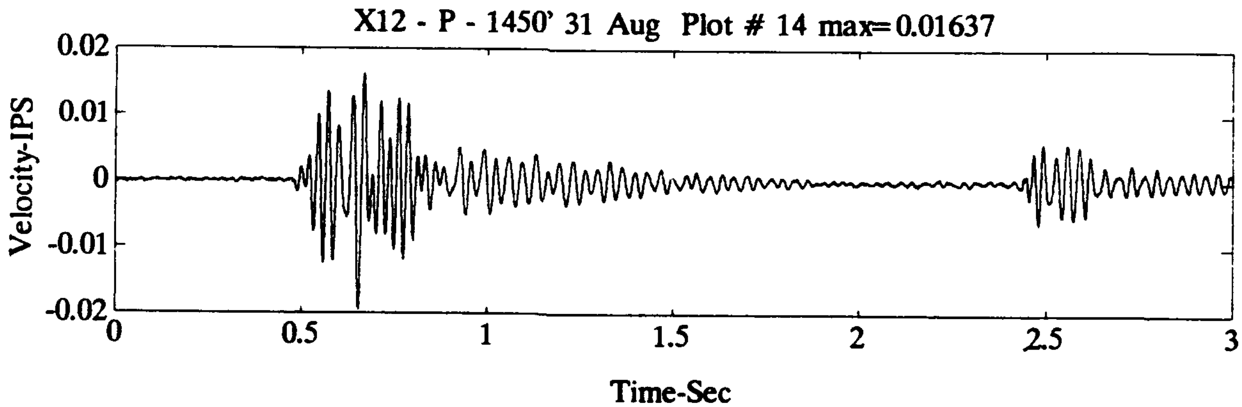
X12 - P - 1450' 31 Aug Plot # 14 max=0.01637
Velocity-IPS
Time-Sec

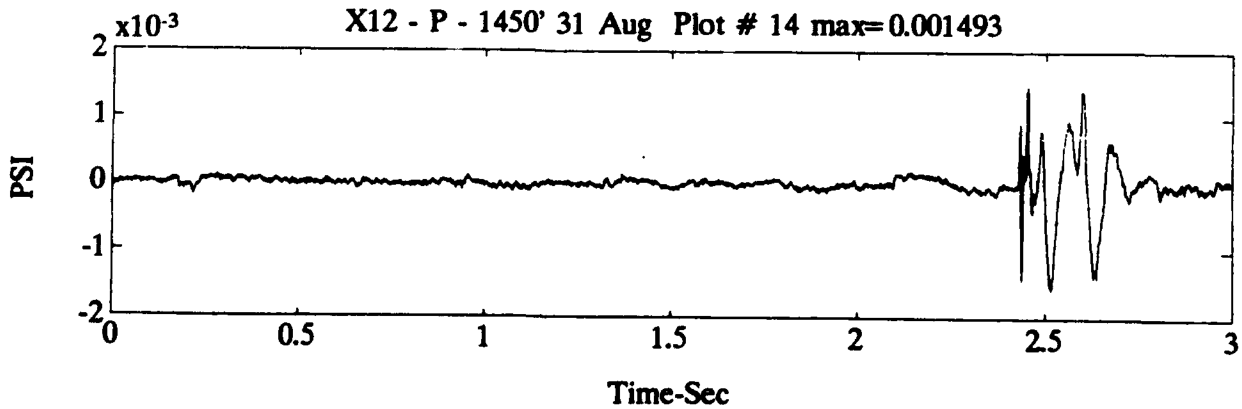
X12 - P - 1450' 31 Aug Plot # 14 max=0.001493
x10-3
PSI
Time-Sec

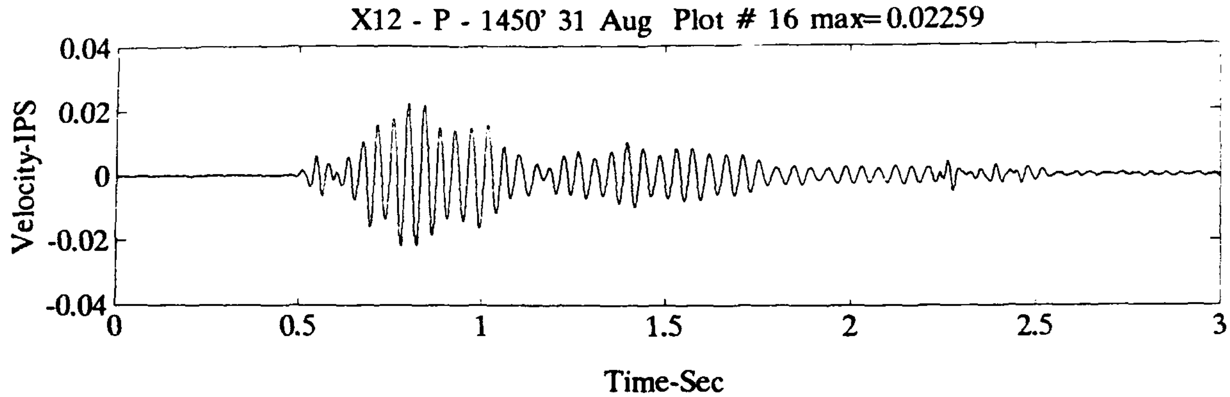
X12 - P - 1450' 31 Aug Plot # 16 max=0.02259
Velocity-IPS
0.04
0.02
0
-0.02
-0.04
0
0.5
1
1.5
2
2.5
3
Time-Sec

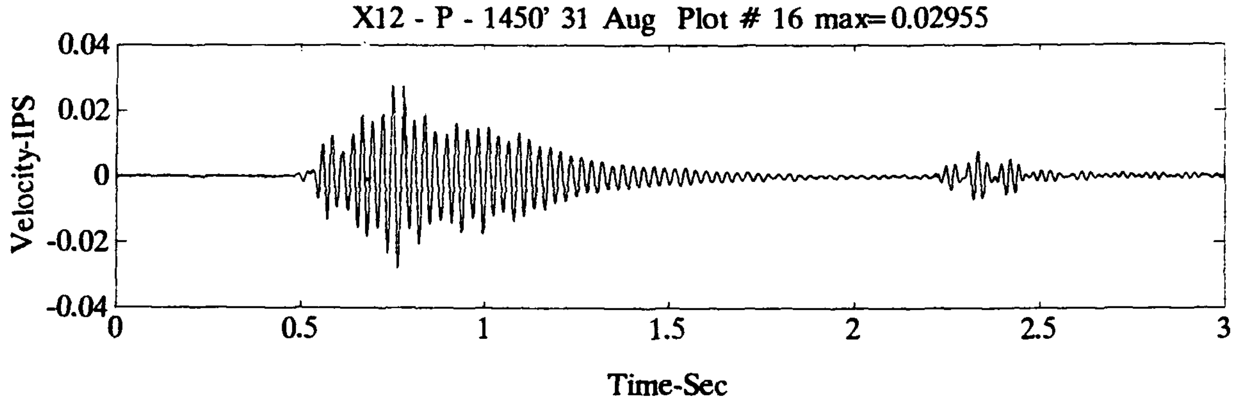
X12 - P - 1450' 31 Aug Plot # 16 max=0.02955
Velocity-IPS
0.04
0.02
0
-0.02
-0.04
0
0.5
1
1.5
2
2.5
3
Time-Sec

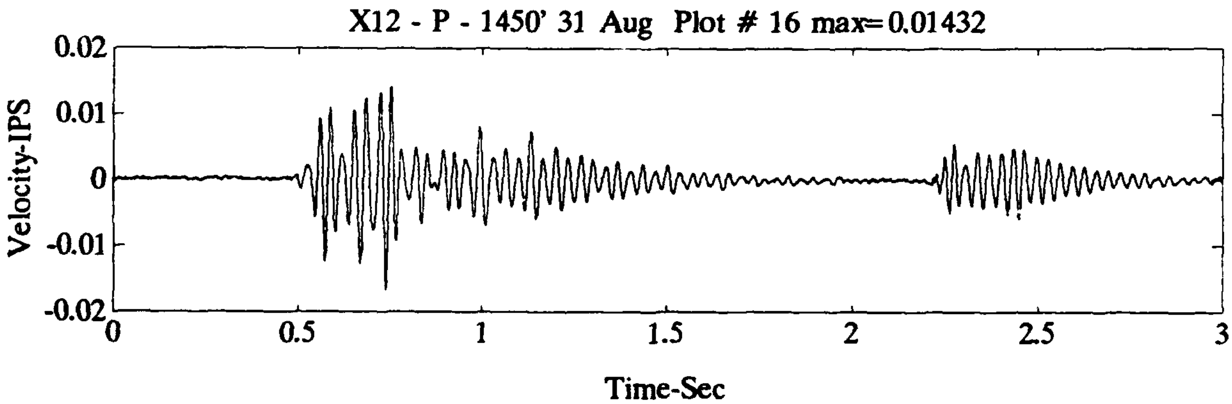
X12 - P - 1450' 31 Aug Plot # 16 max=0.01432
Velocity-IPS
0.02
0.01
0
-0.01
-0.02
0
0.5
1
1.5
2
2.5
3
Time-Sec

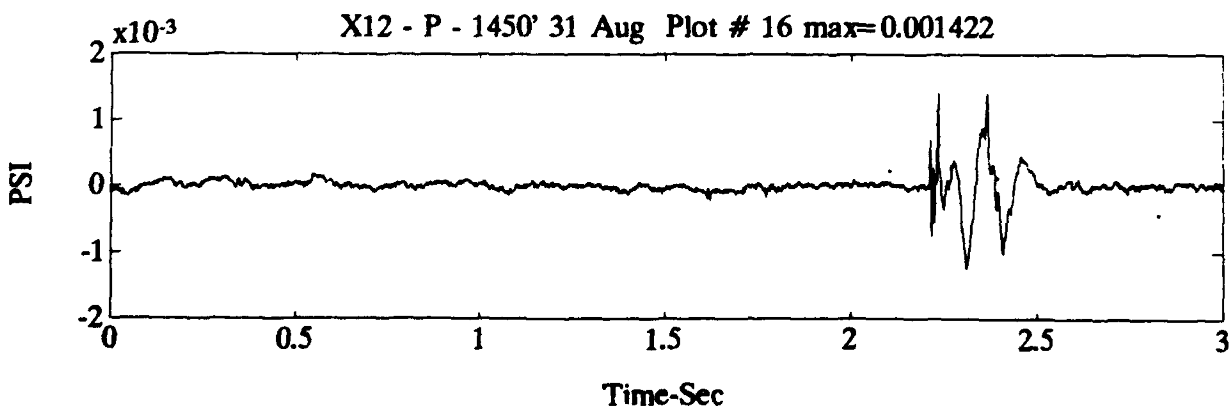
X12 - P - 1450' 31 Aug Plot # 16 max=0.001422
x10-3
PSI
2
1
0
-1
-2
0
0.5
1
1.5
2
2.5
3
Time-Sec

X12 - P - 1450' 31 Aug Plot # 17 max= 0.02108

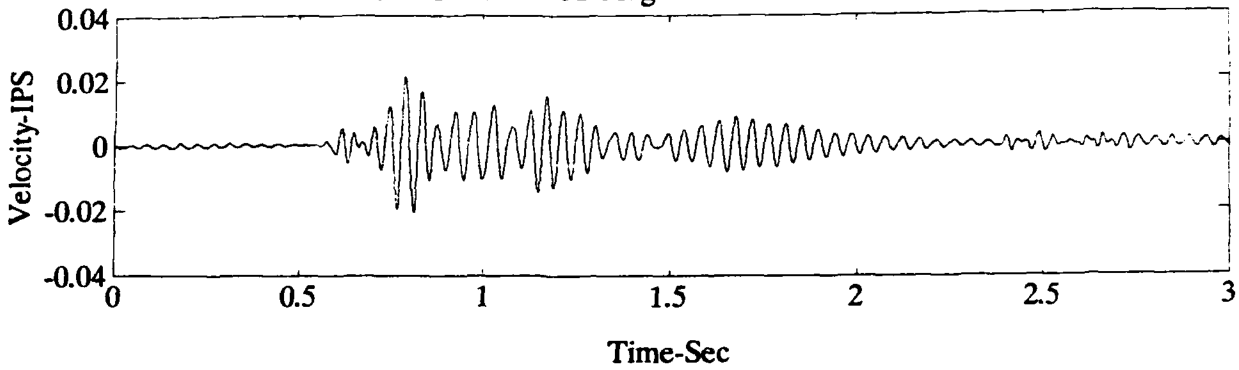

X12 - P - 1450' 31 Aug Plot # 17 max= 0.03088

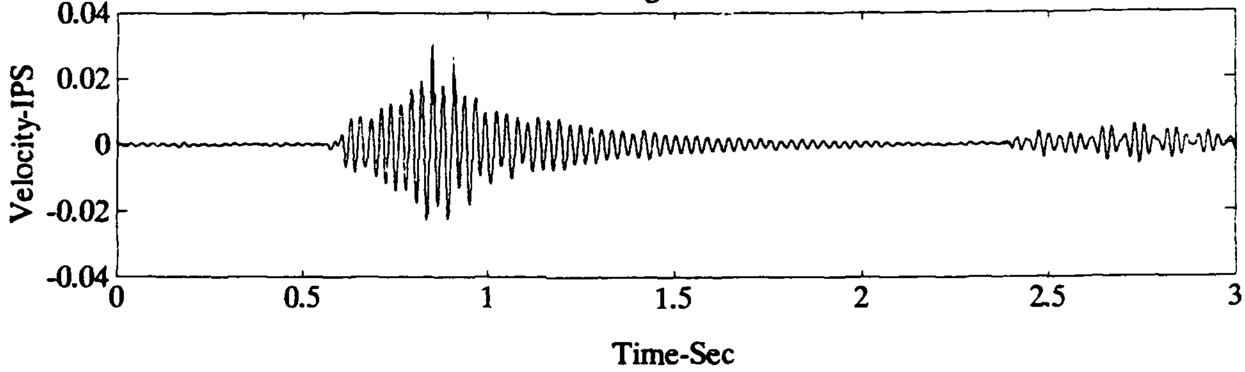

X12 - P - 1450' 31 Aug Plot # 17 max= 0.012

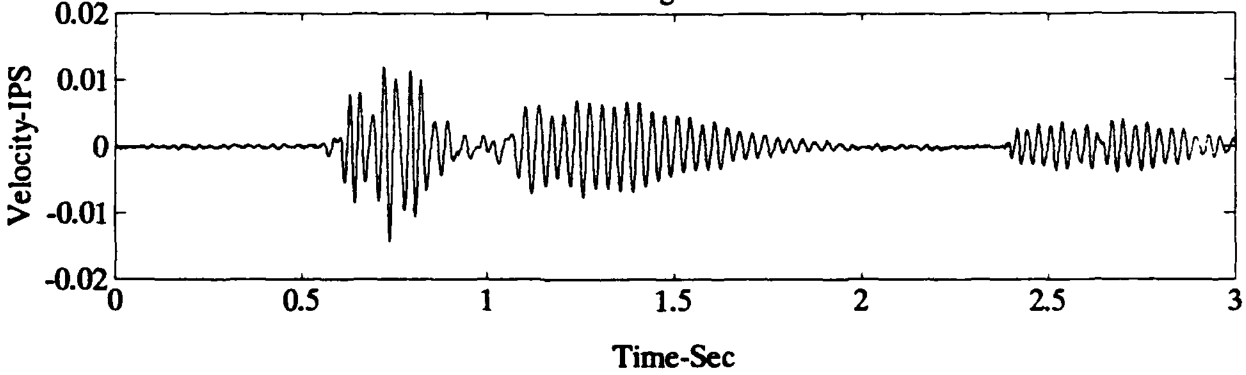

x10-3 X12 - P - 1450' 31 Aug Plot # 17 max= 0.001095

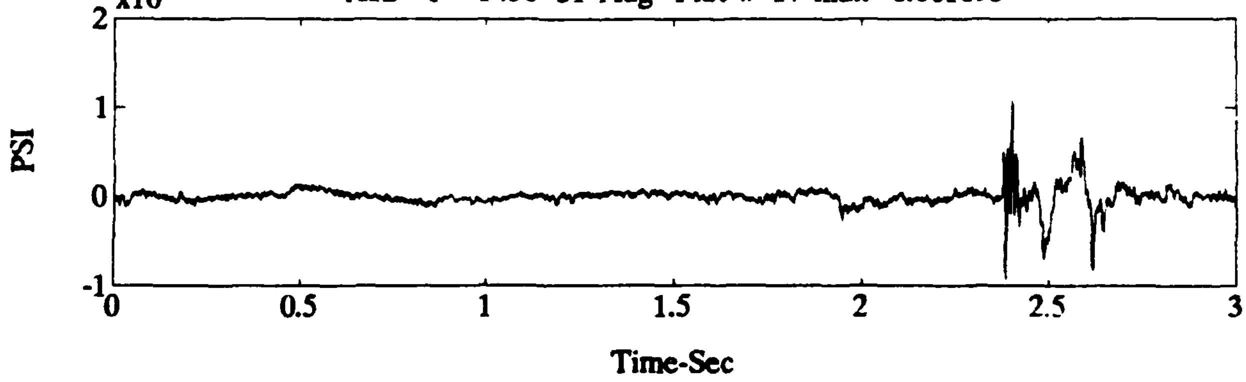

X12 - P - 1450' 31 Aug Plot # 18 max=0.02797

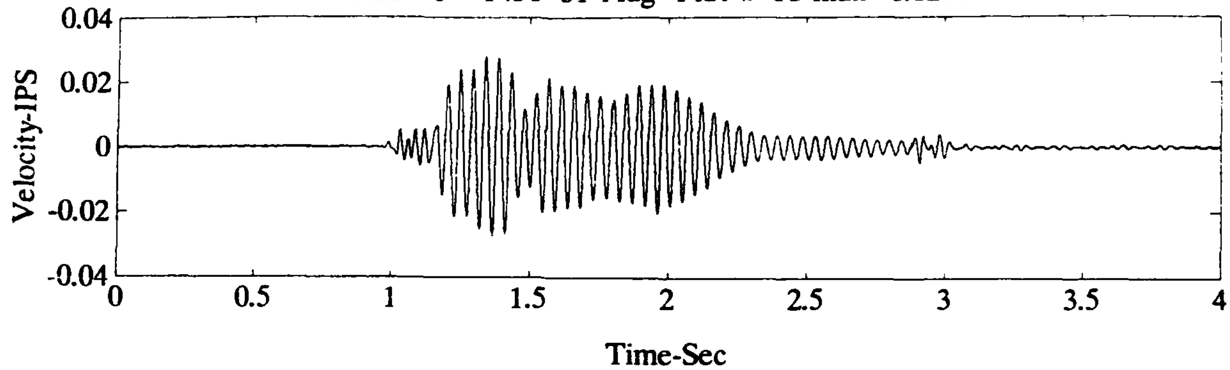

X12 - P - 1450' 31 Aug Plot # 18 max=0.03842

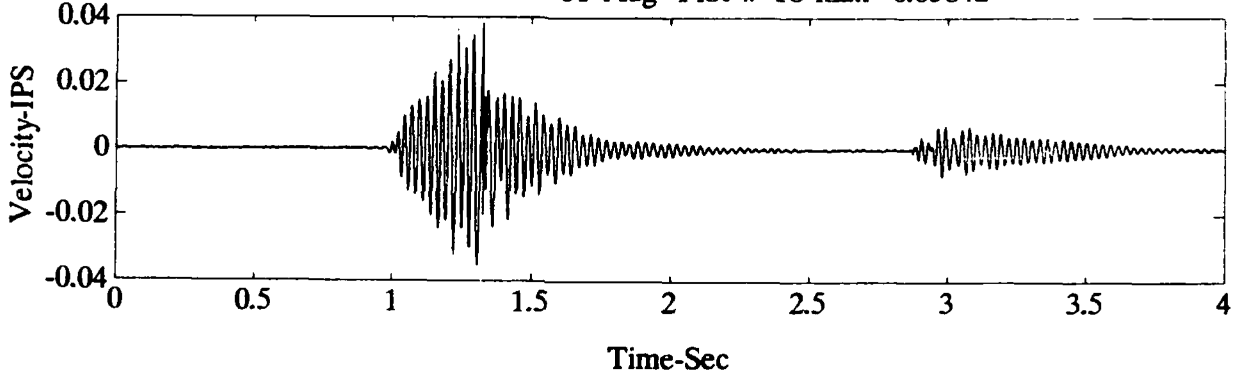

X12 - P - 1450' 31 Aug Plot # 18 max=0.0152

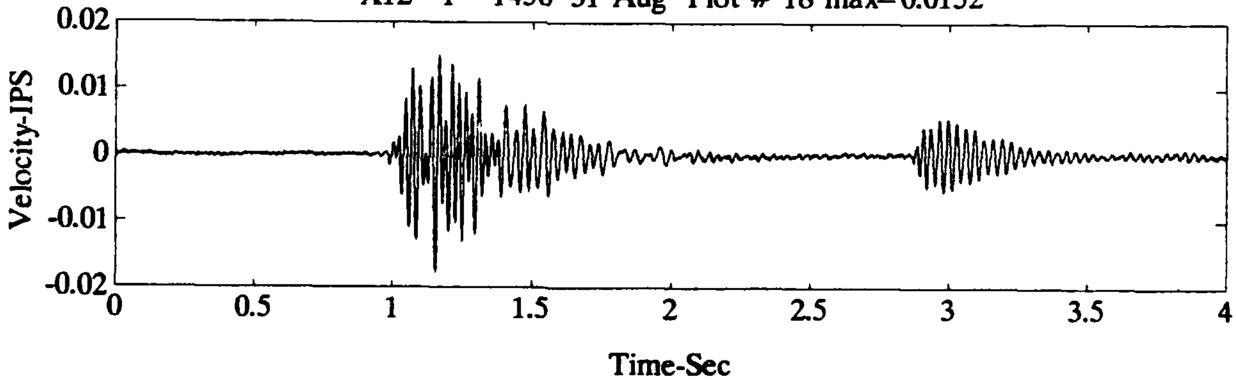

X12 - P - 1450' 31 Aug Plot # 18 max=0.001311

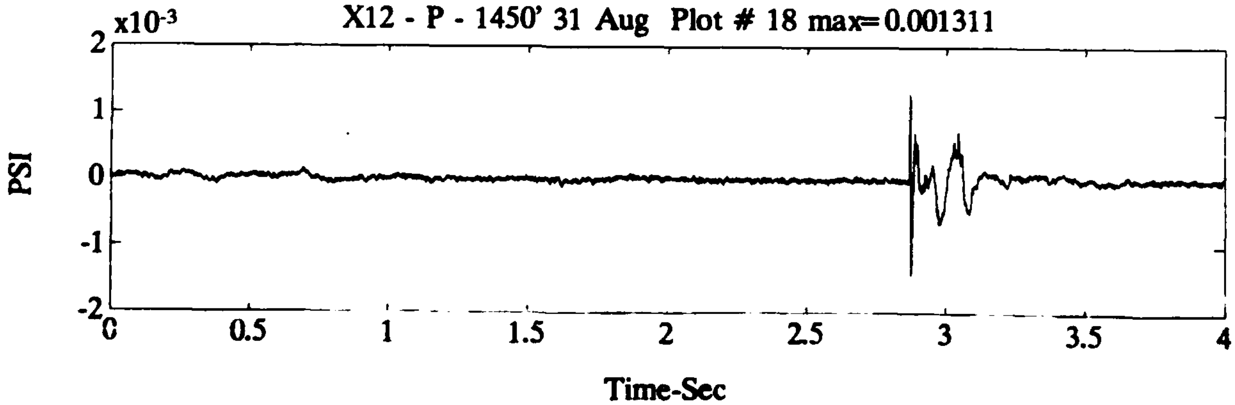

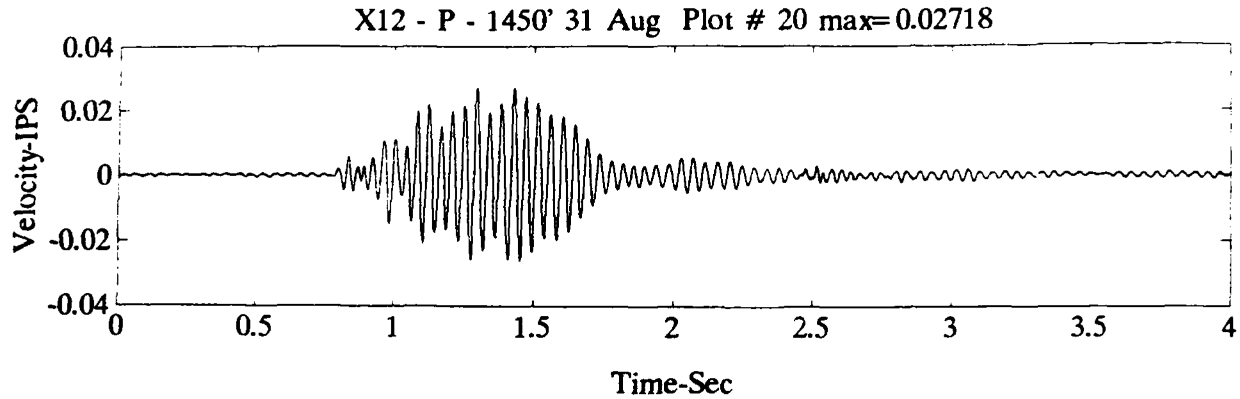
X12 - P - 1450' 31 Aug Plot # 20 max=0.02718
Velocity-IPS
Time-Sec

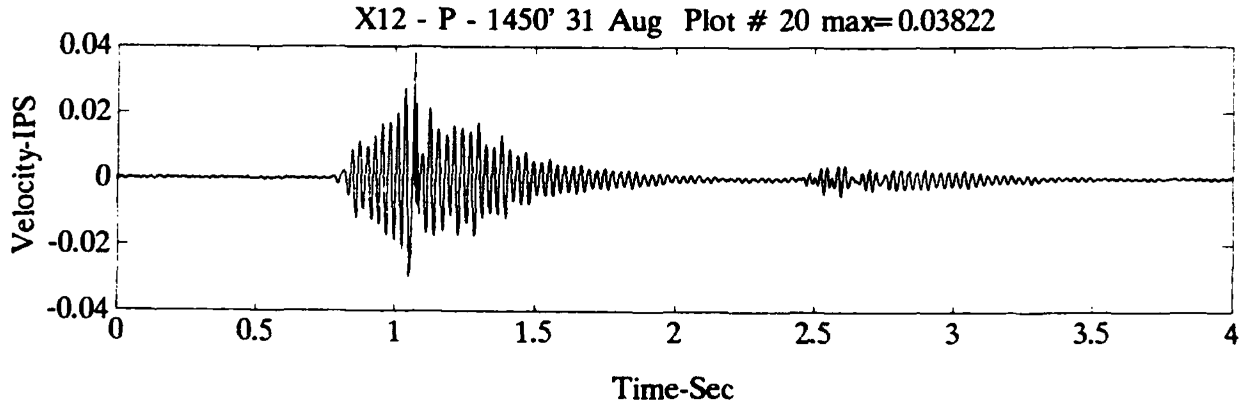
X12 - P - 1450' 31 Aug Plot # 20 max=0.03822
Velocity-IPS
Time-Sec

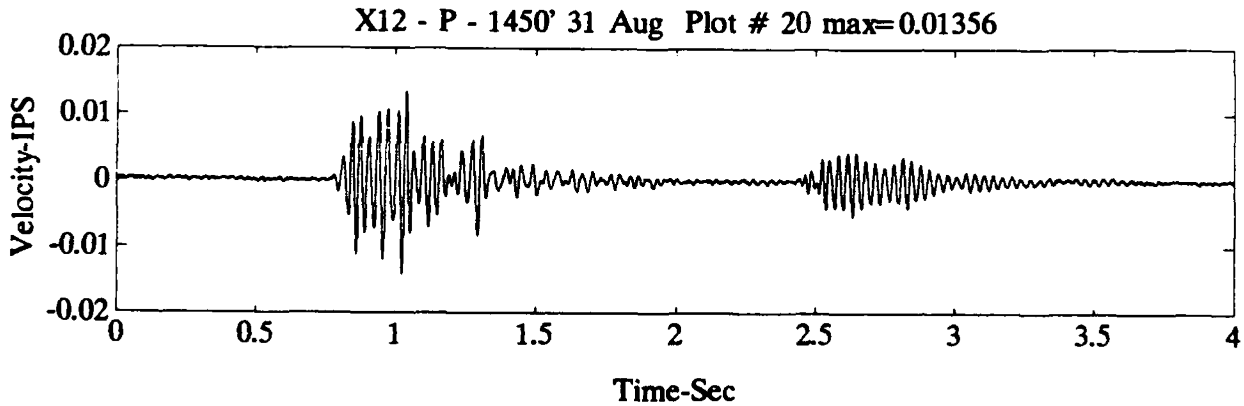
X12 - P - 1450' 31 Aug Plot # 20 max=0.01356
Velocity-IPS
Time-Sec

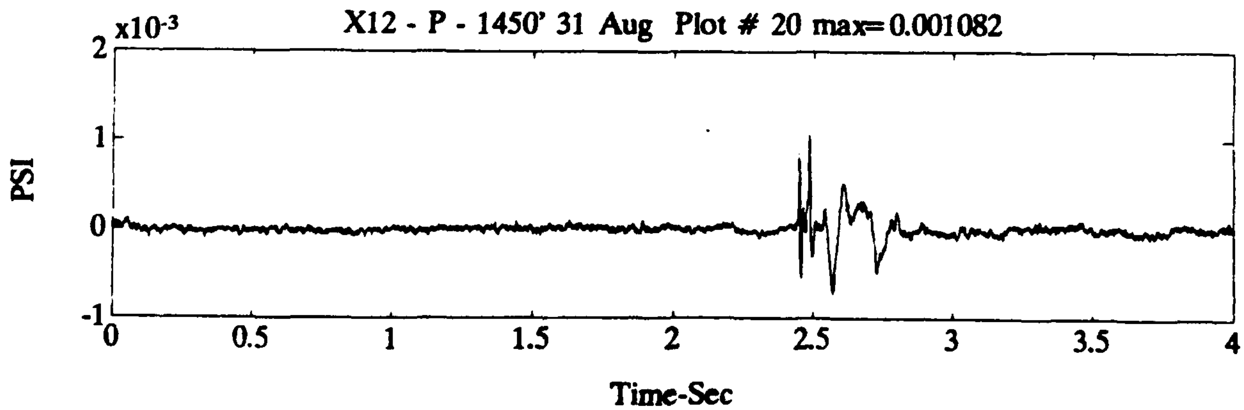
X12 - P - 1450' 31 Aug Plot # 20 max=0.001082
x10-3
PSI
Time-Sec

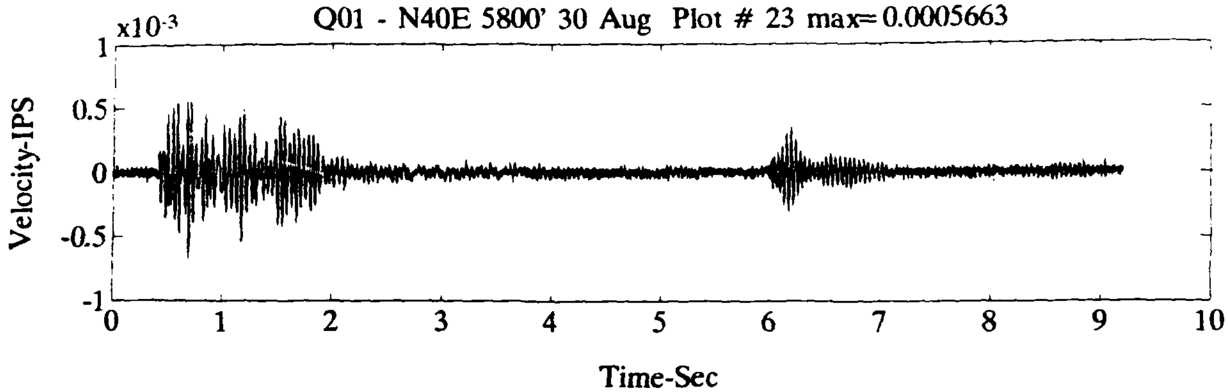
Q01 - N40E 5800' 30 Aug Plot # 23 max=0.0005663
x10-3
Velocity-IPS
Time-Sec

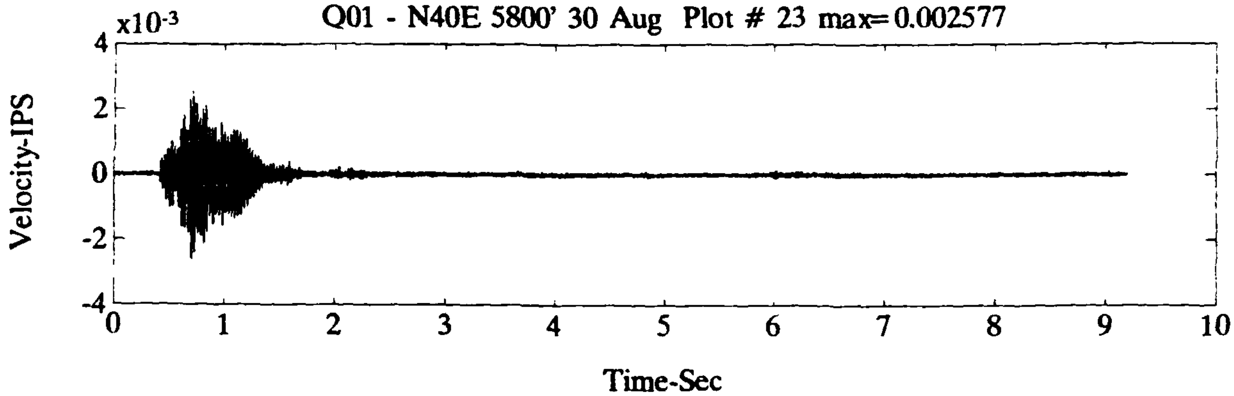
Q01 - N40E 5800' 30 Aug Plot # 23 max=0.002577
x10-3
Velocity-IPS
Time-Sec

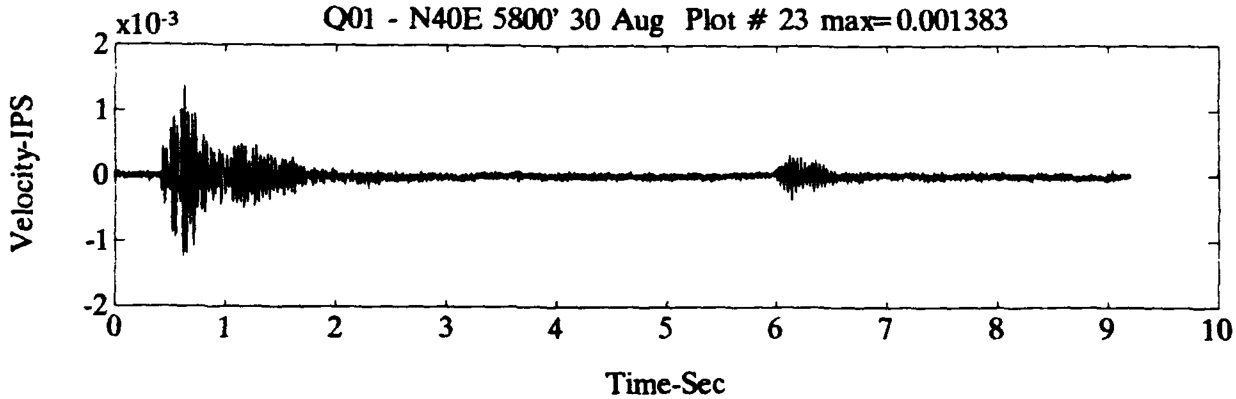
Q01 - N40E 5800' 30 Aug Plot # 23 max=0.001383
x10-3
Velocity-IPS
Time-Sec

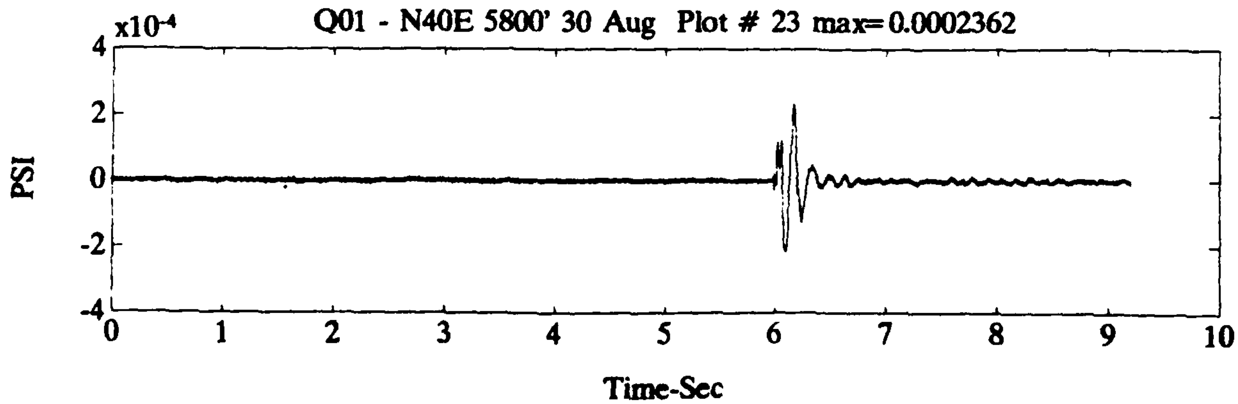
Q01 - N40E 5800' 30 Aug Plot # 23 max=0.0002362
x10-4
PSI
Time-Sec

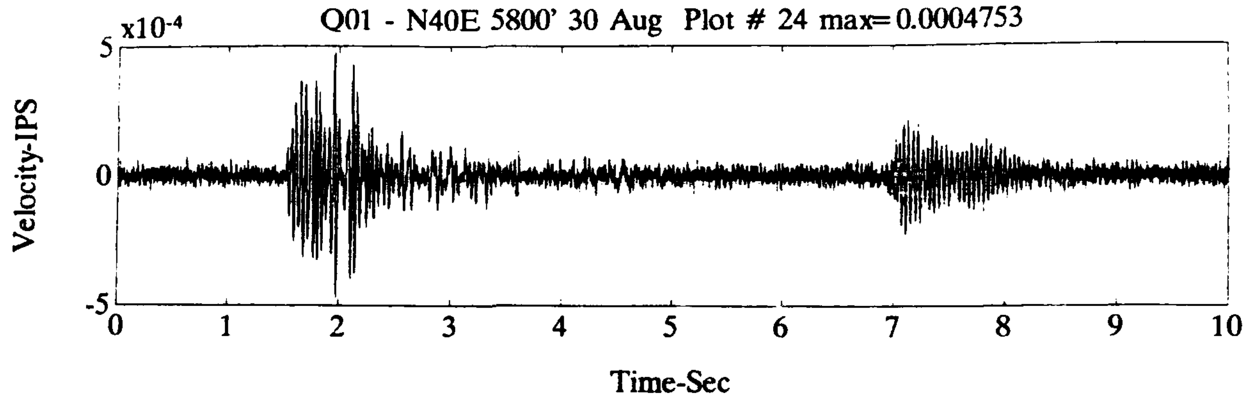
Q01 - N40E 5800' 30 Aug Plot # 24 max=0.0004753
x10-4
Velocity-IPS
Time-Sec

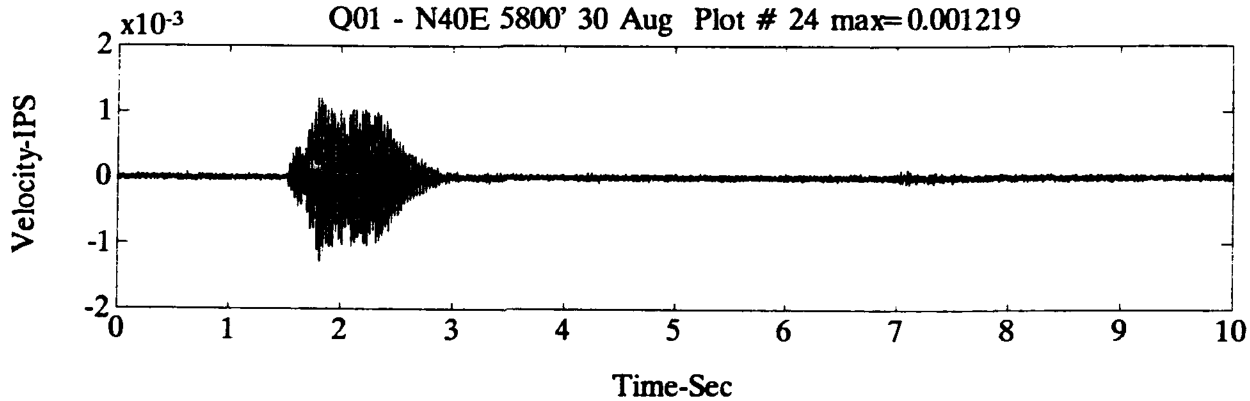
Q01 - N40E 5800' 30 Aug Plot # 24 max=0.001219
x10-3
Velocity-IPS
Time-Sec

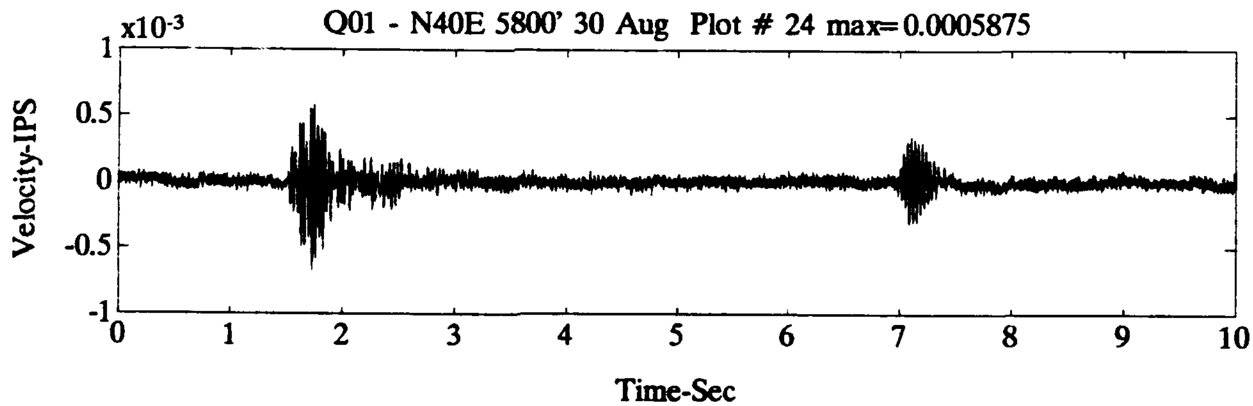
Q01 - N40E 5800' 30 Aug Plot # 24 max=0.0005875
x10-3
Velocity-IPS
Time-Sec

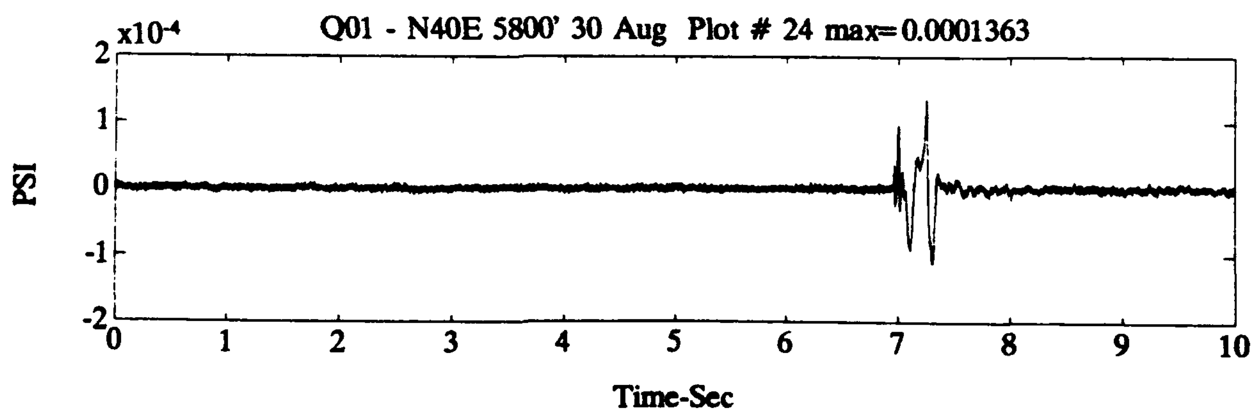
Q01 - N40E 5800' 30 Aug Plot # 24 max=0.0001363
x10-4
PSI
Time-Sec

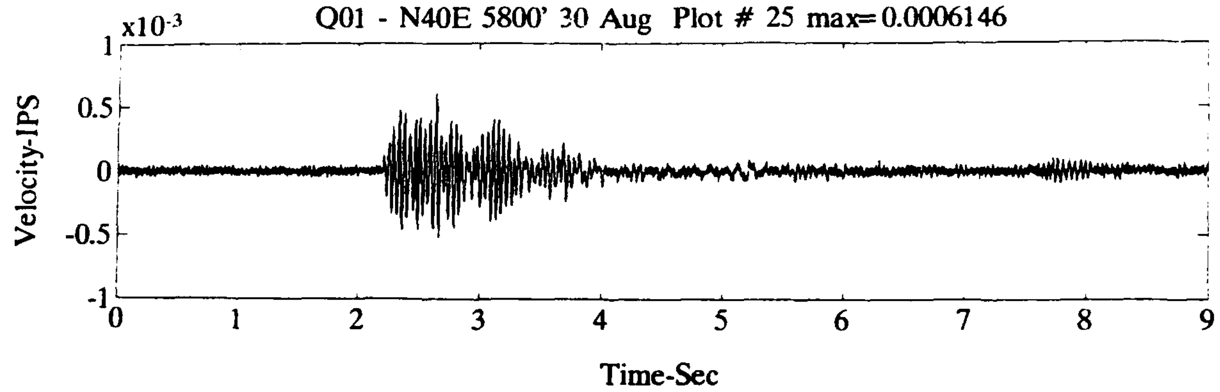
Q01 - N40E 5800' 30 Aug Plot # 25 max=0.0006146
x10-3
Velocity-IPS
Time-Sec

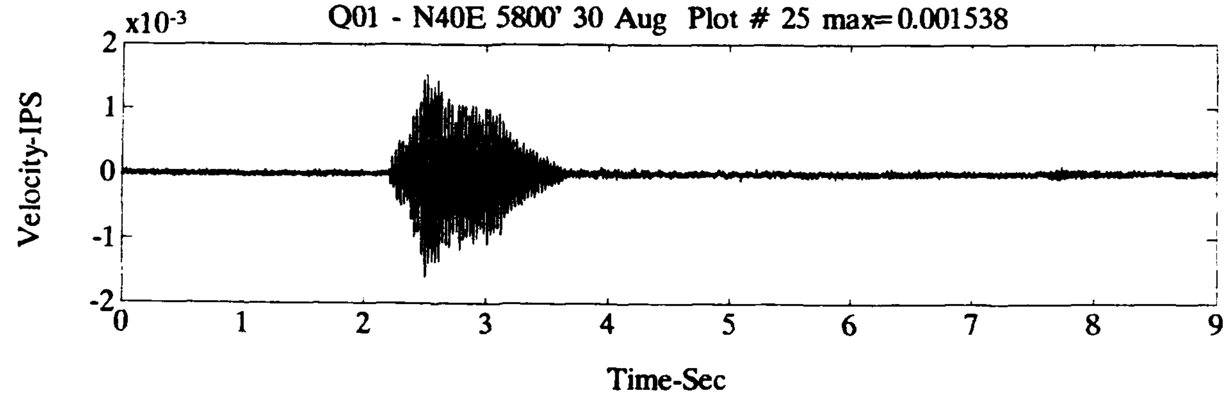
Q01 - N40E 5800' 30 Aug Plot # 25 max=0.001538
x10-3
Velocity-IPS
Time-Sec

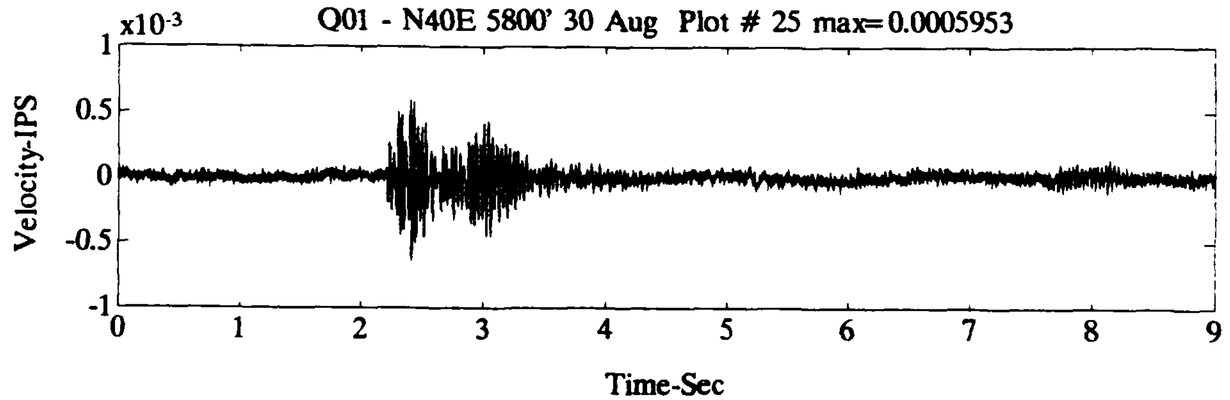
Q01 - N40E 5800' 30 Aug Plot # 25 max=0.0005953
x10-3
Velocity-IPS
Time-Sec

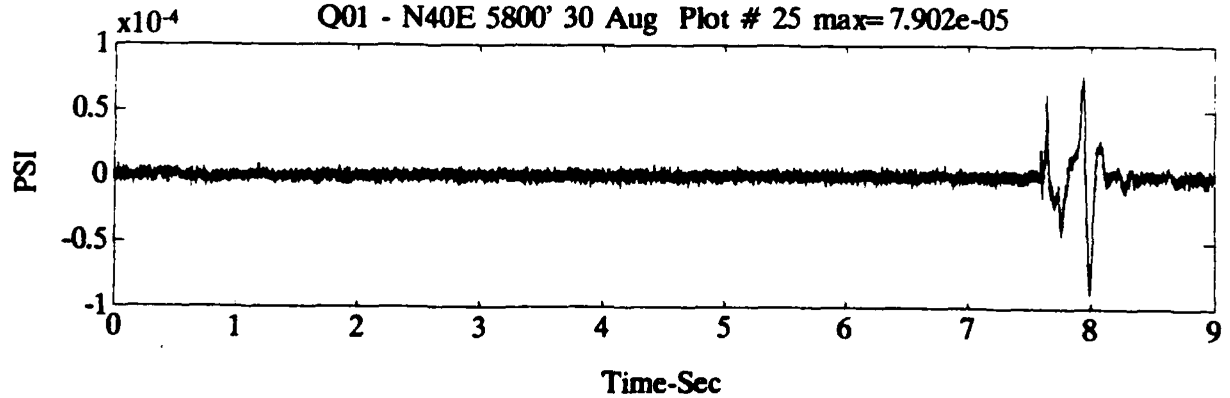
Q01 - N40E 5800' 30 Aug Plot # 25 max=7.902e-05
x10-4
PSI
Time-Sec

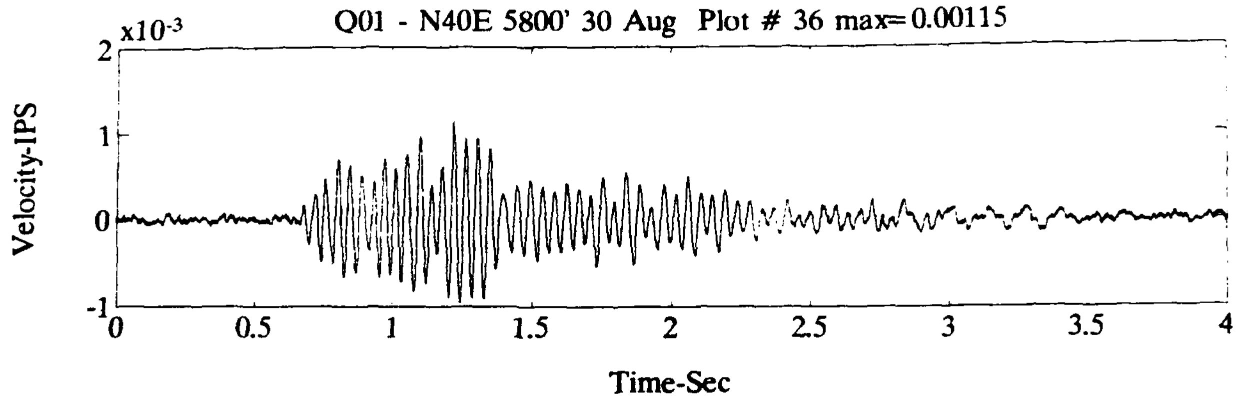
Q01 - N40E 5800' 30 Aug Plot # 36 max=0.00115
x10-3
Velocity-IPS
2
1
0
-1
0
0.5
1
1.5
2
2.5
3
3.5
4
Time-Sec

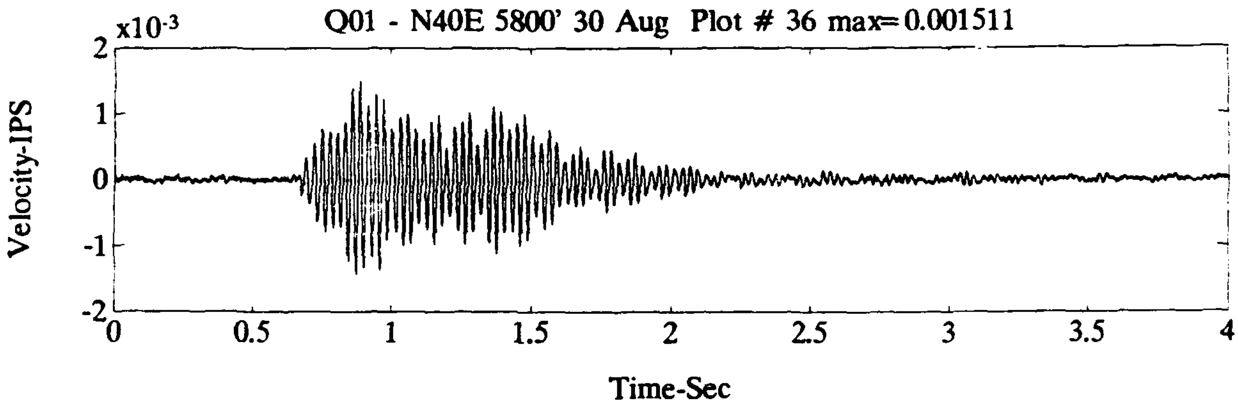
Q01 - N40E 5800' 30 Aug Plot # 36 max=0.001511
x10-3
Velocity-IPS
2
1
0
-1
-2
0
0.5
1
1.5
2
2.5
3
3.5
4
Time-Sec

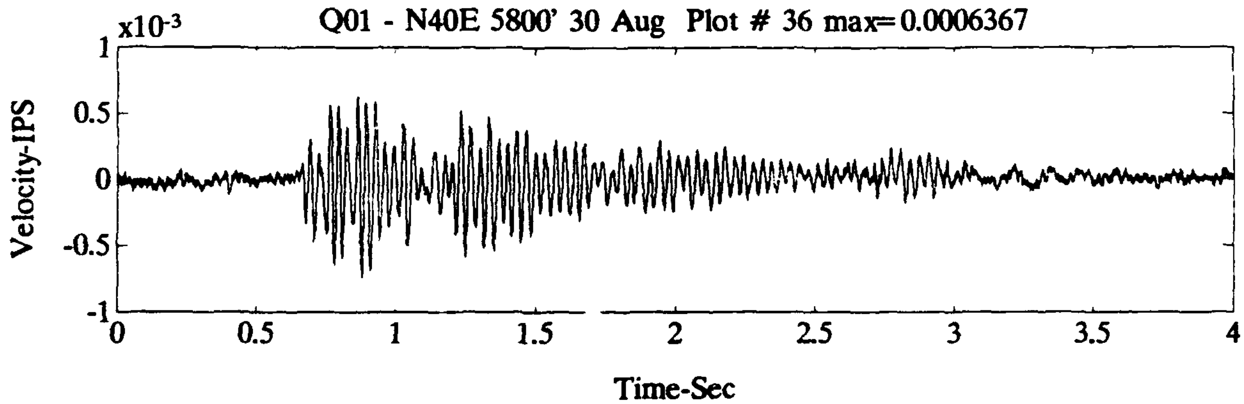
Q01 - N40E 5800' 30 Aug Plot # 36 max=0.0006367
x10-3
Velocity-IPS
1
0.5
0
-0.5
-1
0
0.5
1
1.5
2
2.5
3
3.5
4
Time-Sec

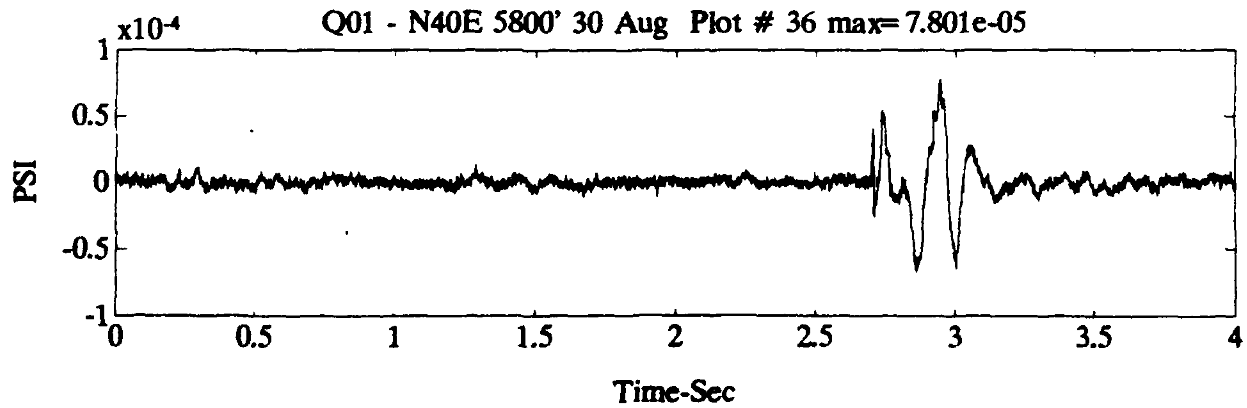
Q01 - N40E 5800' 30 Aug Plot # 36 max=7.801e-05
x10-4
PSI
1
0.5
0
-0.5
-1
0
0.5
1
1.5
2
2.5
3
3.5
4
Time-Sec

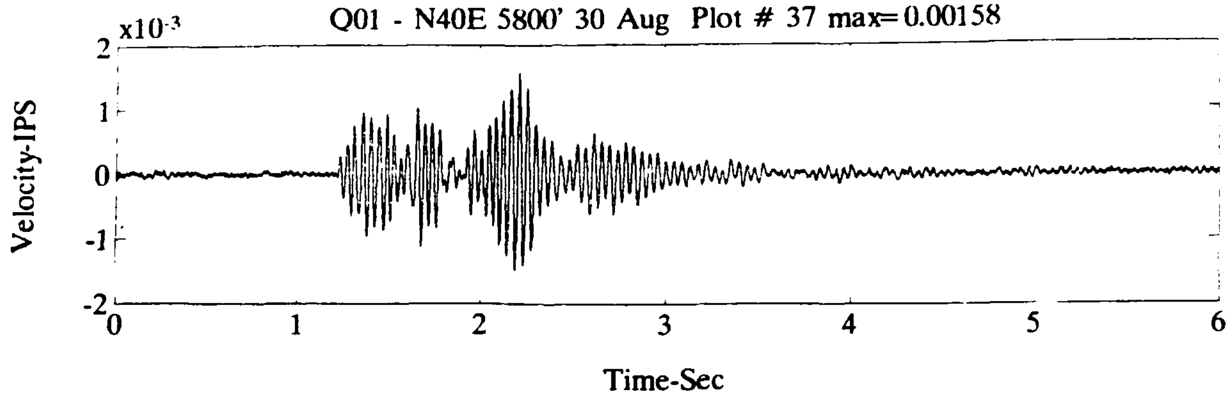
Q01 - N40E 5800' 30 Aug Plot # 37 max=0.00158
x10-3
Velocity-IPS
Time-Sec

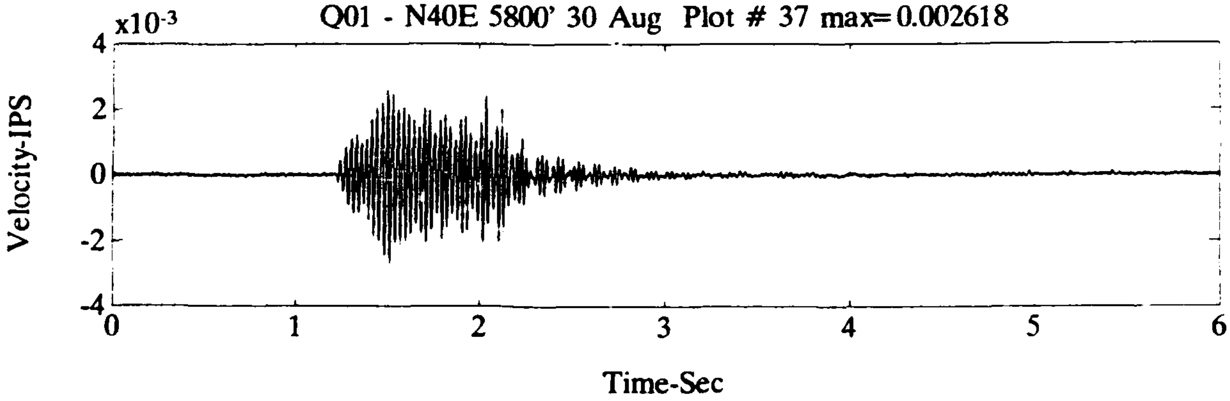
Q01 - N40E 5800' 30 Aug Plot # 37 max=0.002618
x10-3
Velocity-IPS
Time-Sec

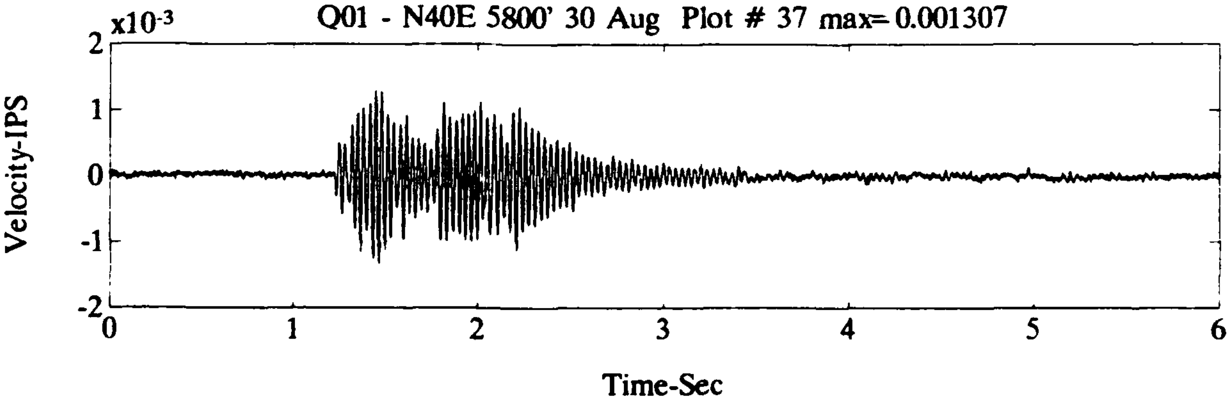
Q01 - N40E 5800' 30 Aug Plot # 37 max=0.001307
x10-3
Velocity-IPS
Time-Sec

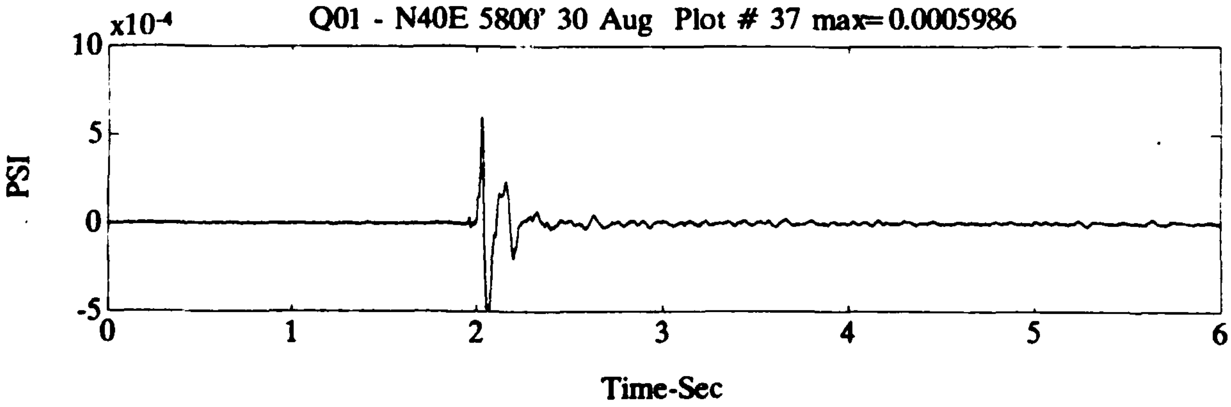
Q01 - N40E 5800' 30 Aug Plot # 37 max=0.0005986
x10-4
PSI
Time-Sec

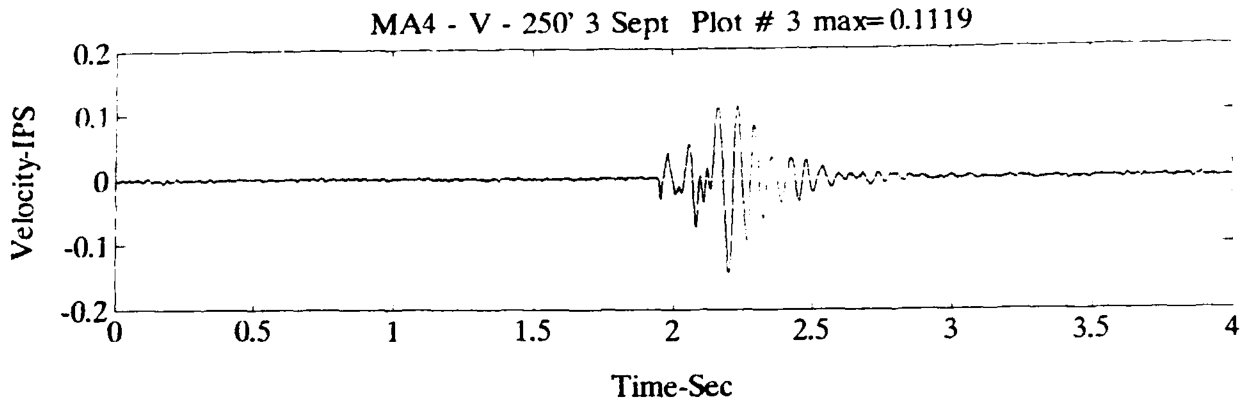
MA4 - V - 250' 3 Sept Plot # 3 max=0.1119
Velocity-IPS
Time-Sec

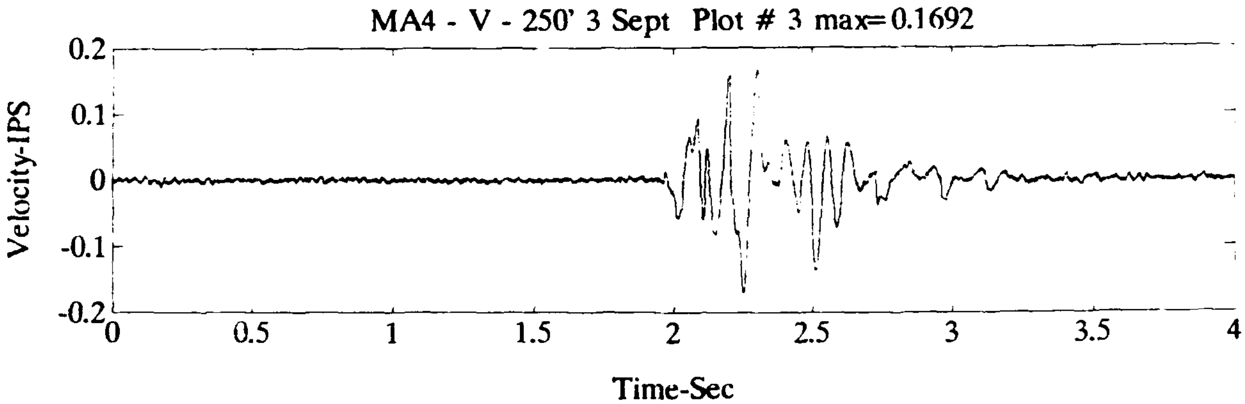
MA4 - V - 250' 3 Sept Plot # 3 max=0.1692
Velocity-IPS
Time-Sec

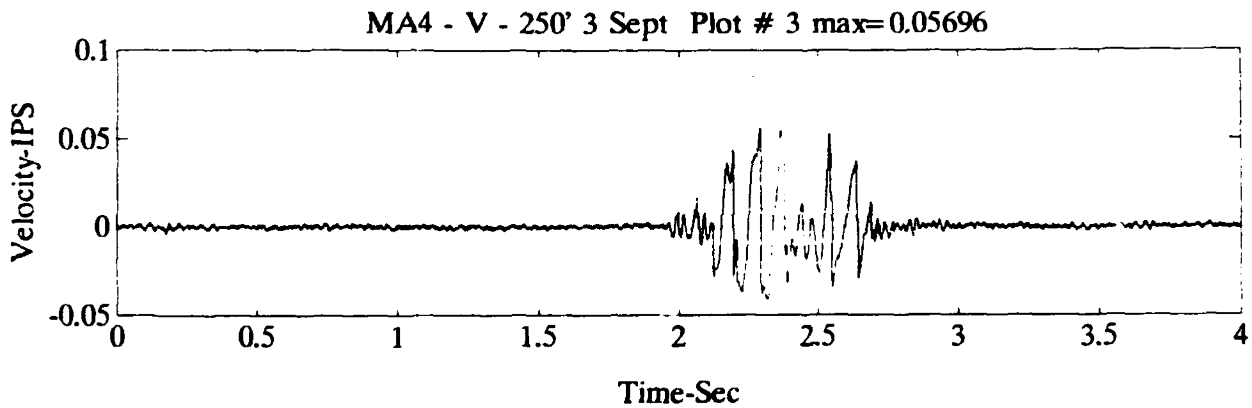
MA4 - V - 250' 3 Sept Plot # 3 max=0.05696
Velocity-IPS
Time-Sec

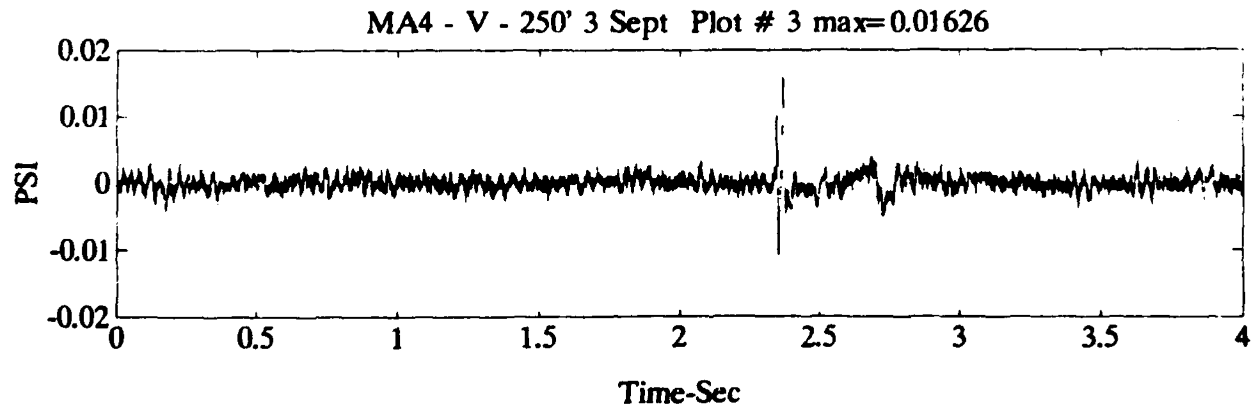
MA4 - V - 250' 3 Sept Plot # 3 max=0.01626
PSI
Time-Sec

MA4 - V - 250' 3 Sept Plot # 10 max=0.06813

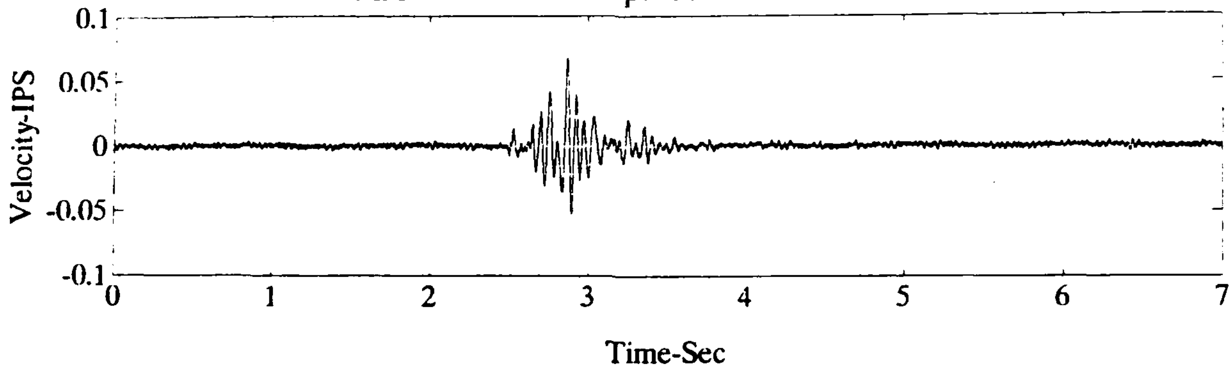

MA4 - V - 250' 3 Sept Plot # 10 max=0.06178

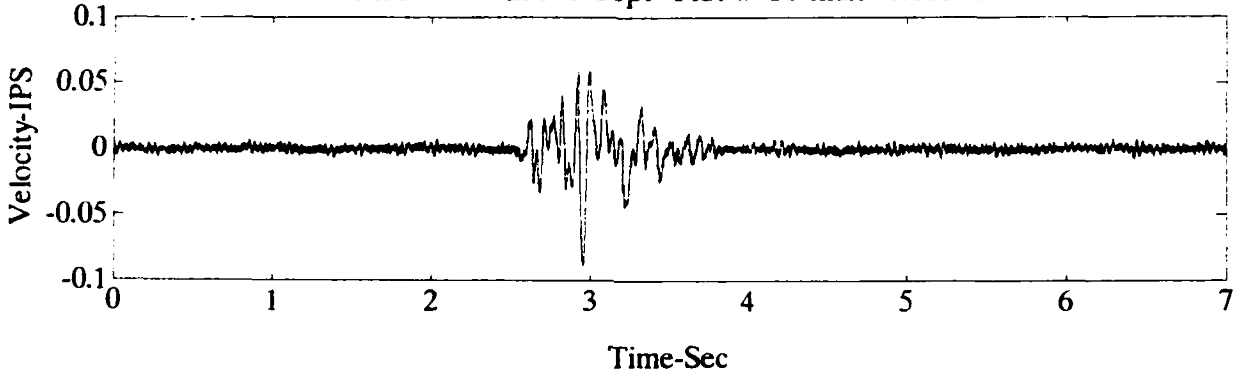

MA4 - V - 250' 3 Sept Plot # 10 max=0.04018

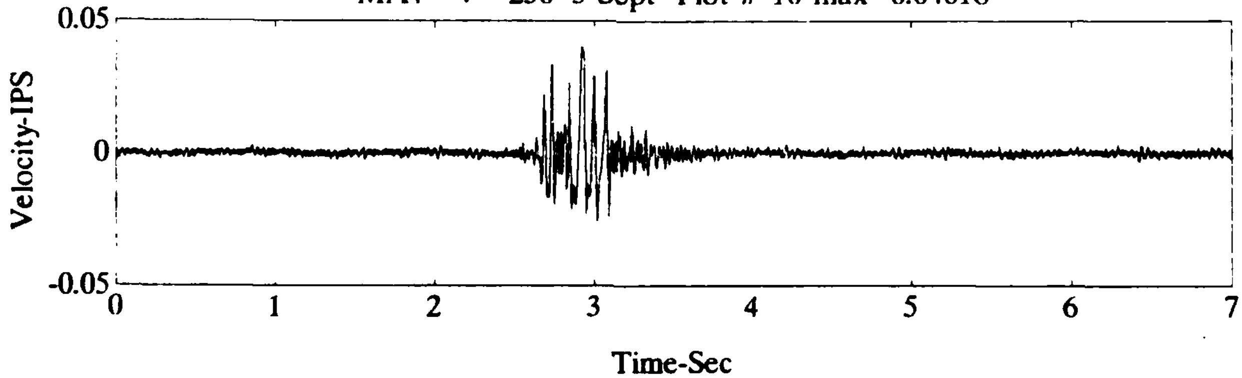

MA4 - V - 250' 3 Sept Plot # 10 max=0.02308

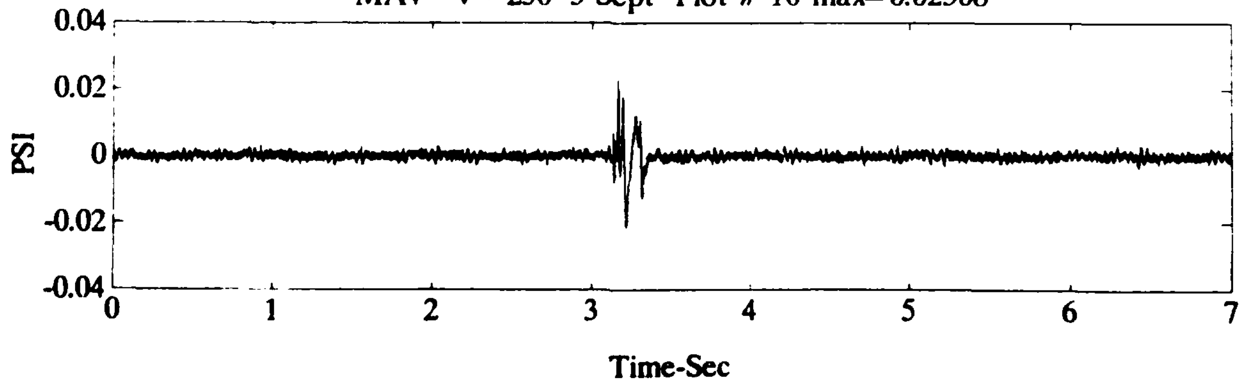

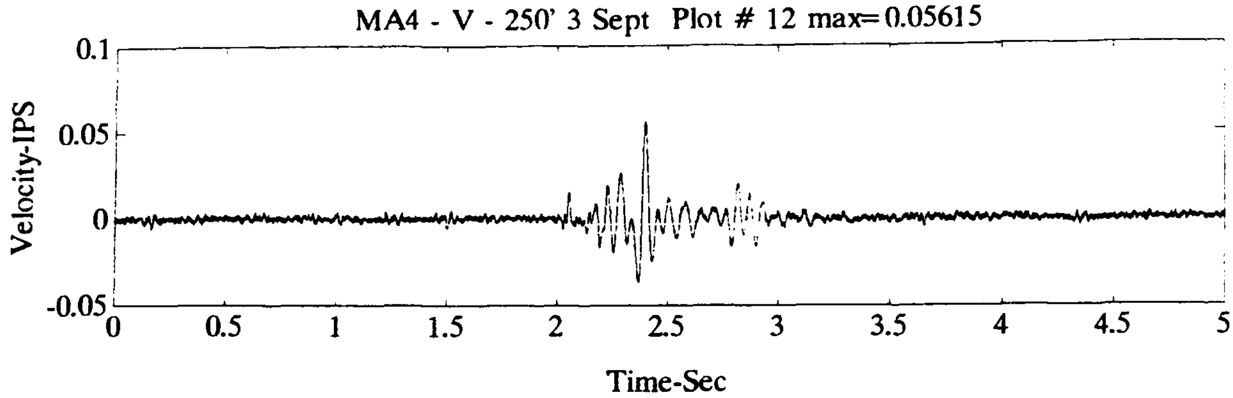
MA4 - V - 250' 3 Sept Plot # 12 max=0.05615
Velocity-IPS
0.1
0.05
0
-0.05
0
0.5
1
1.5
2
2.5
3
3.5
4
4.5
5
Time-Sec

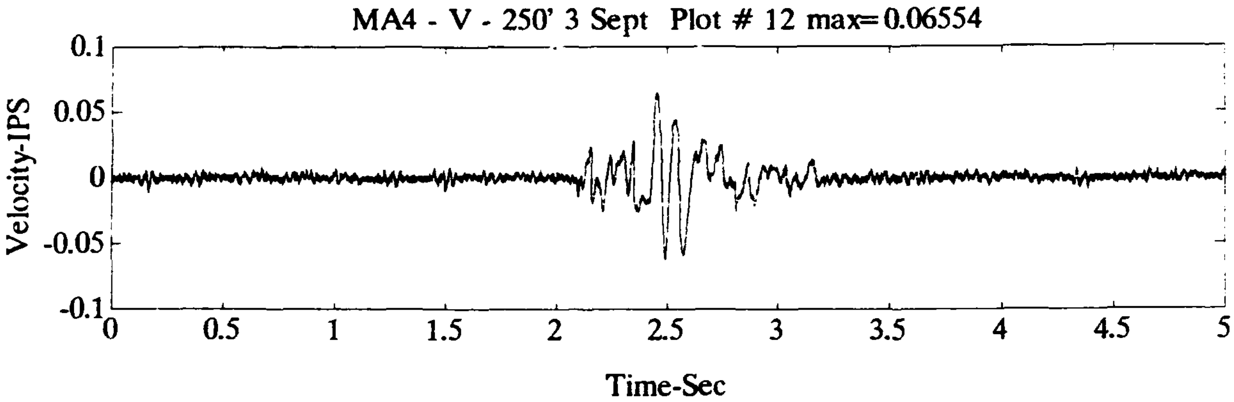
MA4 - V - 250' 3 Sept Plot # 12 max=0.06554
Velocity-IPS
0.1
0.05
0
-0.05
-0.1
0
0.5
1
1.5
2
2.5
3
3.5
4
4.5
5
Time-Sec

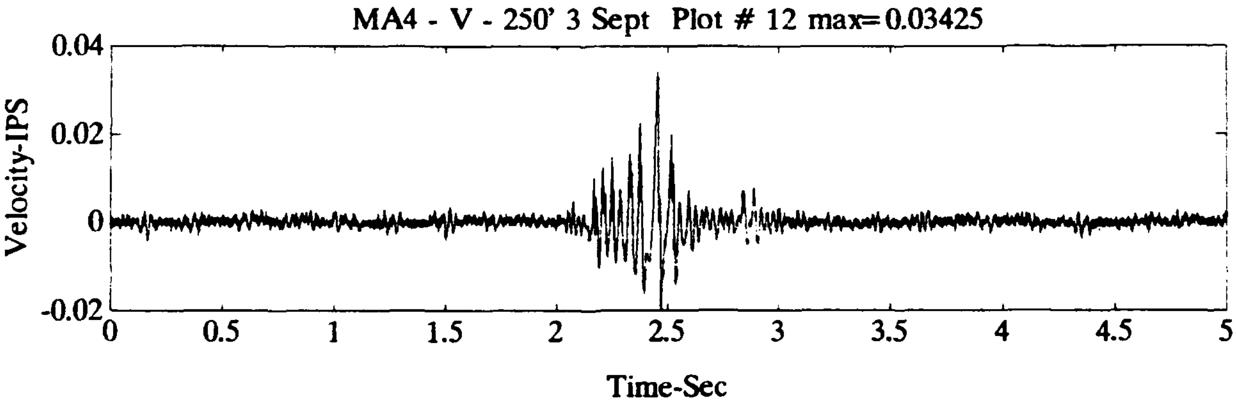
MA4 - V - 250' 3 Sept Plot # 12 max=0.03425
Velocity-IPS
0.04
0.02
0
-0.02
0
0.5
1
1.5
2
2.5
3
3.5
4
4.5
5
Time-Sec

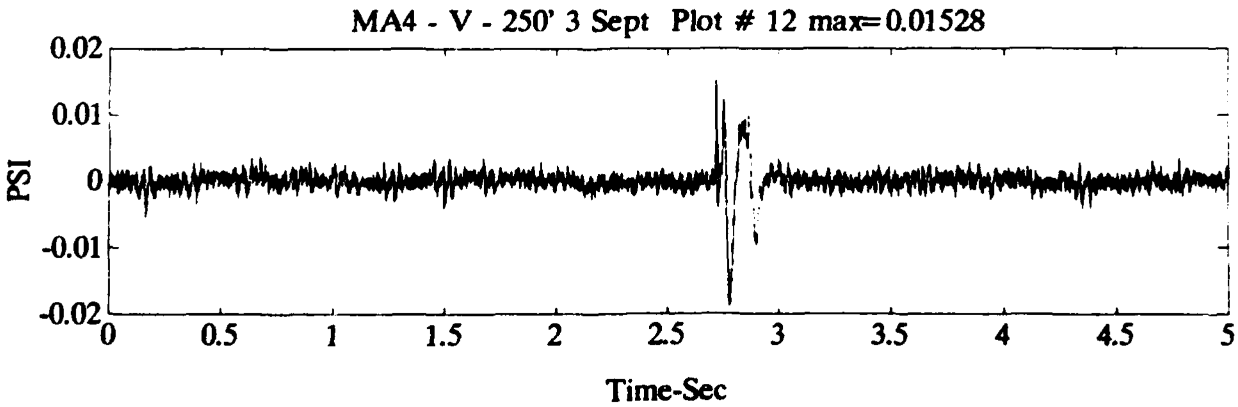
MA4 - V - 250' 3 Sept Plot # 12 max=0.01528
PSI
0.02
0.01
0
-0.01
-0.02
0
0.5
1
1.5
2
2.5
3
3.5
4
4.5
5
Time-Sec

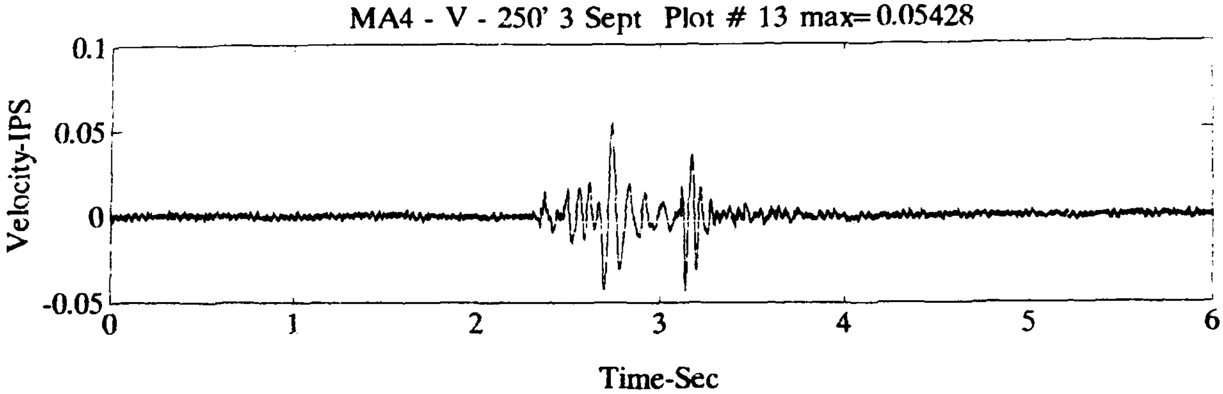
MA4 - V - 250' 3 Sept Plot # 13 max=0.05428
Velocity-IPS
Time-Sec

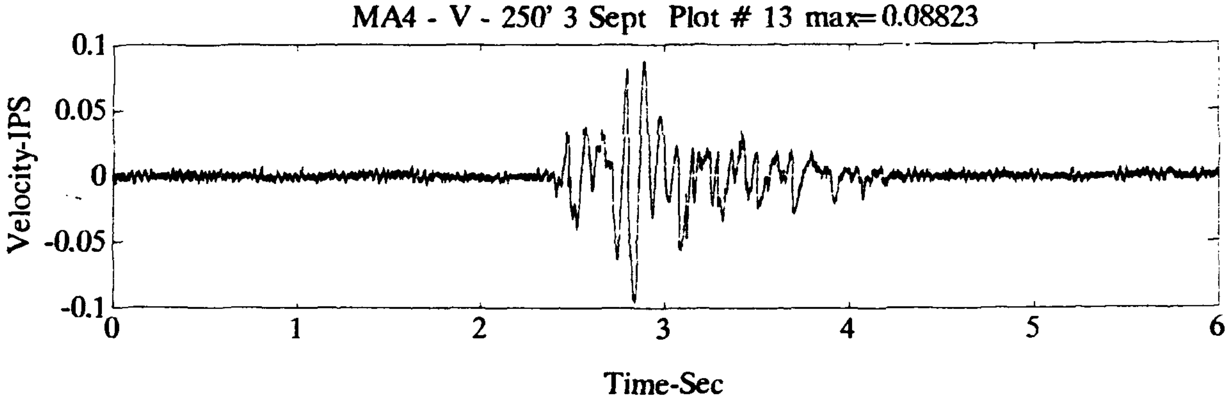
MA4 - V - 250' 3 Sept Plot # 13 max=0.08823
Velocity-IPS
Time-Sec

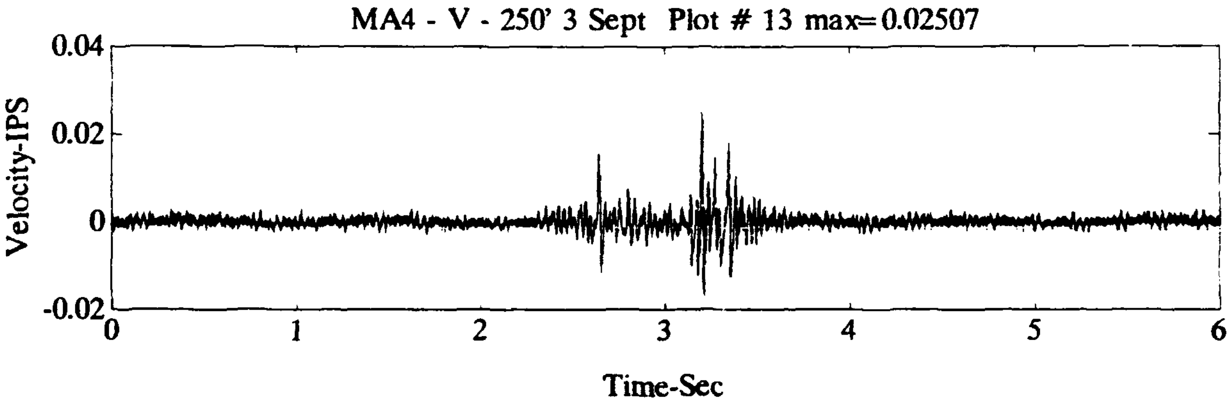
MA4 - V - 250' 3 Sept Plot # 13 max=0.02507
Velocity-IPS
Time-Sec

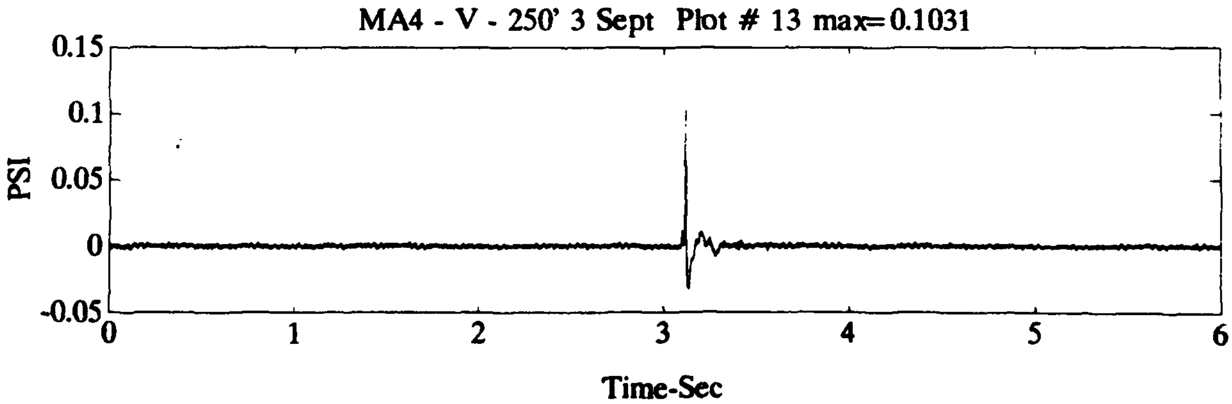
MA4 - V - 250' 3 Sept Plot # 13 max=0.1031
PSI
Time-Sec

MA4 - V - 250' 3 Sept Plot # 22 max=0.0356

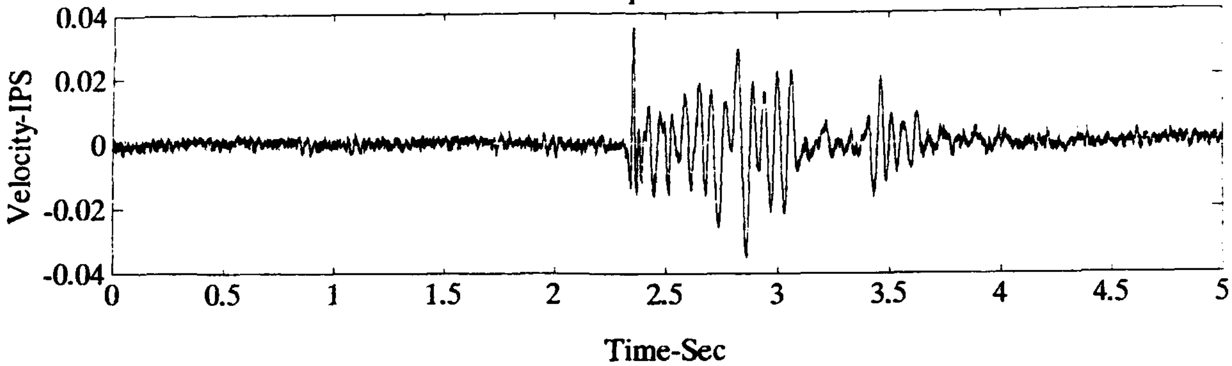

MA4 - V - 250' 3 Sept Plot # 22 max=0.04368

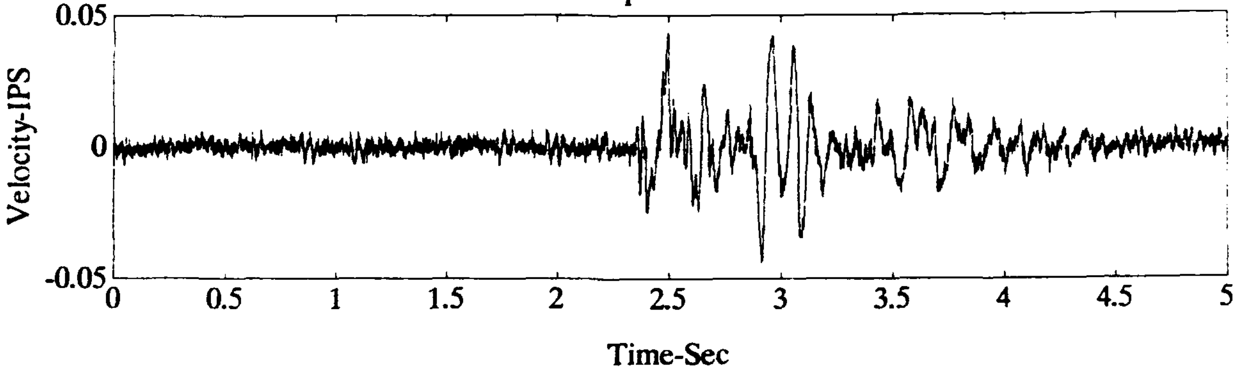

MA4 - V - 250' 3 Sept Plot # 22 max=0.0244

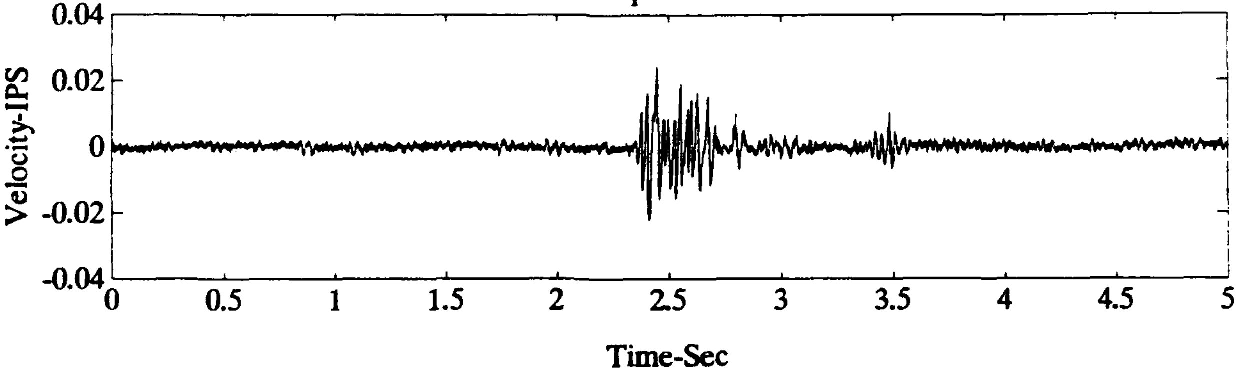

MA4 - V - 250' 3 Sept Plot # 22 max=0.02832

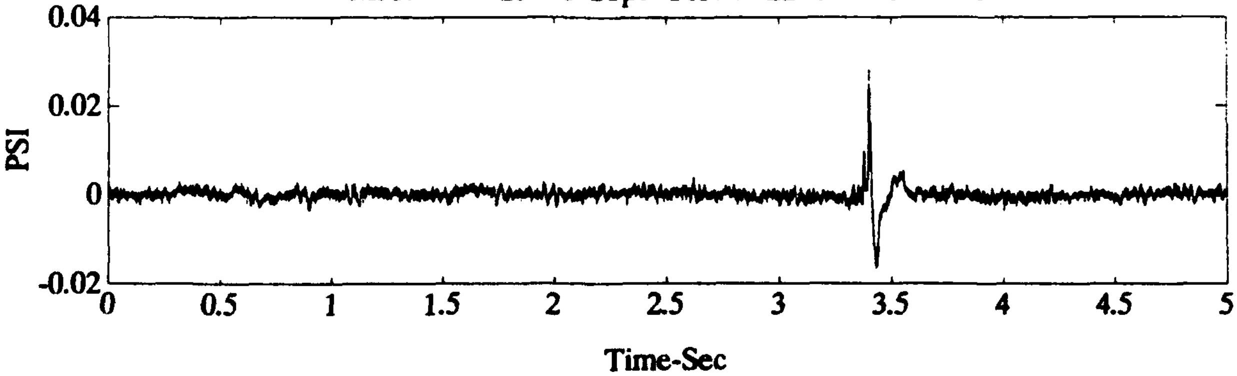

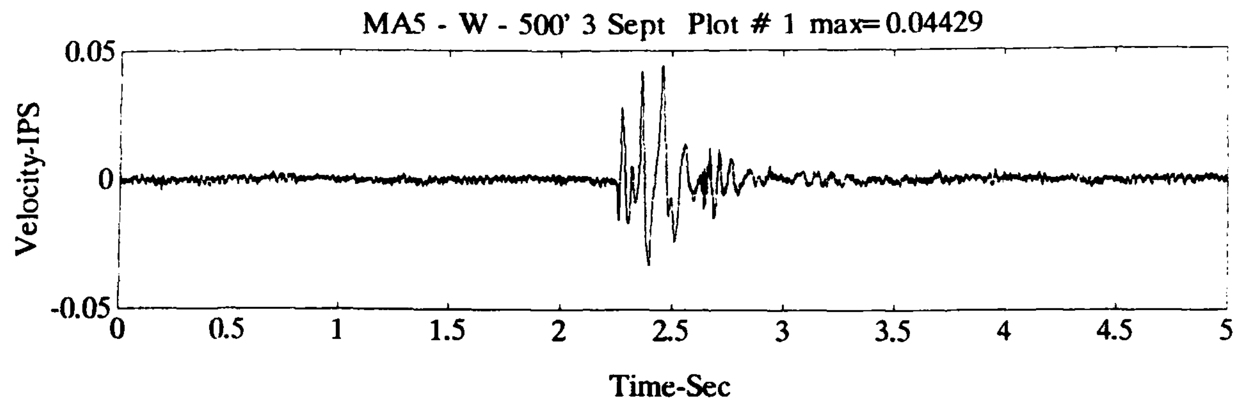
MA5 - W - 500' 3 Sept Plot # 1 max= 0.04429
Velocity-IPS
Time-Sec

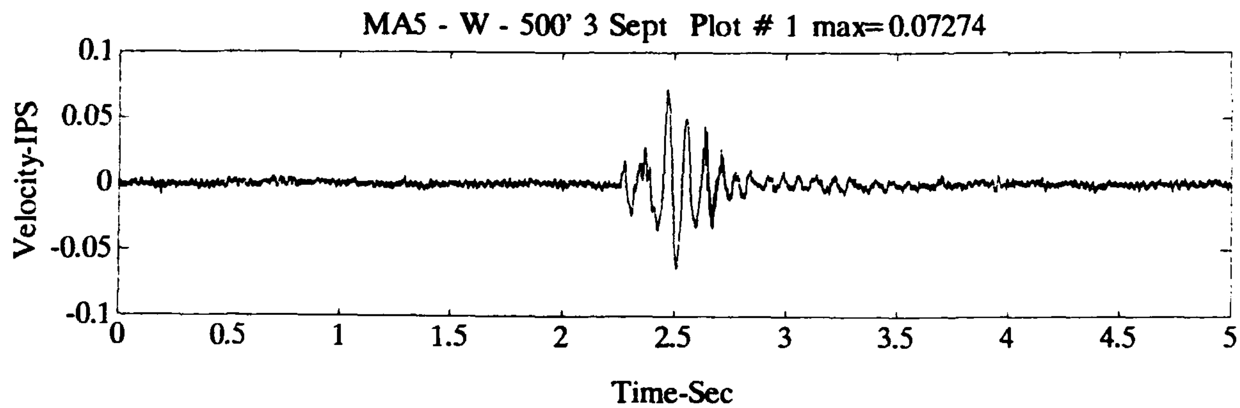
MA5 - W - 500' 3 Sept Plot # 1 max= 0.07274
Velocity-IPS
Time-Sec

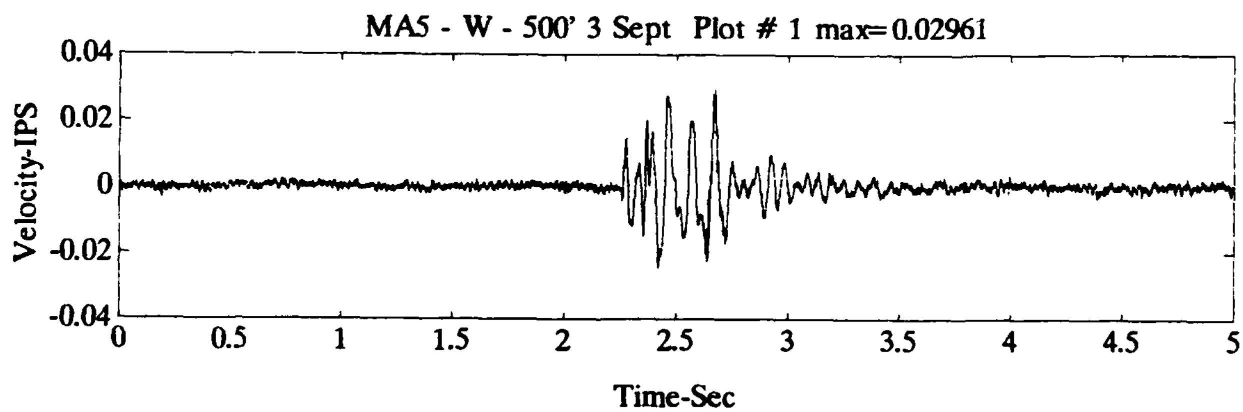
MA5 - W - 500' 3 Sept Plot # 1 max= 0.02961
Velocity-IPS
Time-Sec

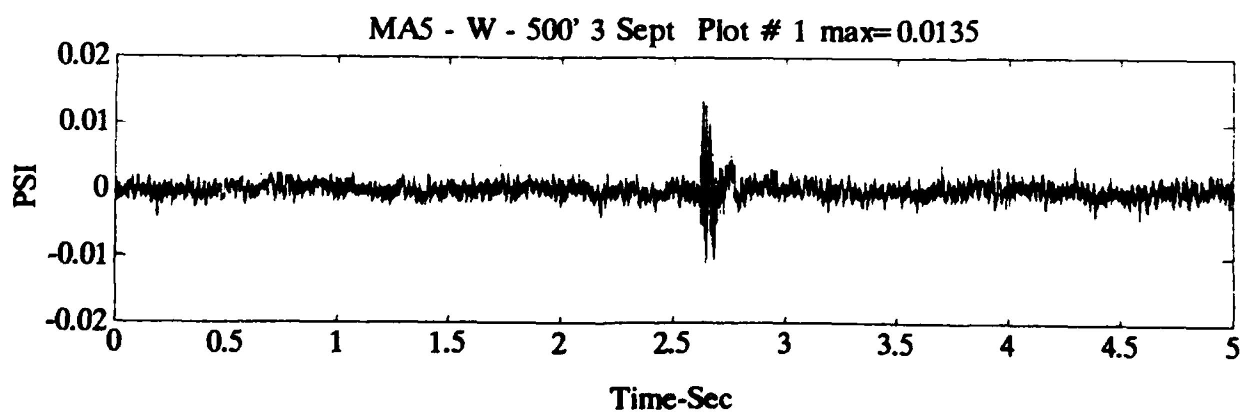
MA5 - W - 500' 3 Sept Plot # 1 max= 0.0135
PSI
Time-Sec

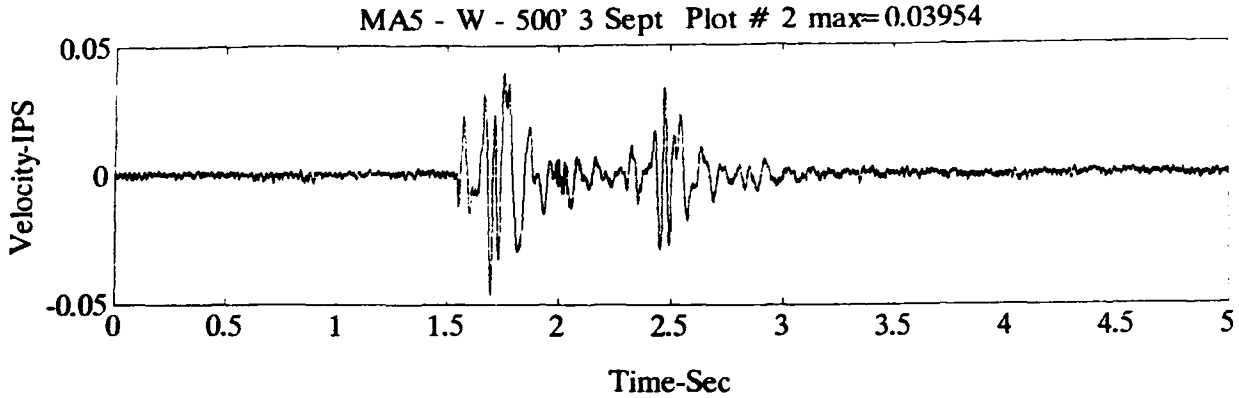
MA5 - W - 500' 3 Sept Plot # 2 max=0.03954
Velocity-IPS
0.05
0
-0.05
0
0.5
1
1.5
2
2.5
3
3.5
4
4.5
5
Time-Sec

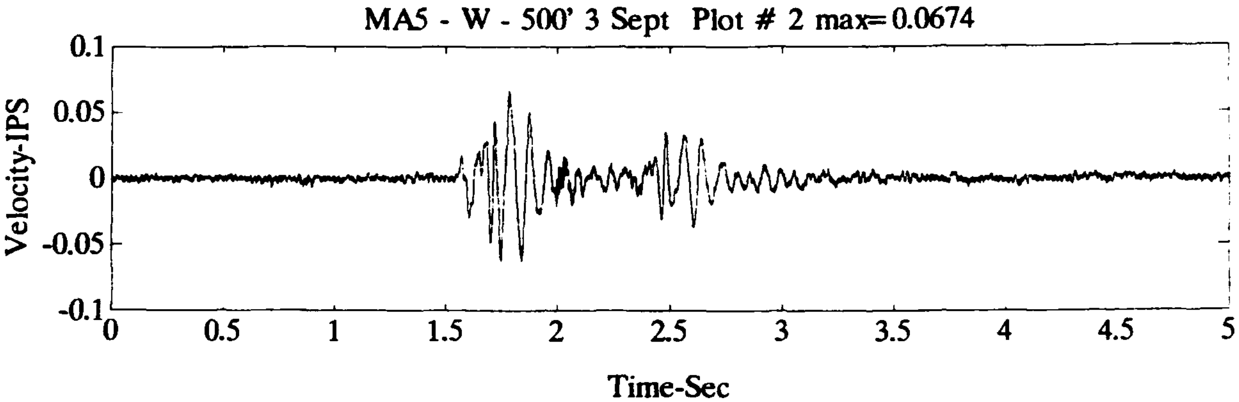
MA5 - W - 500' 3 Sept Plot # 2 max=0.0674
Velocity-IPS
0.1
0.05
0
-0.05
-0.1
0
0.5
1
1.5
2
2.5
3
3.5
4
4.5
5
Time-Sec

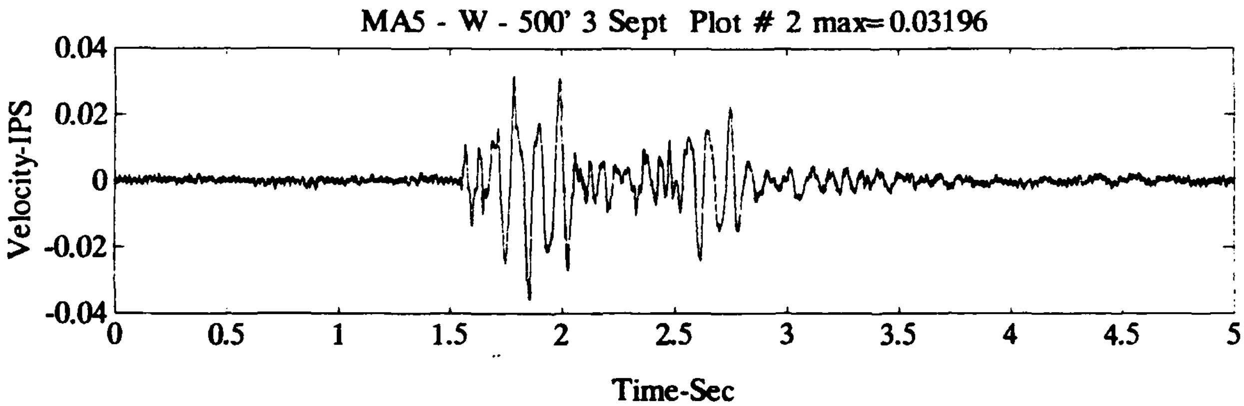
MA5 - W - 500' 3 Sept Plot # 2 max=0.03196
Velocity-IPS
0.04
0.02
0
-0.02
-0.04
0
0.5
1
1.5
2
2.5
3
3.5
4
4.5
5
Time-Sec

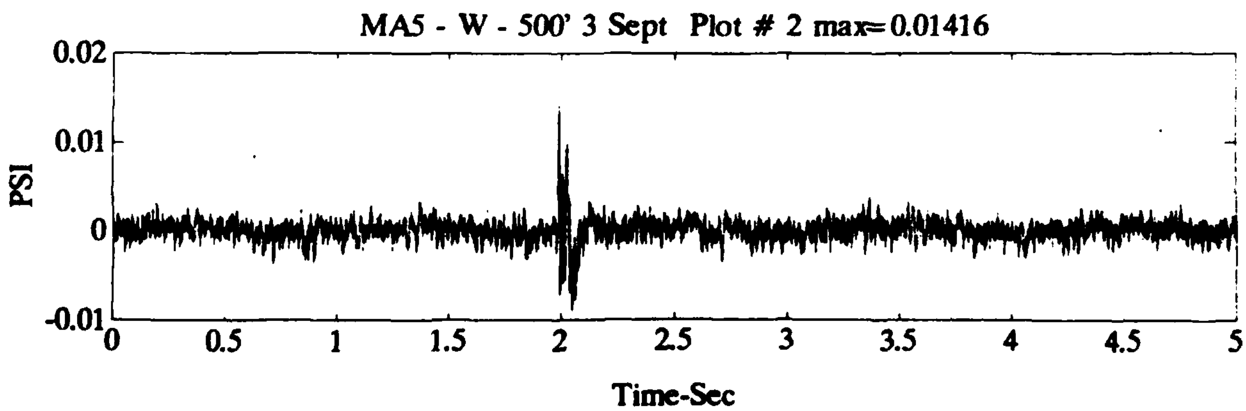
MA5 - W - 500' 3 Sept Plot # 2 max=0.01416
PSI
0.02
0.01
0
-0.01
0
0.5
1
1.5
2
2.5
3
3.5
4
4.5
5
Time-Sec

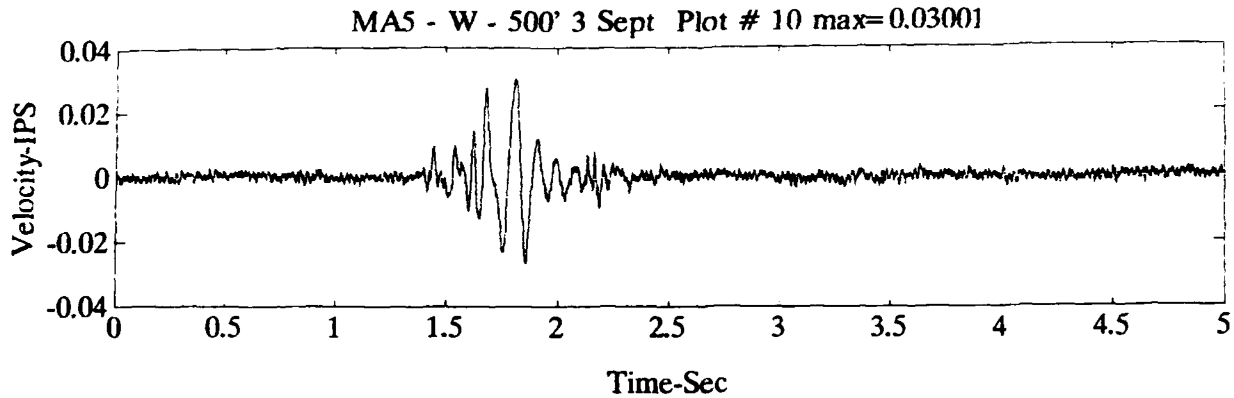
MA5 - W - 500' 3 Sept Plot # 10 max=0.03001
Velocity-IPS
Time-Sec

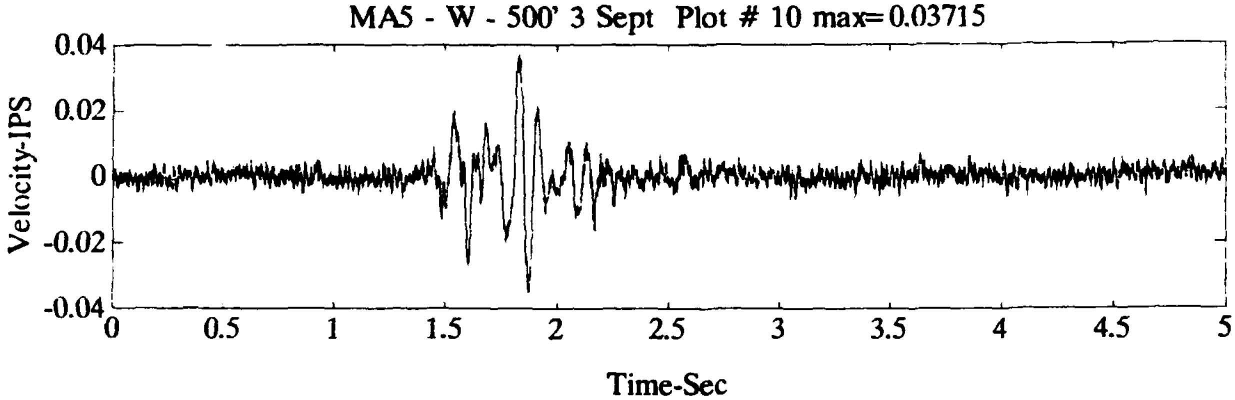
MA5 - W - 500' 3 Sept Plot # 10 max=0.03715
Velocity-IPS
Time-Sec

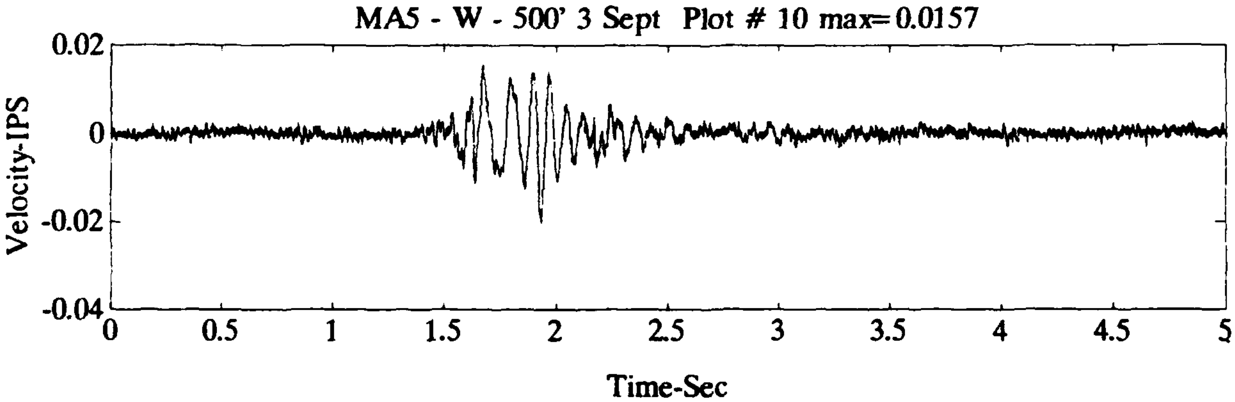
MA5 - W - 500' 3 Sept Plot # 10 max=0.0157
Velocity-IPS
Time-Sec

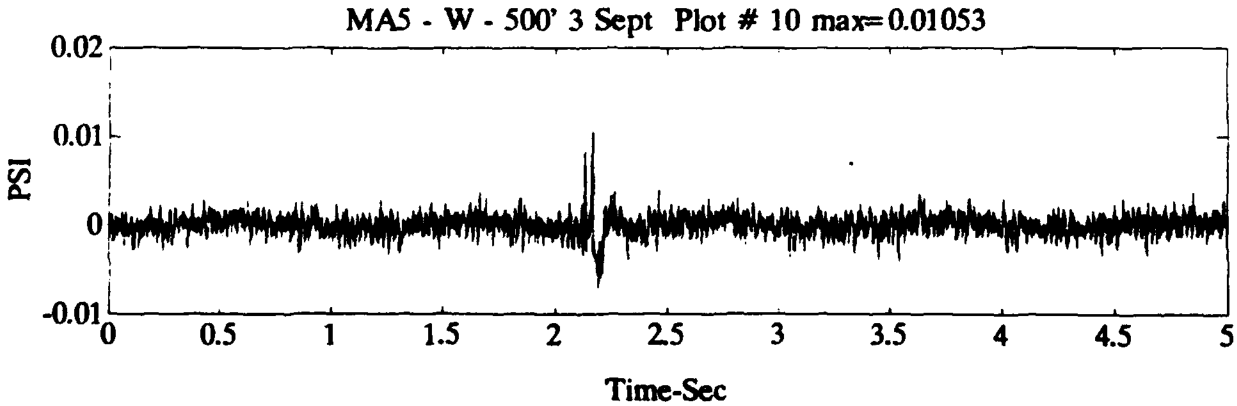
MA5 - W - 500' 3 Sept Plot # 10 max=0.01053
PSI
Time-Sec

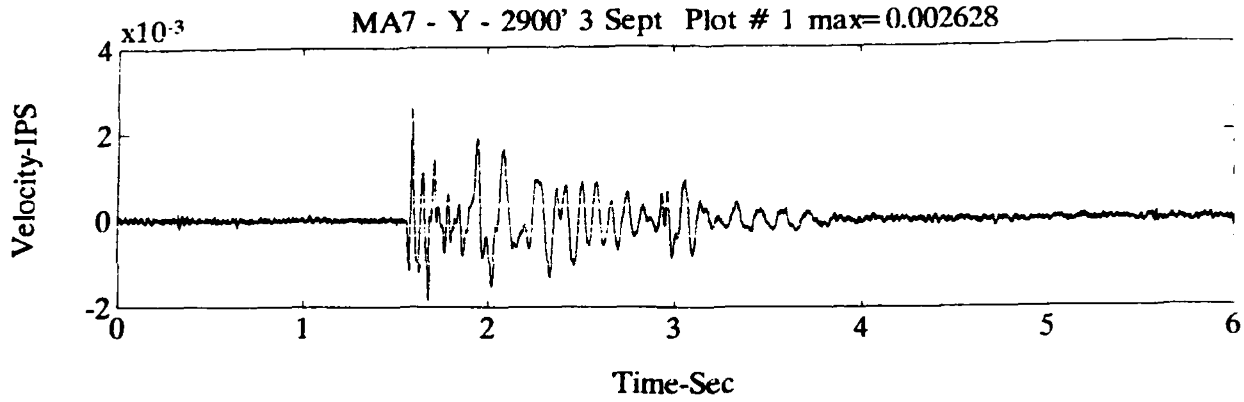
MA7 - Y - 2900' 3 Sept Plot # 1 max=0.002628
x10-3
Velocity-IPS
Time-Sec

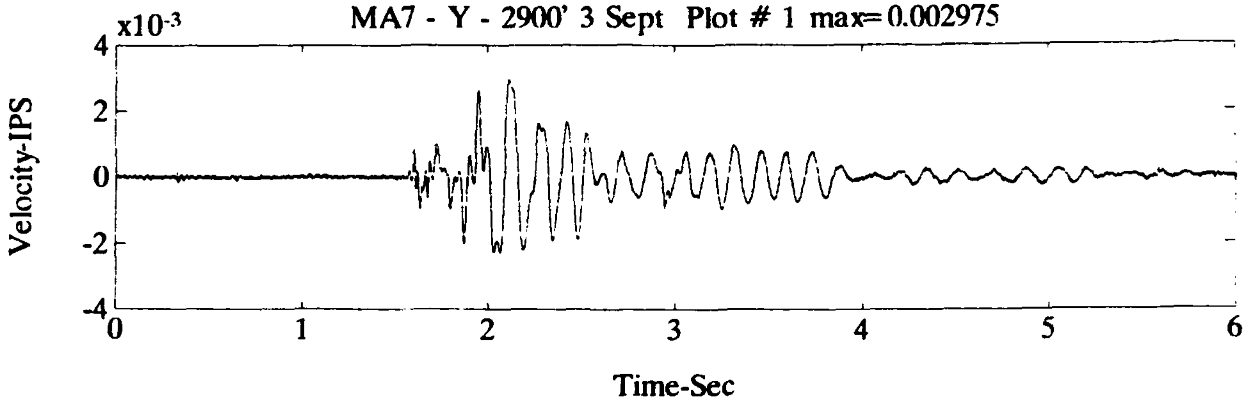
MA7 - Y - 2900' 3 Sept Plot # 1 max=0.002975
x10-3
Velocity-IPS
Time-Sec

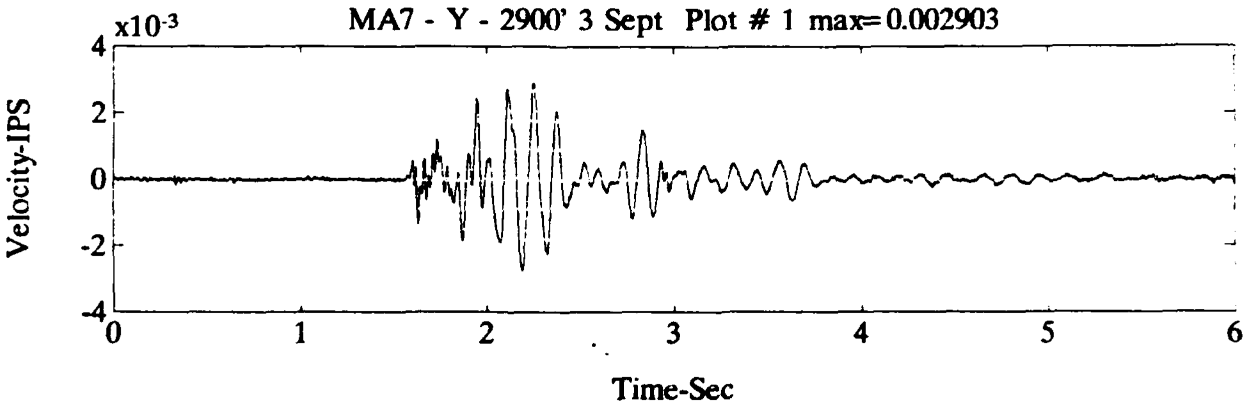
MA7 - Y - 2900' 3 Sept Plot # 1 max=0.002903
x10-3
Velocity-IPS
Time-Sec

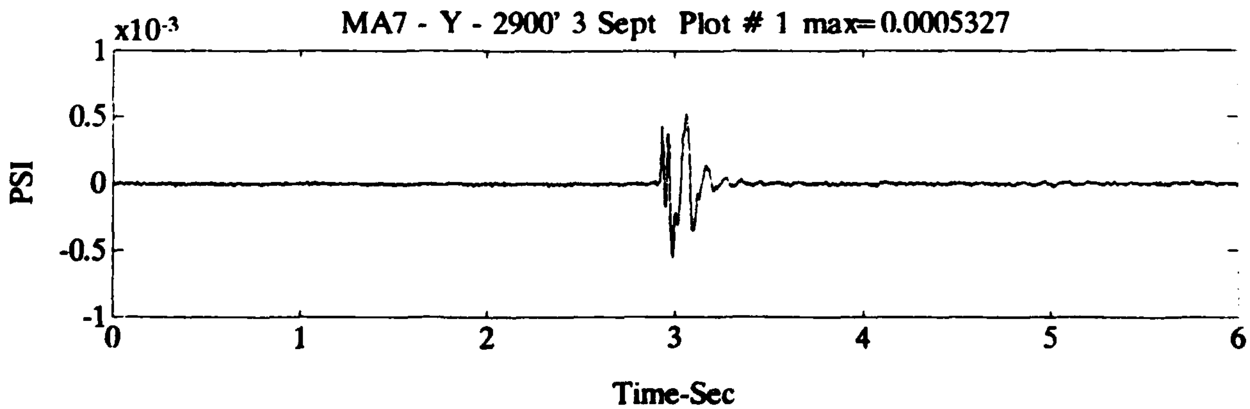
MA7 - Y - 2900' 3 Sept Plot # 1 max=0.0005327
x10-3
PSI
Time-Sec

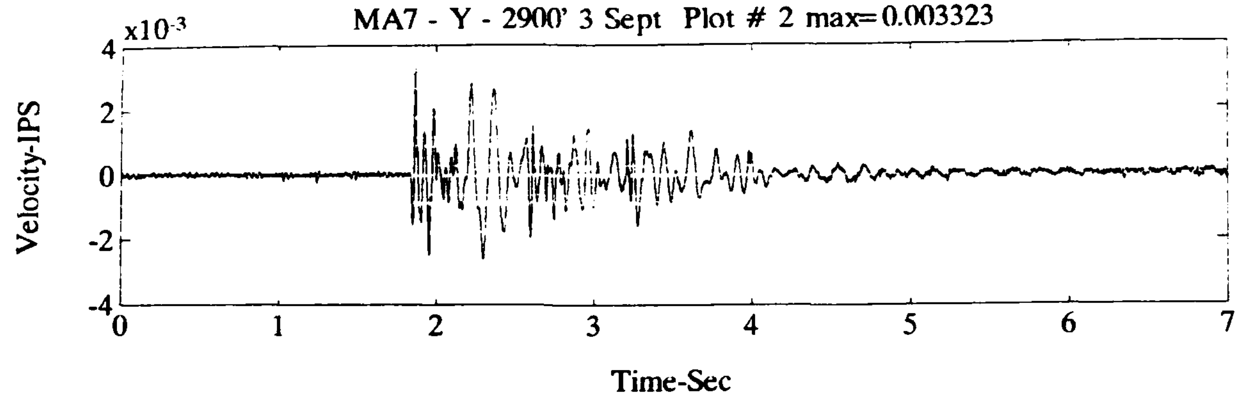
MA7 - Y - 2900' 3 Sept Plot # 2 max=0.003323
x10-3
Velocity-IPS
Time-Sec

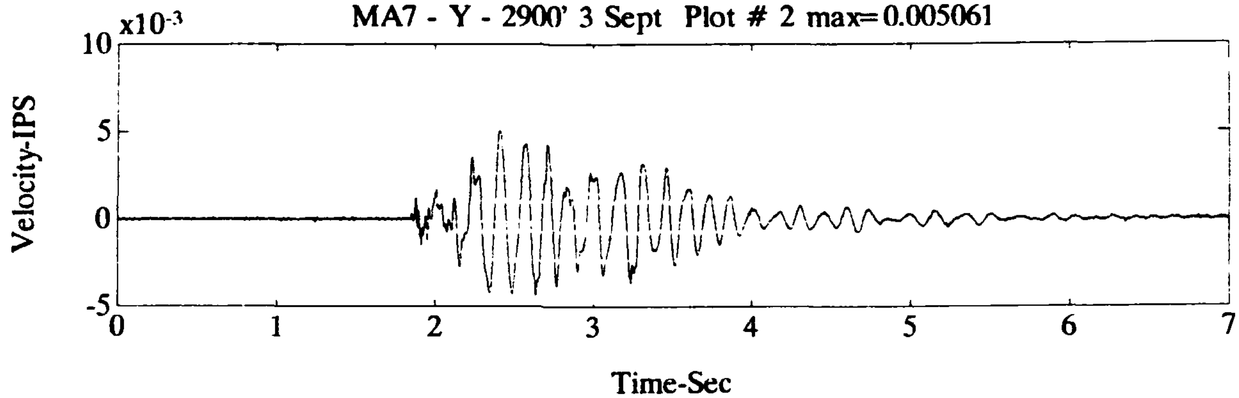
MA7 - Y - 2900' 3 Sept Plot # 2 max=0.005061
x10-3
Velocity-IPS
Time-Sec

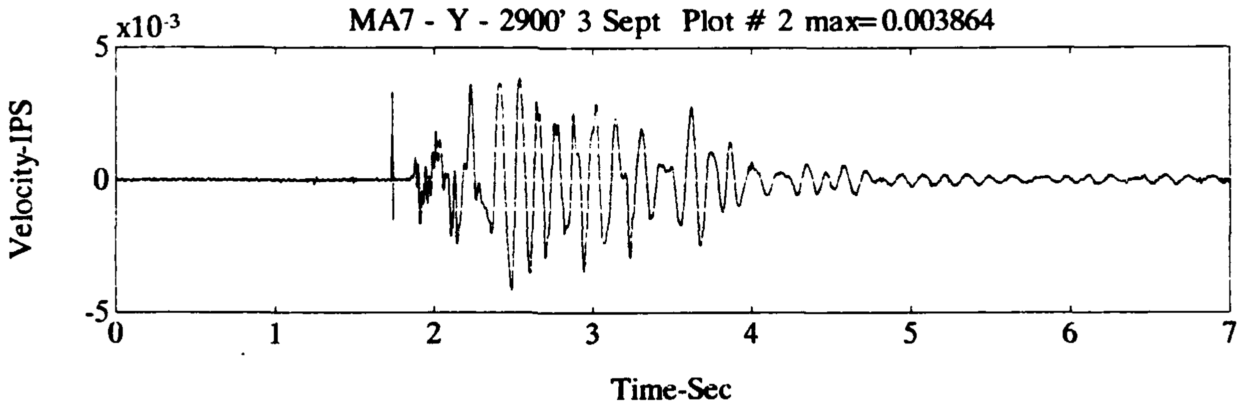
MA7 - Y - 2900' 3 Sept Plot # 2 max=0.003864
x10-3
Velocity-IPS
Time-Sec

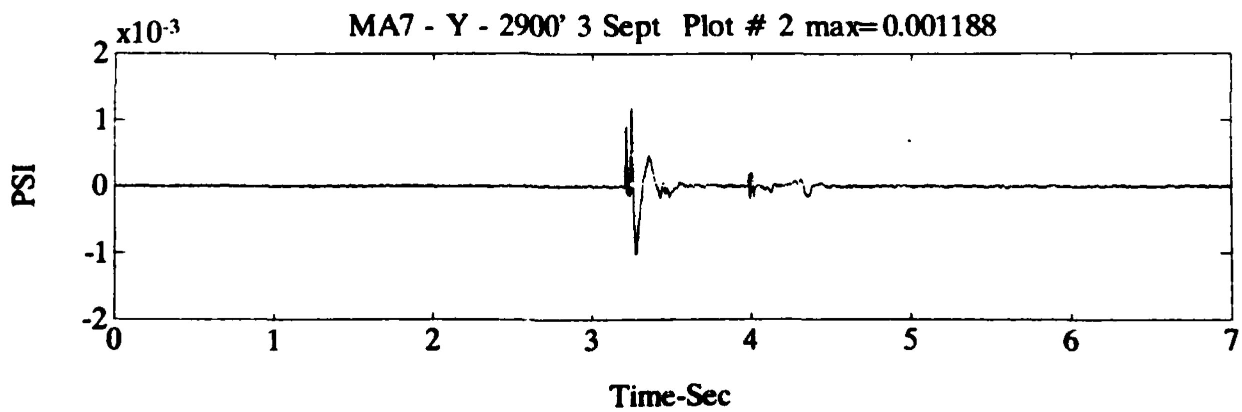
MA7 - Y - 2900' 3 Sept Plot # 2 max=0.001188
x10-3
PSI
Time-Sec

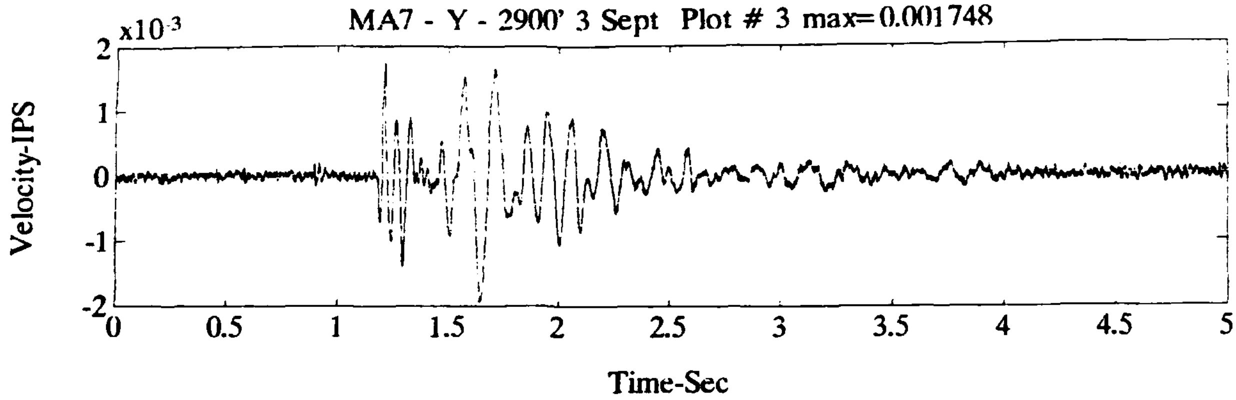
MA7 - Y - 2900' 3 Sept Plot # 3 max=0.001748
x10-3
Velocity-IPS
Time-Sec

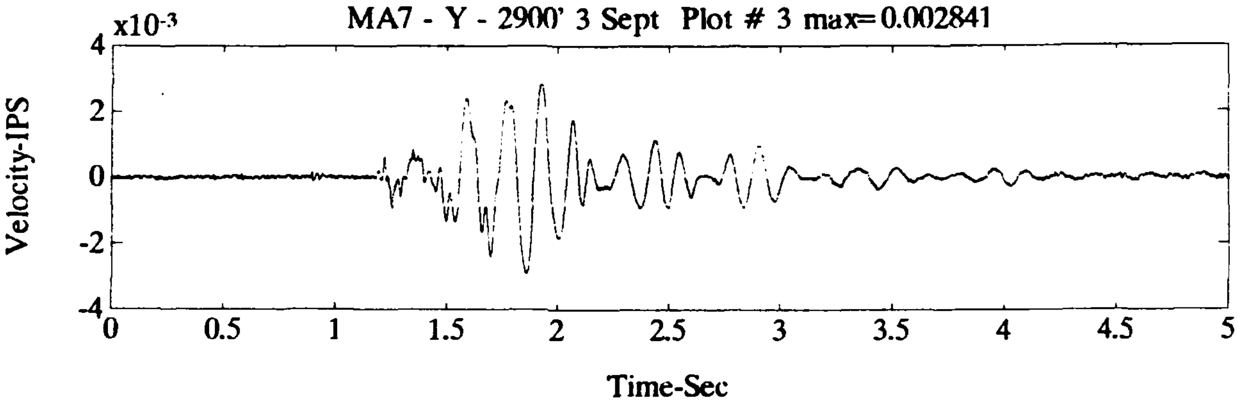
MA7 - Y - 2900' 3 Sept Plot # 3 max=0.002841
x10-3
Velocity-IPS
Time-Sec

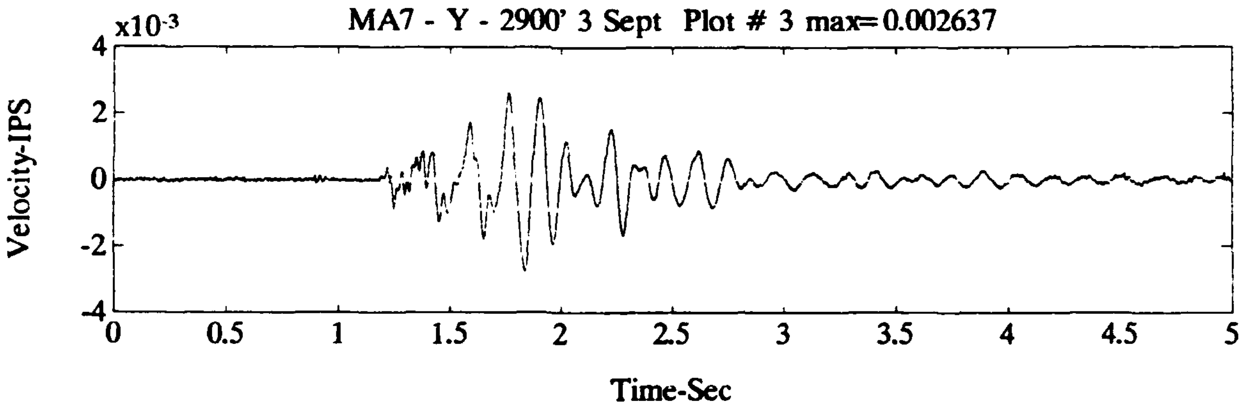
MA7 - Y - 2900' 3 Sept Plot # 3 max=0.002637
x10-3
Velocity-IPS
Time-Sec

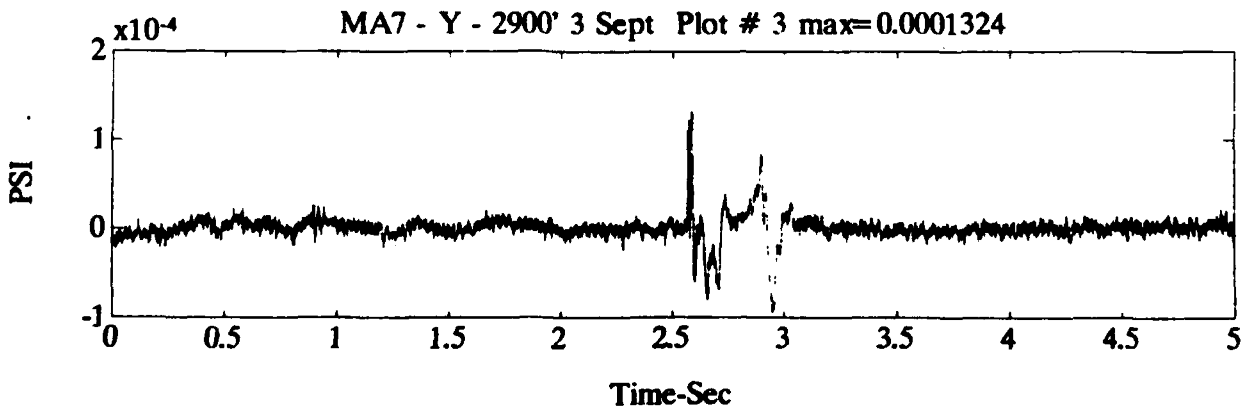
MA7 - Y - 2900' 3 Sept Plot # 3 max=0.0001324
x10-4
PSI
Time-Sec

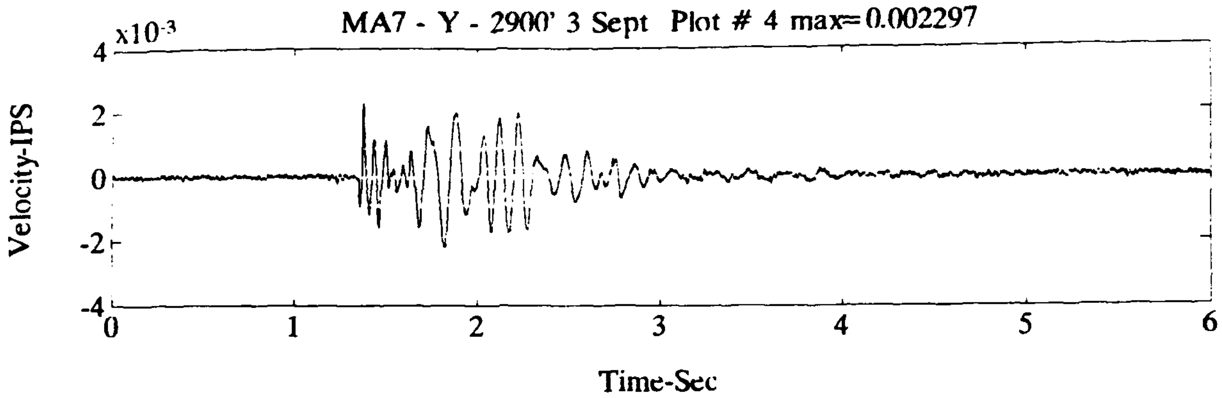
MA7 - Y - 2900' 3 Sept Plot # 4 max=0.002297
x10-3
Velocity-IPS
Time-Sec

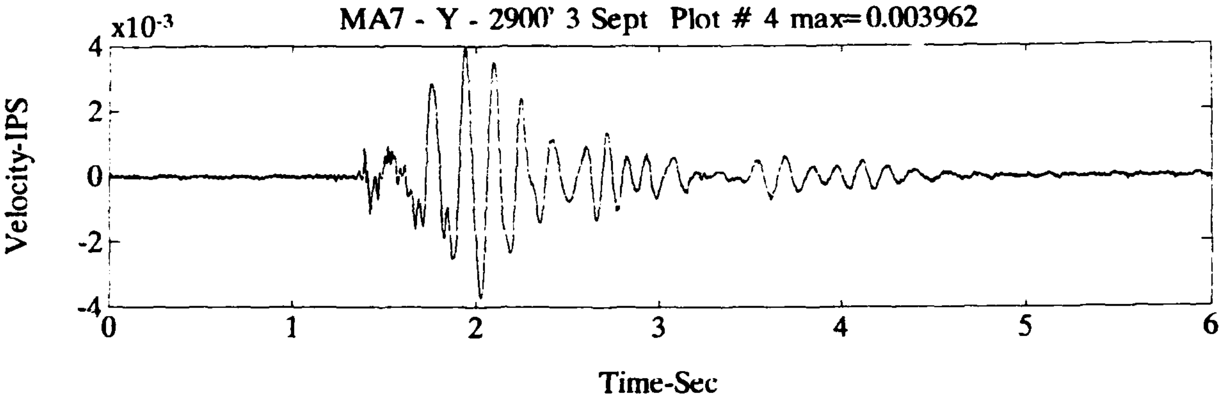
MA7 - Y - 2900' 3 Sept Plot # 4 max=0.003962
x10-3
Velocity-IPS
Time-Sec

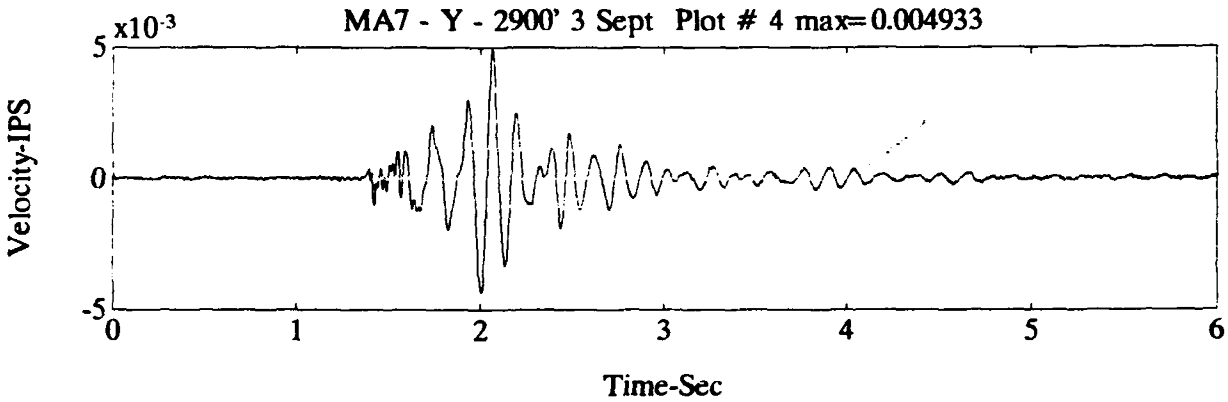
MA7 - Y - 2900' 3 Sept Plot # 4 max=0.004933
x10-3
Velocity-IPS
Time-Sec

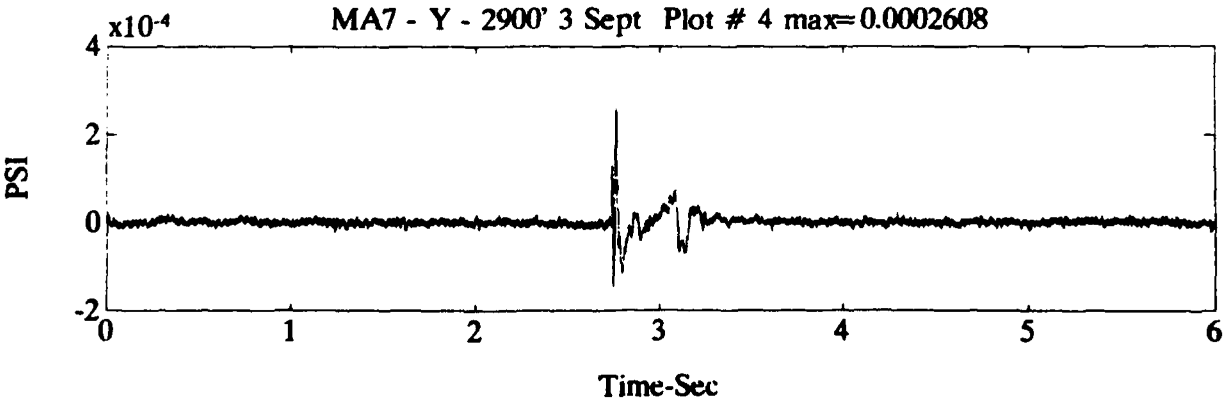
MA7 - Y - 2900' 3 Sept Plot # 4 max=0.0002608
x10-4
PSI
Time-Sec

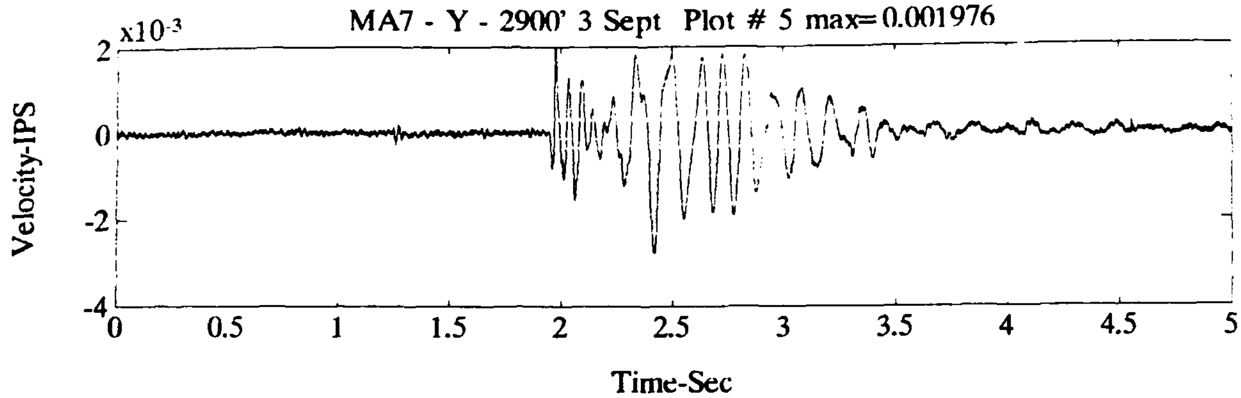
MA7 - Y - 2900' 3 Sept Plot # 5 max=0.001976
x10-3
Velocity-IPS
2
0
-2
-4
0
0.5
1
1.5
2
2.5
3
3.5
4
4.5
5
Time-Sec

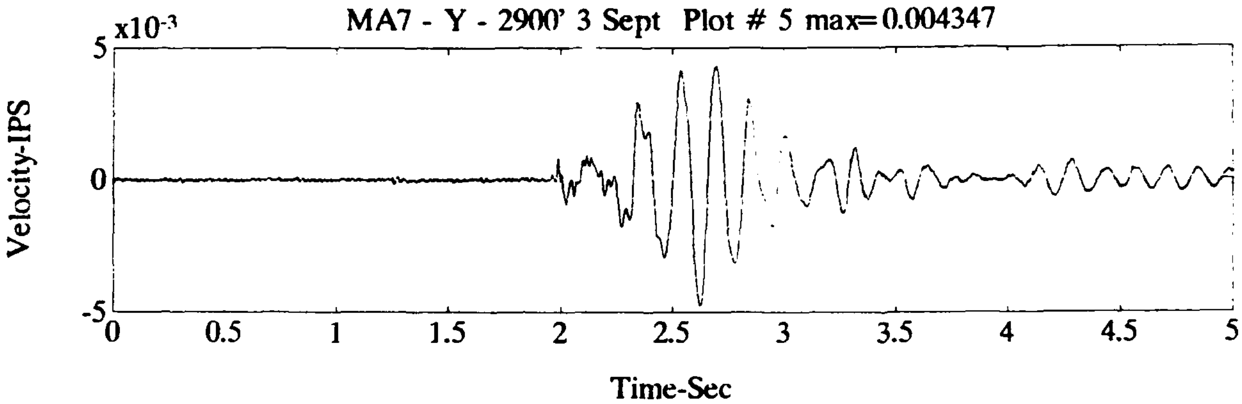
MA7 - Y - 2900' 3 Sept Plot # 5 max=0.004347
x10-3
Velocity-IPS
5
0
-5
0
0.5
1
1.5
2
2.5
3
3.5
4
4.5
5
Time-Sec

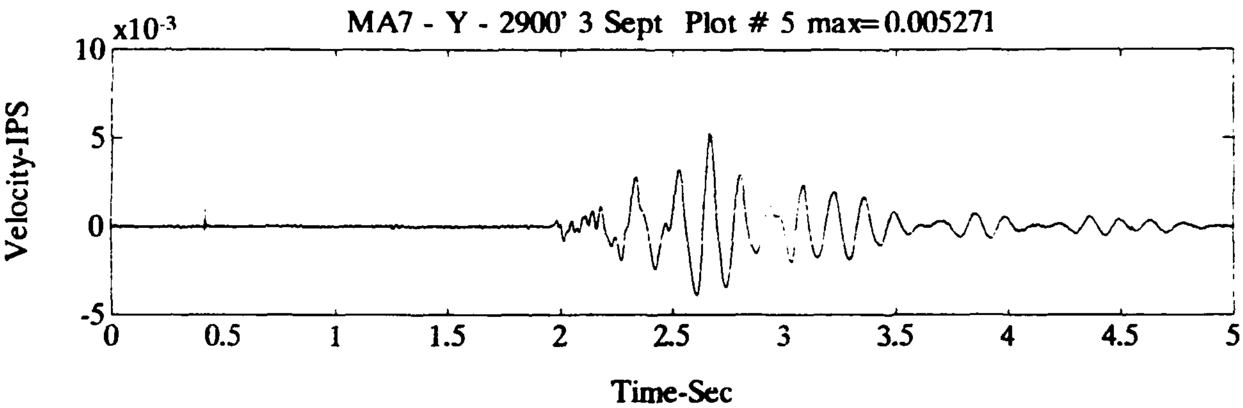
MA7 - Y - 2900' 3 Sept Plot # 5 max=0.005271
x10-3
Velocity-IPS
10
5
0
-5
0
0.5
1
1.5
2
2.5
3
3.5
4
4.5
5
Time-Sec

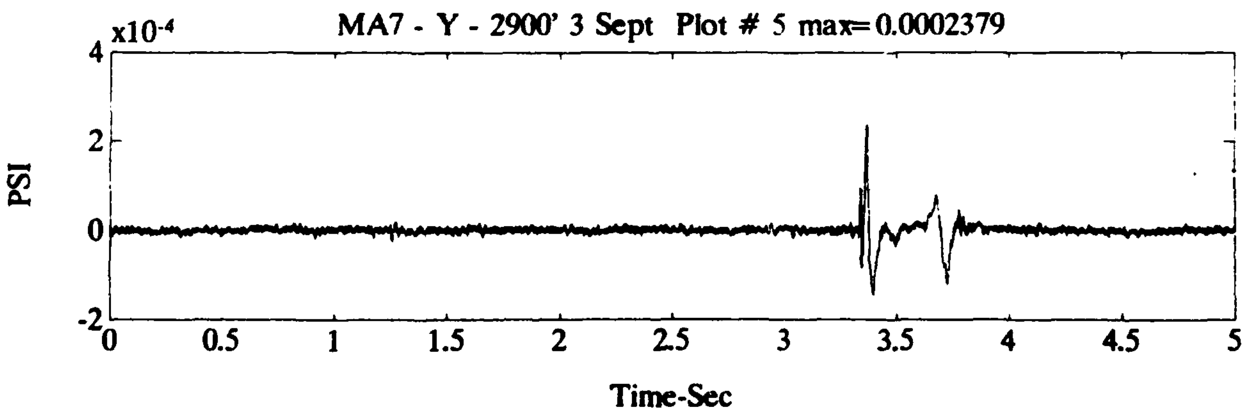
MA7 - Y - 2900' 3 Sept Plot # 5 max=0.0002379
x10-4
PSI
4
2
0
-2
0
0.5
1
1.5
2
2.5
3
3.5
4
4.5
5
Time-Sec

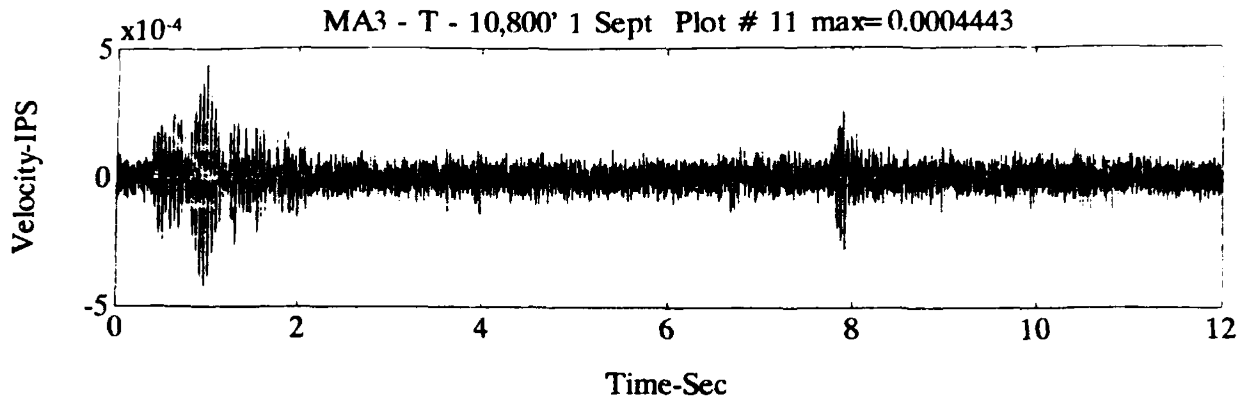
MA3 - T - 10,800' 1 Sept Plot # 11 max=0.0004443
x10-4
Velocity-IPS
Time-Sec

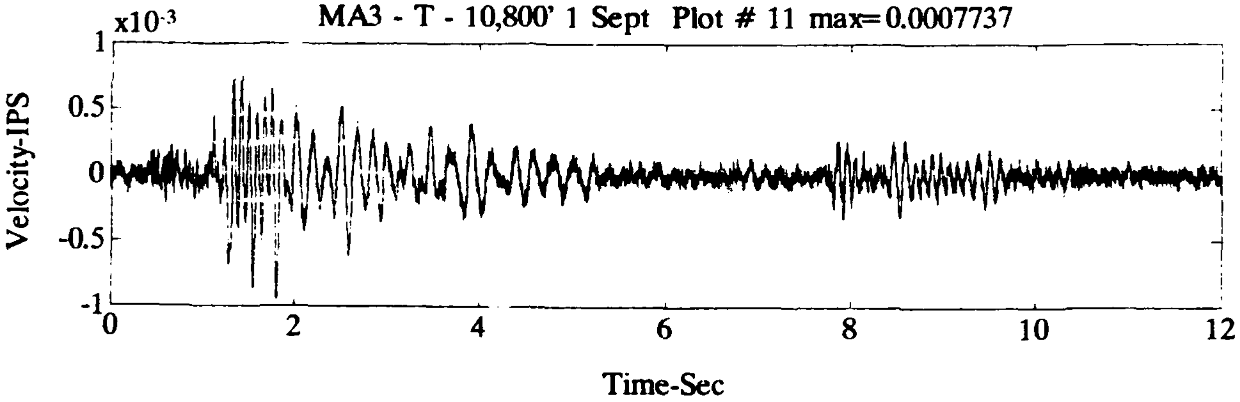
MA3 - T - 10,800' 1 Sept Plot # 11 max=0.0007737
x10-3
Velocity-IPS
Time-Sec

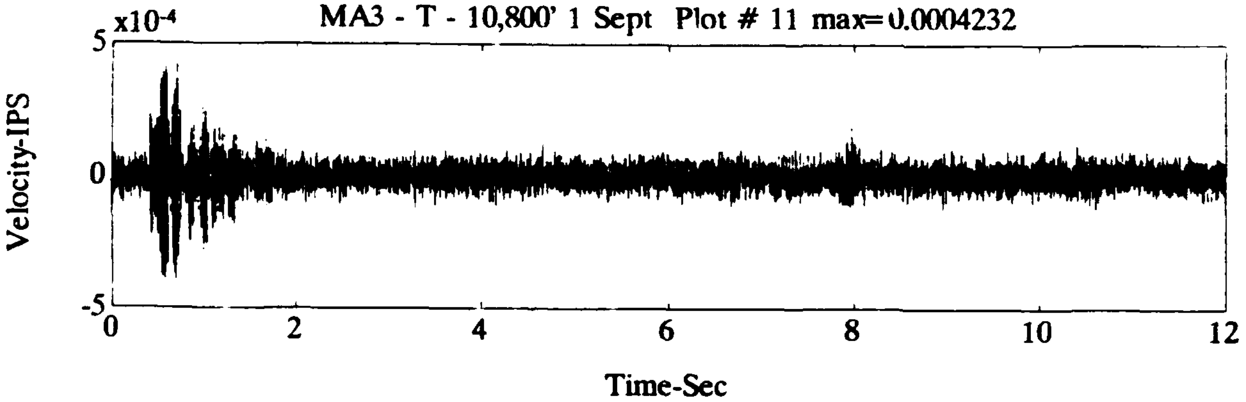
MA3 - T - 10,800' 1 Sept Plot # 11 max=0.0004232
x10-4
Velocity-IPS
Time-Sec

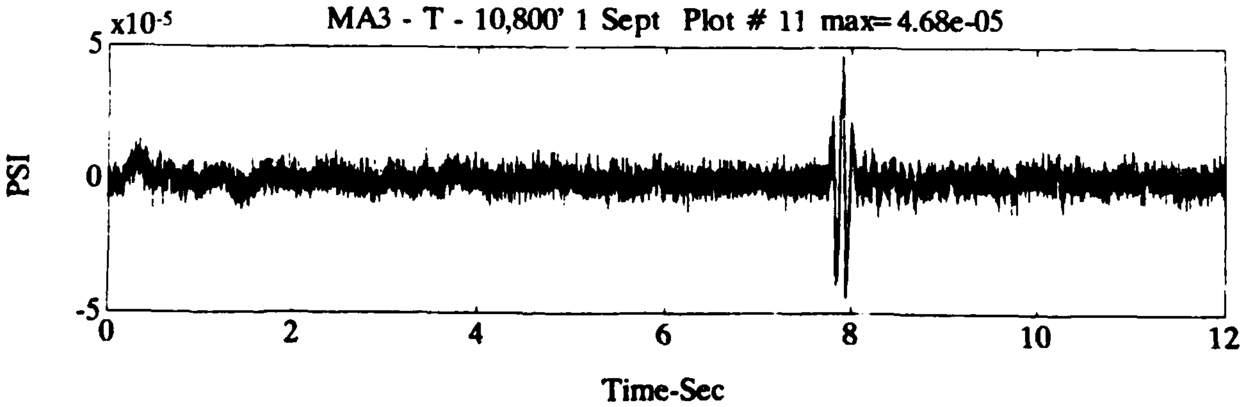
MA3 - T - 10,800' 1 Sept Plot # 11 max=4.68e-05
x10-5
PSI
Time-Sec

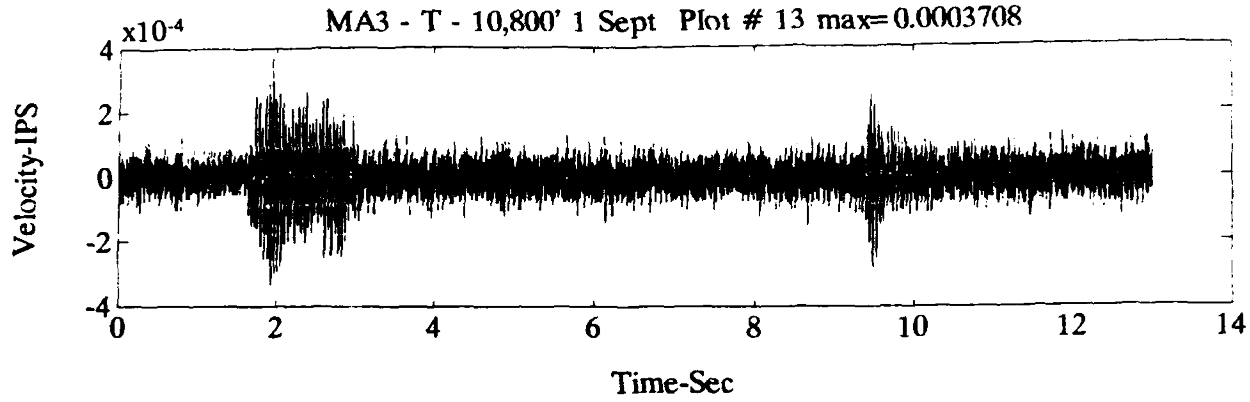
MA3 - T - 10,800' 1 Sept Plot # 13 max=0.0003708
x10-4
Velocity-IPS
Time-Sec

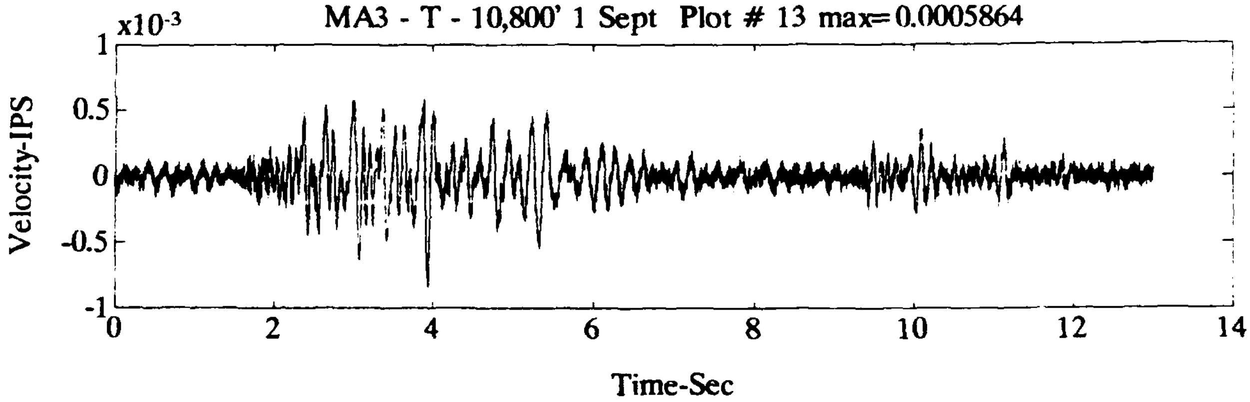
MA3 - T - 10,800' 1 Sept Plot # 13 max=0.0005864
x10-3
Velocity-IPS
Time-Sec

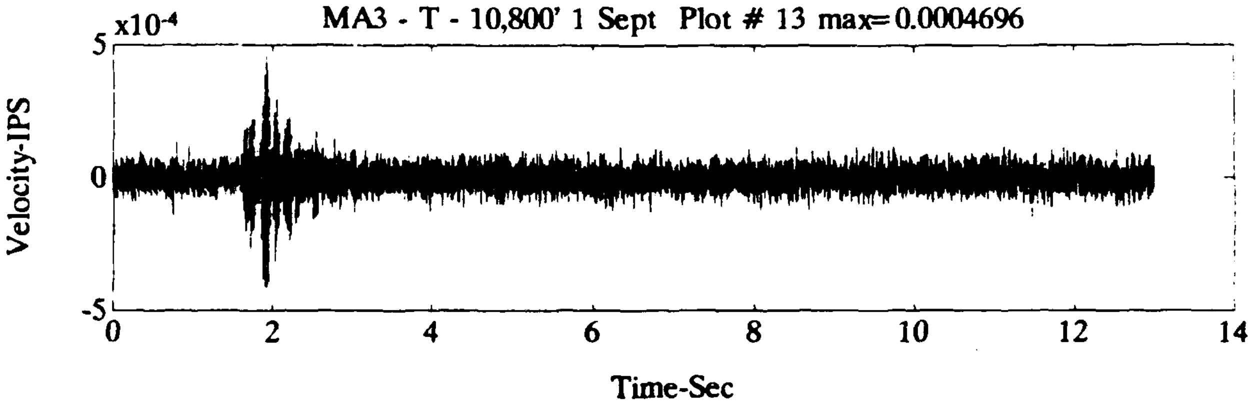
MA3 - T - 10,800' 1 Sept Plot # 13 max=0.0004696
x10-4
Velocity-IPS
Time-Sec

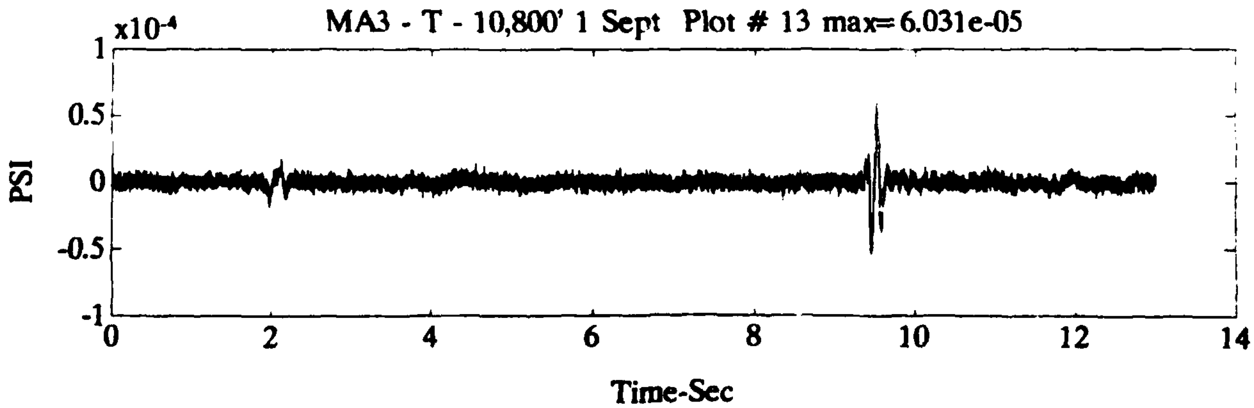
MA3 - T - 10,800' 1 Sept Plot # 13 max=6.031e-05
x10-4
PSI
Time-Sec

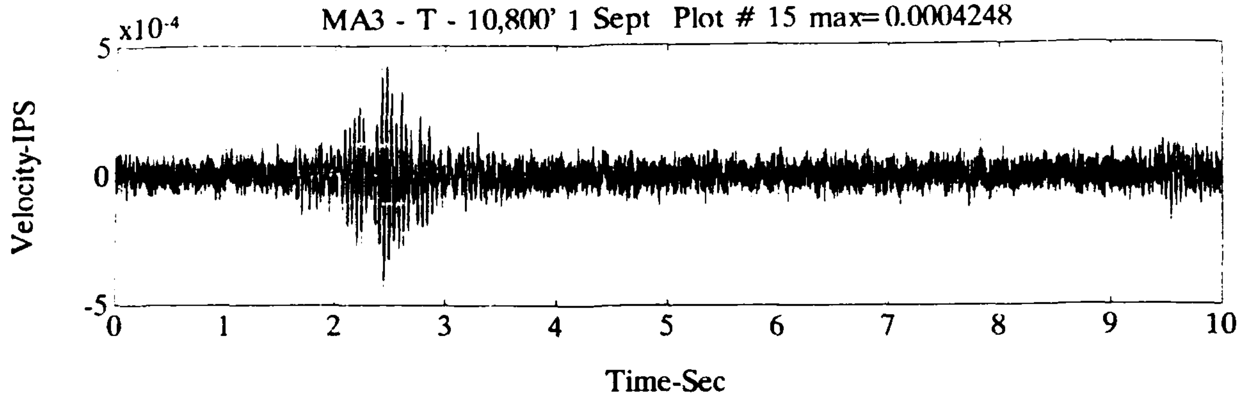
MA3 - T - 10,800' 1 Sept Plot # 15 max=0.0004248
x10-4
Velocity-IPS
Time-Sec

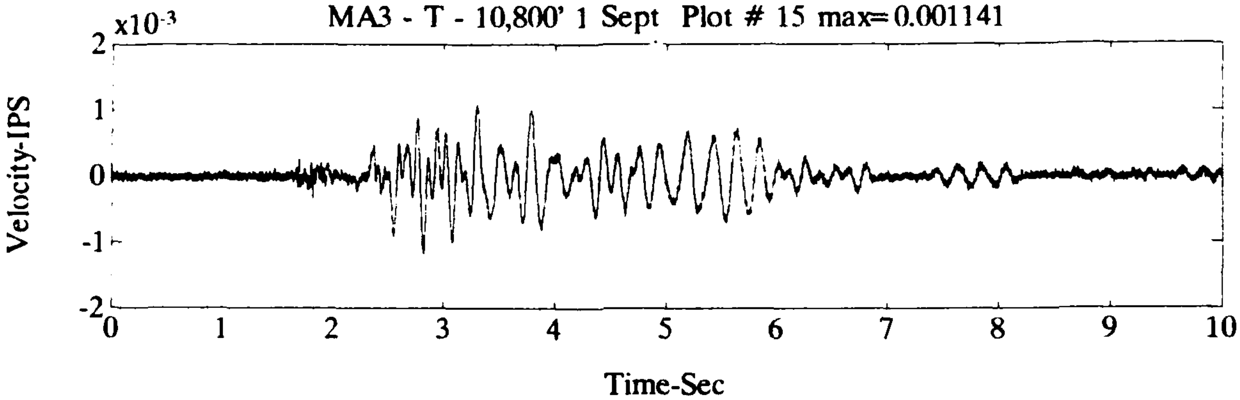
MA3 - T - 10,800' 1 Sept Plot # 15 max=0.001141
x10-3
Velocity-IPS
Time-Sec

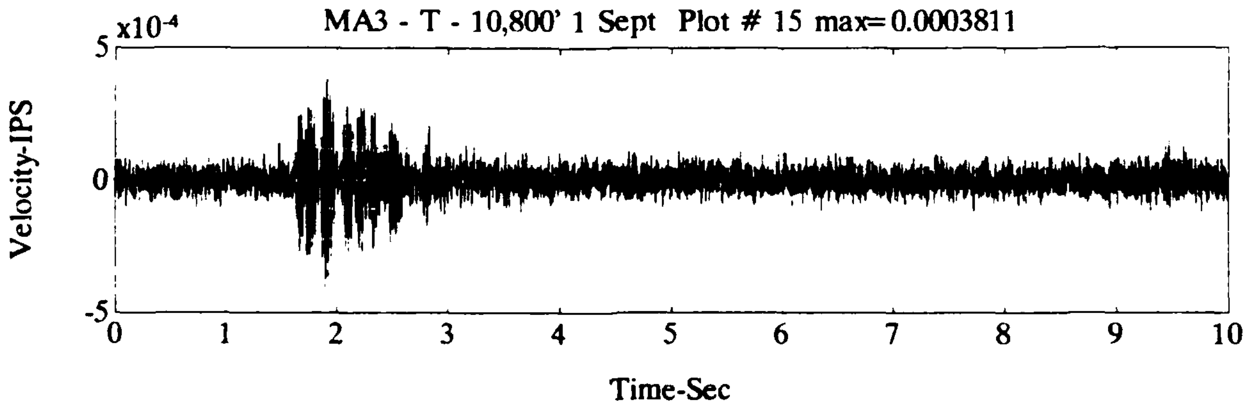
MA3 - T - 10,800' 1 Sept Plot # 15 max=0.0003811
x10-4
Velocity-IPS
Time-Sec

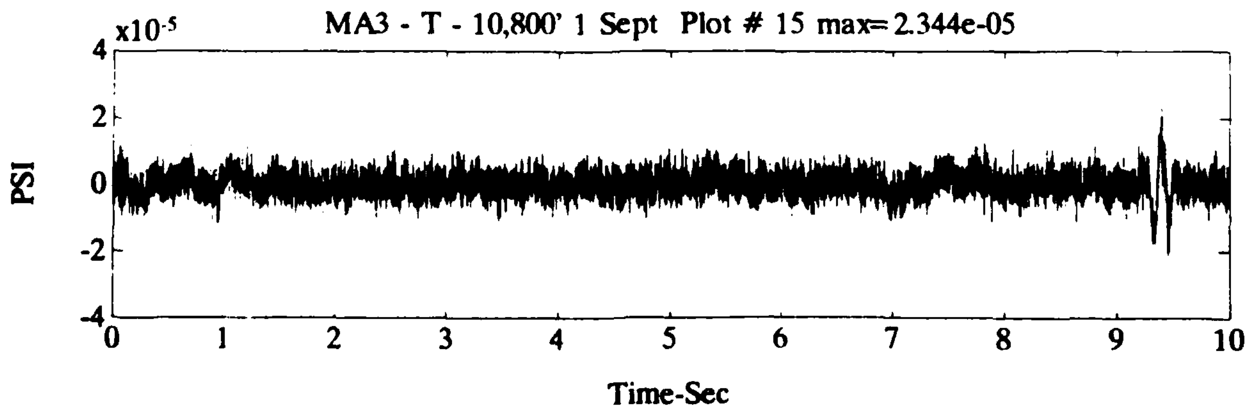
MA3 - T - 10,800' 1 Sept Plot # 15 max=2.344e-05
x10-5
PSI
Time-Sec

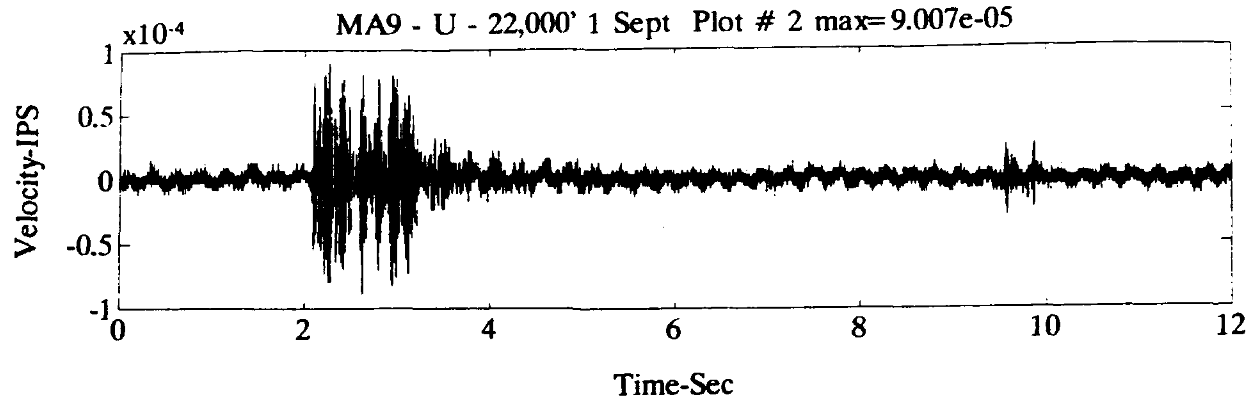
MA9 - U - 22,000' 1 Sept Plot # 2 max=9.007e-05
x10-4
Velocity-IPS
1
0.5
0
-0.5
-1
0
2
4
6
8
10
12
Time-Sec

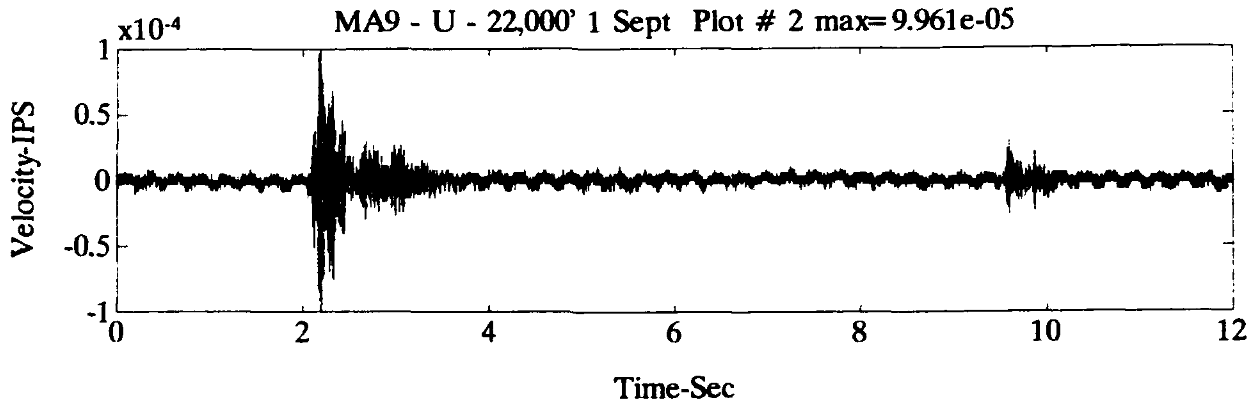
MA9 - U - 22,000' 1 Sept Plot # 2 max=9.961e-05
x10-4
Velocity-IPS
1
0.5
0
-0.5
-1
0
2
4
6
8
10
12
Time-Sec

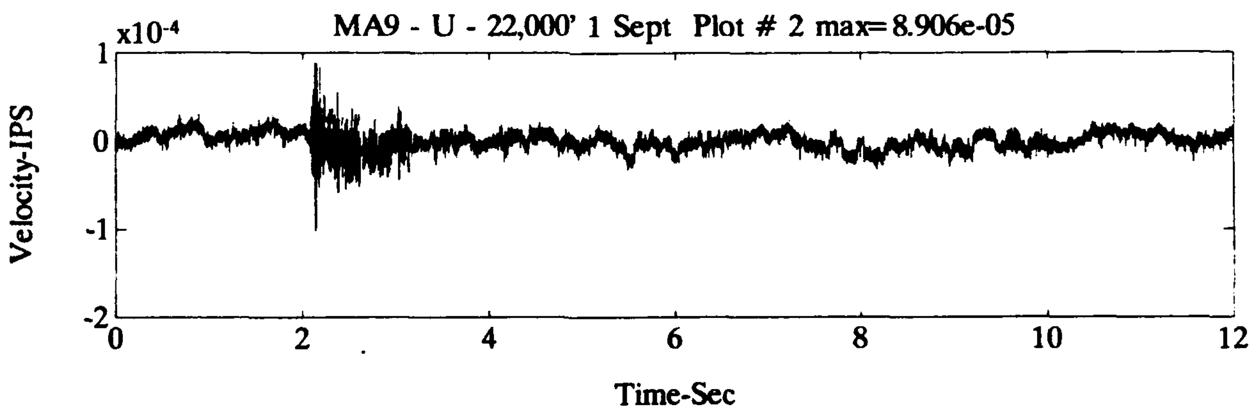
MA9 - U - 22,000' 1 Sept Plot # 2 max=8.906e-05
x10-4
Velocity-IPS
1
0
-1
-2
0
2
4
6
8
10
12
Time-Sec

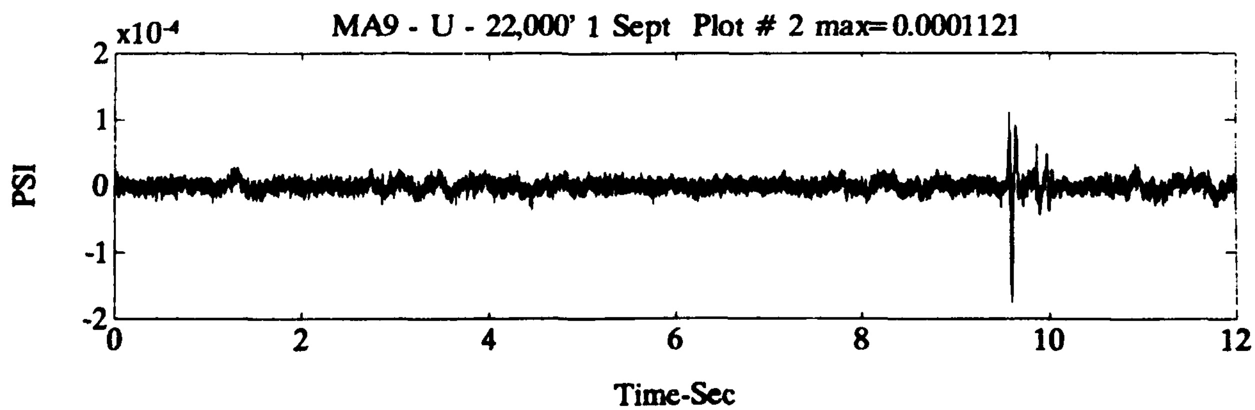
MA9 - U - 22,000' 1 Sept Plot # 2 max=0.0001121
x10-4
PSI
2
1
0
-1
-2
0
2
4
6
8
10
12
Time-Sec

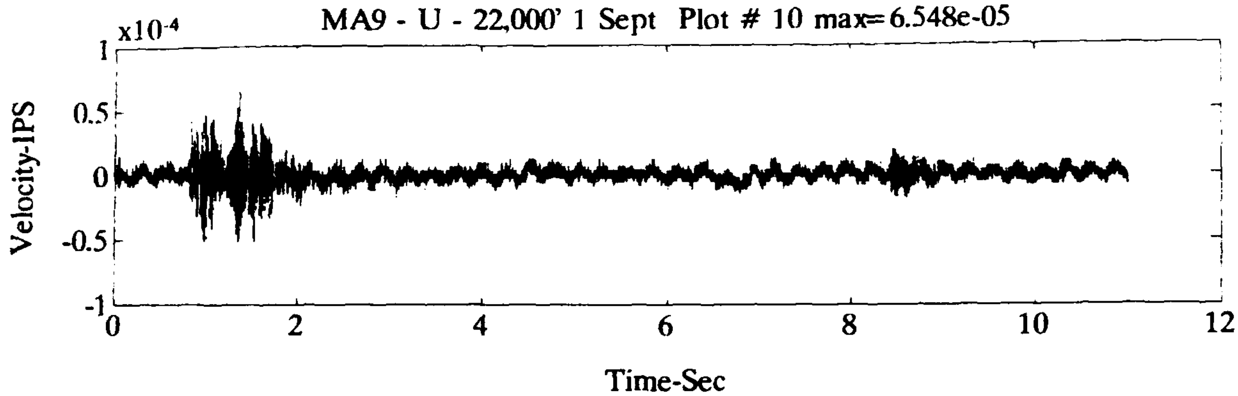
MA9 - U - 22,000' 1 Sept Plot # 10 max=6.548e-05
x10-4
Velocity-IPS
1
0.5
0
-0.5
-1
0
2
4
6
8
10
12
Time-Sec

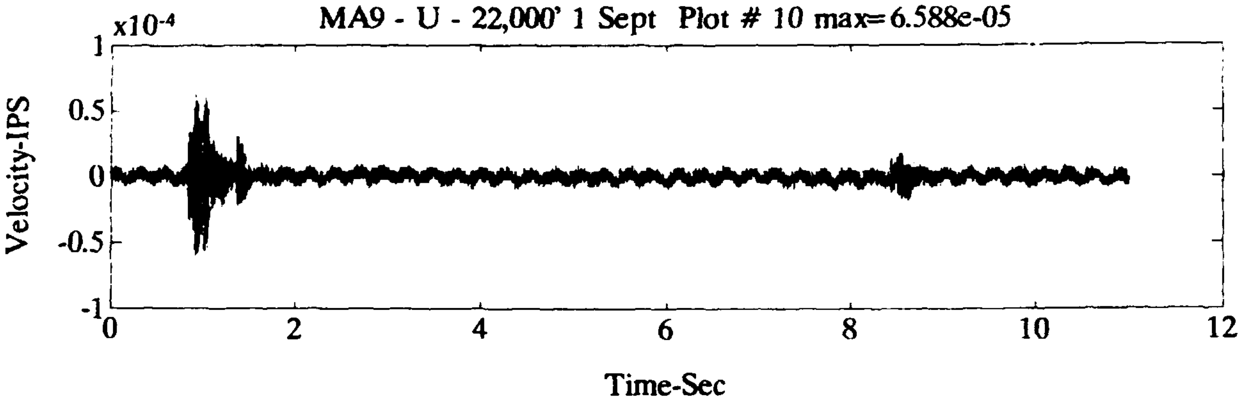
MA9 - U - 22,000' 1 Sept Plot # 10 max=6.588e-05
x10-4
Velocity-IPS
1
0.5
0
-0.5
-1
0
2
4
6
8
10
12
Time-Sec

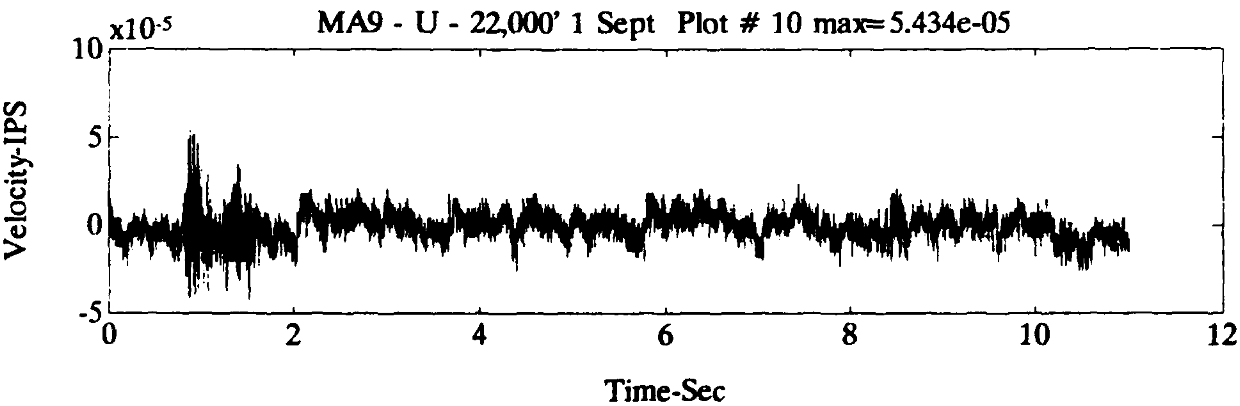
MA9 - U - 22,000' 1 Sept Plot # 10 max=5.434e-05
x10-5
Velocity-IPS
10
5
0
-5
0
2
4
6
8
10
12
Time-Sec

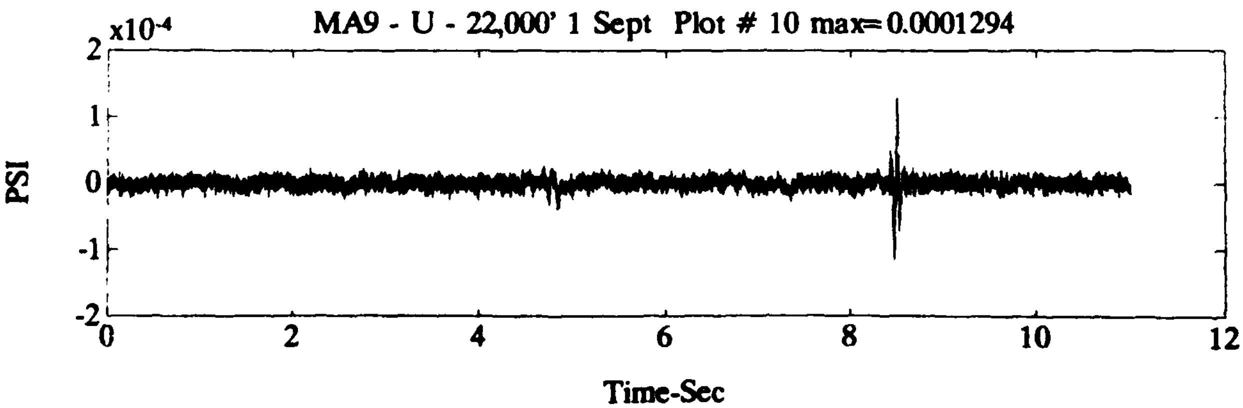
MA9 - U - 22,000' 1 Sept Plot # 10 max=0.0001294
x10-4
PSI
2
1
0
-1
-2
0
2
4
6
8
10
12
Time-Sec

MA9 - U - 22,000' 1 Sept Plot # 19 max=0.0002255

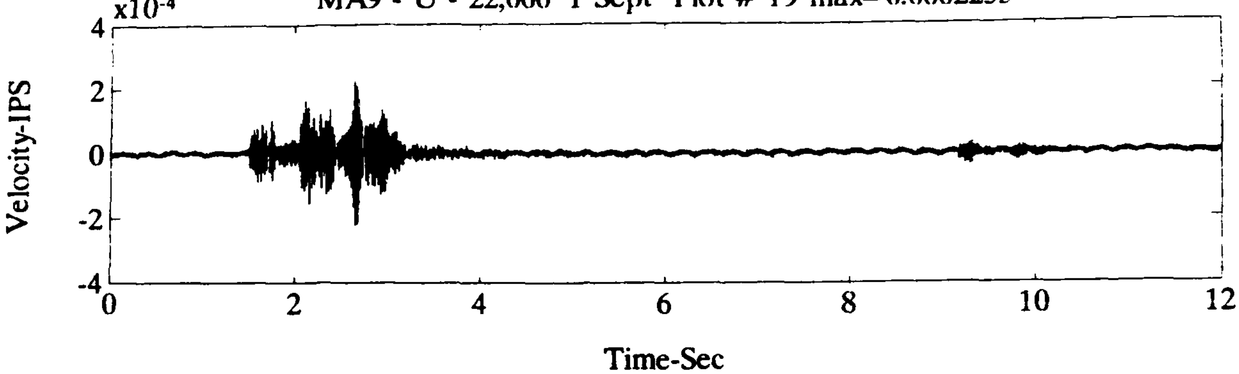

MA9 - U - 22,000' 1 Sept Plot # 19 max=0.0002324

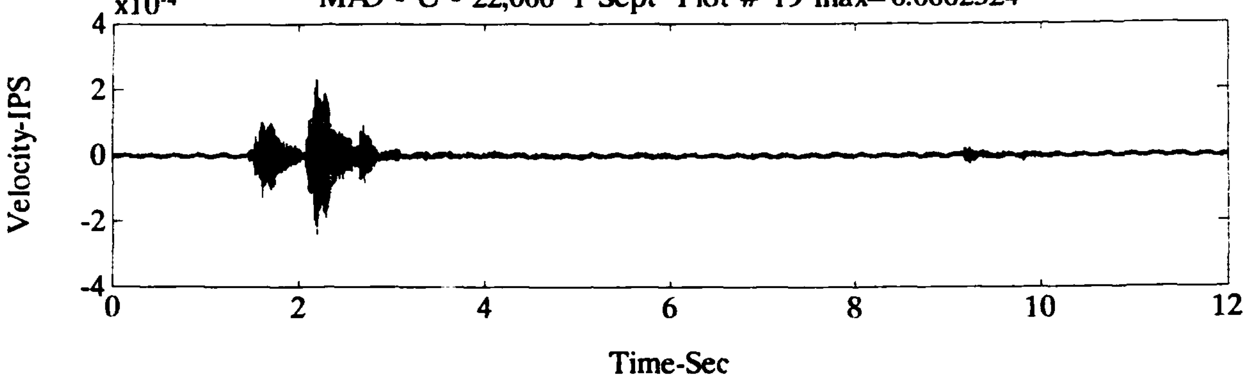

MA9 - U - 22,000' 1 Sept Plot # 19 max=0.0001568

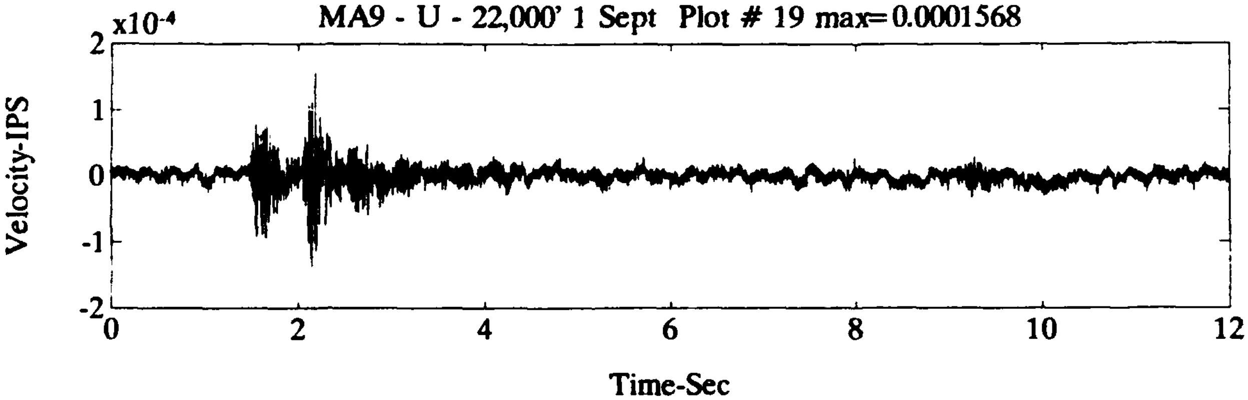

MA9 - U - 22,000' 1 Sept Plot # 19 max=0.0001323

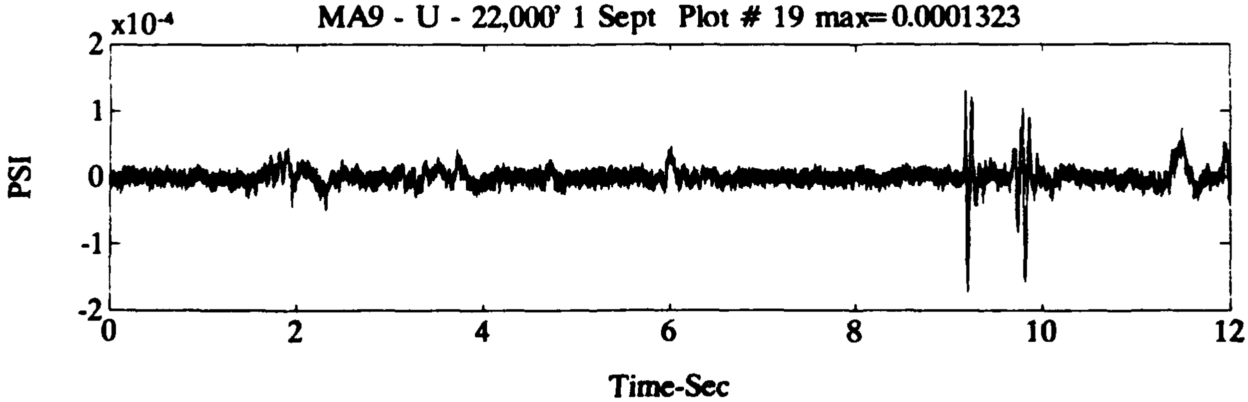

Appendix C: Plots of Peak Particle Velocities and Air

Air Overpressures Versus Scaled Range

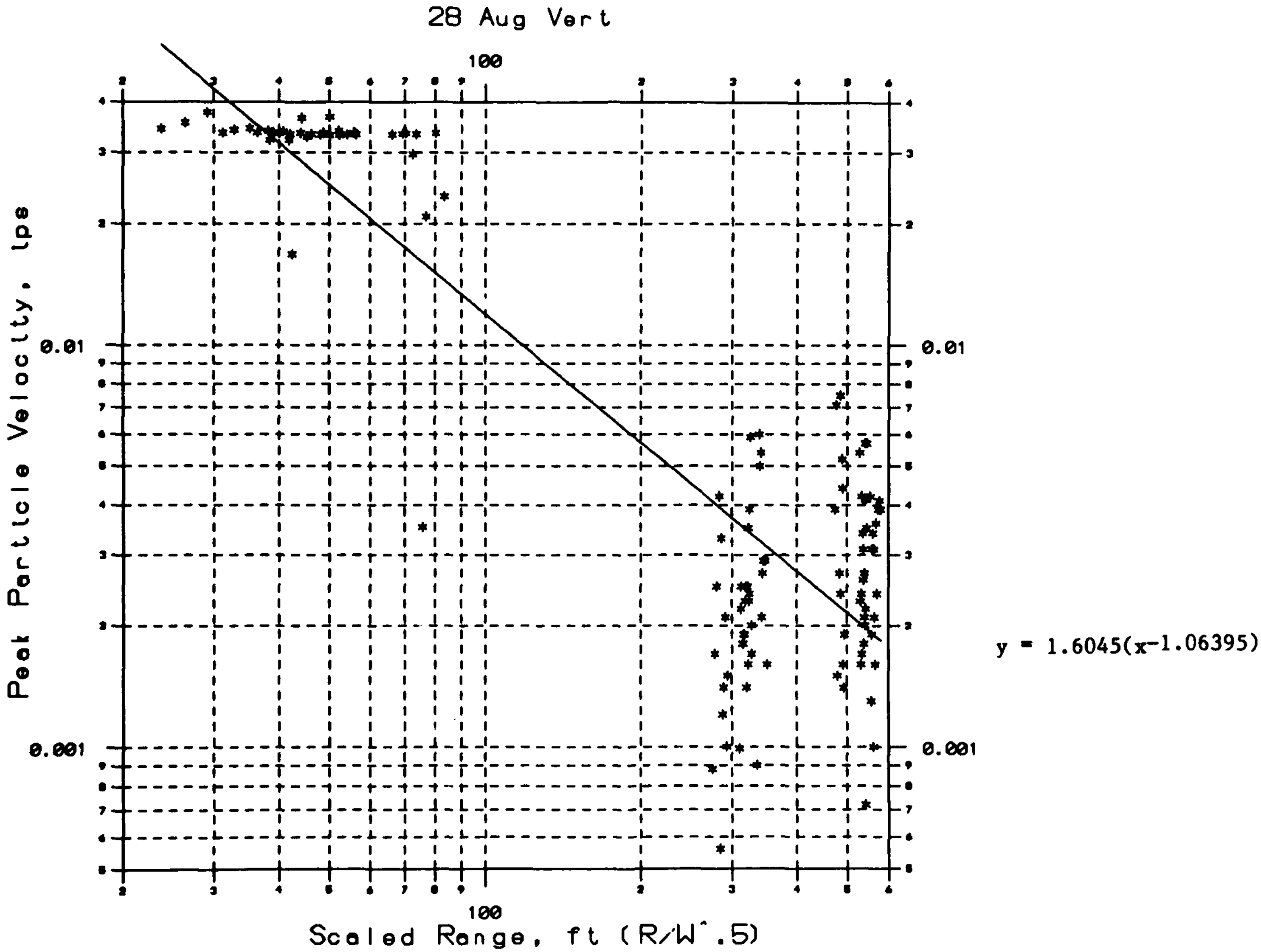
28 Aug Vert
100
0.01
0.001
Peak Particle Velocity, ips
Scaled Range, ft (R/W^.5)
y = 1.6045(x^-1.06395)

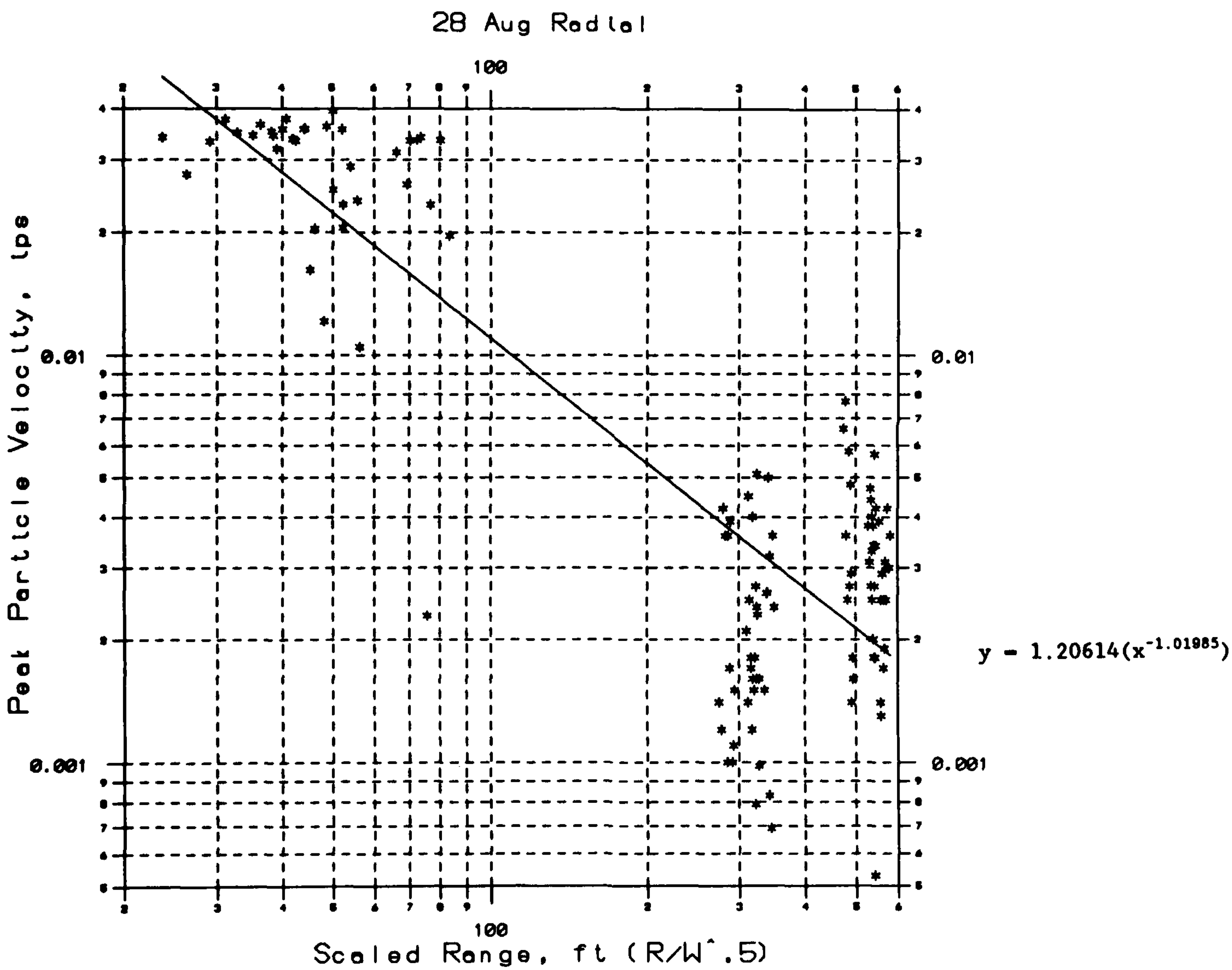
28 Aug Radial
Peak Particle Velocity, ips
Scaled Range, ft (R/W^.5)
100
0.01
0.001
y = 1.20614(x^-1.01985)

28 Aug Transverse

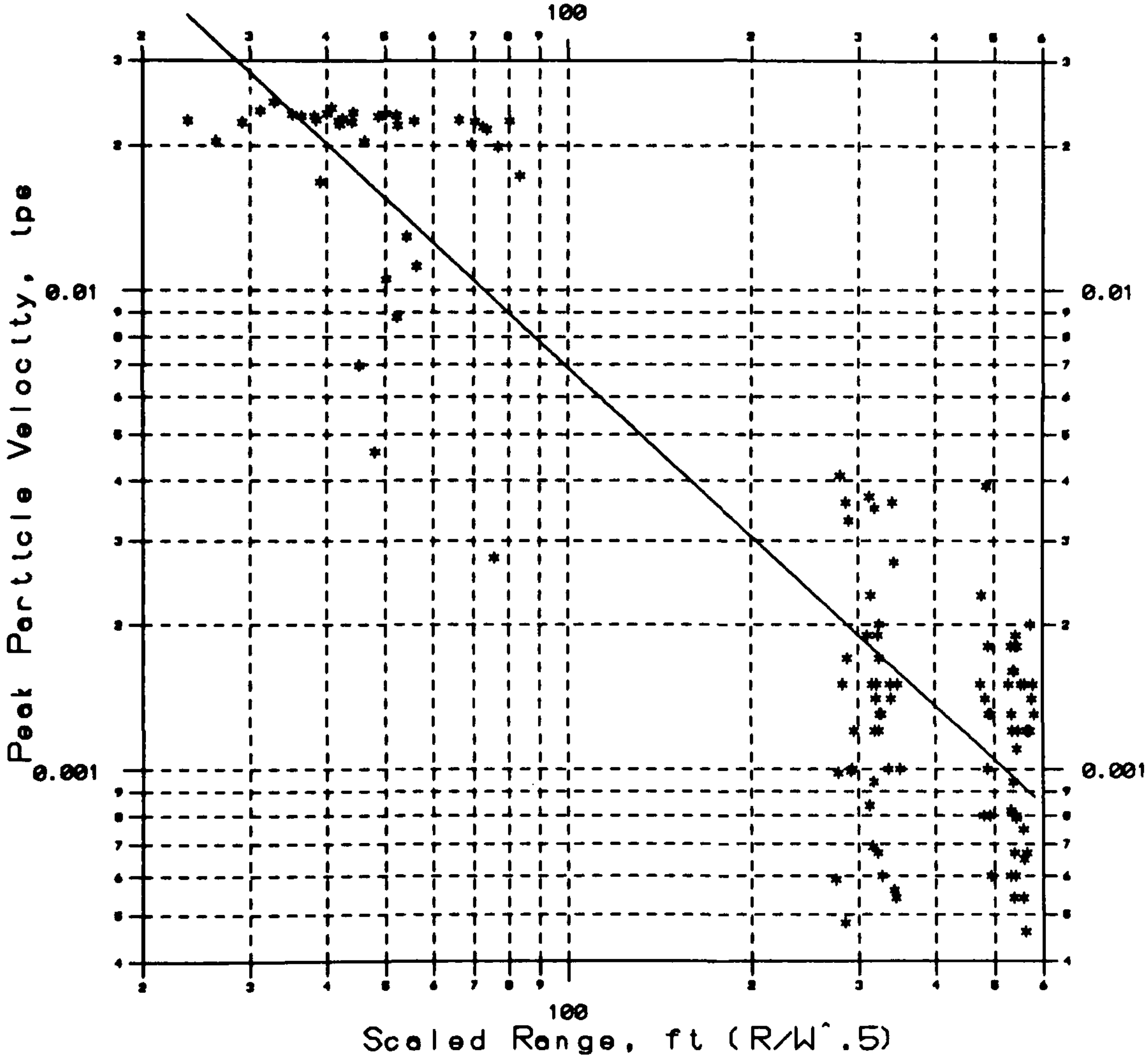

$y = 1.52418(x^{-1.17219})$

28 Aug Vertical

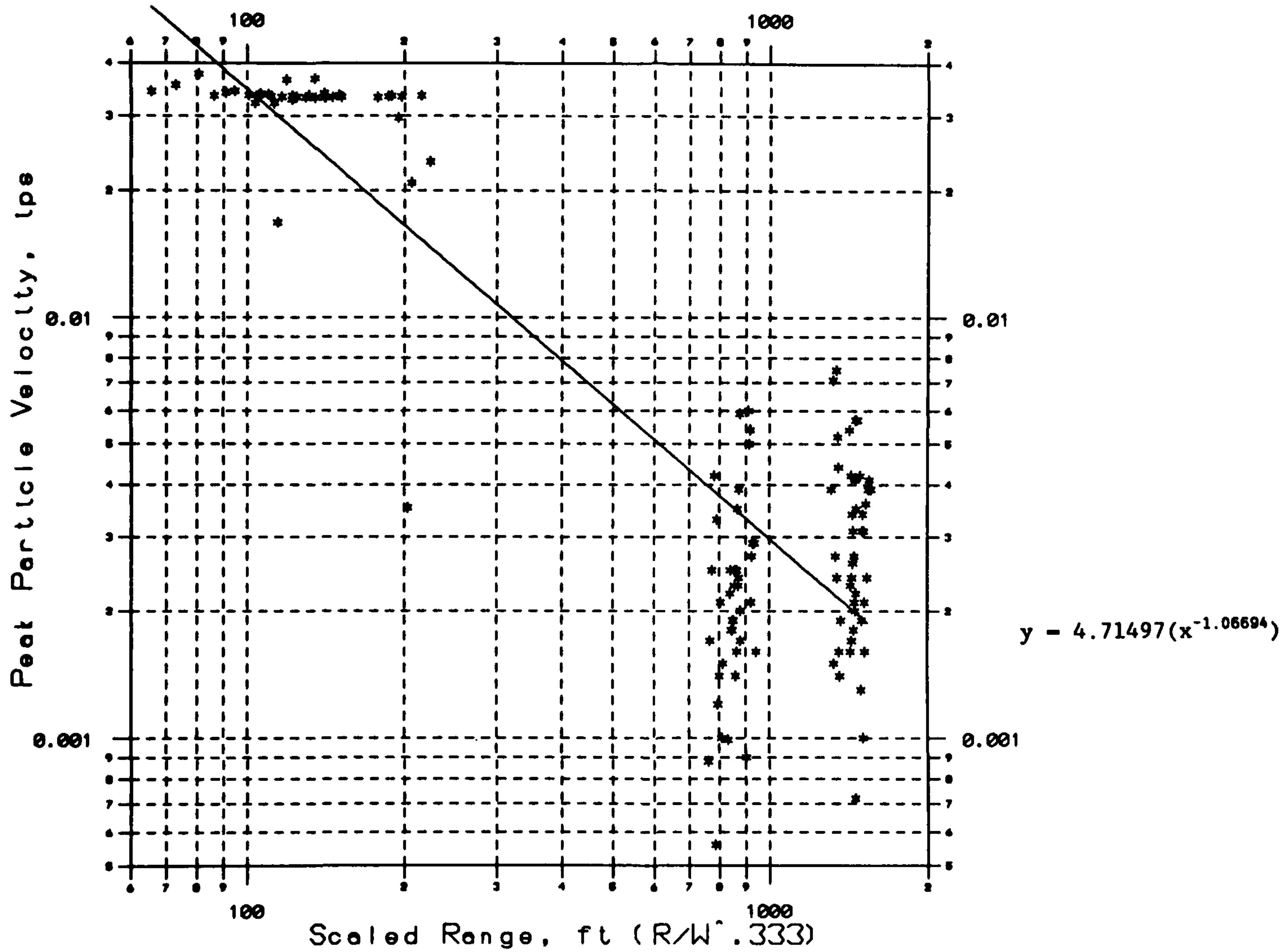

28 Aug Radial

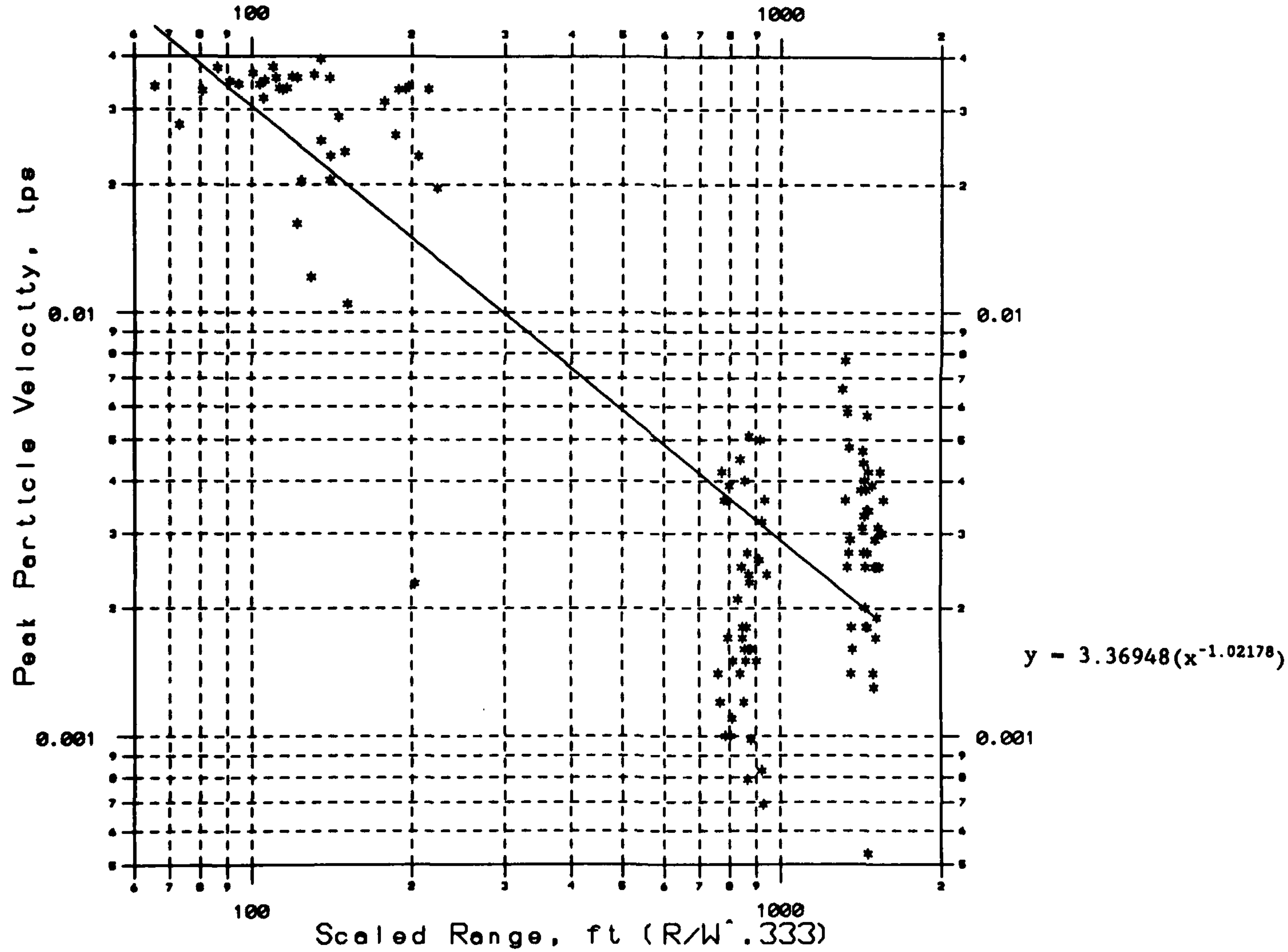

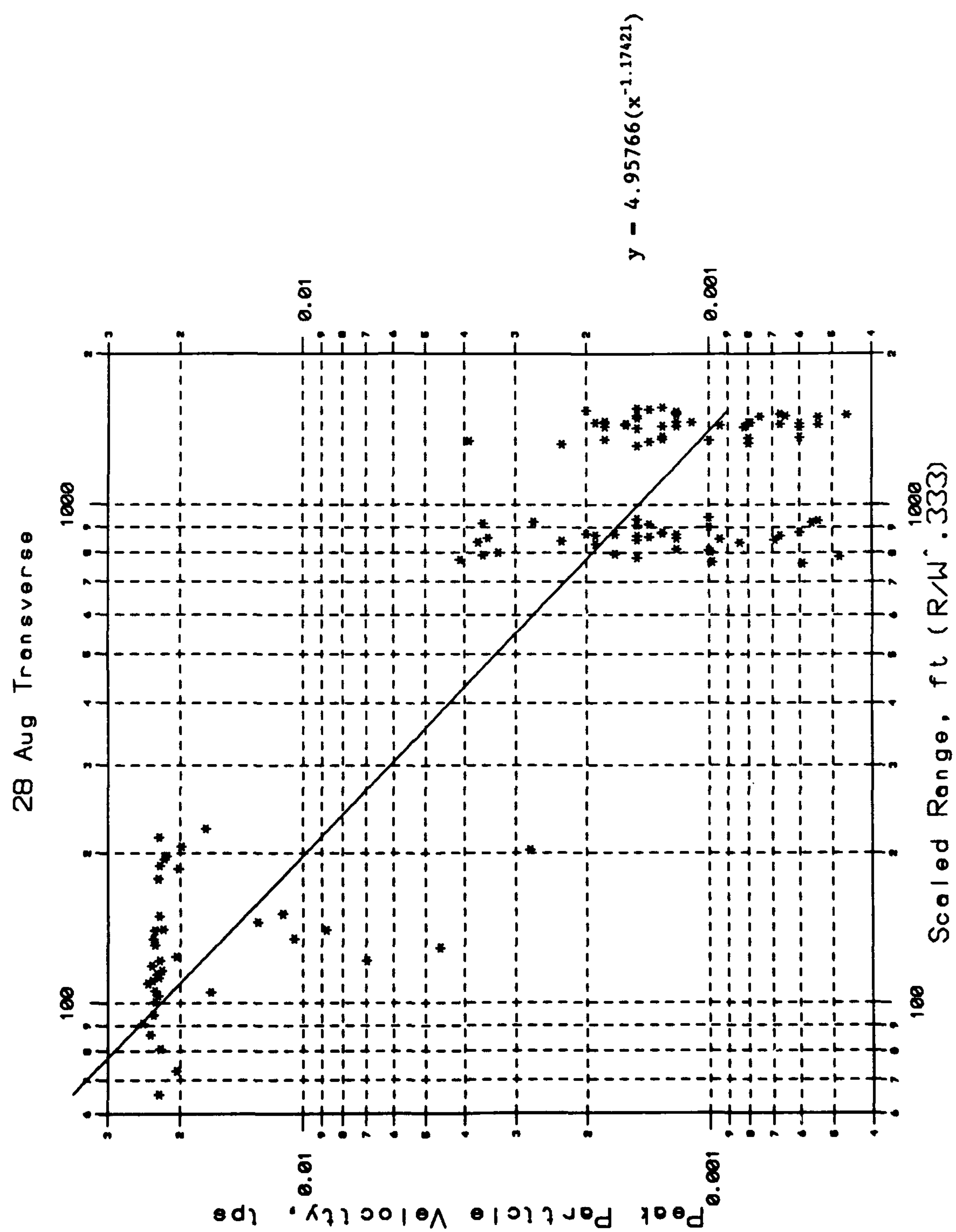

28 Aug Transverse
y - 4.95766(x^-1.17421)
0.01
0.001
100
1000
Scaled Range, ft (R/W^.333)
Peak Particle Velocity, ips

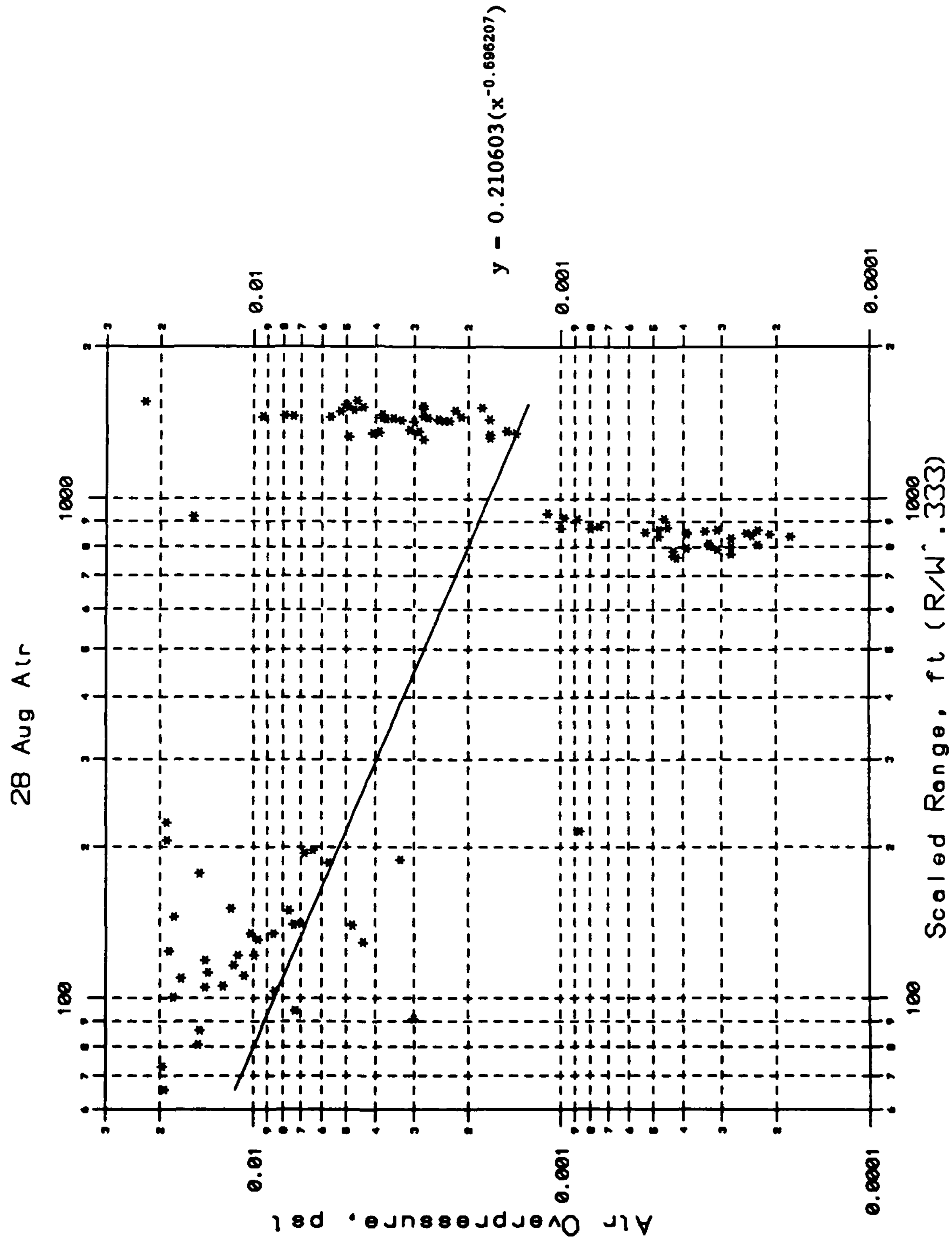
28 Aug Air
y = 0.210603(x^-0.696207)
Scaled Range, ft (R/W^.333)
Air Overpressure, psi
100
1000
0.01
0.001
0.0001

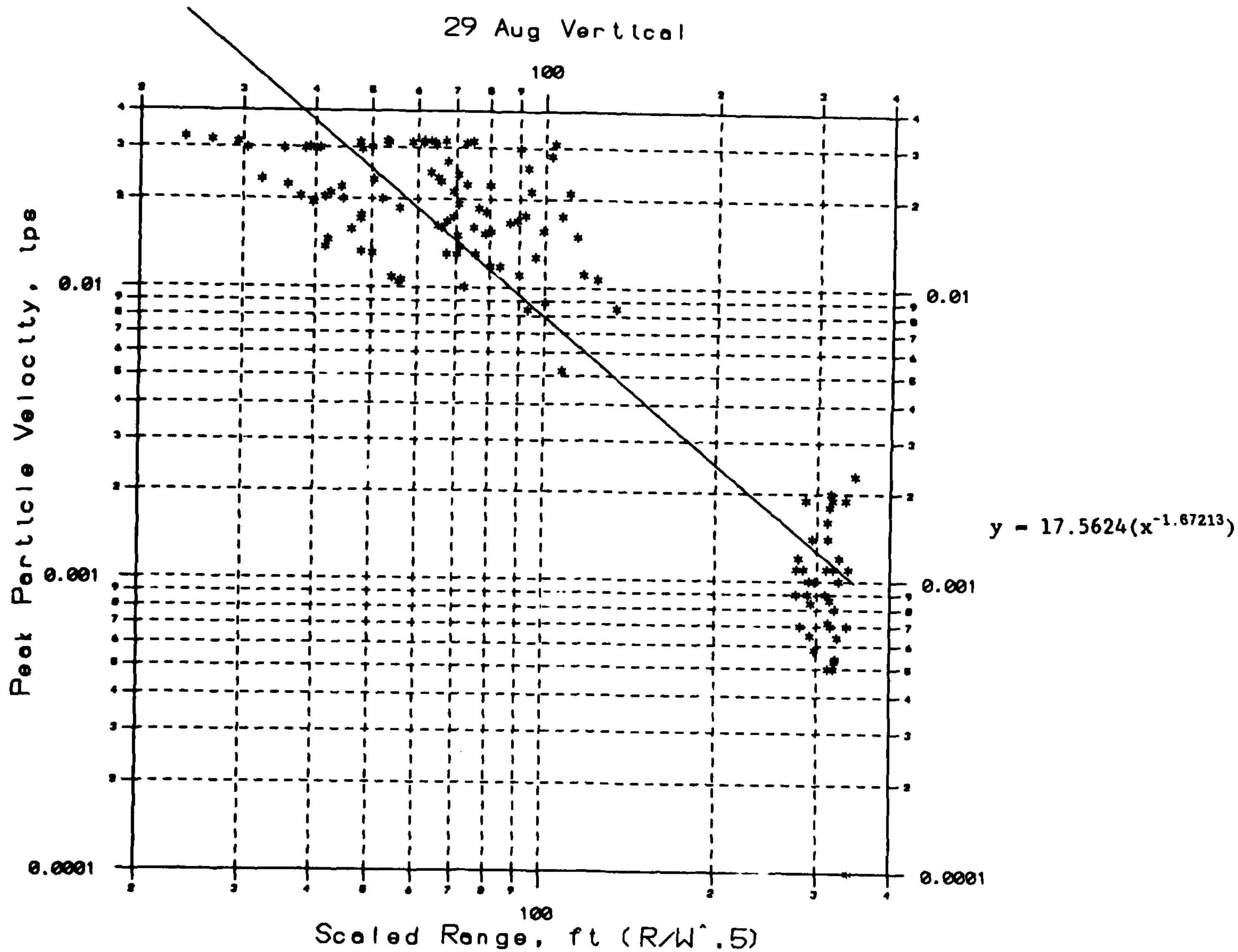

29 Aug Vertical
Peak Particle Velocity, ips
Scaled Range, ft (R/W^.5)
100
0.01
0.001
0.0001
y = 17.5624(x^-1.67213)

29 Aug Radial

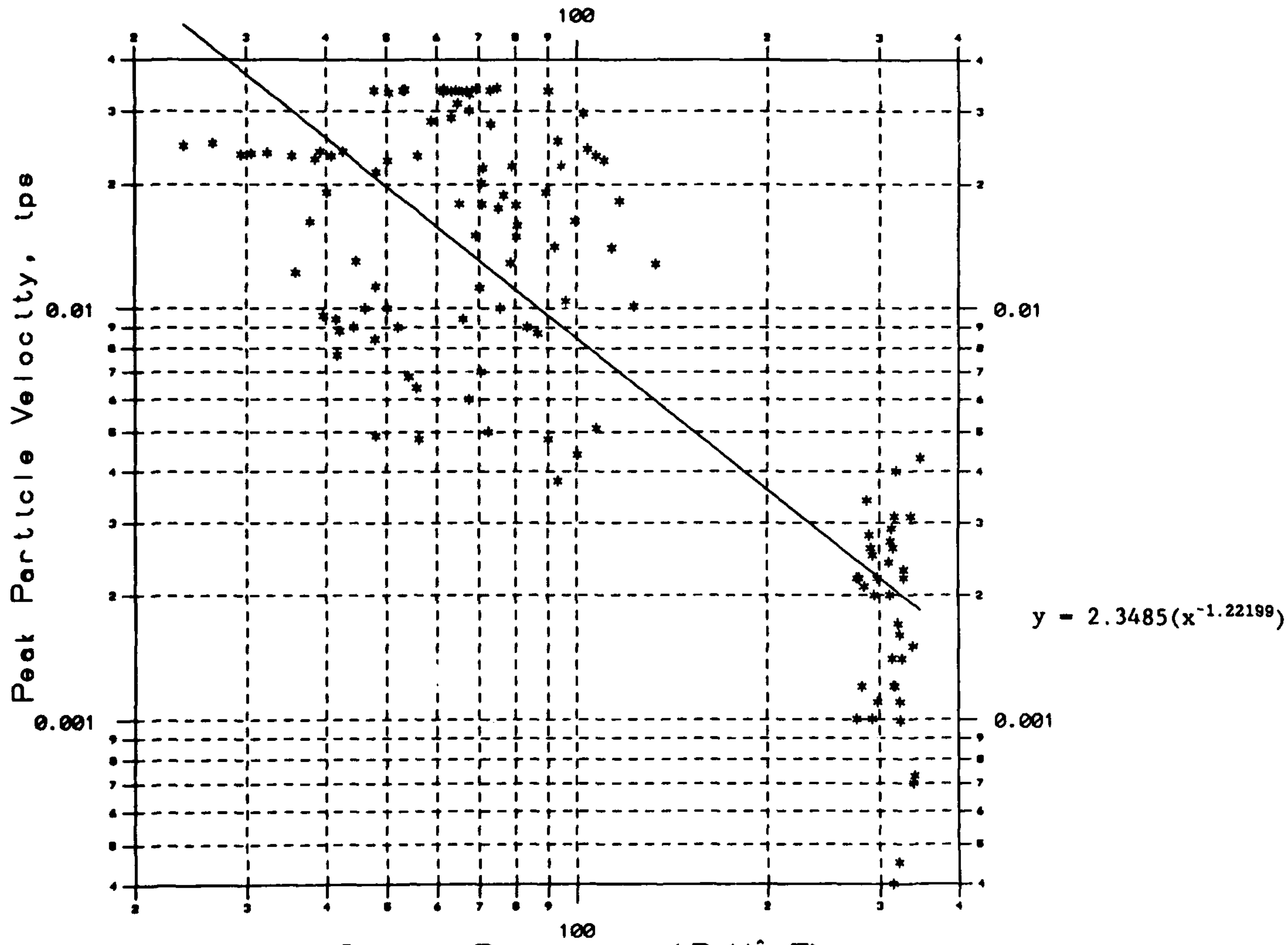

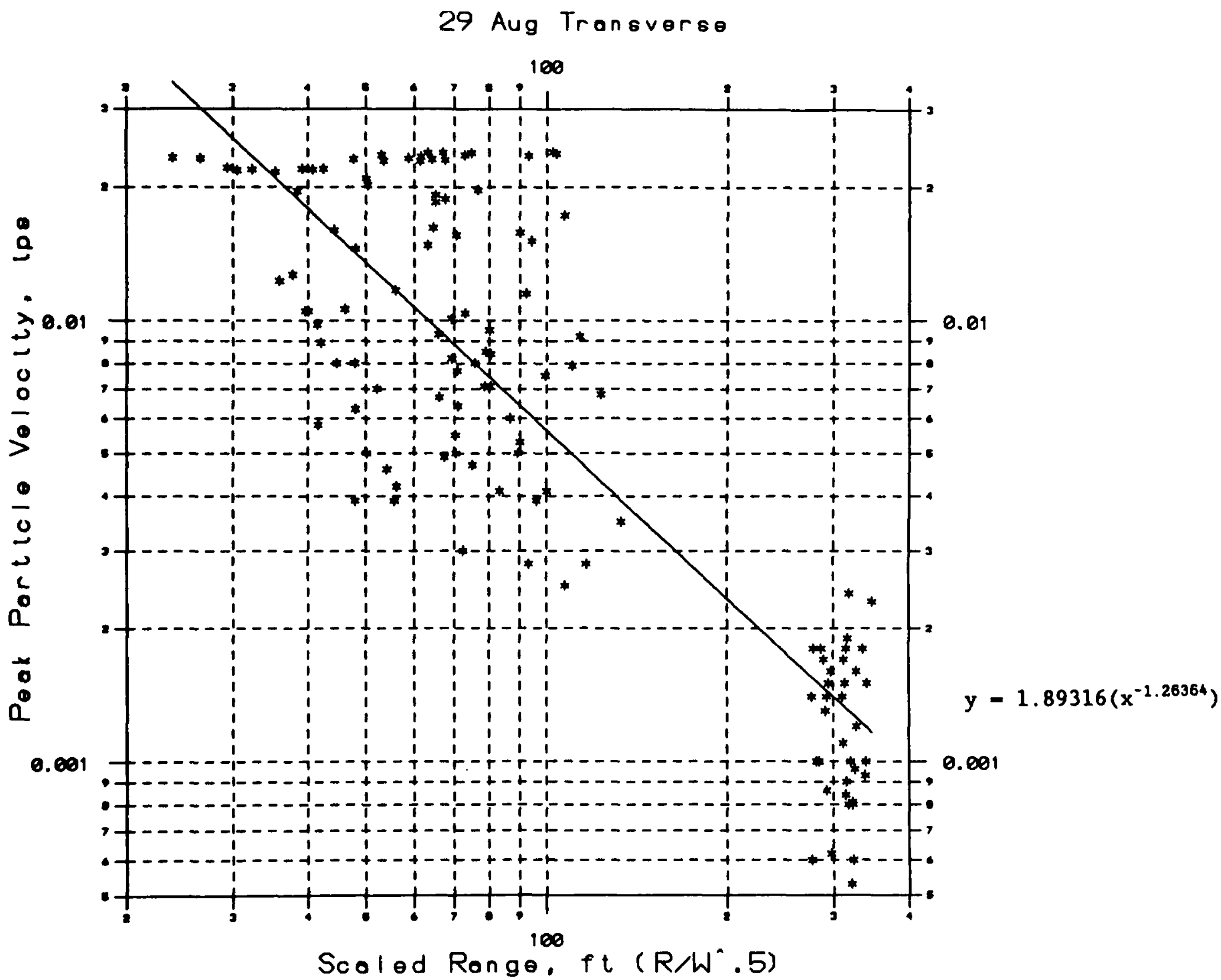

29 Aug Transverse
100
0.01
0.001
Peak Particle Velocity, ips
Scaled Range, ft (R/W^.5)
y = 1.89316(x^-1.26364)

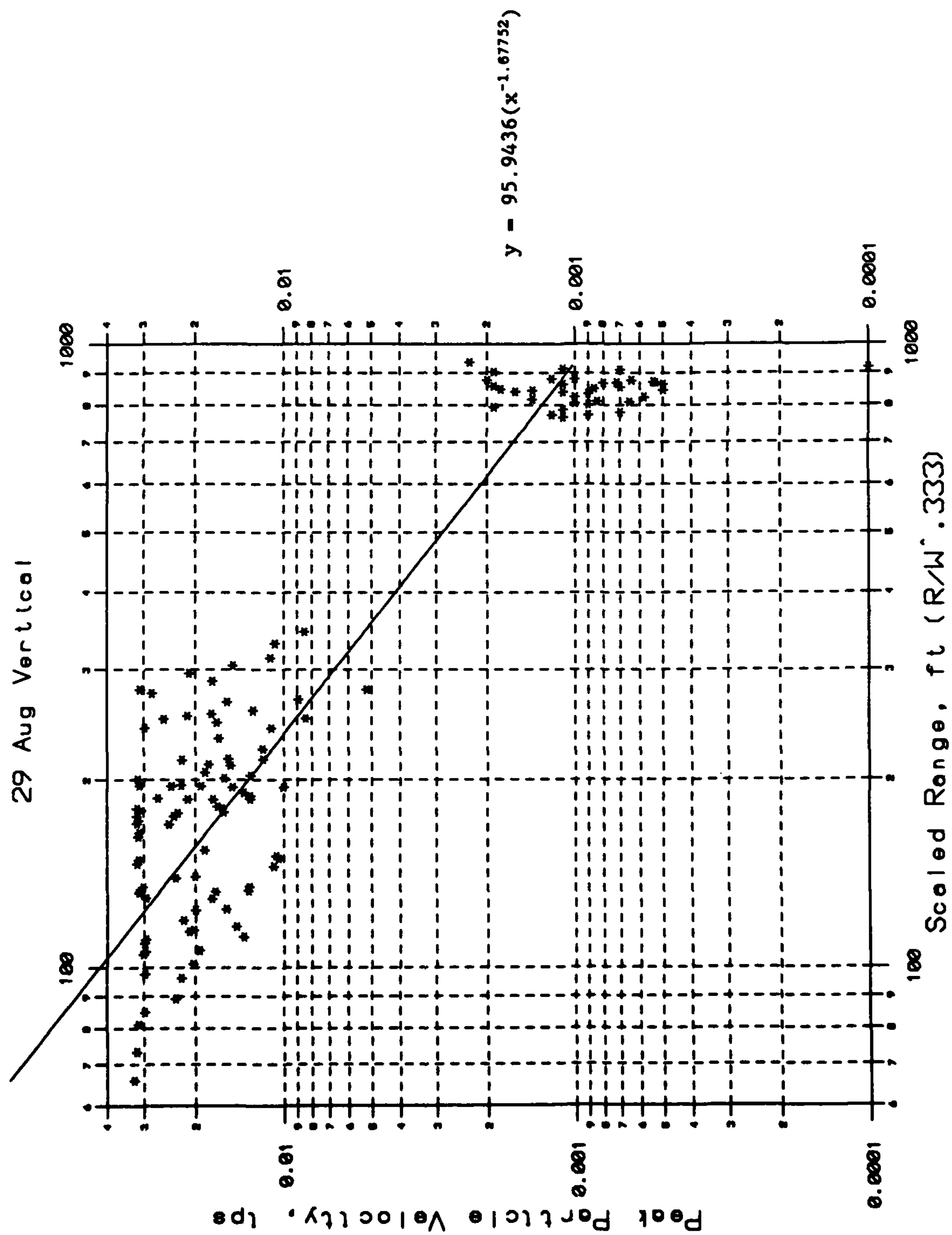
29 Aug Vertical
y = 95.9436(x^-1.67752)
Peak Particle Velocity, ips
Scaled Range, ft (R/W^.333)
0.01
0.001
0.0001
100
1000

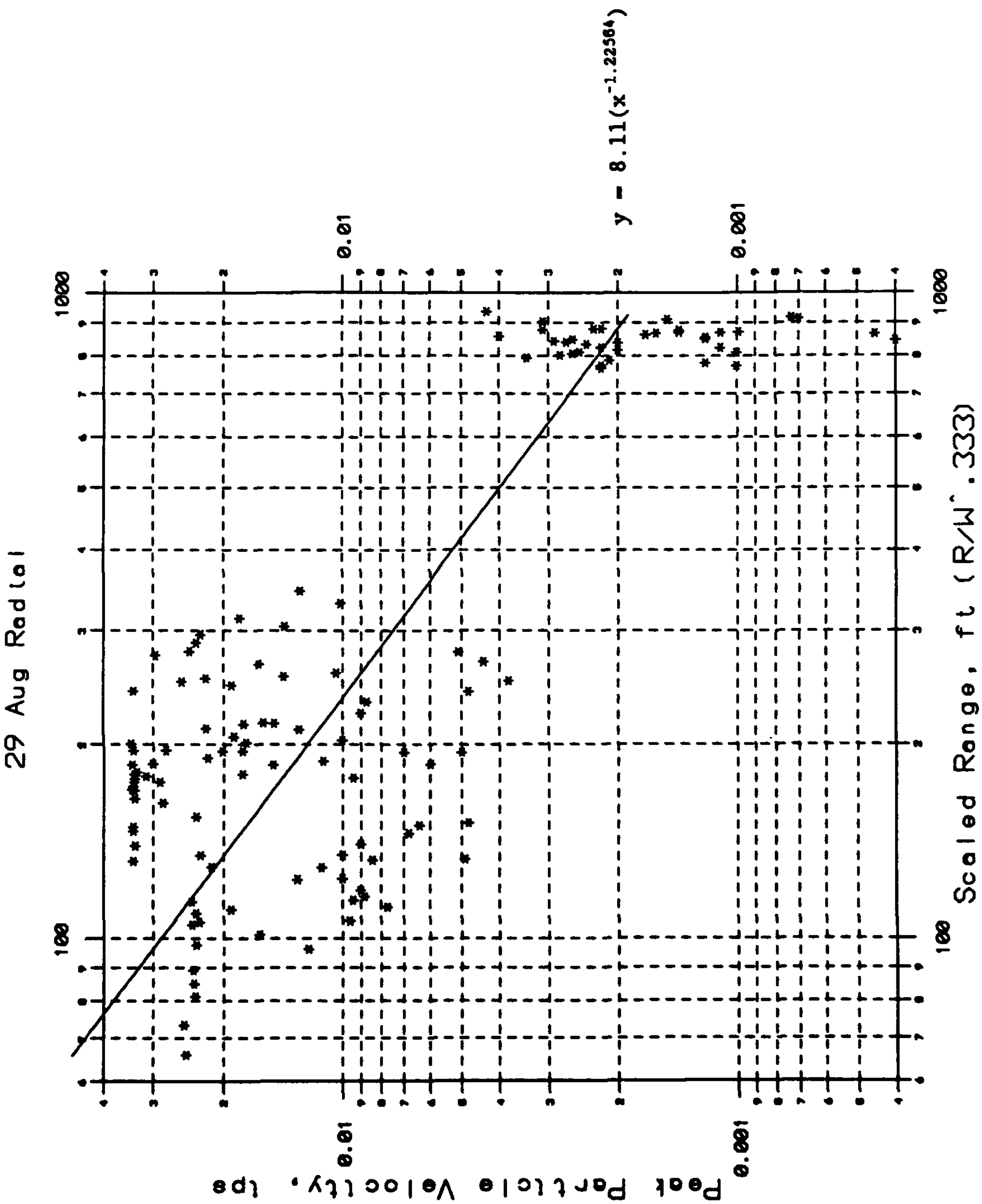

29 Aug Radial
y = 8.11(x^-1.22564)
0.01
0.001
1000
100
Scaled Range, ft (R/W^.333)
Peak Particle Velocity, ips

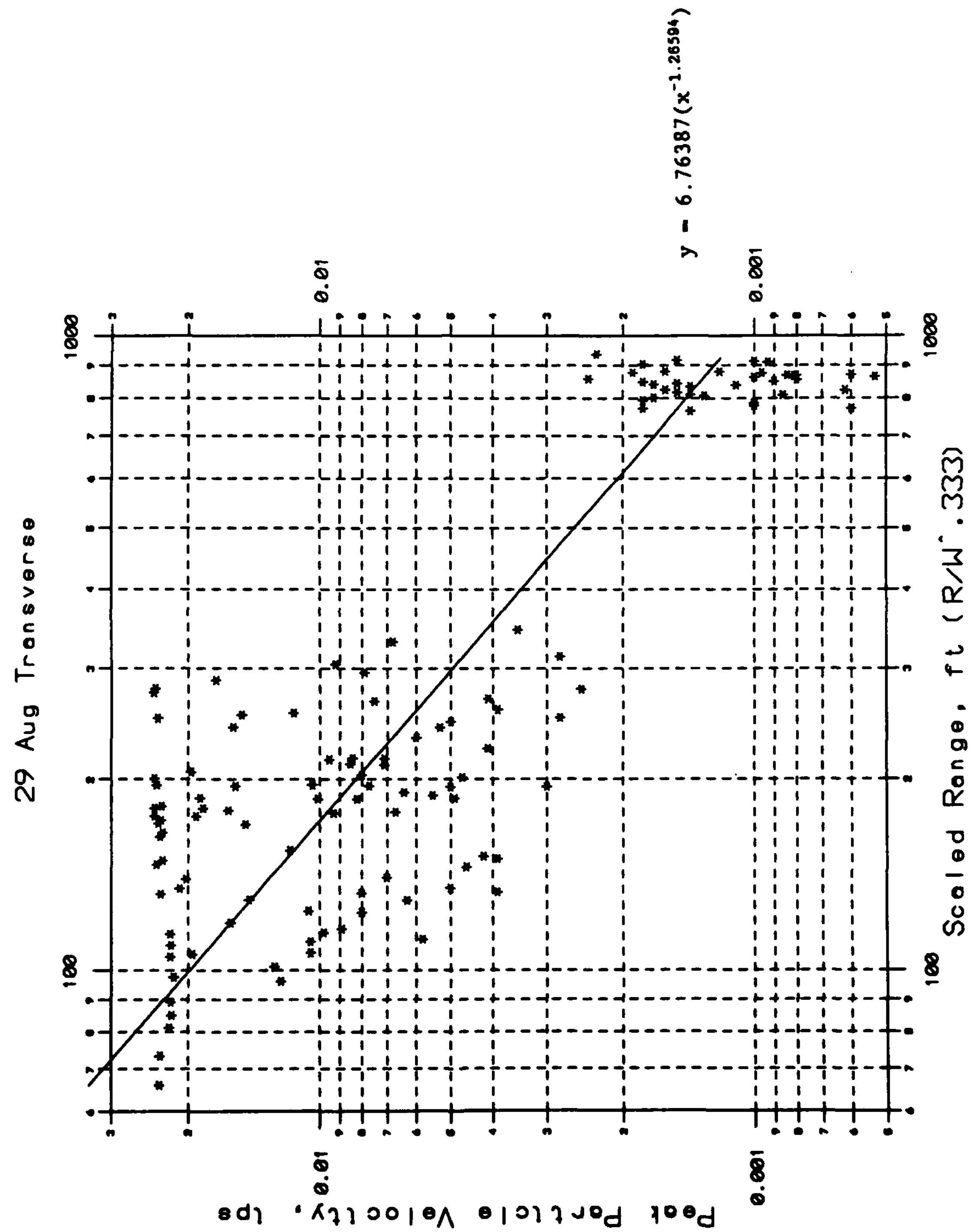
29 Aug Transverse
y = 6.76387(x^-1.26594)
Scaled Range, ft (R/W^.333)
Peak Particle Velocity, ips
100
1000
0.01
0.001

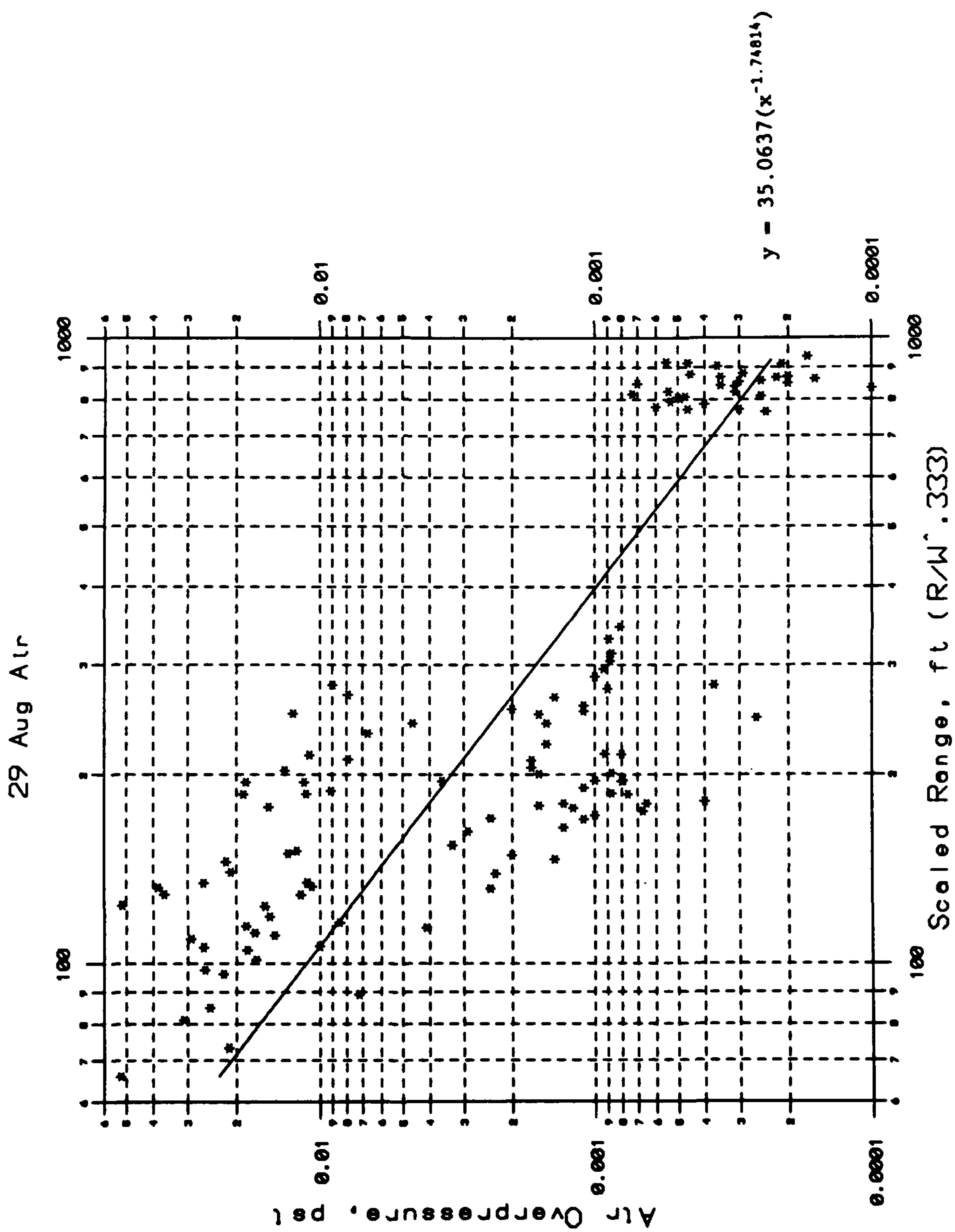
29 Aug Air
y = 35.0637(x^-1.74814)
Scaled Range, ft (R/W^.333)
Air Overpressure, psi
100
1000
0.01
0.001
0.0001

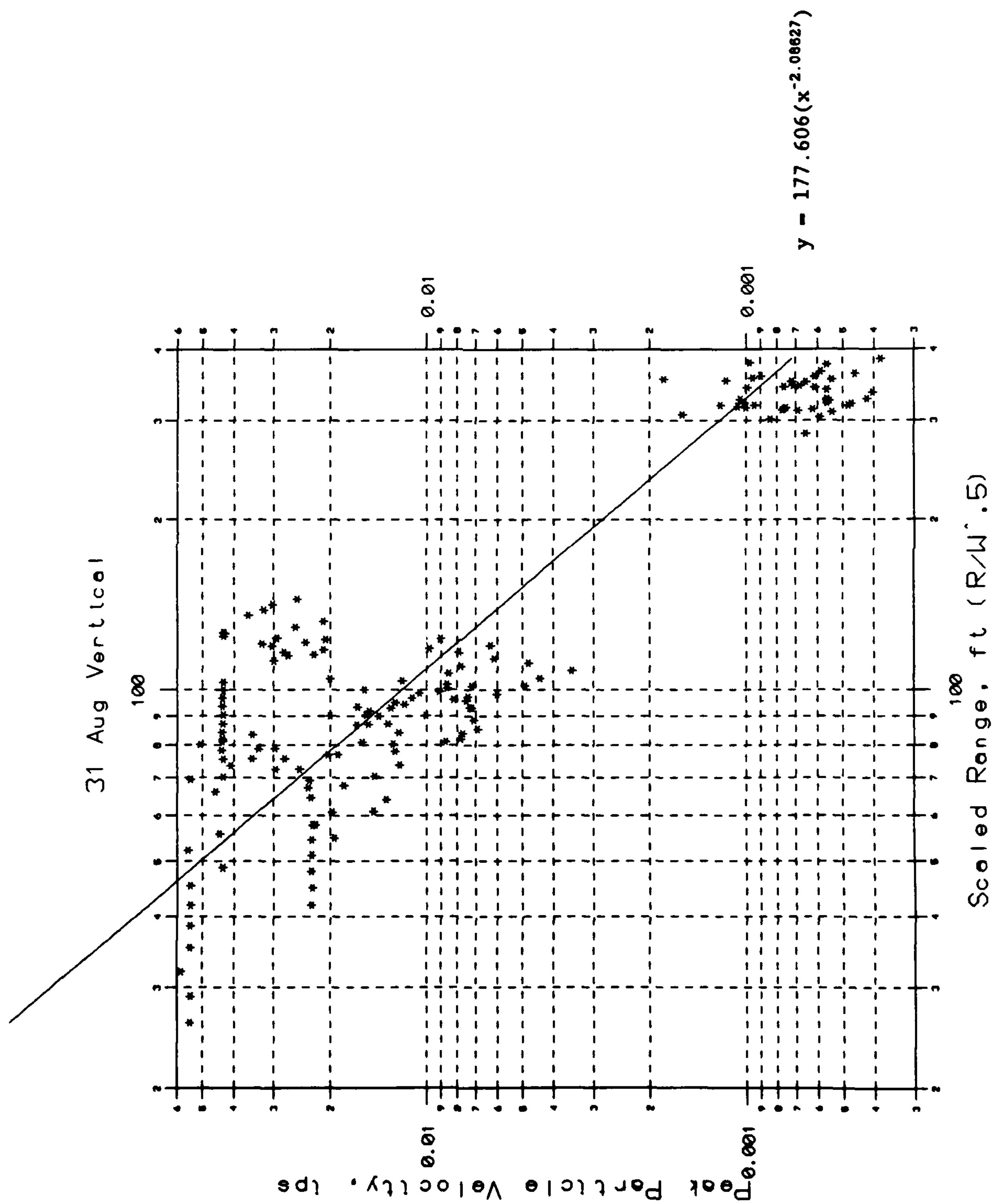
31 Aug Vertical
y = 177.606(x^-2.08627)
Scaled Range, ft (R/W^.5)
Peak Particle Velocity, ips
100
0.01
0.001

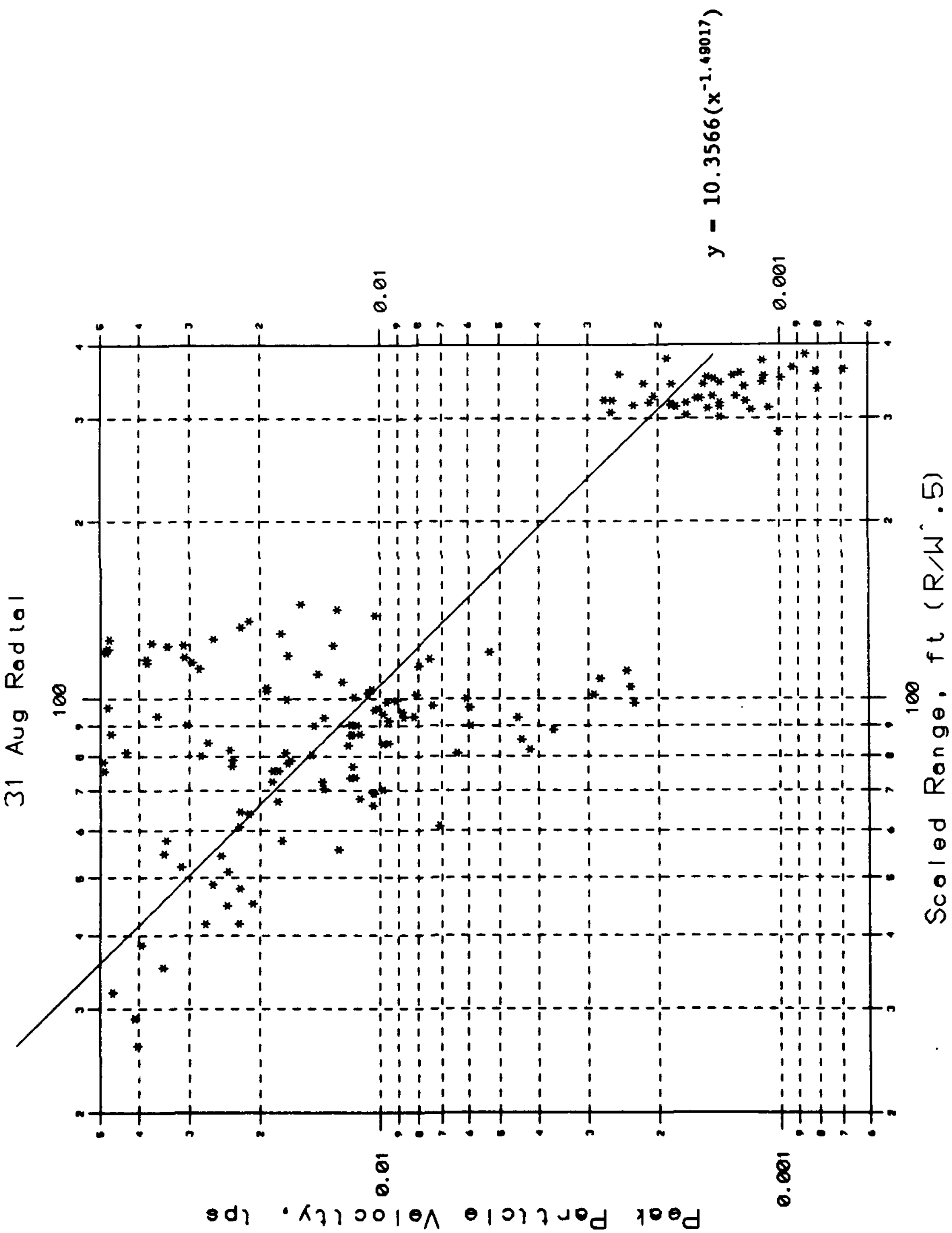
31 Aug Radial
y = 10.3566(x^-1.49017)
Scaled Range, ft (R/W^.5)
Peak Particle Velocity, ips
100
0.01
0.001

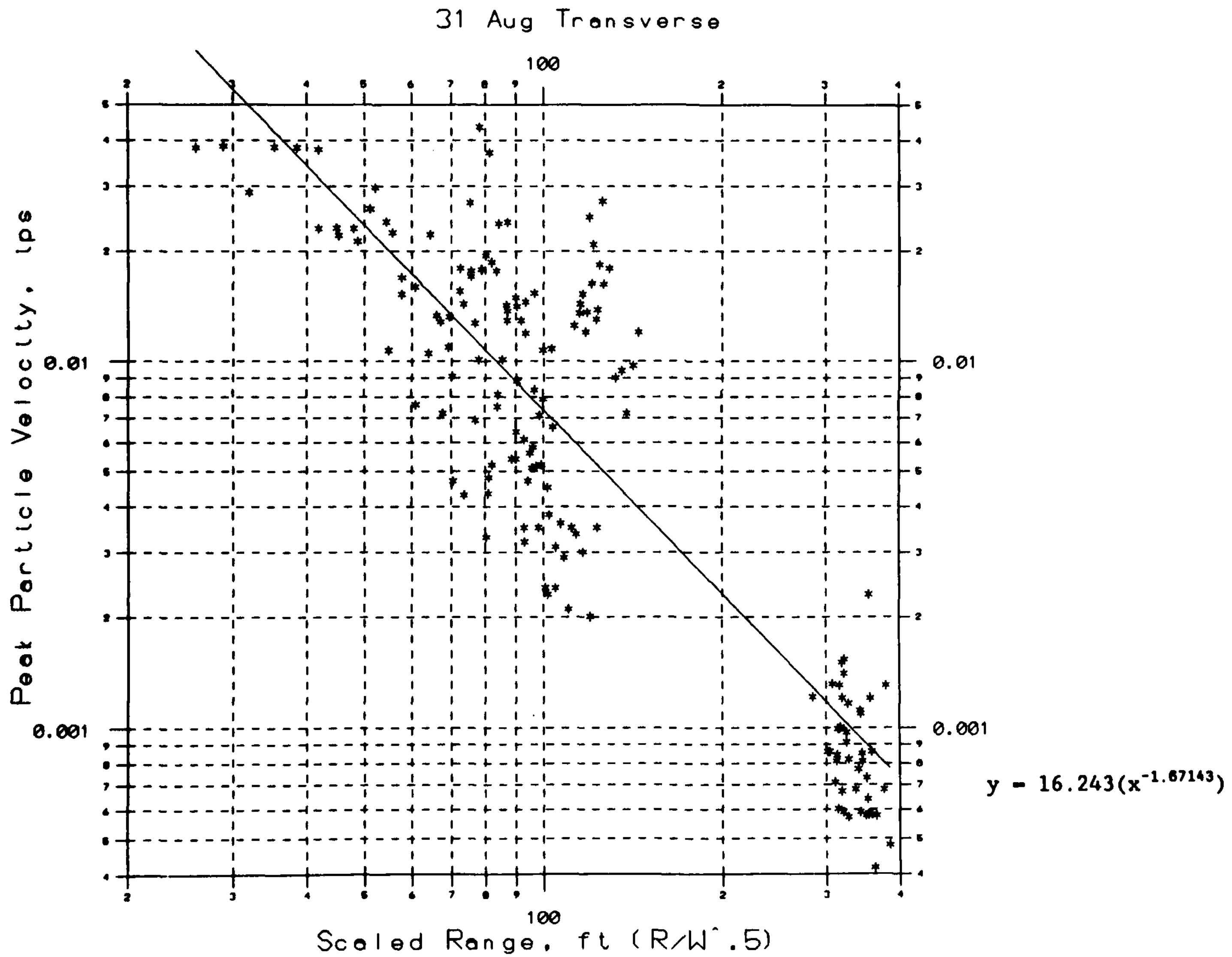
31 Aug Transverse
Peak Particle Velocity, ips
Scaled Range, ft (R/W^.5)
0.01
0.001
100
y = 16.243(x^-1.67143)

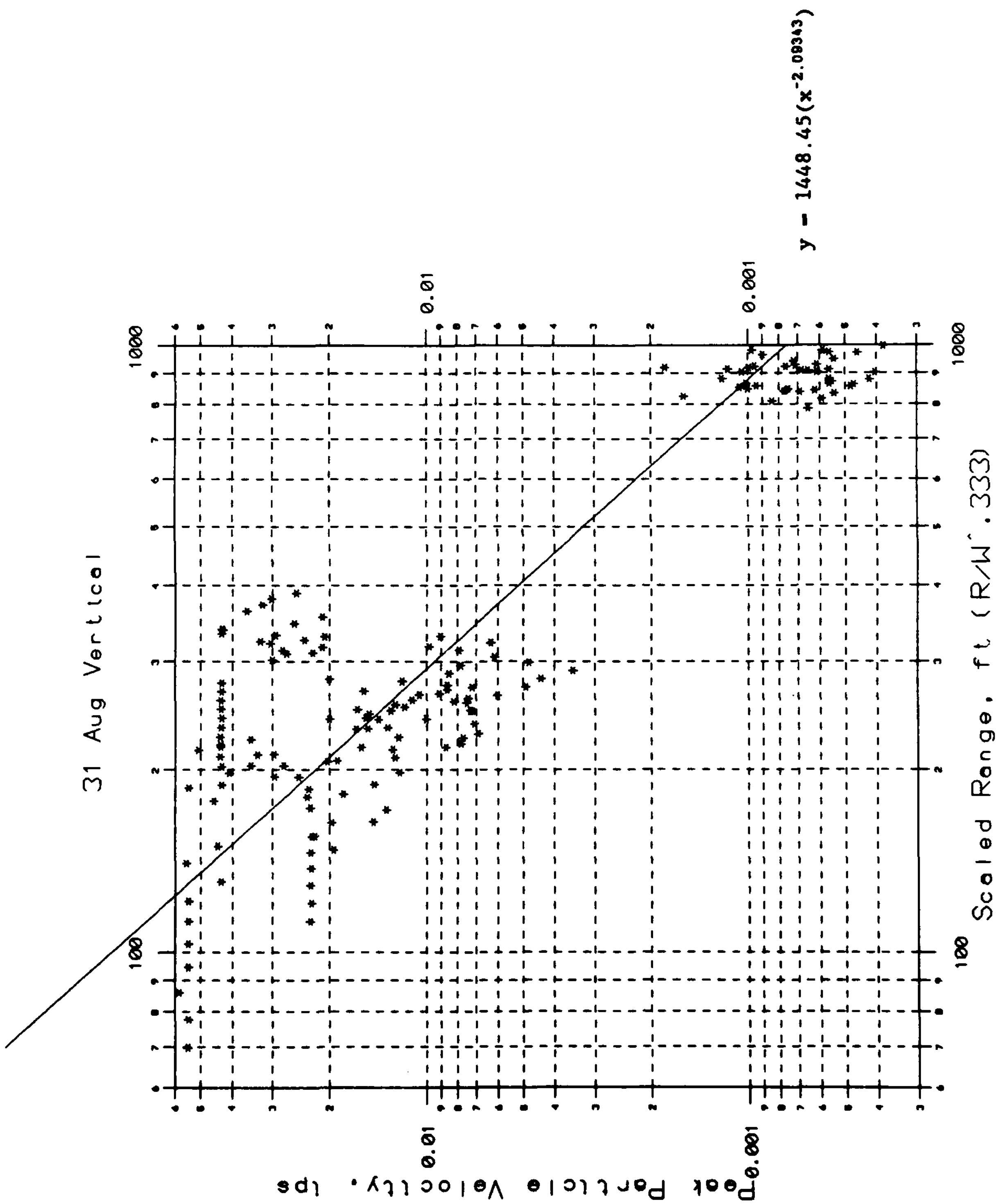
31 Aug Vertical
y = 1448.45(x^-2.09343)
Scaled Range, ft (R/W^.333)
Peak Particle Velocity, ips
100
1000
0.01
0.001

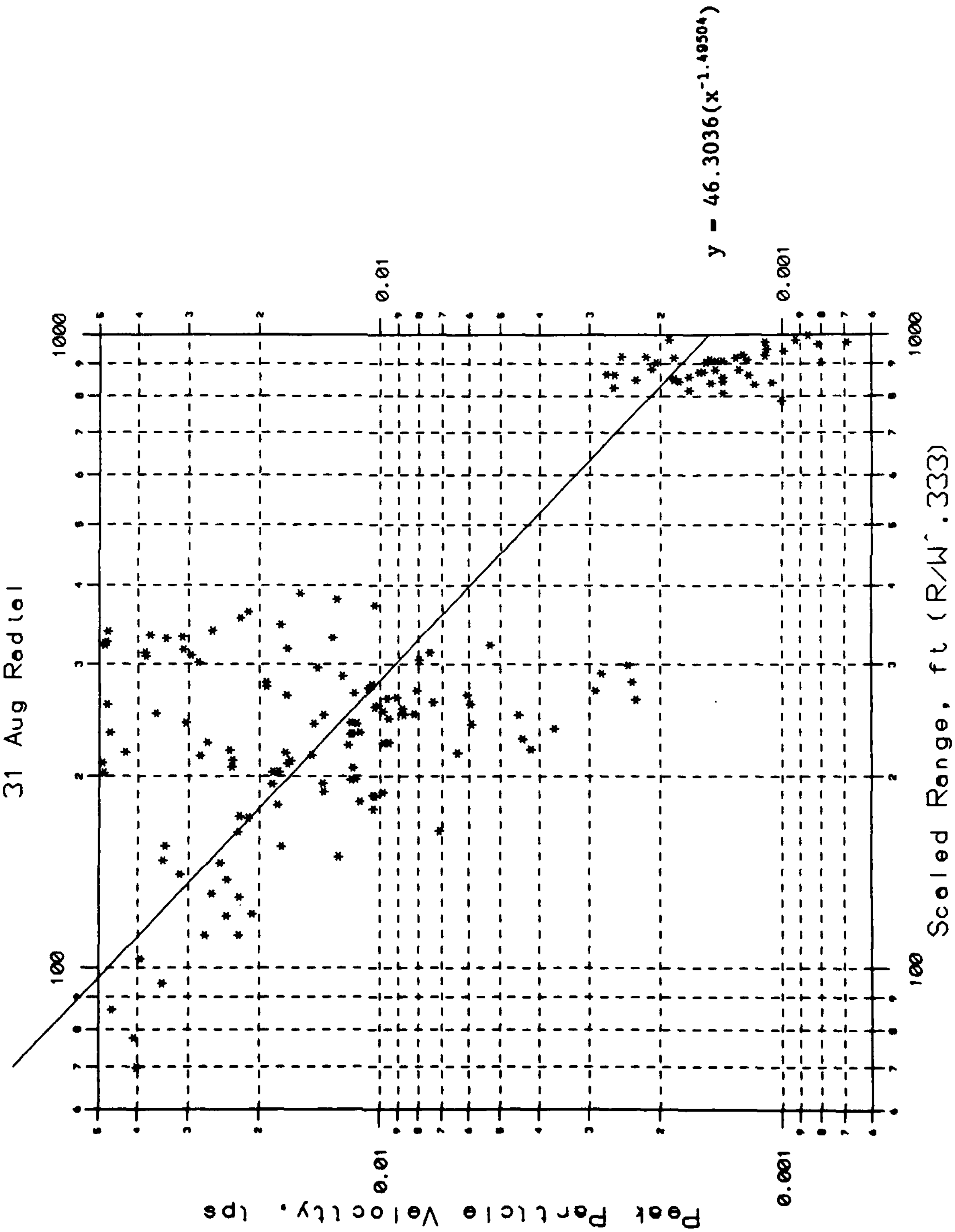
31 Aug Radial
y = 46.3036(x^-1.49504)
Scaled Range, ft (R/W^.333)
Peak Particle Velocity, ips
100
1000
0.01
0.001

31 Aug Transverse

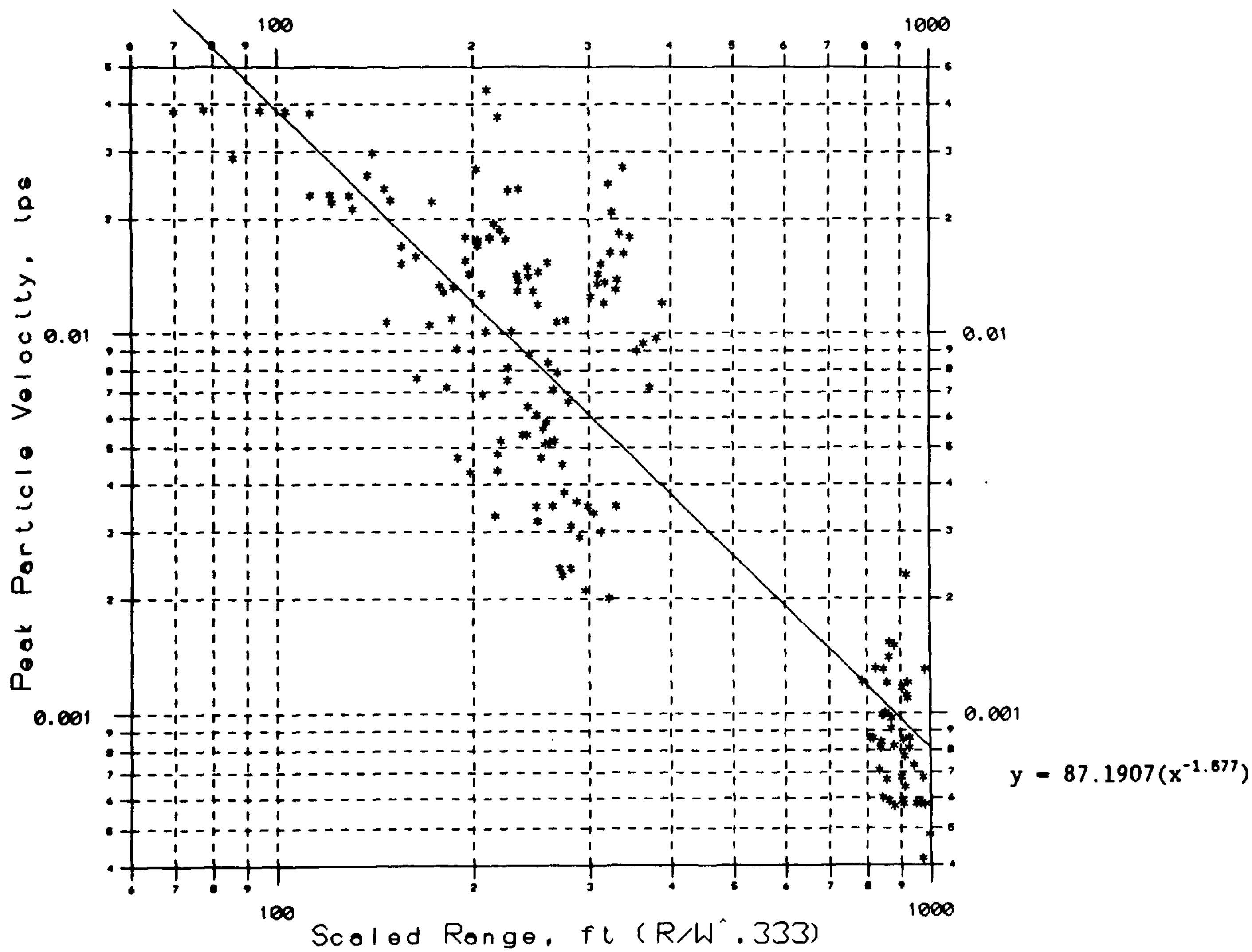

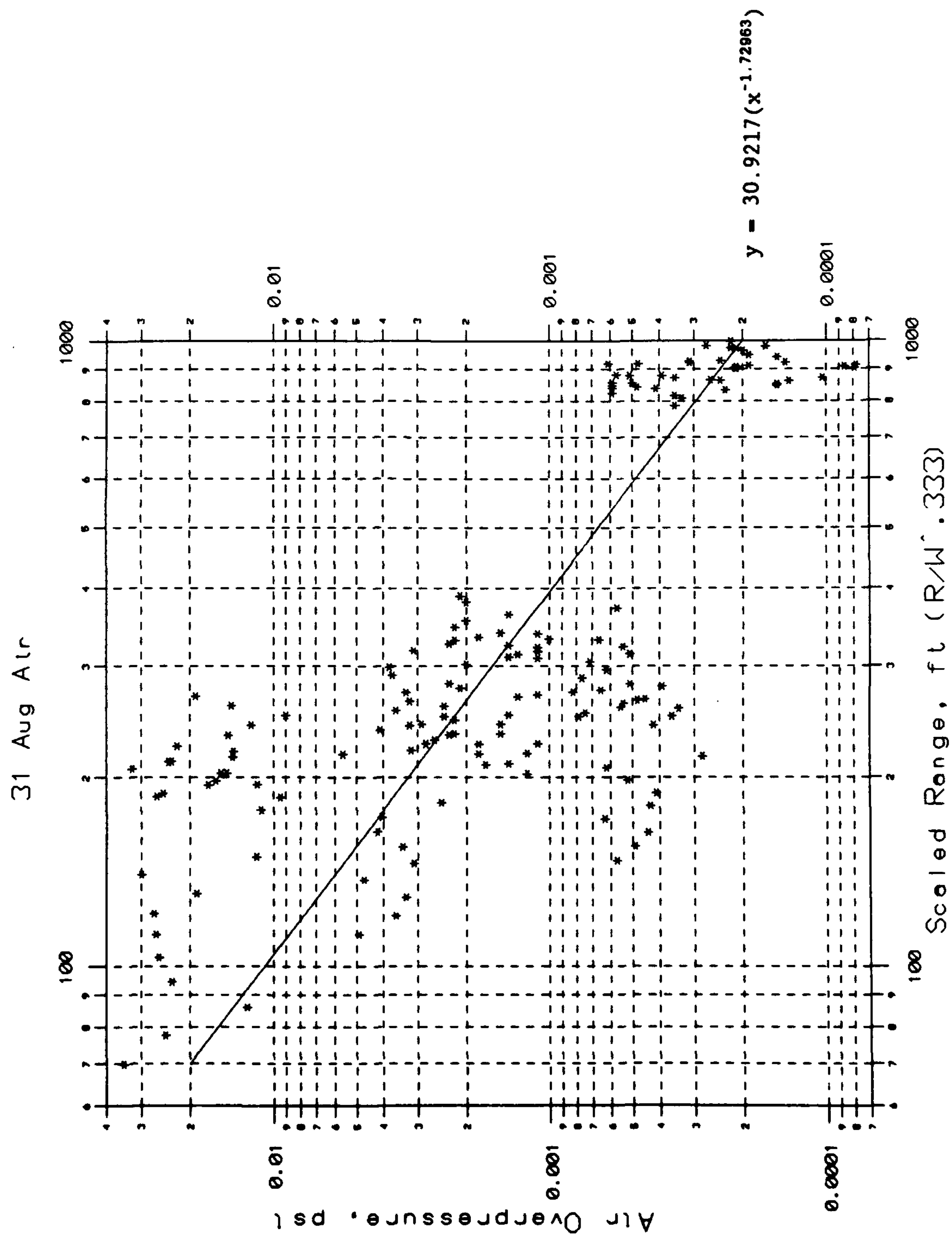
31 Aug Air
y = 30.9217(x^-1.72963)
Air Overpressure, psi
Scaled Range, ft (R/W^.333)
0.01
0.001
0.0001
100
1000

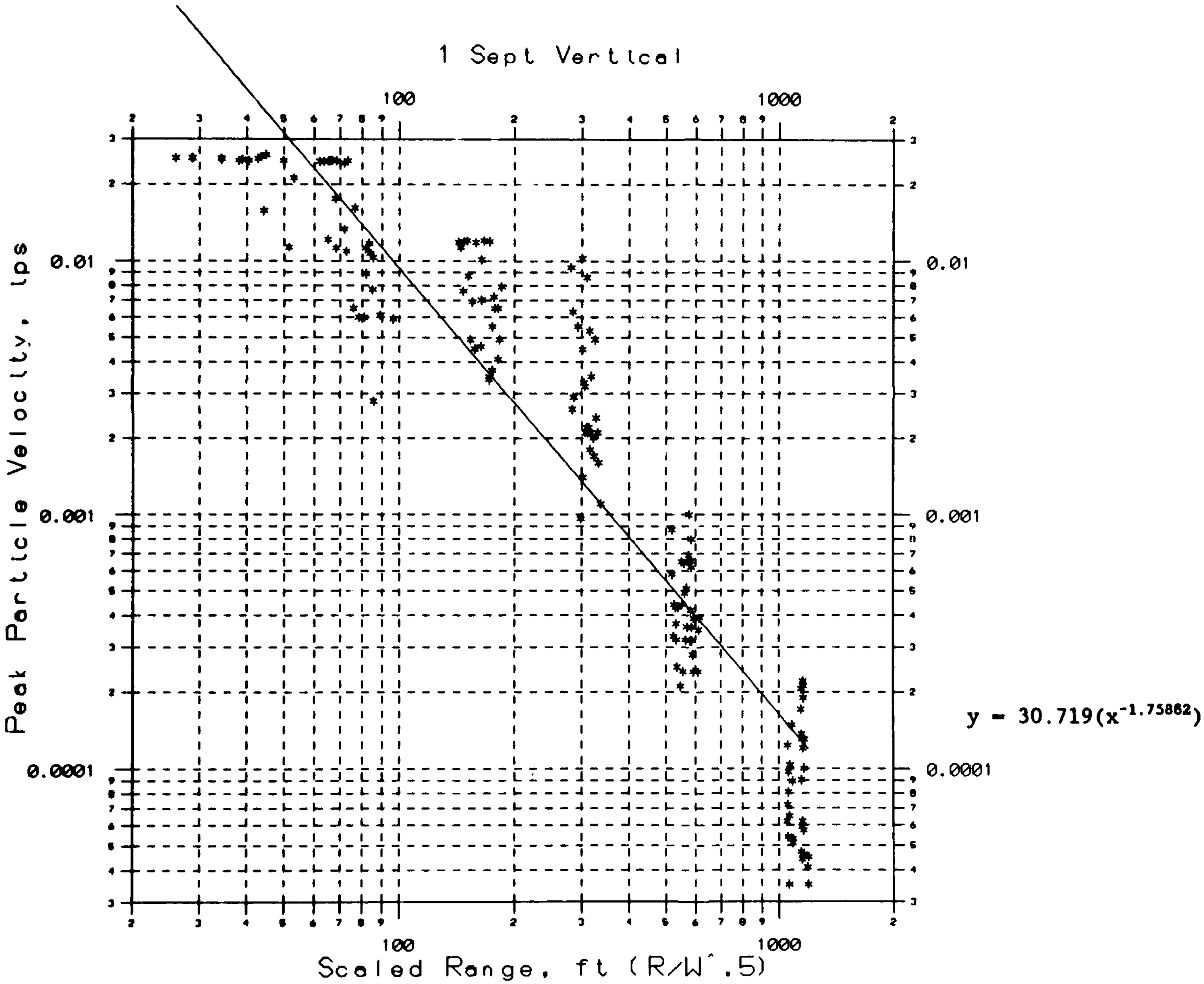

1 Sept Vertical
Peak Particle Velocity, ips
Scaled Range, ft (R/W^.5)
y = 30.719(x^-1.75862)

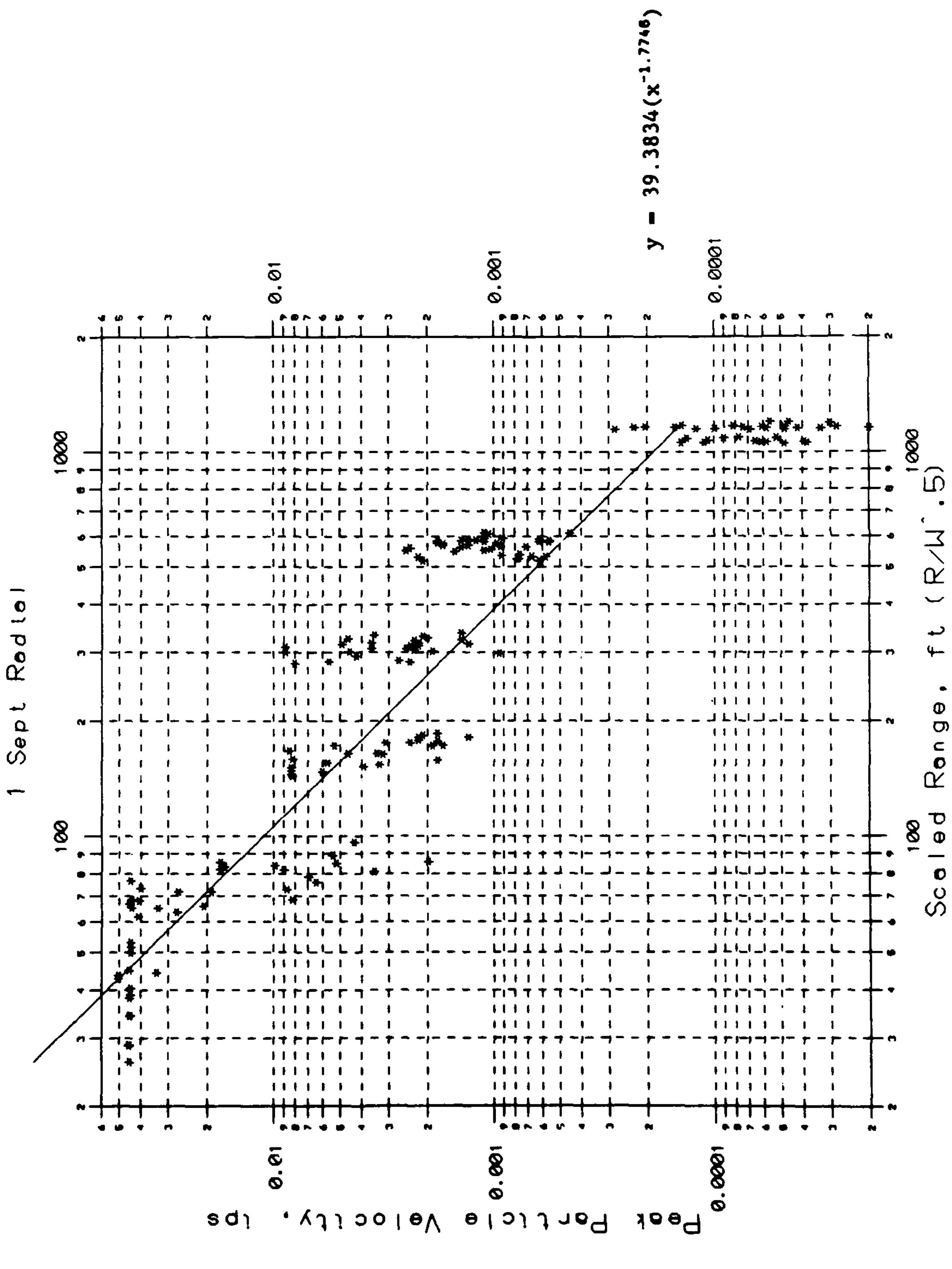
1 Sept Radial
y = 39.3834(x^-1.7746)
Scaled Range, ft (R/W^.5)
Peak Particle Velocity, ips
0.01
0.001
0.0001
100
1000

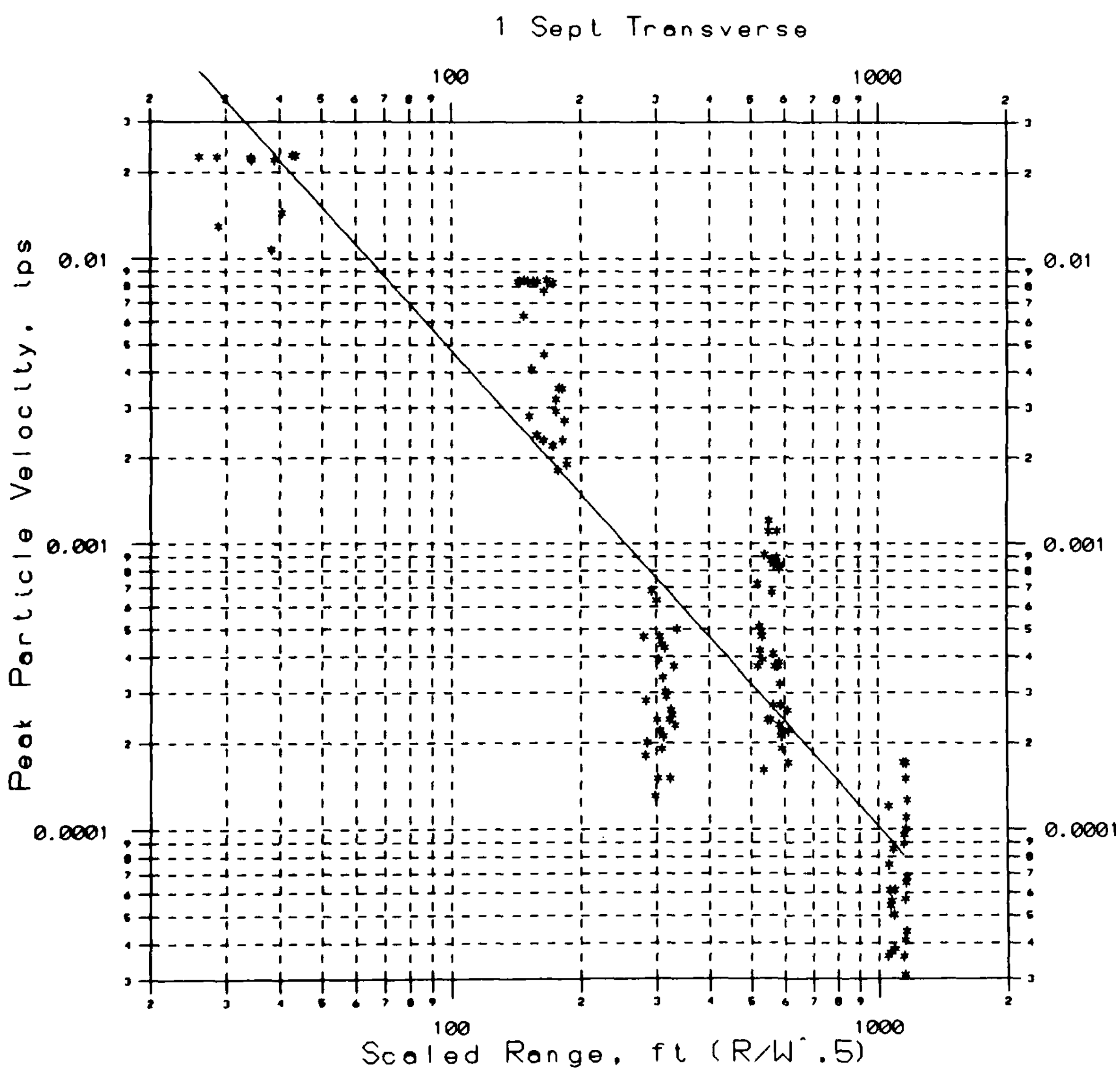

$y = 10.3959(x^{-1.66985})$

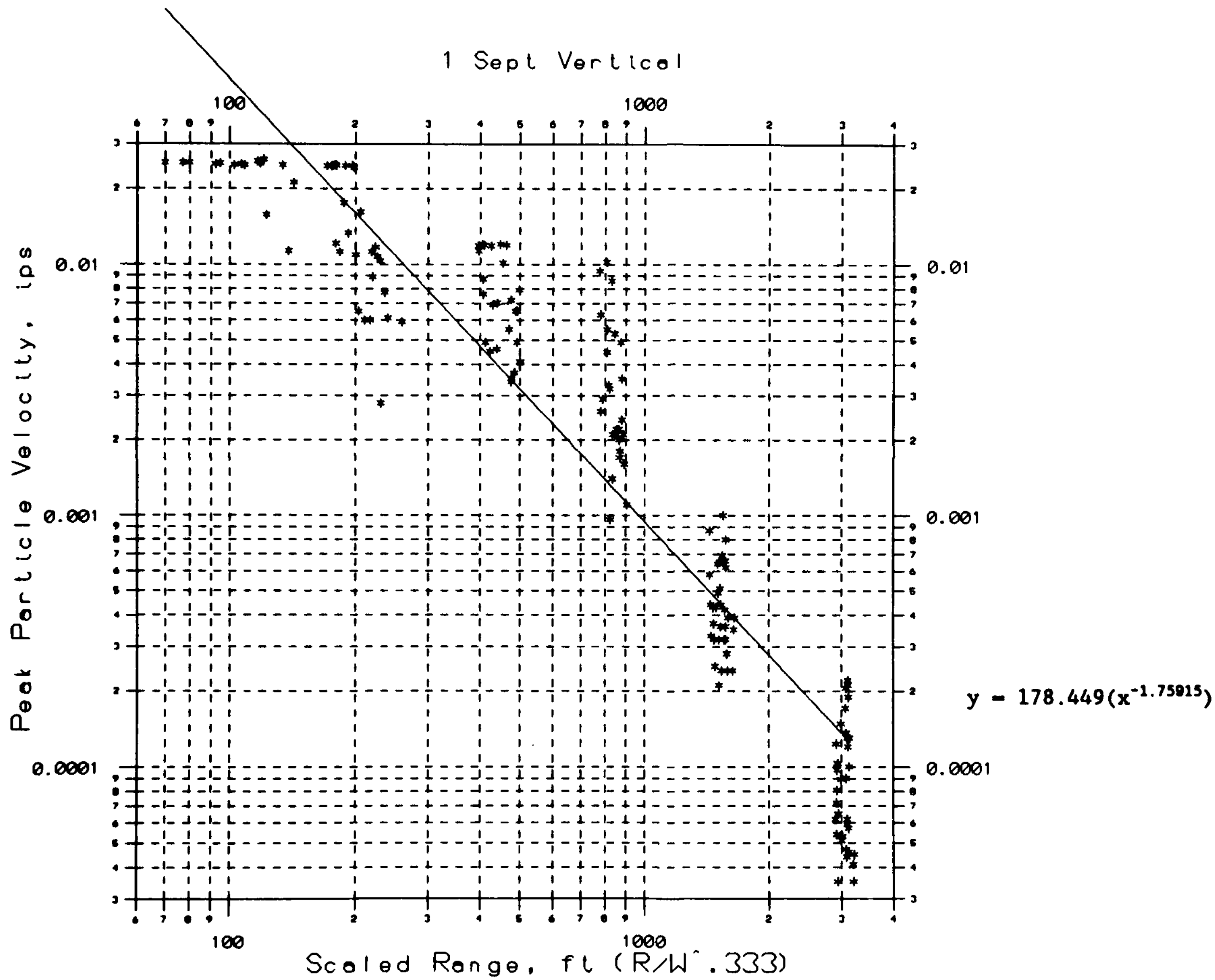

1 Sept Vertical
Peak Particle Velocity, ips
Scaled Range, ft (R/W^.333)
y = 178.449(x^-1.75915)
100
1000
0.01
0.001
0.0001

1 Sept Radial

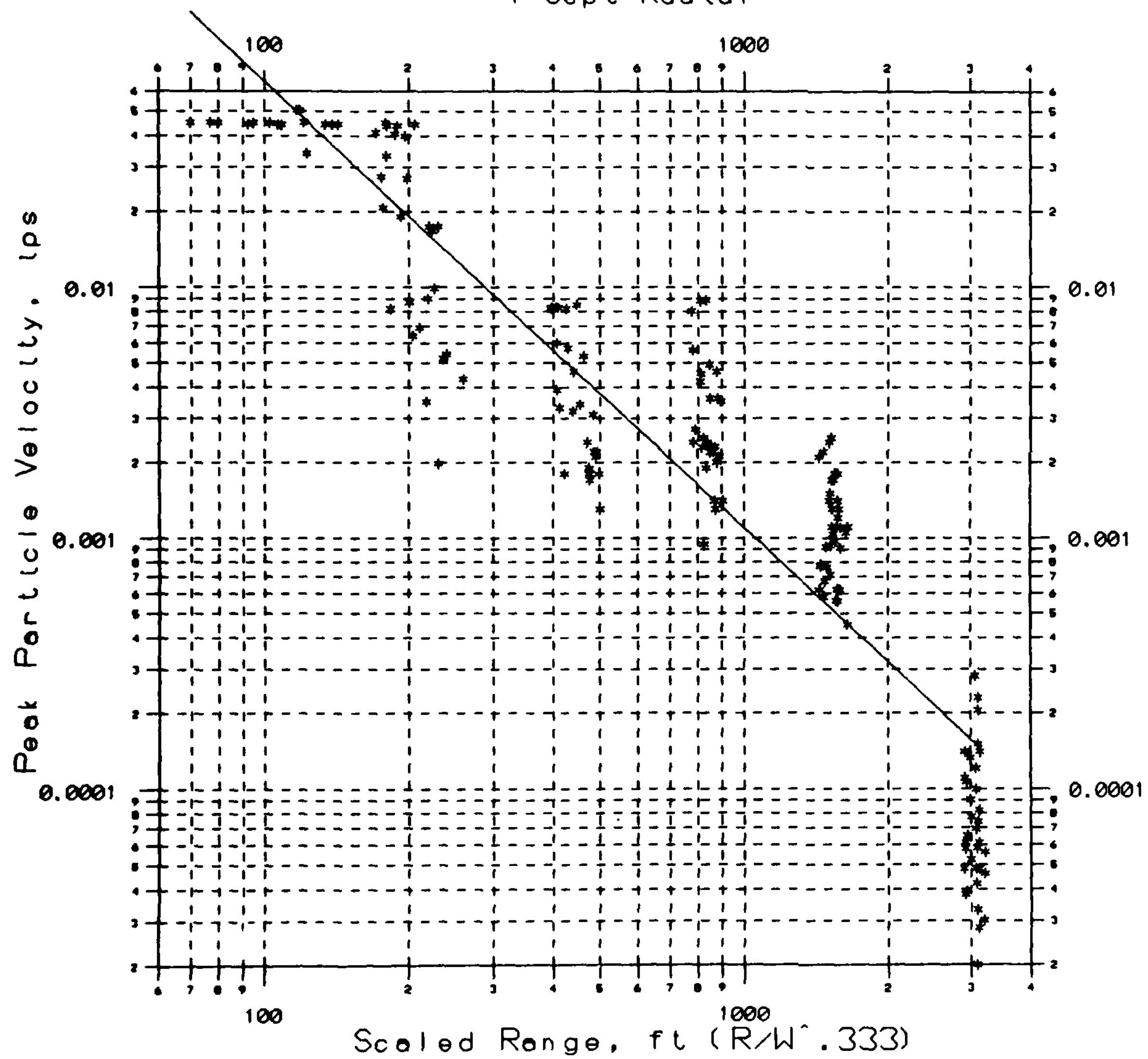

$y = 231.959(x^{-1.7748})$

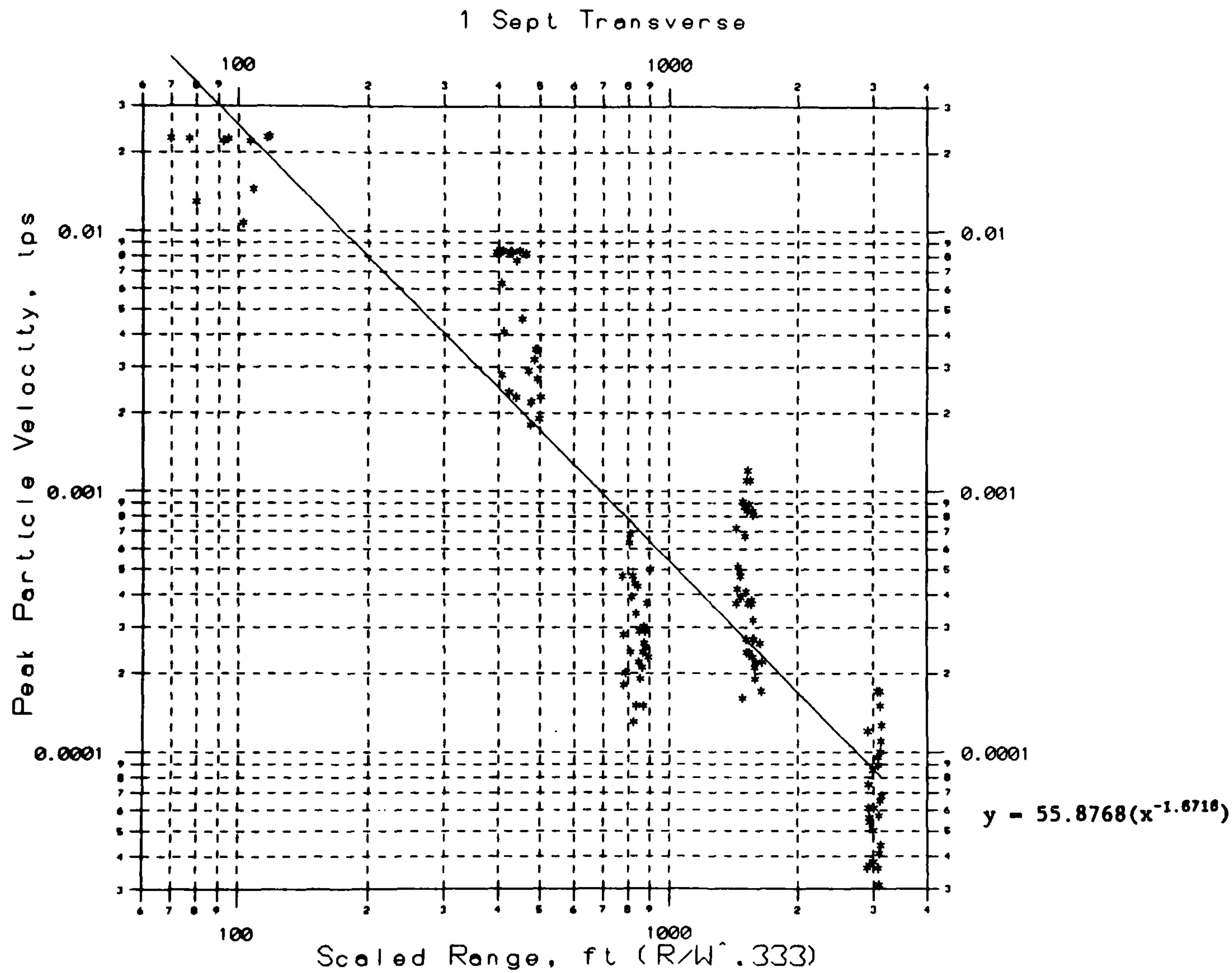
1 Sept Transverse
Peak Particle Velocity, ips
Scaled Range, ft (R/W^.333)
0.01
0.001
0.0001
100
1000
y = 55.8768(x^-1.6716)

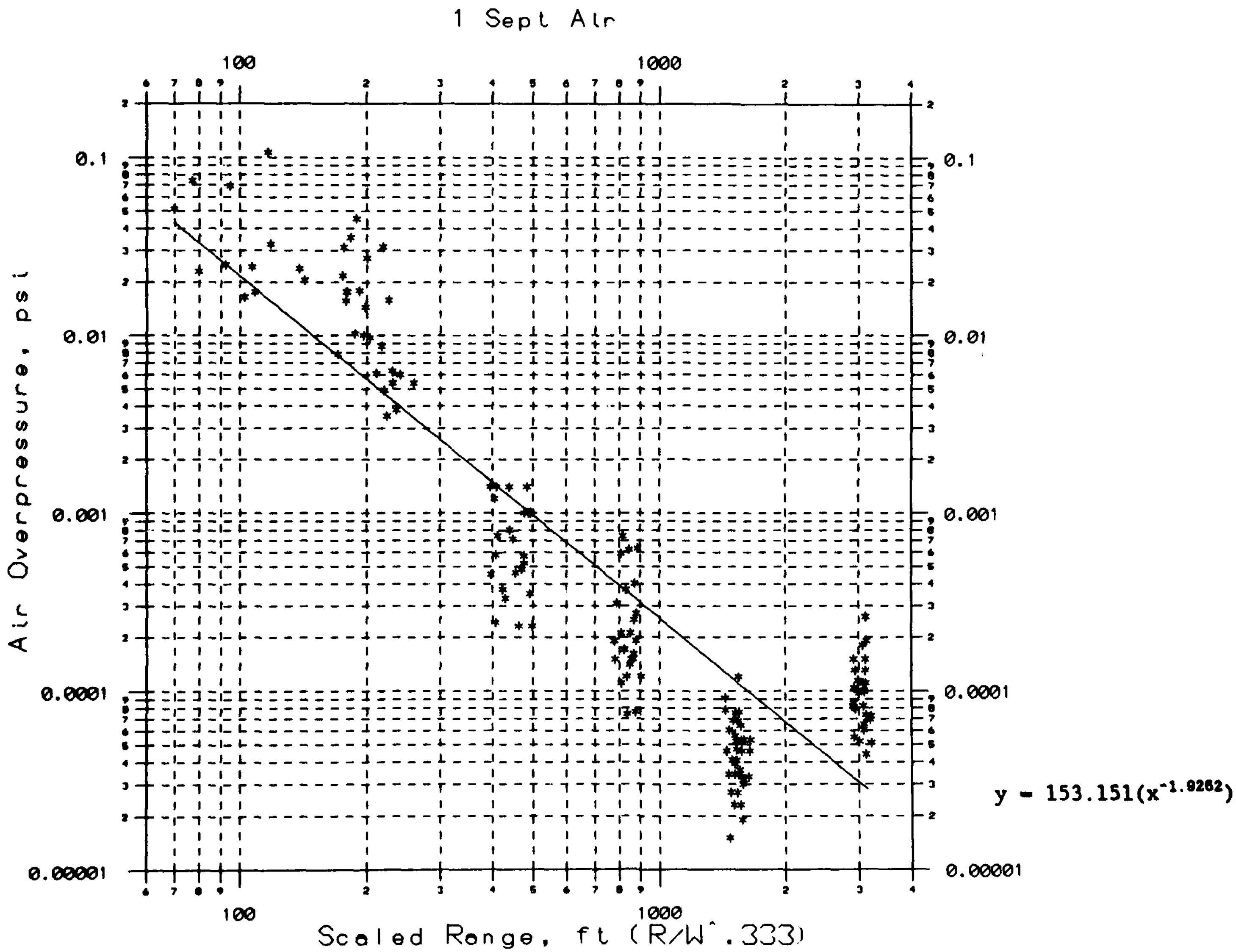
1 Sept Air
Air Overpressure, psi
Scaled Range, ft (R/W^.333)
y = 153.151(x^-1.9262)
0.1
0.01
0.001
0.0001
0.00001
100
1000

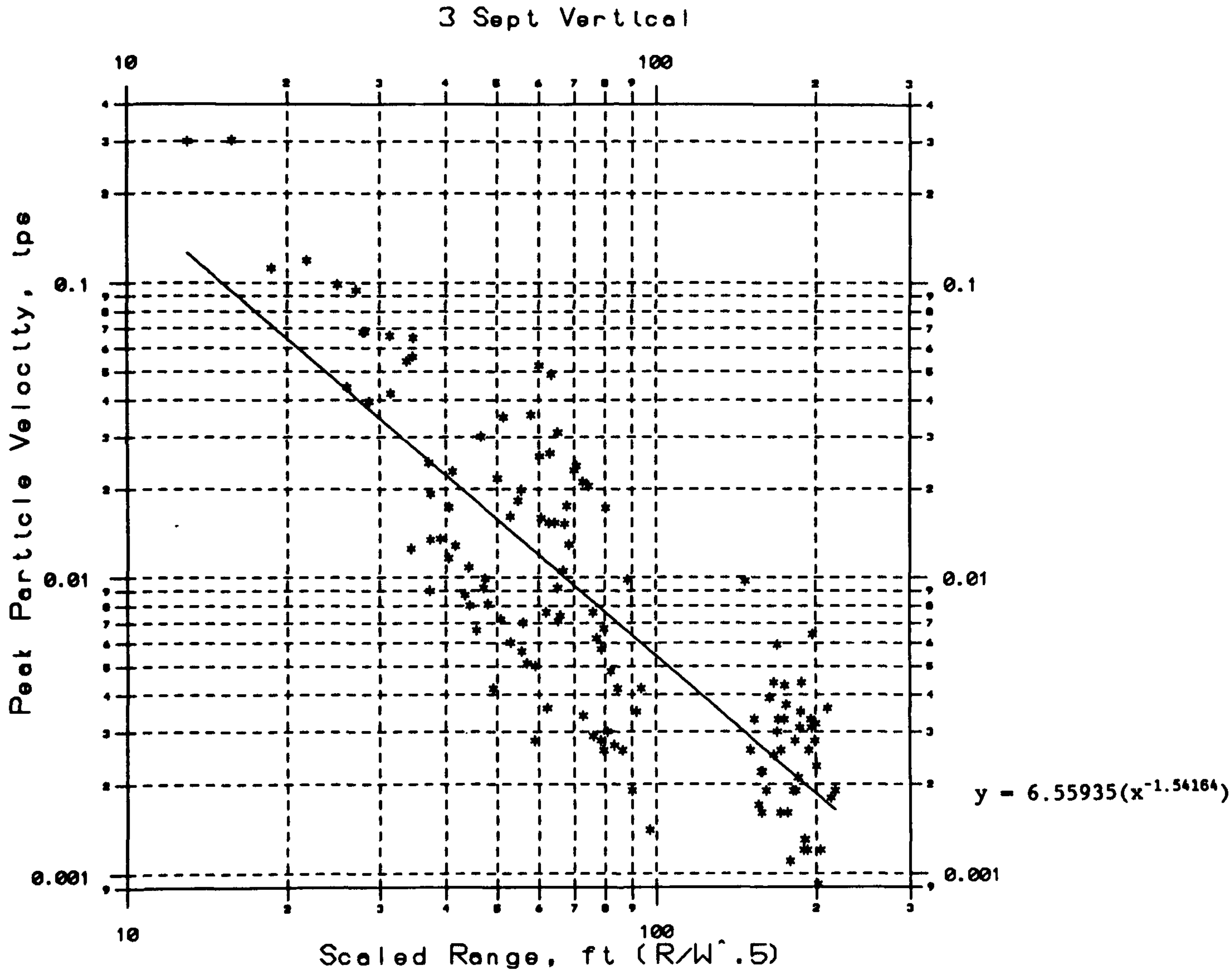

3 Sept Vertical
Peak Particle Velocity, ips
Scaled Range, ft (R/W^.5)
10
100
0.1
0.01
0.001
y = 6.55935(x^-1.54164)

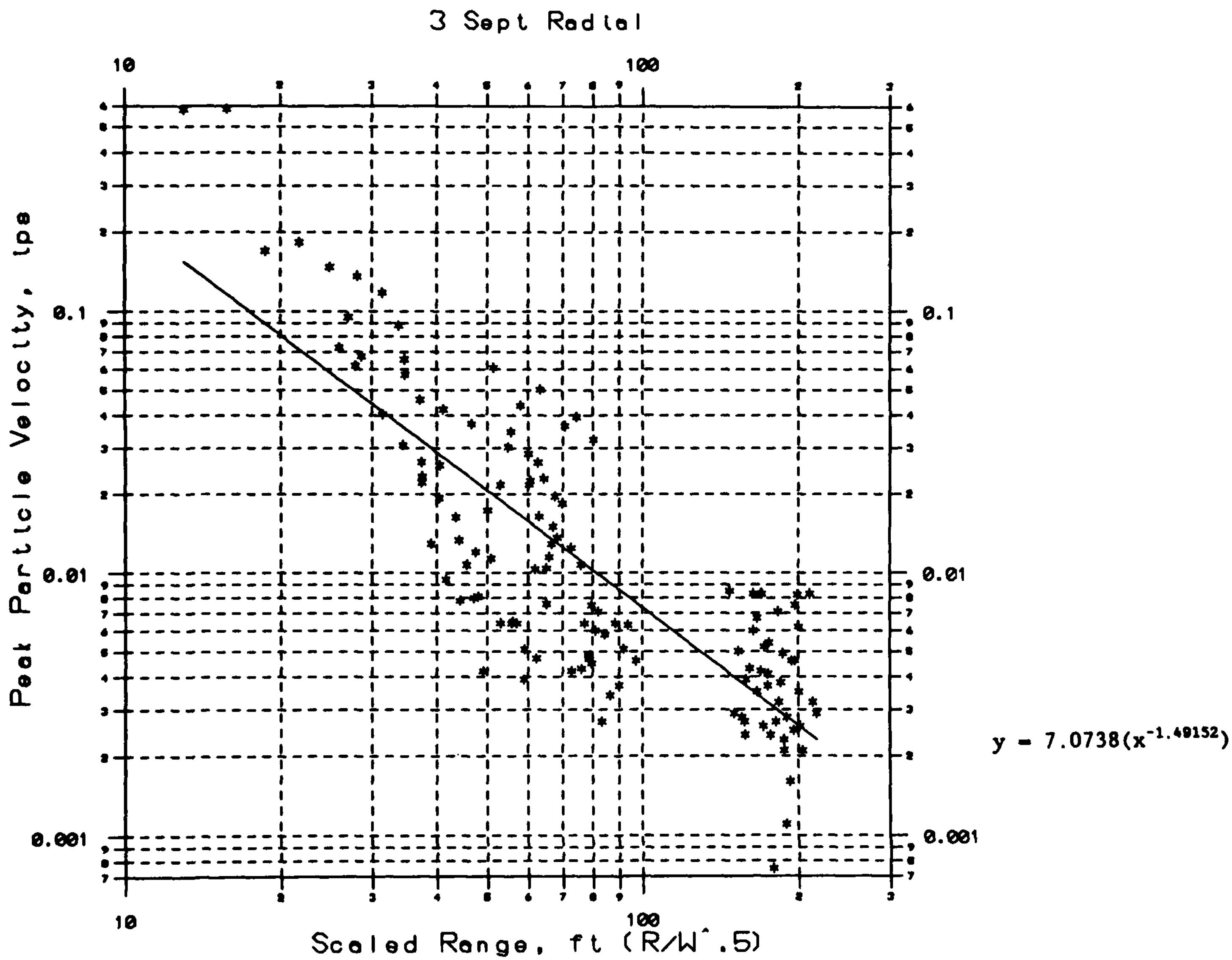

3 Sept Radial
Peak Particle Velocity, ips
Scaled Range, ft (R/W^.5)
10
100
0.1
0.01
0.001
y = 7.0738(x^-1.49152)

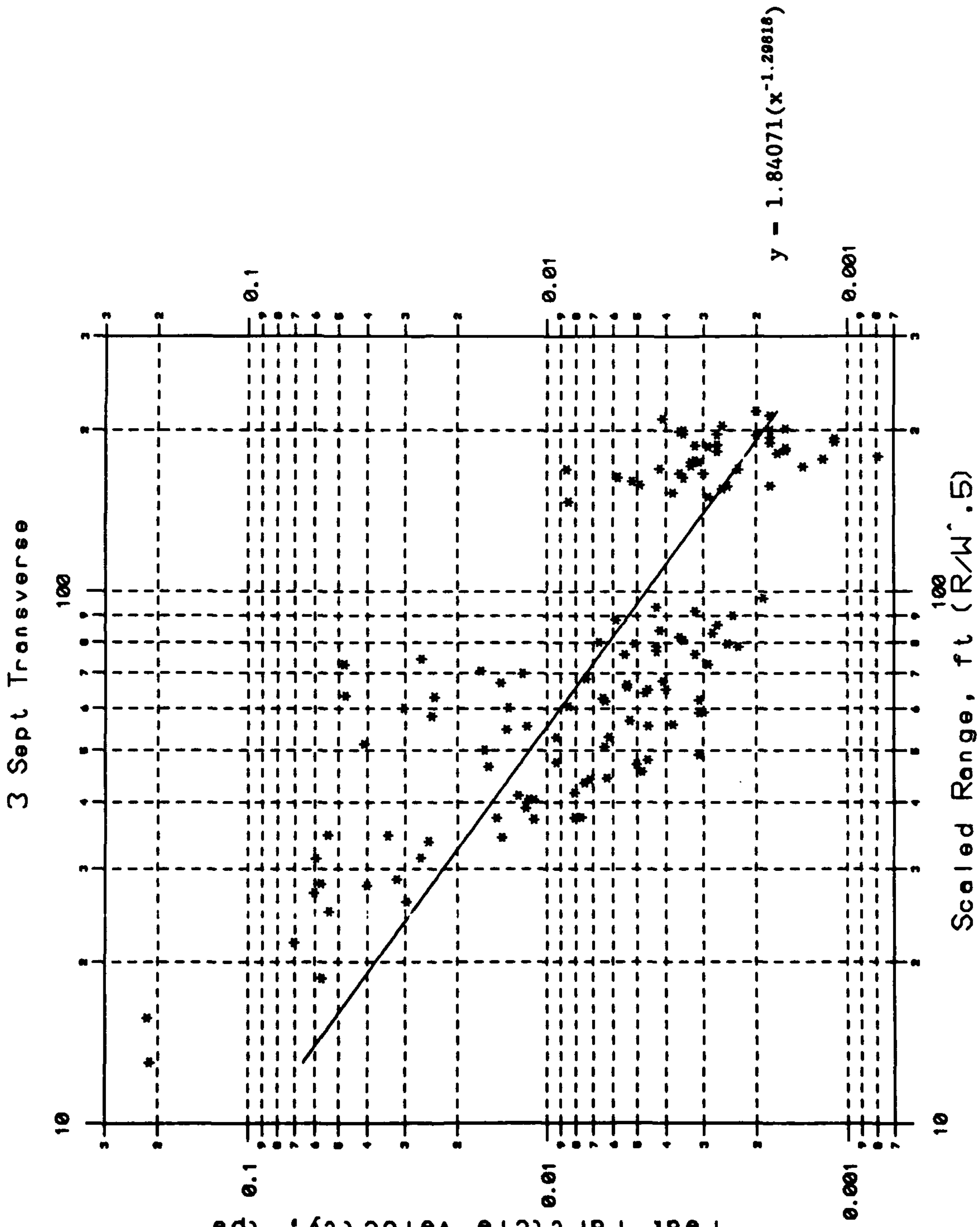
3 Sept Transverse
Peak Particle Velocity, ips
Scaled Range, ft (R/W^.5)
y - 1.84071(x^-1.29818)
0.1
0.01
0.001
10
100

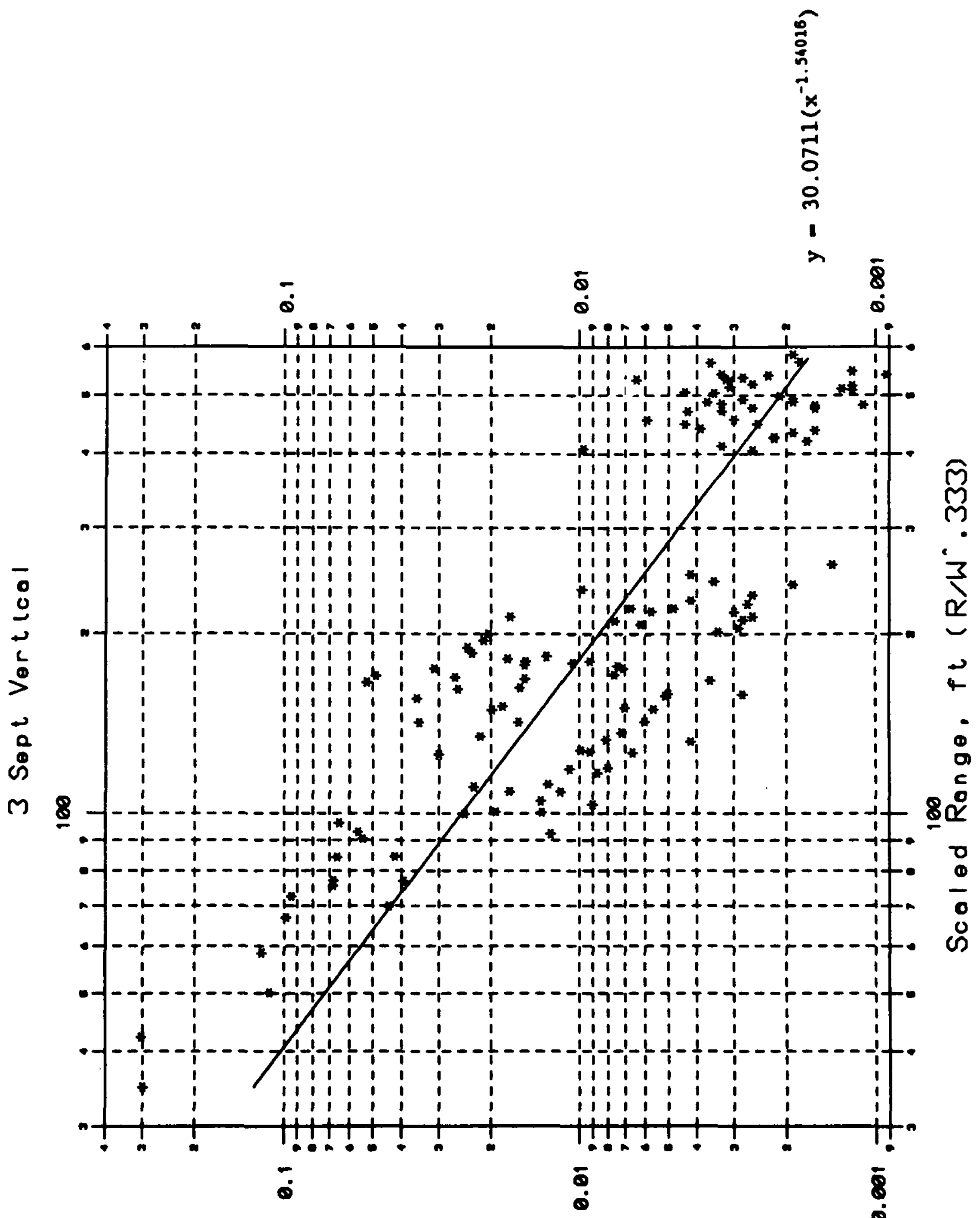

3 Sept Vertical
y = 30.0711(x^-1.54016)
Peak Particle Velocity, ips
Scaled Range, ft (R/W^.333)
100
0.1
0.01
0.001

3 Sept Radial

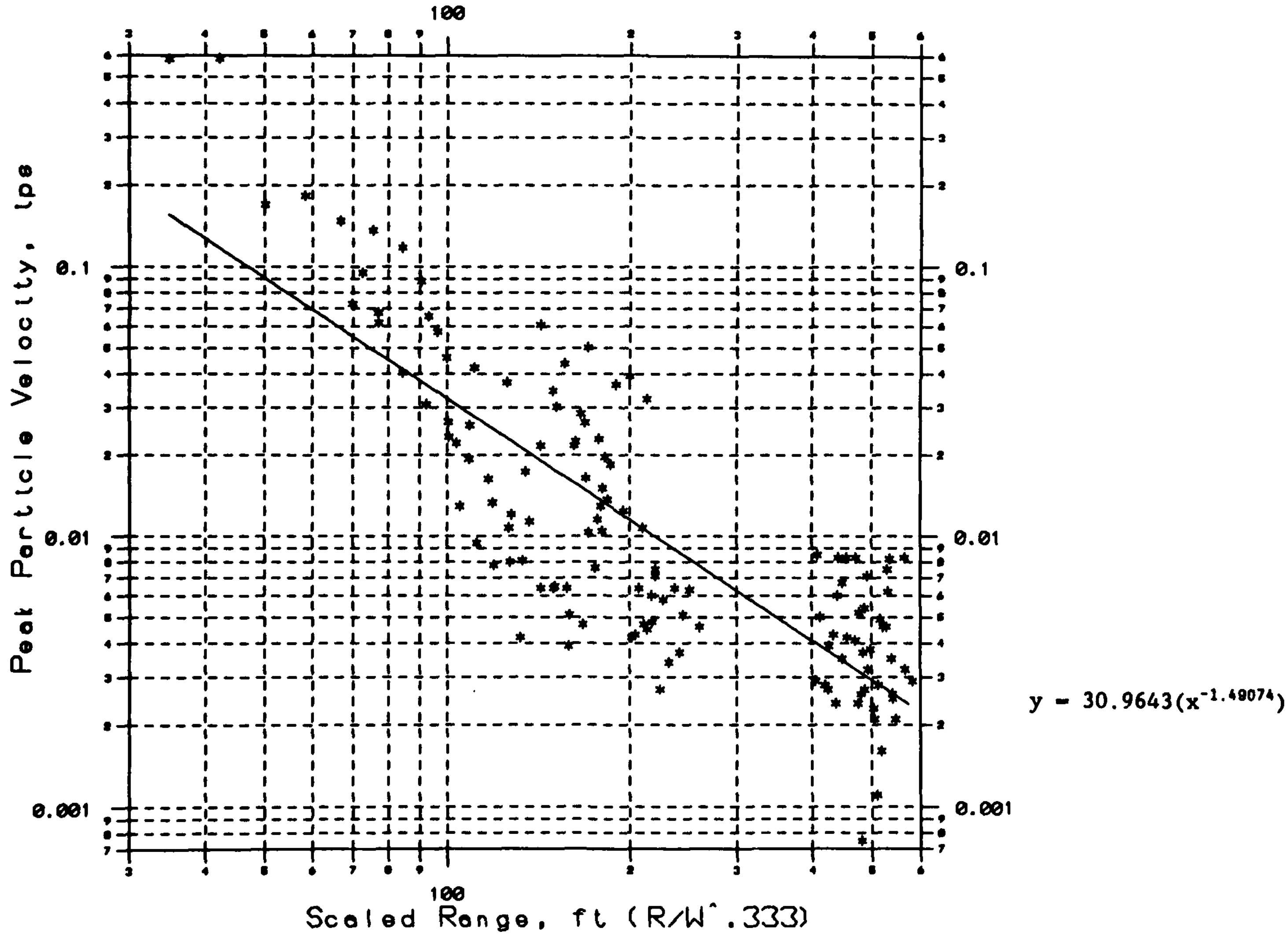

3 Sept Transverse

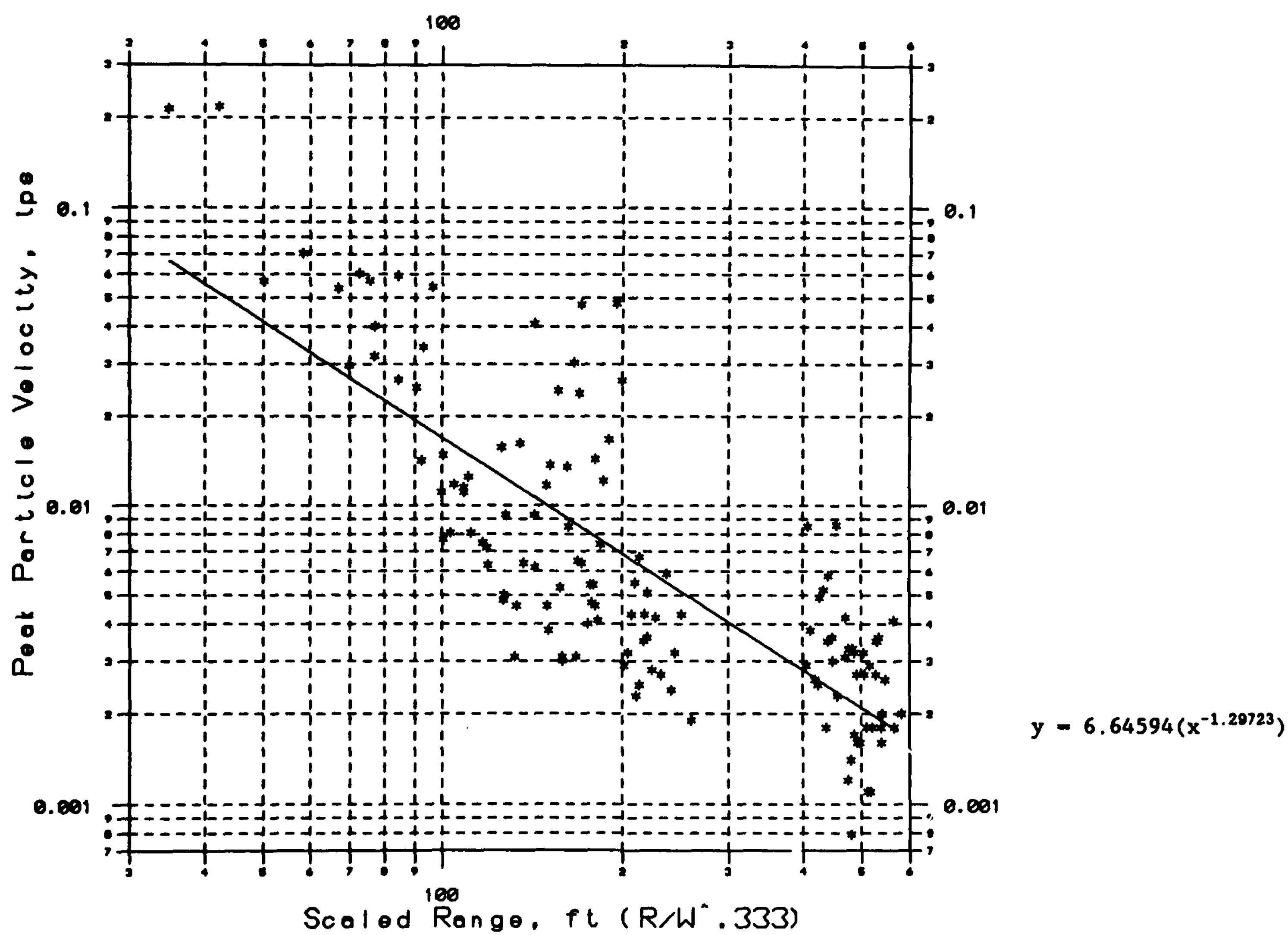

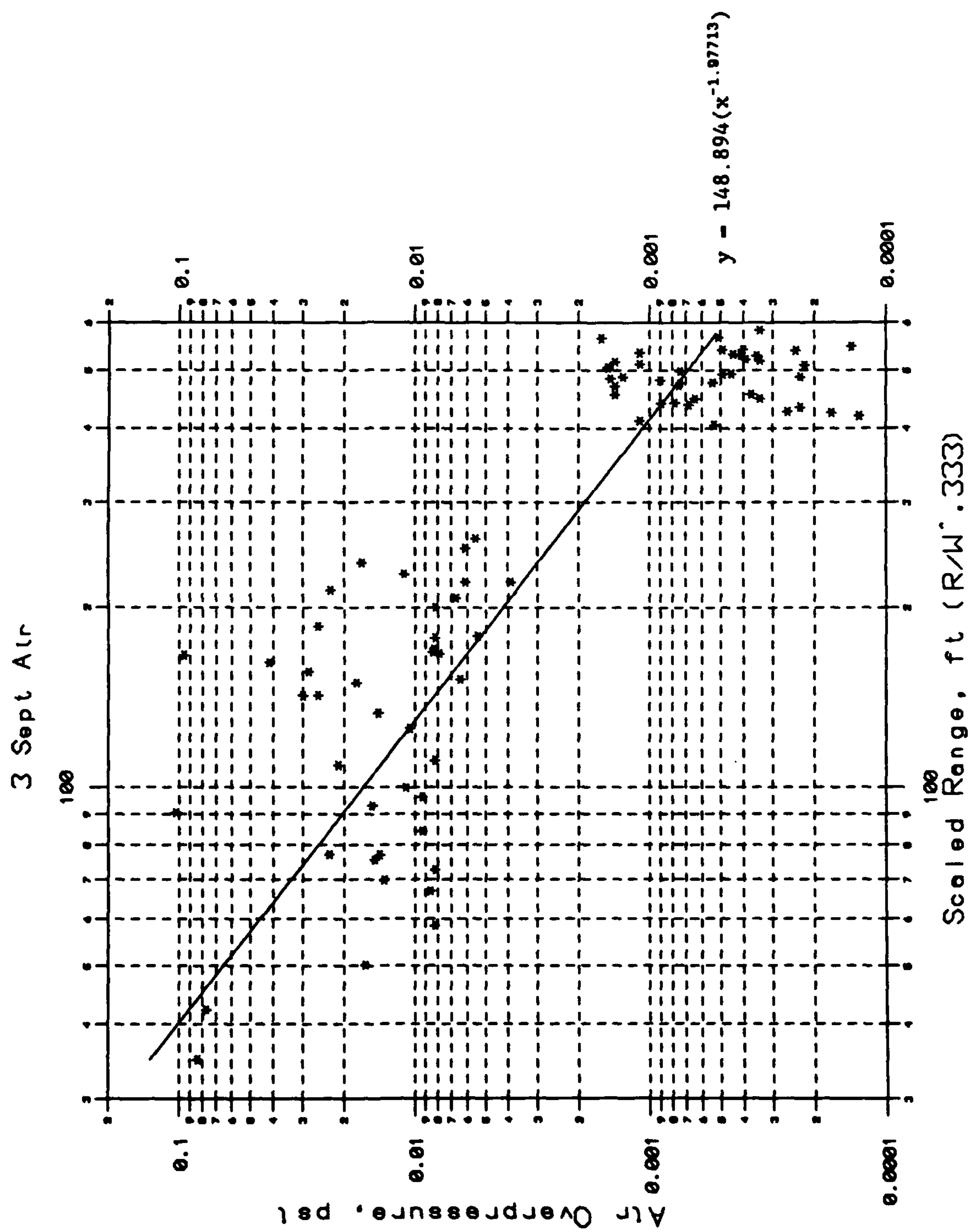

3 Sept Air
y = 148.894(x^-1.97713)
Scaled Range, ft (R/W^.333)
Air Overpressure, psi
0.1
0.01
0.001
0.0001
100

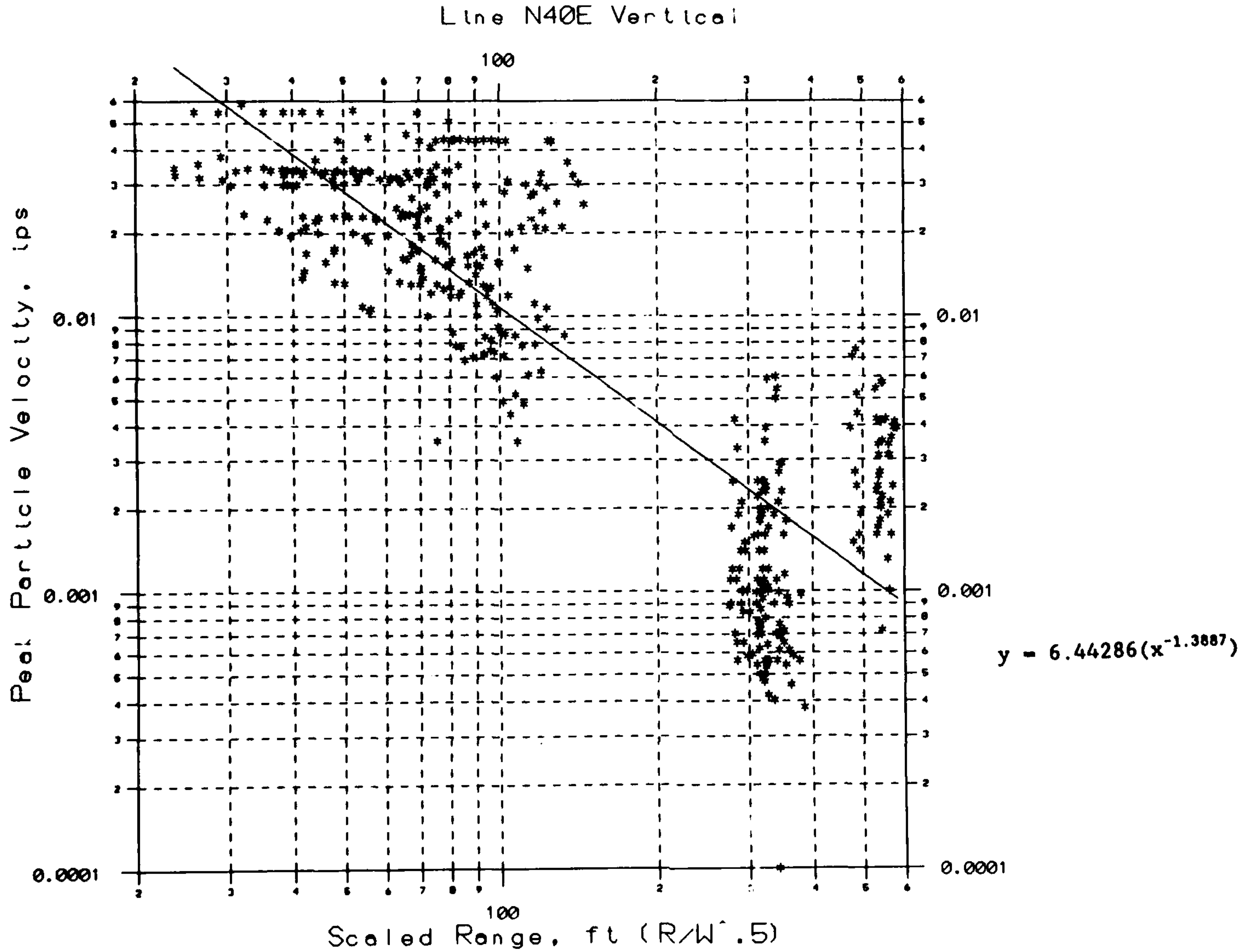

Line N40E Vertical
Peak Particle Velocity, ips
Scaled Range, ft (R/W^.5)
0.01
0.001
0.0001
100
y = 6.44286(x^-1.3887)

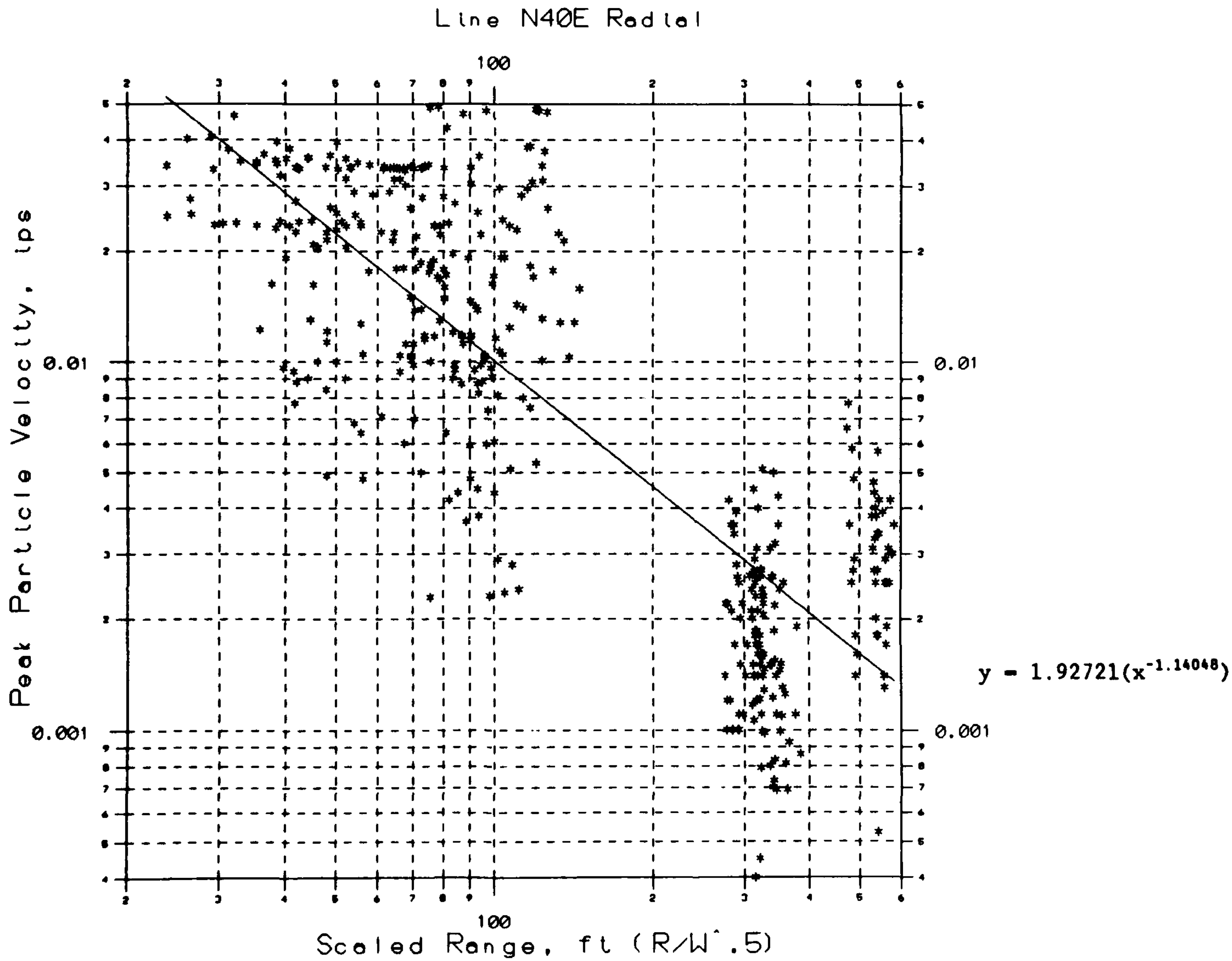

Line N40E Radial
100
0.01
0.001
Peak Particle Velocity, ips
Scaled Range, ft (R/W^.5)
y = 1.92721(x^-1.14048)

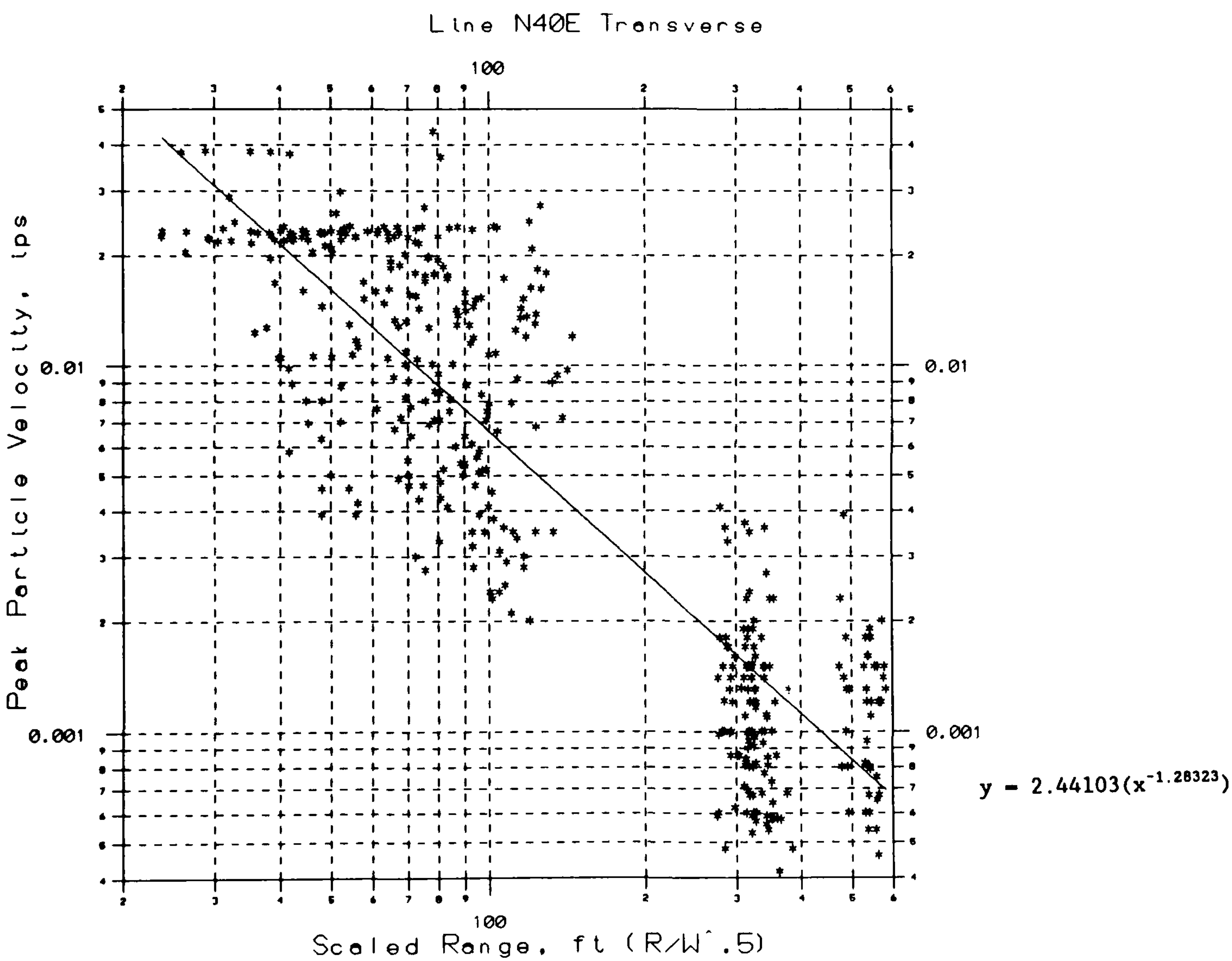
Line N40E Transverse
100
0.01
0.001
Peak Particle Velocity, ips
Scaled Range, ft (R/W^.5)
y = 2.44103(x^-1.28323)

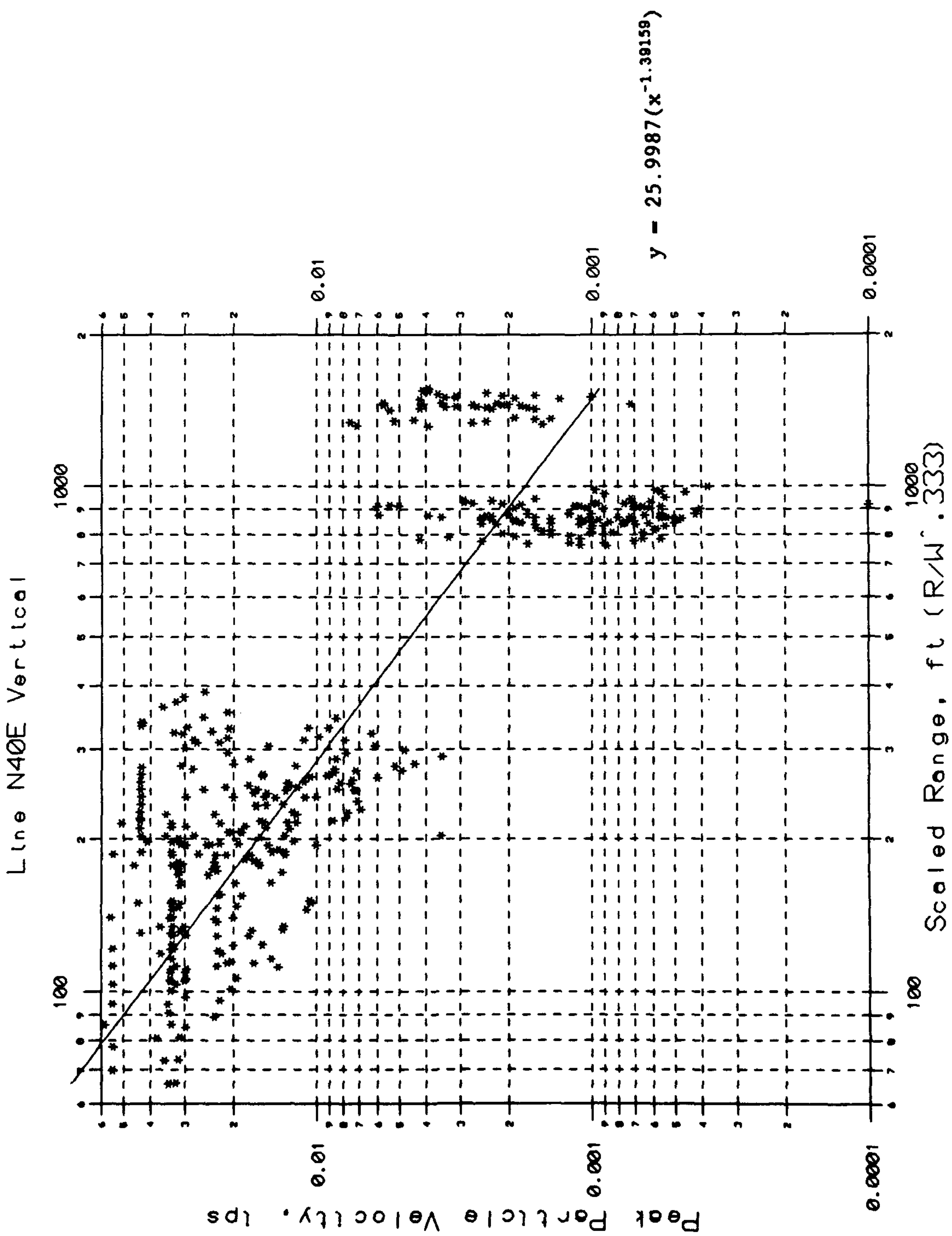
Line N40E Vertical
y = 25.9987(x^-1.38159)
Scaled Range, ft (R/W^.333)
Peak Particle Velocity, ips
100
1000
0.01
0.001
0.0001

Line N40E Radial

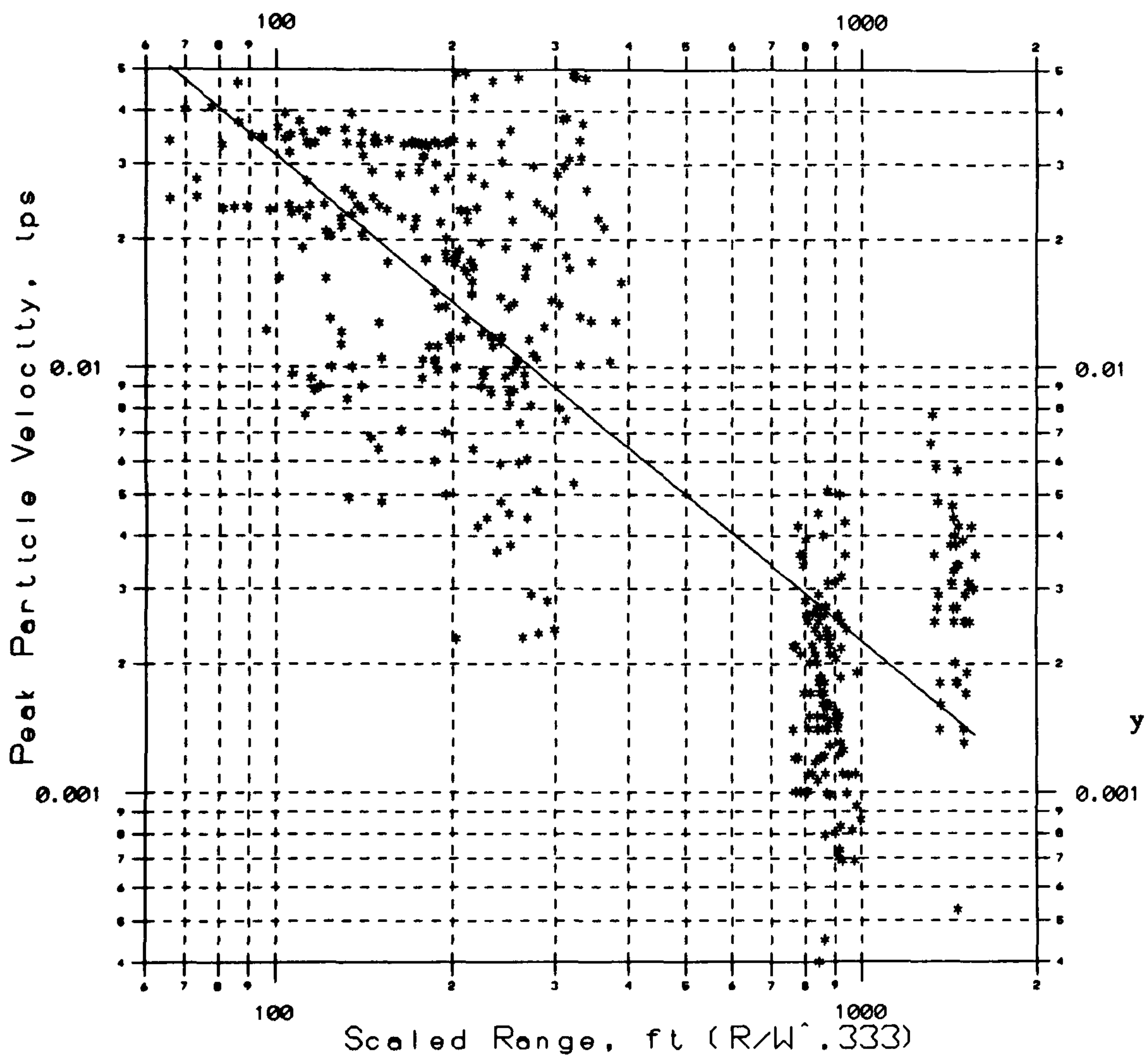

$y = 6.05231(x^{-1.1428})$

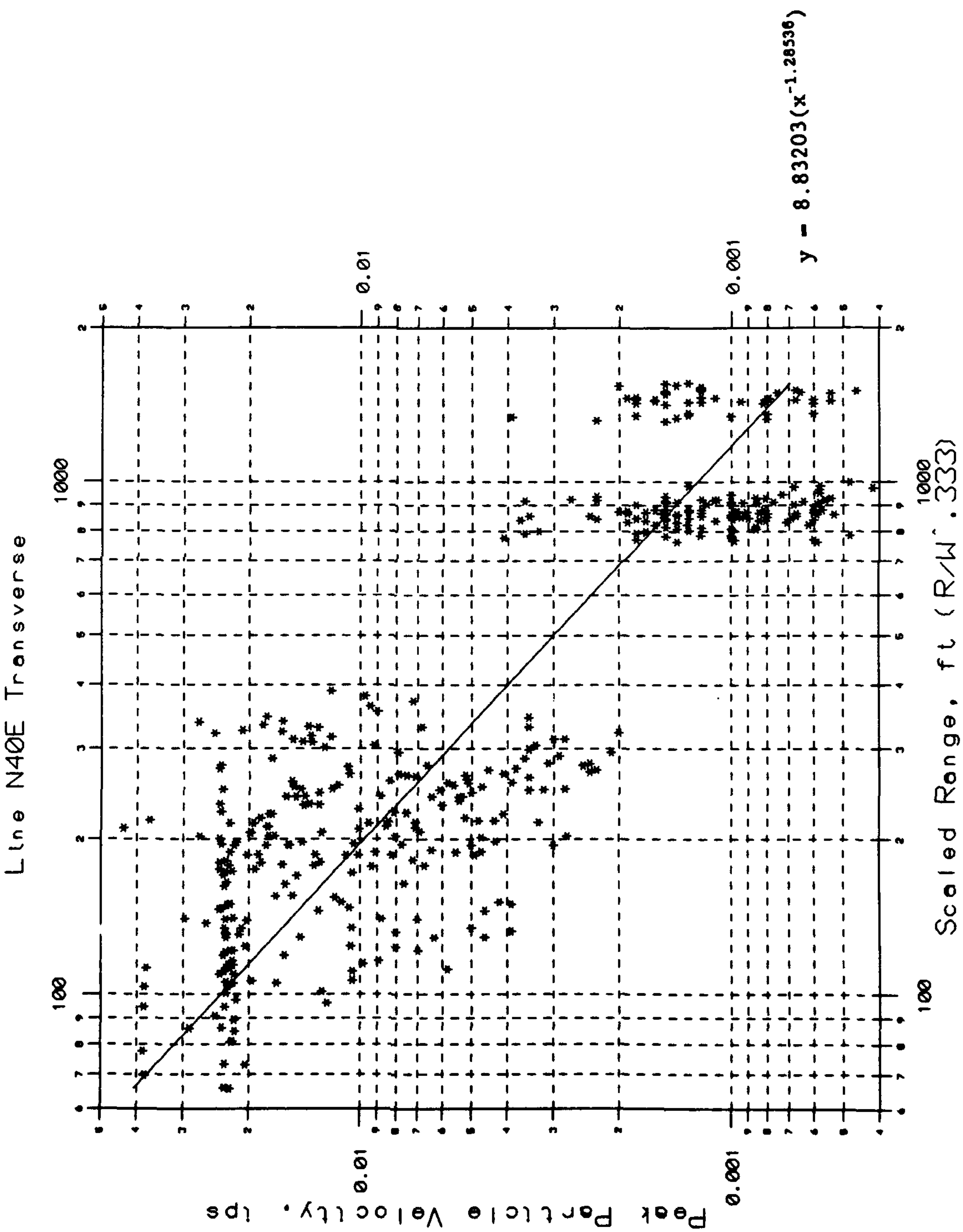
Line N40E Transverse
y = 8.83203(x^-1.28536)
Scaled Range, ft (R/W^.333)
Peak Particle Velocity, ips
100
1000
0.01
0.001

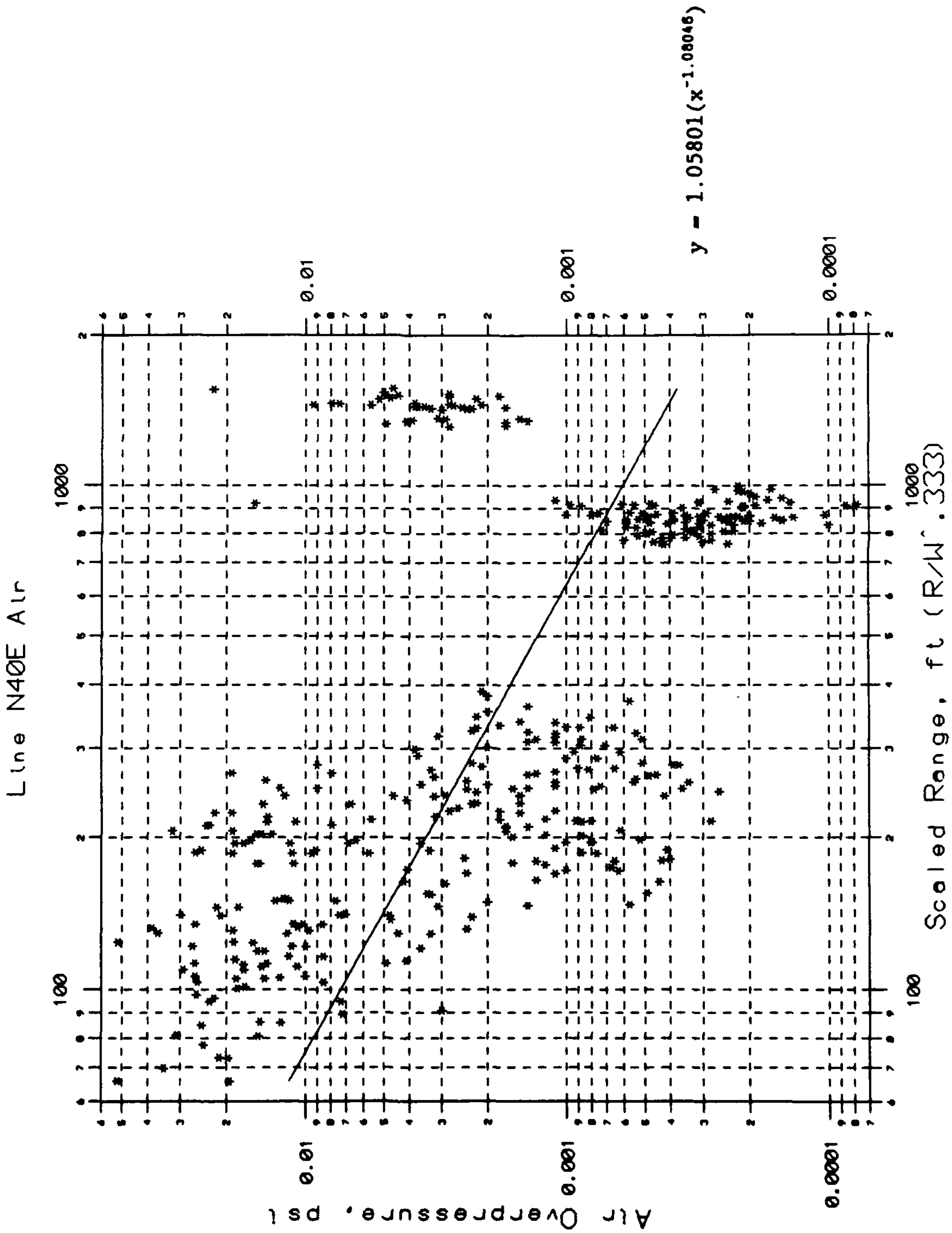
Line N40E Air
y = 1.05801(x^-1.08046)
Air Overpressure, psi
Scaled Range, ft (R/W^.333)
0.01
0.001
0.0001
100
1000

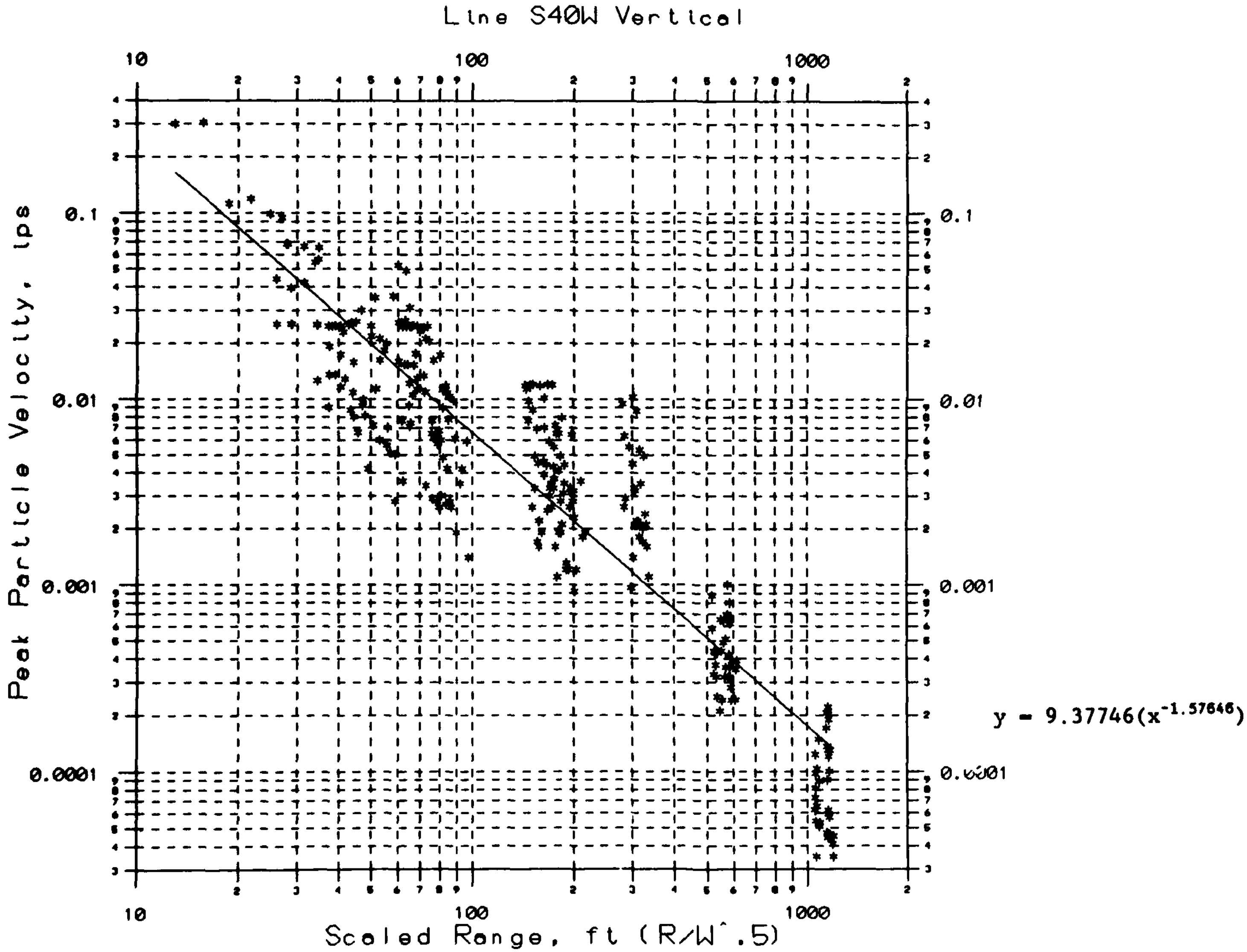
Line S40W Vertical
Peak Particle Velocity, ips
Scaled Range, ft (R/W^.5)
y = 9.37746(x^-1.57646)
10
100
1000
0.1
0.01
0.001
0.0001

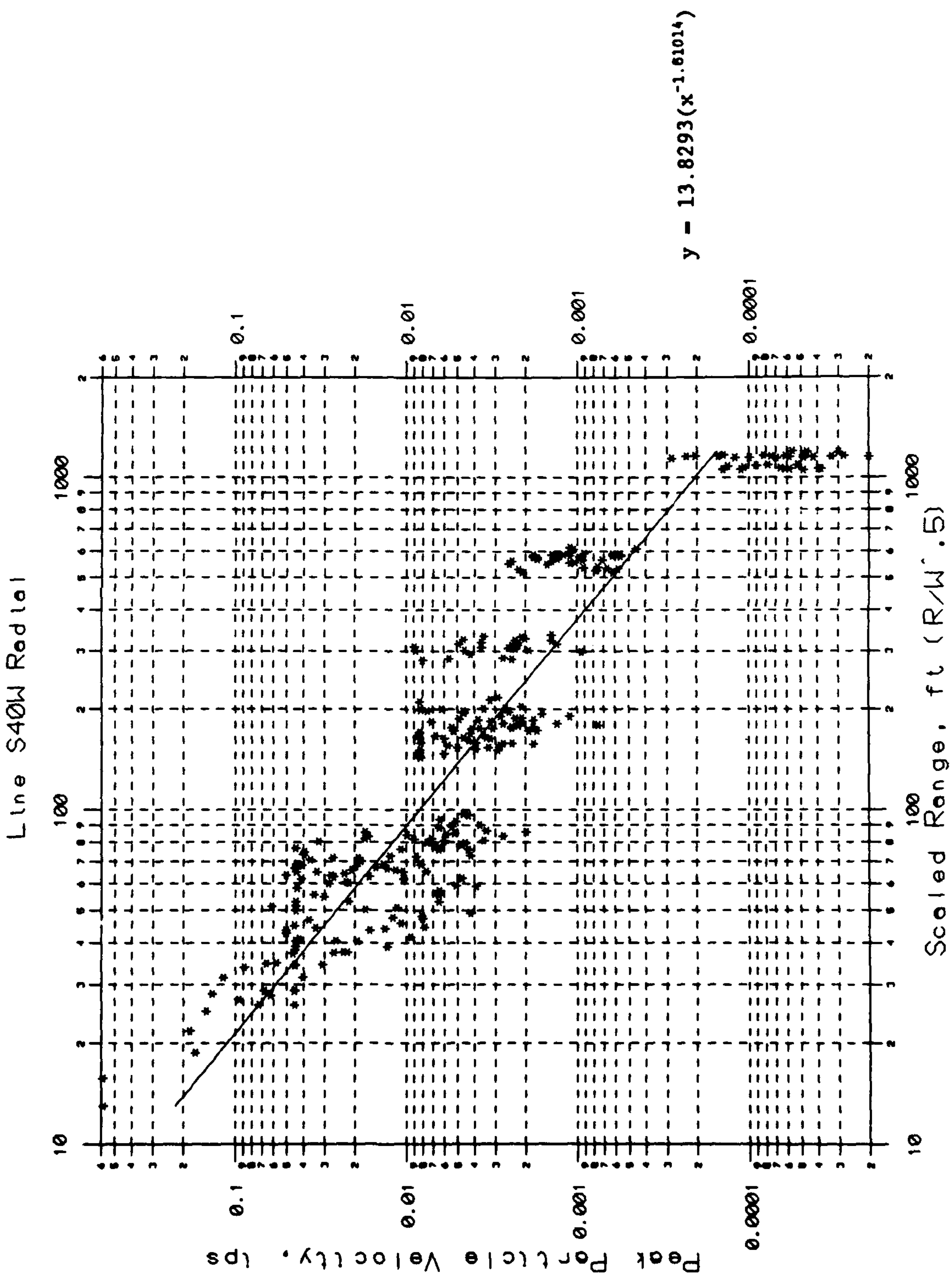

Line S40W Radial
y = 13.8293(x^-1.61014)
10
100
1000
0.1
0.01
0.001
0.0001
Scaled Range, ft (R/W^.5)
Peak Particle Velocity, ips

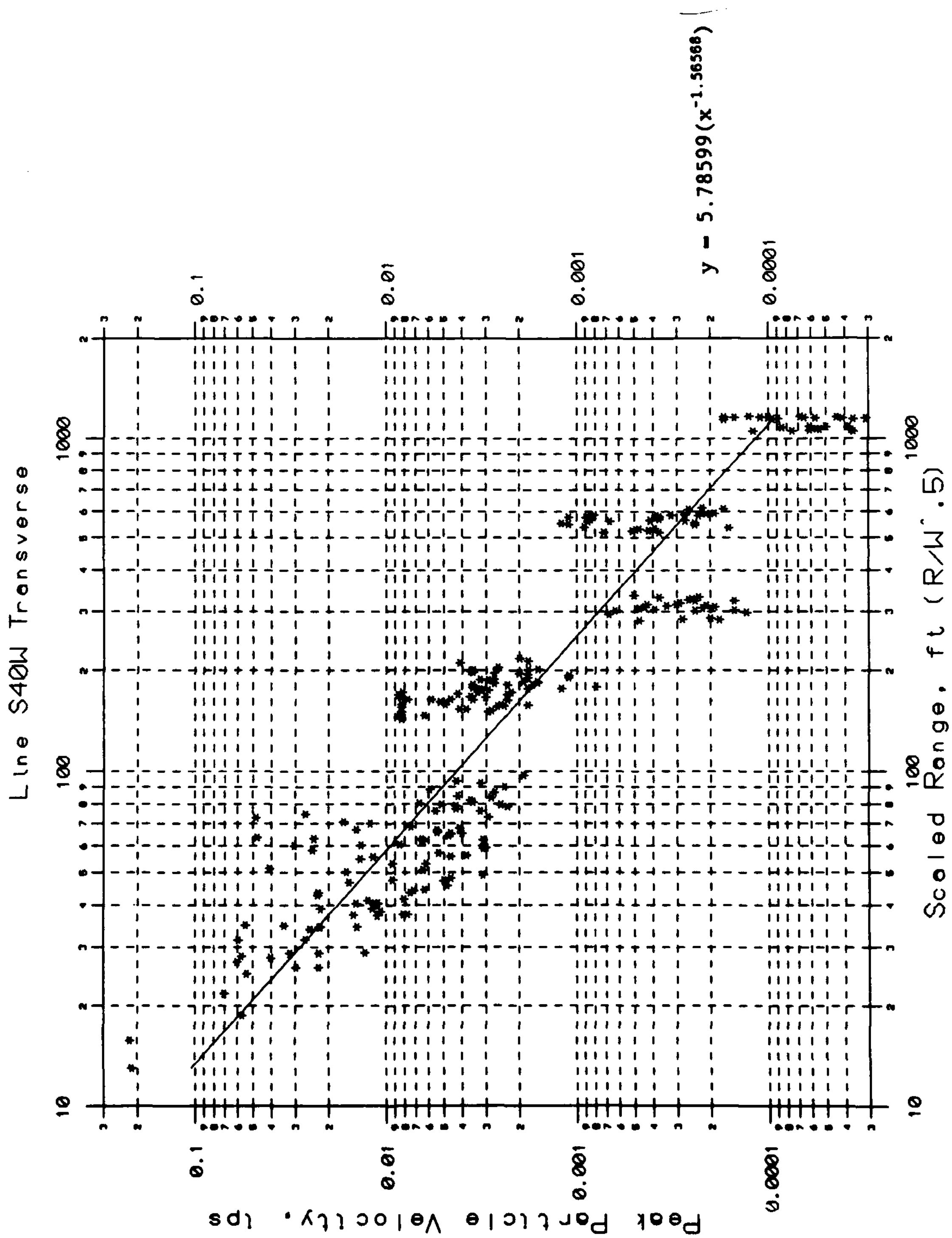
Line S40W Transverse
y = 5.78599(x^-1.56568)
Peak Particle Velocity, ips
Scaled Range, ft (R/W^.5)
0.1
0.01
0.001
0.0001
10
100
1000

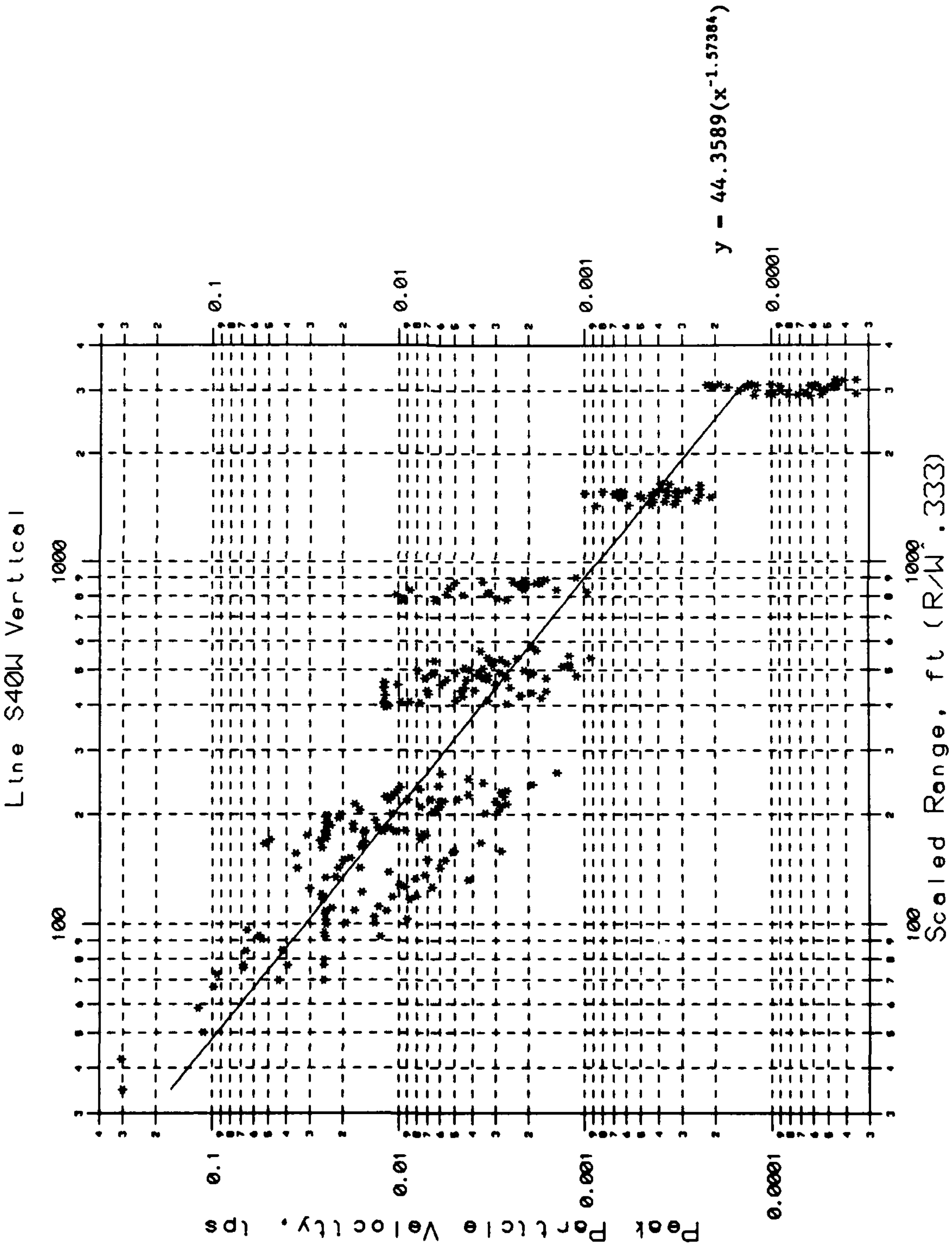

Line S40W Vertical
y = 44.3589(x^-1.57384)
Peak Particle Velocity, ips
Scaled Range, ft (R/W^.333)
0.1
0.01
0.001
0.0001
100
1000

Line S40W Radial

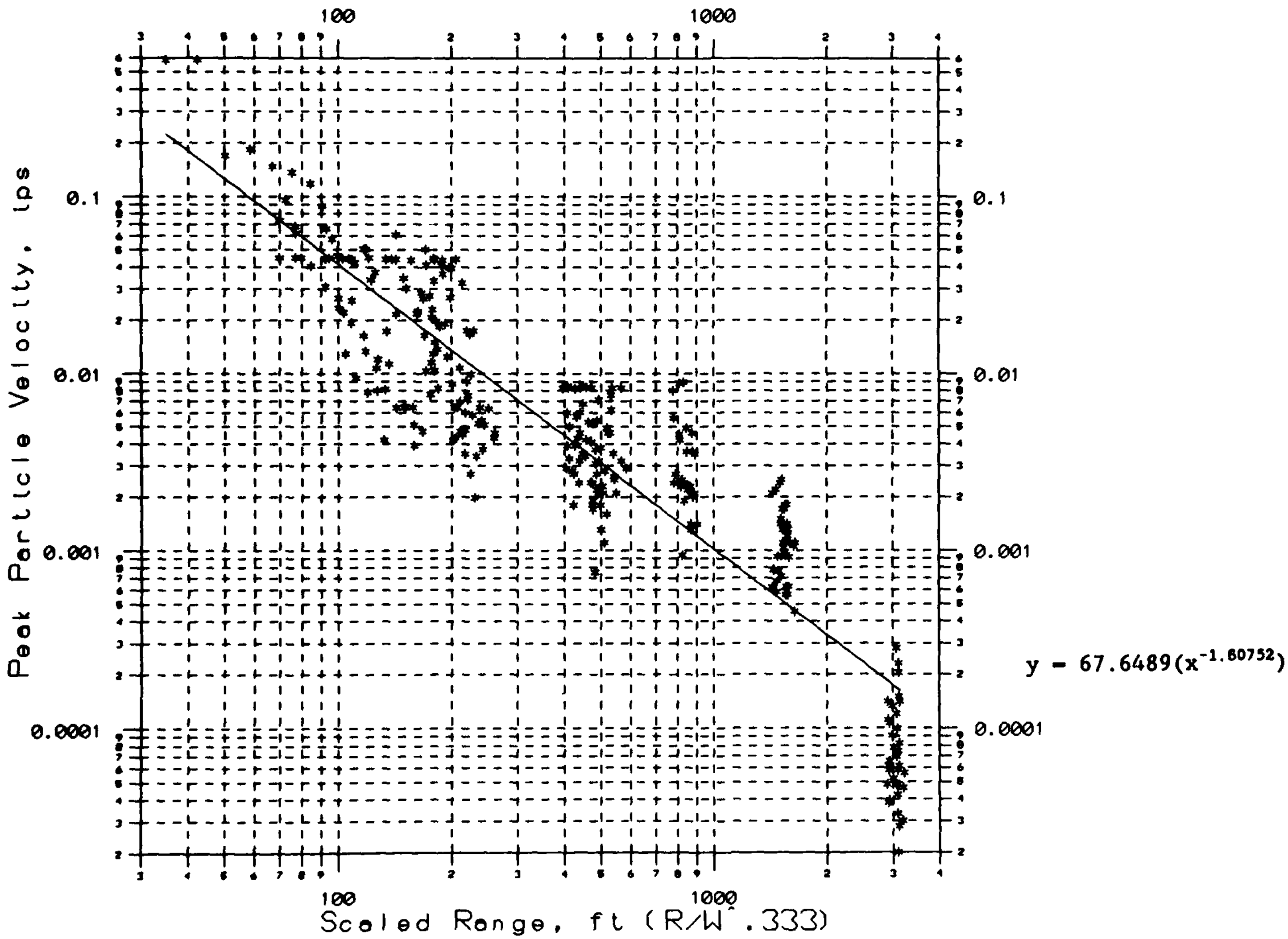

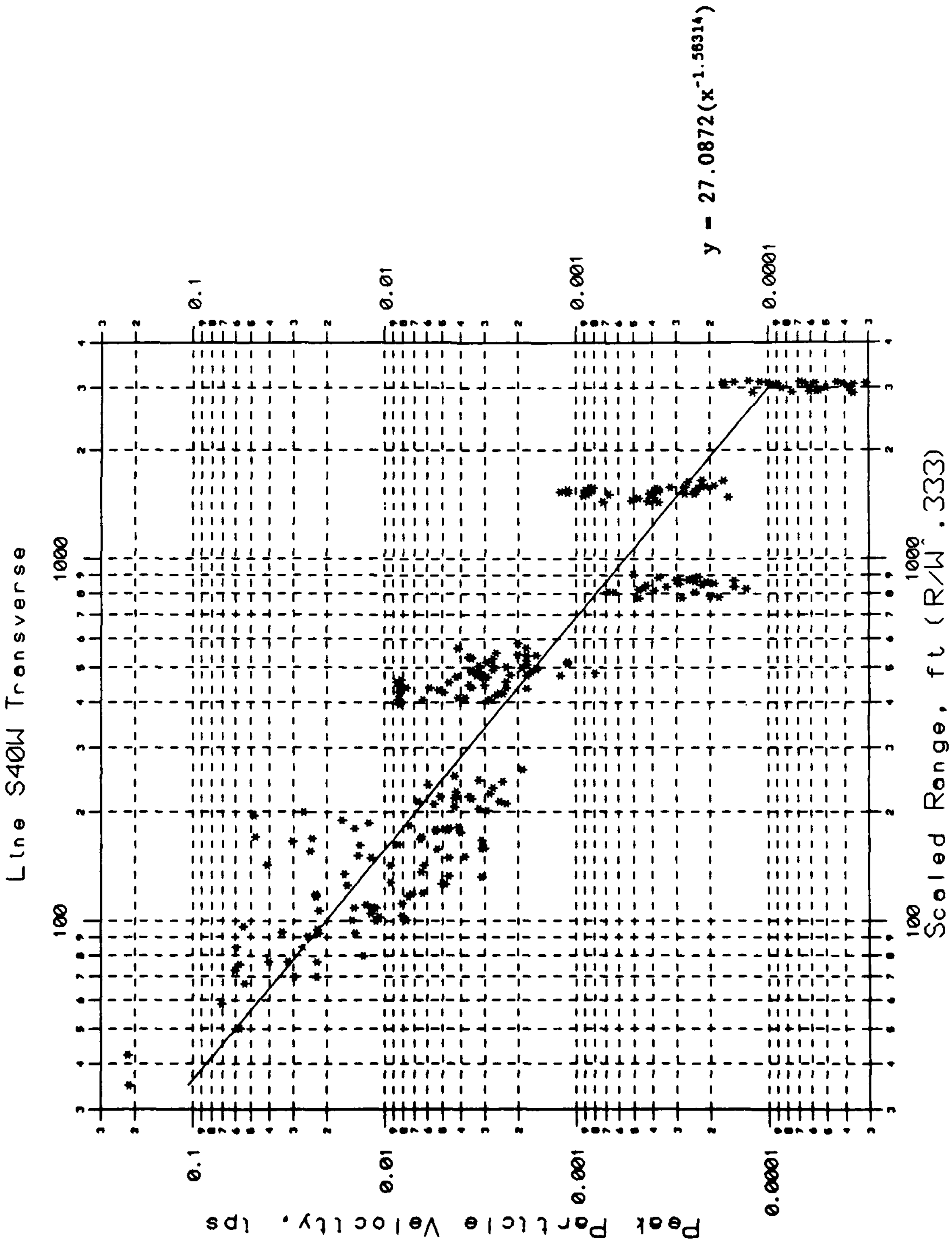
Line S40W Transverse
y = 27.0872(x^-1.56314)
Peak Particle Velocity, ips
Scaled Range, ft (R/W^.333)
0.1
0.01
0.001
0.0001
100
1000

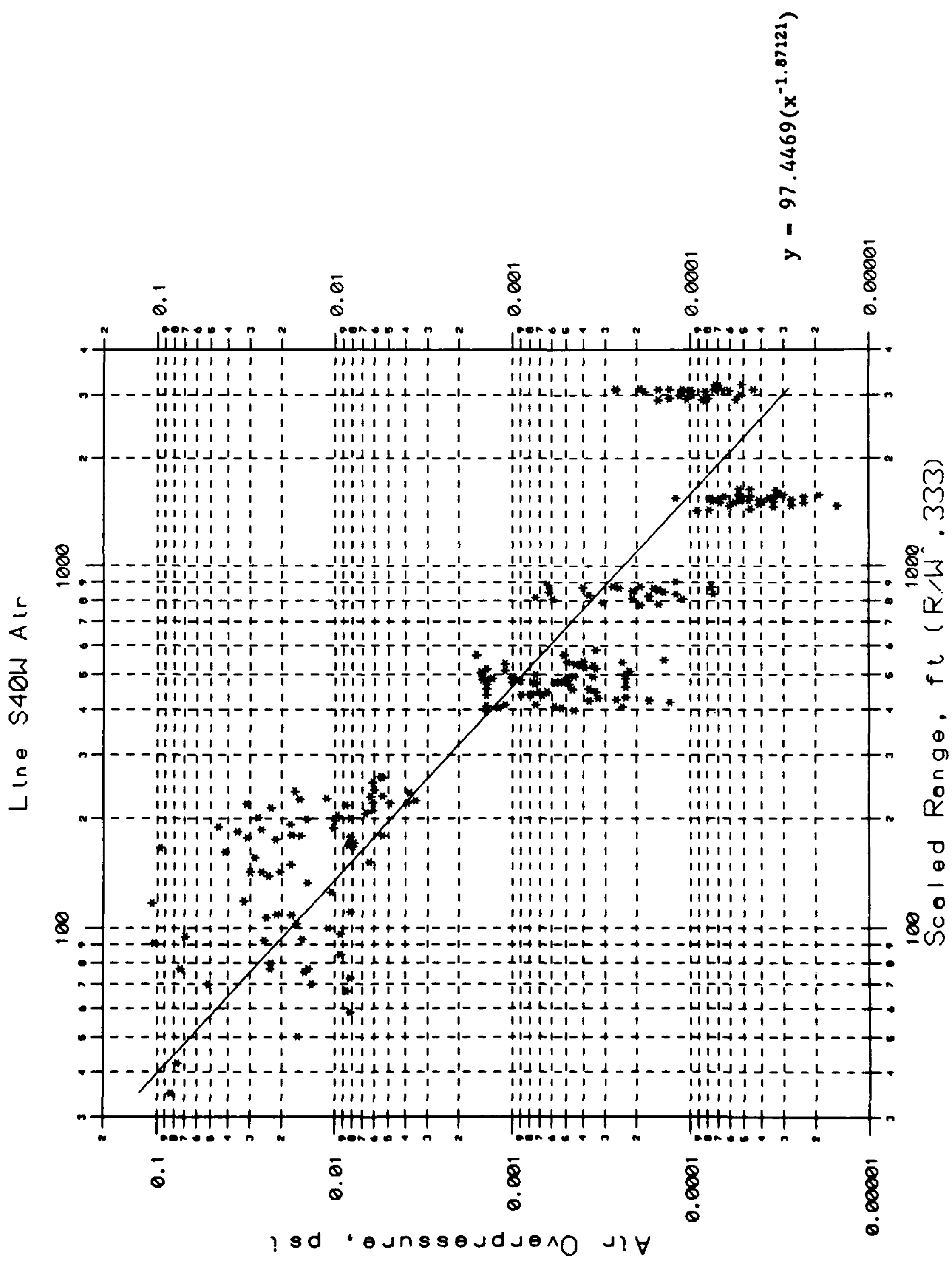
Line S40W Air
y = 97.4469(x^-1.87121)
Scaled Range, ft (R/W^.333)
Air Overpressure, psi
0.1
0.01
0.001
0.0001
0.00001
100
1000

Appendix D: Selected Power Spectral Density Plots

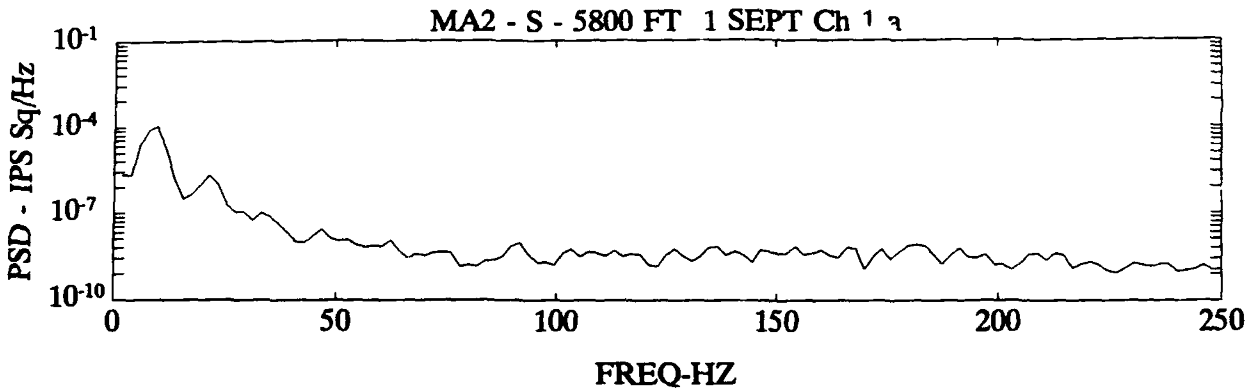
MA2 - S - 5800 FT 1 SEPT Ch 1 a
PSD - IPS Sq/Hz
10^{-1}
10^{-4}
10^{-7}
10^{-10}
0
50
100
150
200
250
FREQ-HZ

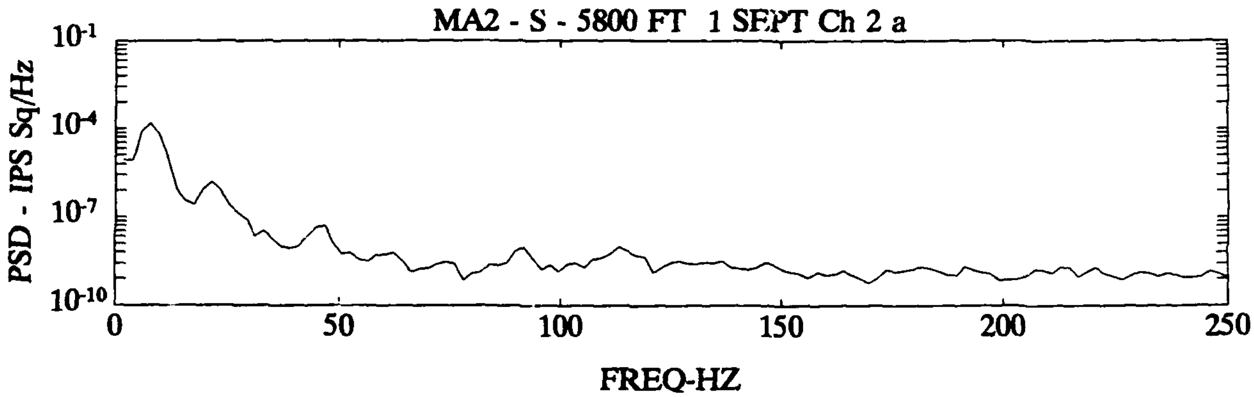
MA2 - S - 5800 FT 1 SEPT Ch 2 a
PSD - IPS Sq/Hz
10^{-1}
10^{-4}
10^{-7}
10^{-10}
0
50
100
150
200
250
FREQ-HZ

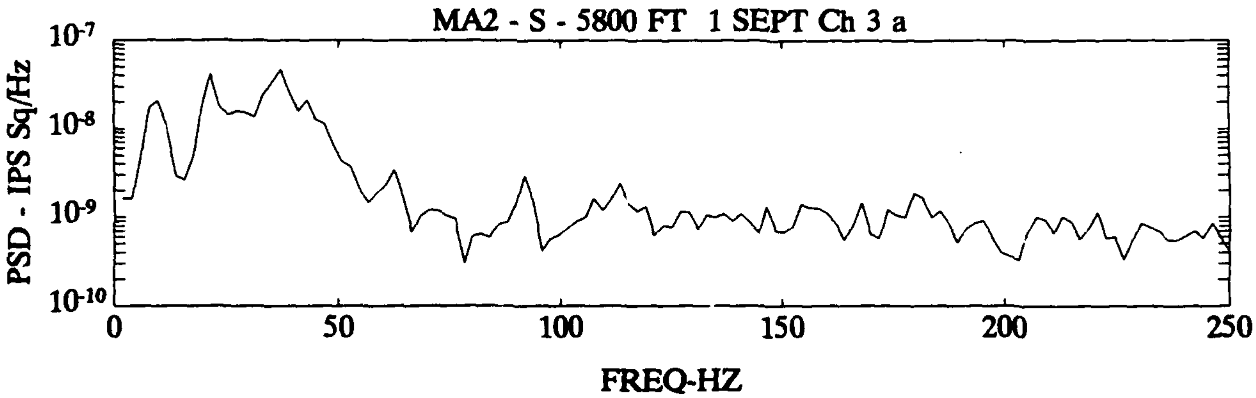
MA2 - S - 5800 FT 1 SEPT Ch 3 a
PSD - IPS Sq/Hz
10^{-7}
10^{-8}
10^{-9}
10^{-10}
0
50
100
150
200
250
FREQ-HZ

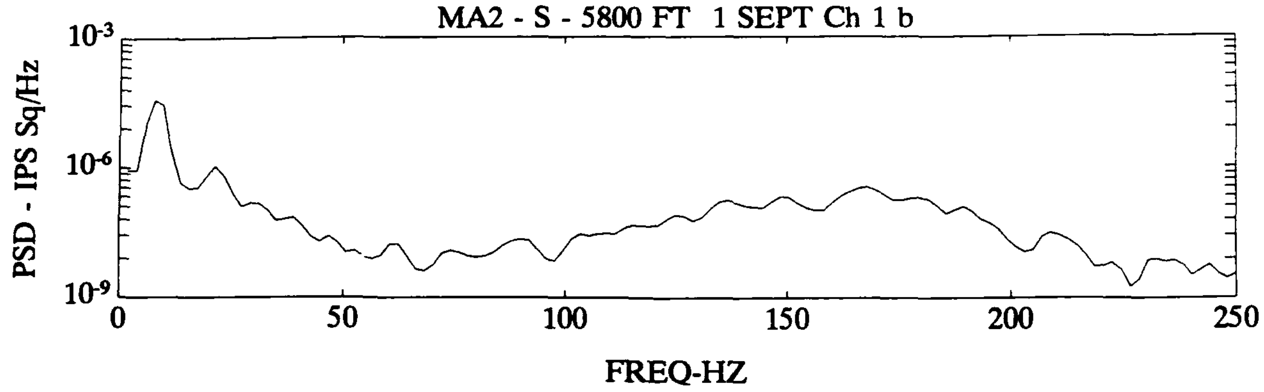
MA2 - S - 5800 FT 1 SEPT Ch 1 b
PSD - IPS Sq/Hz
10^{-3}
10^{-6}
10^{-9}
0
50
100
150
200
250
FREQ-HZ

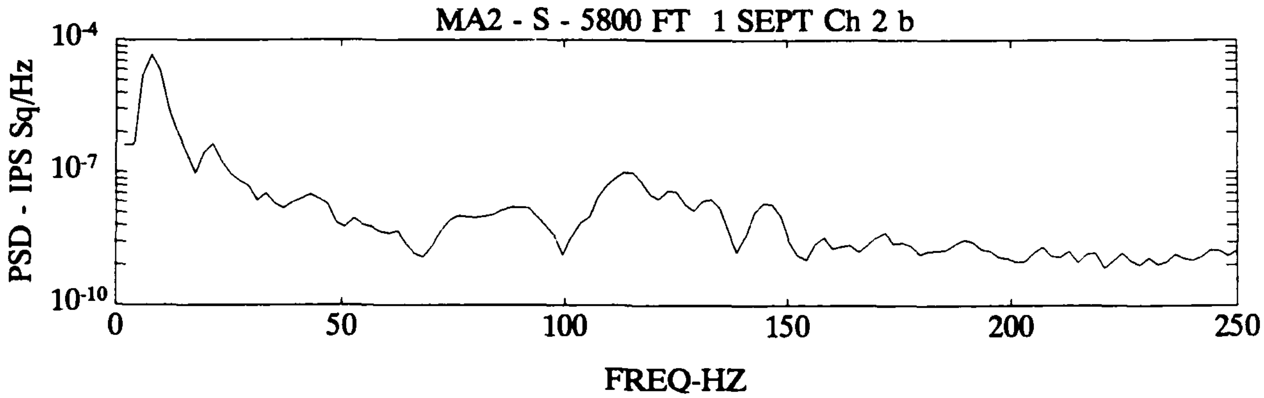
MA2 - S - 5800 FT 1 SEPT Ch 2 b
PSD - IPS Sq/Hz
10^{-4}
10^{-7}
10^{-10}
0
50
100
150
200
250
FREQ-HZ

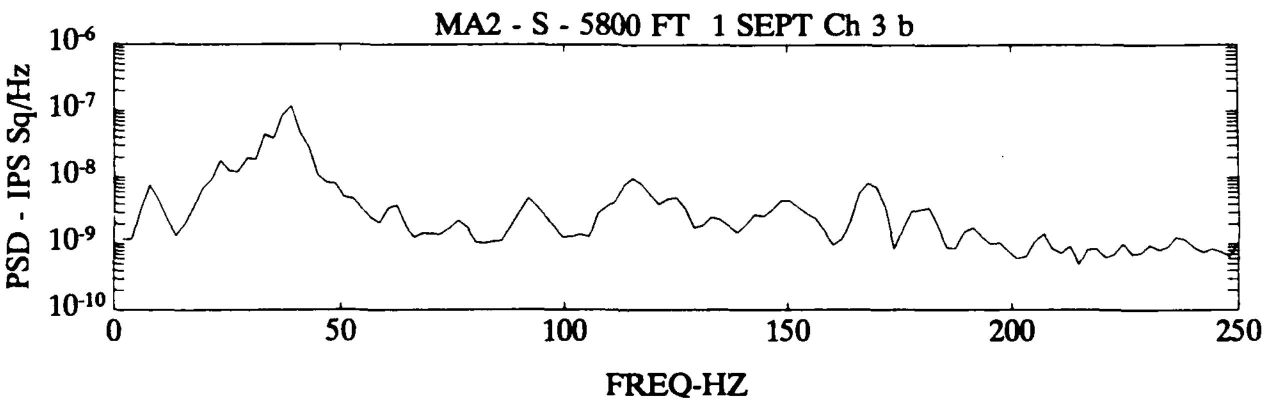
MA2 - S - 5800 FT 1 SEPT Ch 3 b
PSD - IPS Sq/Hz
10^{-6}
10^{-7}
10^{-8}
10^{-9}
10^{-10}
0
50
100
150
200
250
FREQ-HZ

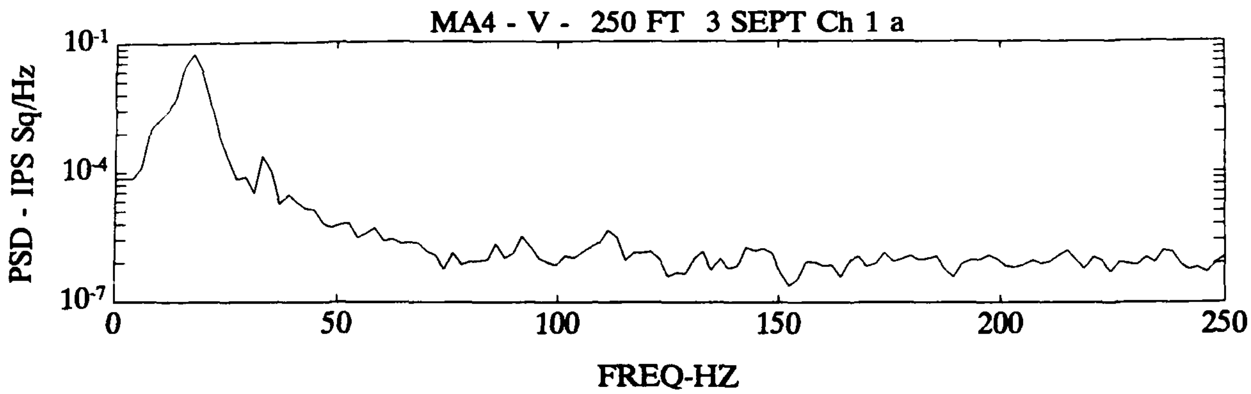

MA4 - V - 250 FT 3 SEPT Ch 1 a
PSD - IPS Sq/Hz
10^{-1}
10^{-4}
10^{-7}
0
50
100
150
200
250
FREQ-HZ

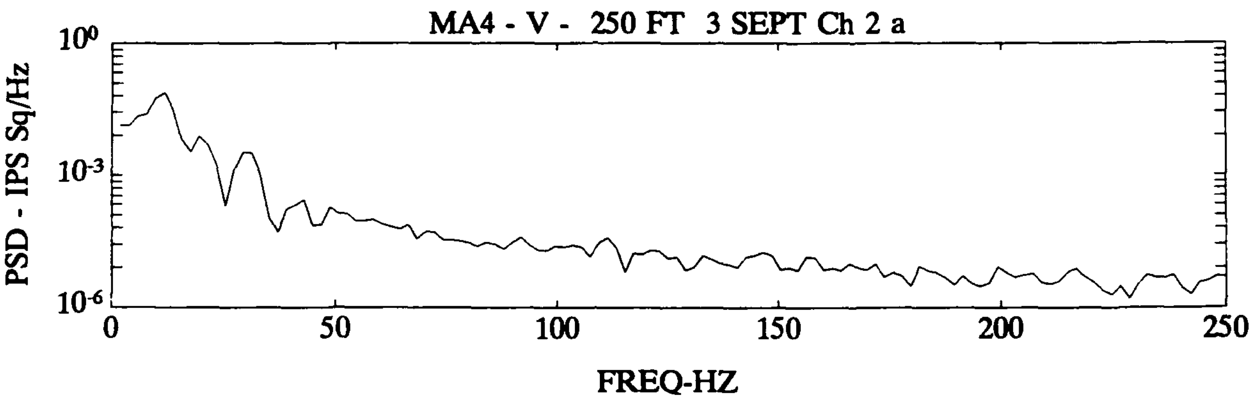

MA4 - V - 250 FT 3 SEPT Ch 2 a
PSD - IPS Sq/Hz
10^{0}
10^{-3}
10^{-6}
0
50
100
150
200
250
FREQ-HZ

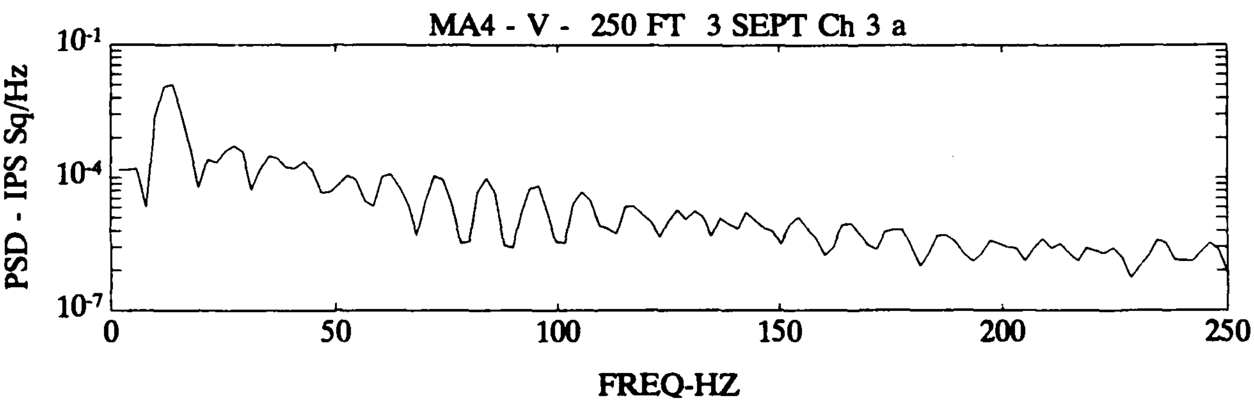

MA4 - V - 250 FT 3 SEPT Ch 3 a
PSD - IPS Sq/Hz
10^{-1}
10^{-4}
10^{-7}
0
50
100
150
200
250
FREQ-HZ

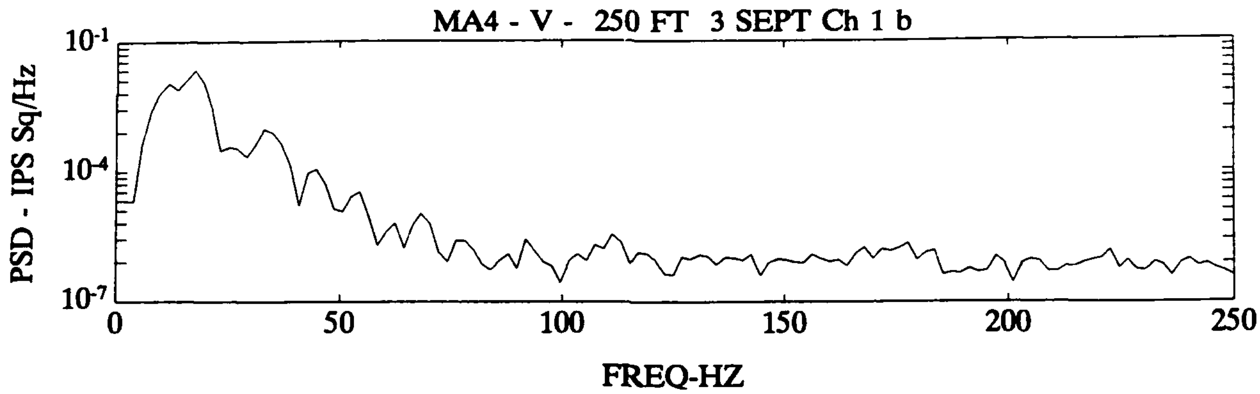
MA4 - V - 250 FT 3 SEPT Ch 1 b
PSD - IPS Sq/Hz
10^{-1}
10^{-4}
10^{-7}
0
50
100
150
200
250
FREQ-HZ

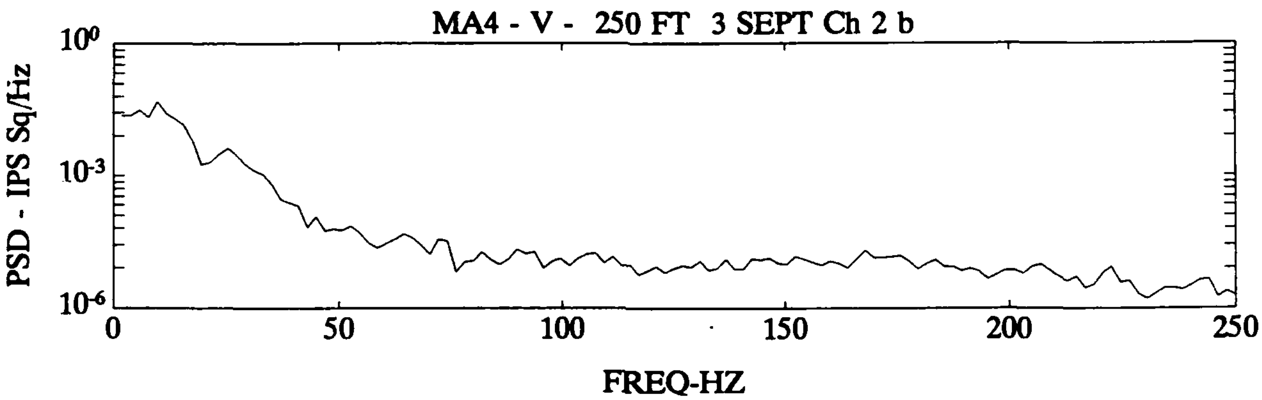
MA4 - V - 250 FT 3 SEPT Ch 2 b
PSD - IPS Sq/Hz
10^{0}
10^{-3}
10^{-6}
0
50
100
150
200
250
FREQ-HZ

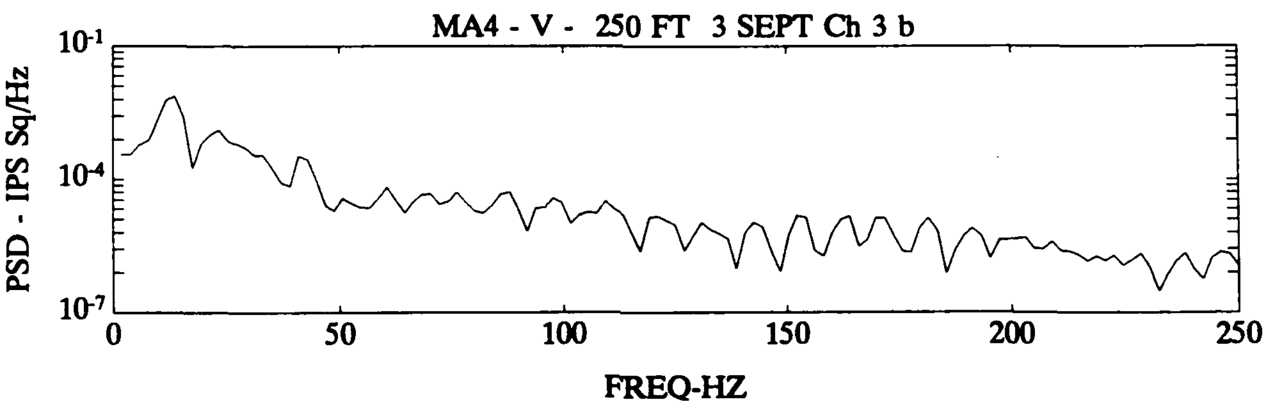
MA4 - V - 250 FT 3 SEPT Ch 3 b
PSD - IPS Sq/Hz
10^{-1}
10^{-4}
10^{-7}
0
50
100
150
200
250
FREQ-HZ

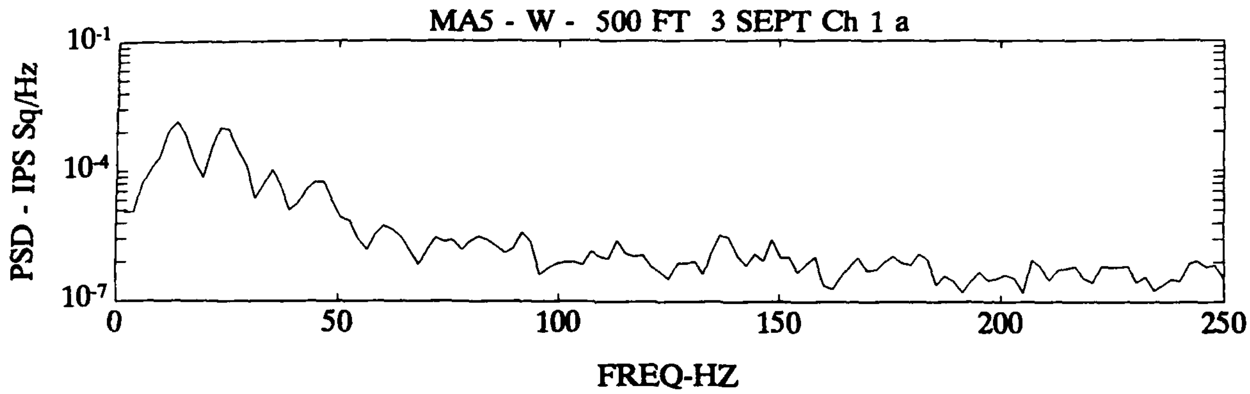
MA5 - W - 500 FT 3 SEPT Ch 1 a
PSD - IPS Sq/Hz
FREQ-HZ

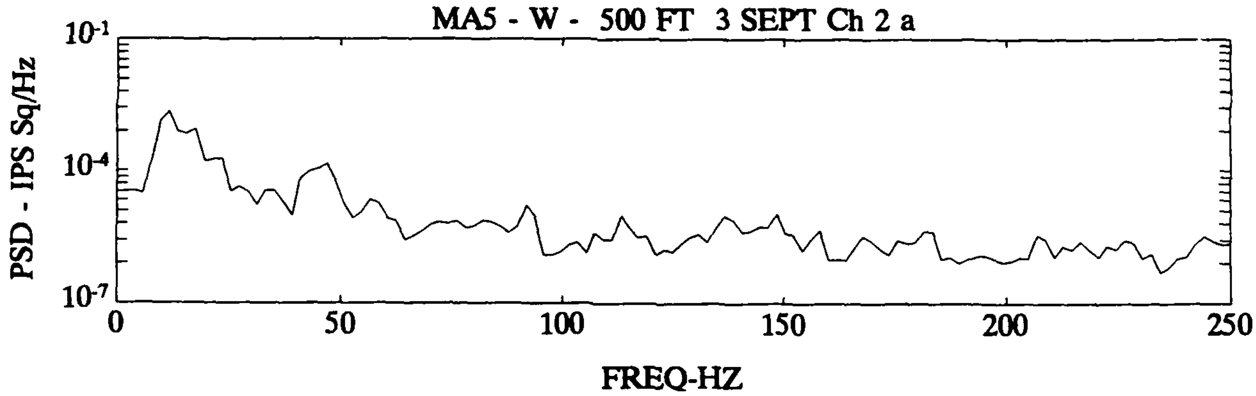
MA5 - W - 500 FT 3 SEPT Ch 2 a
PSD - IPS Sq/Hz
FREQ-HZ

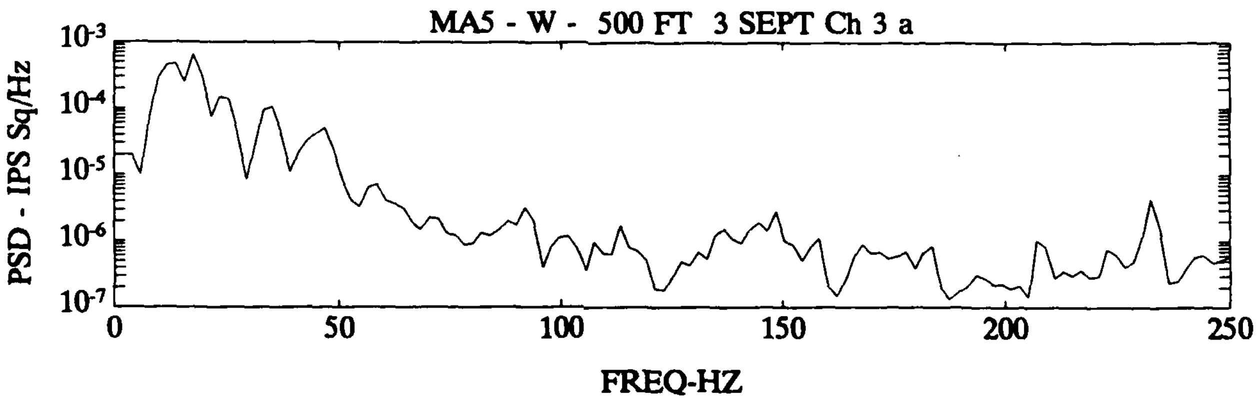
MA5 - W - 500 FT 3 SEPT Ch 3 a
PSD - IPS Sq/Hz
FREQ-HZ

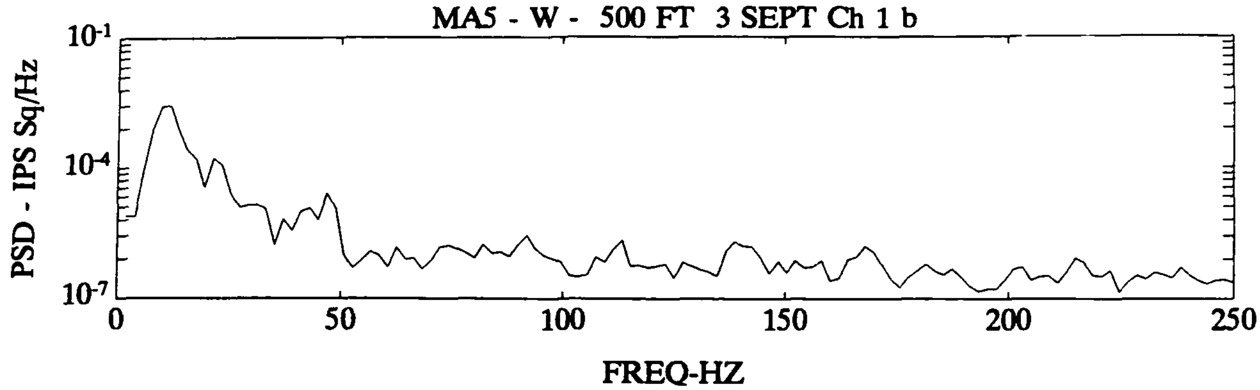
MA5 - W - 500 FT 3 SEPT Ch 1 b
PSD - IPS Sq/Hz
FREQ-HZ

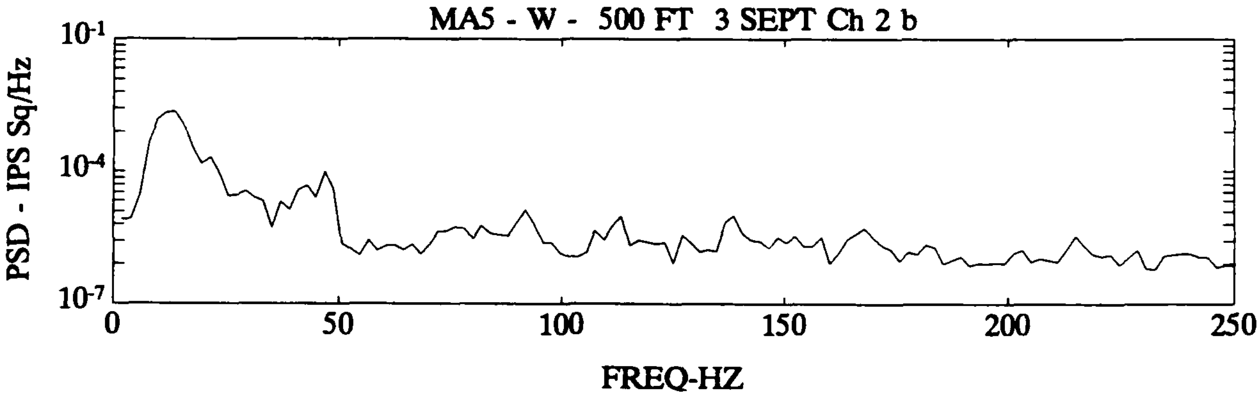
MA5 - W - 500 FT 3 SEPT Ch 2 b
PSD - IPS Sq/Hz
FREQ-HZ

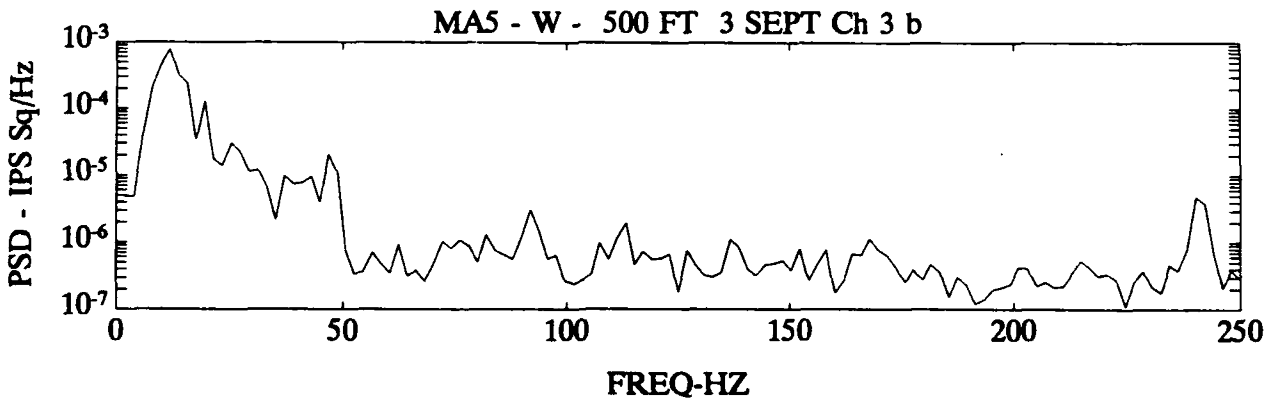
MA5 - W - 500 FT 3 SEPT Ch 3 b
PSD - IPS Sq/Hz
FREQ-HZ

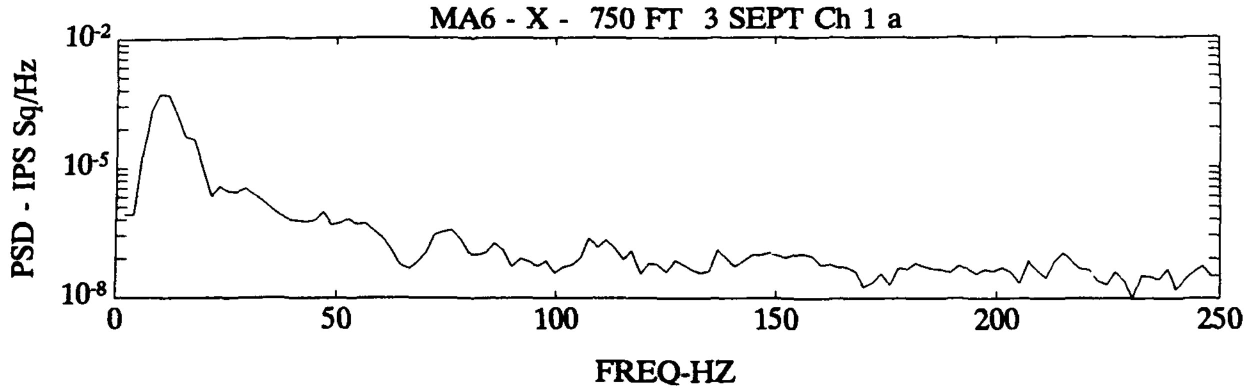
MA6 - X - 750 FT 3 SEPT Ch 1 a
PSD - IPS Sq/Hz
10^{-2}
10^{-5}
10^{-8}
0
50
100
150
200
250
FREQ-HZ

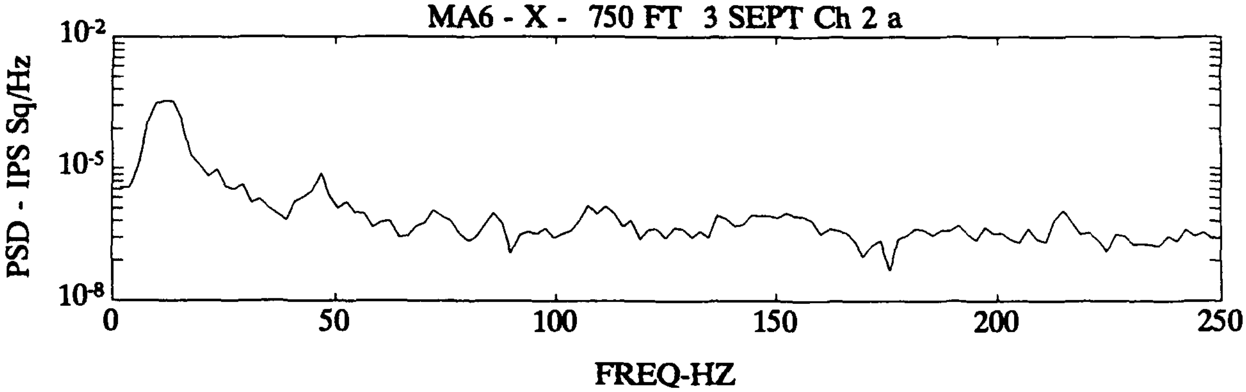
MA6 - X - 750 FT 3 SEPT Ch 2 a
PSD - IPS Sq/Hz
10^{-2}
10^{-5}
10^{-8}
0
50
100
150
200
250
FREQ-HZ

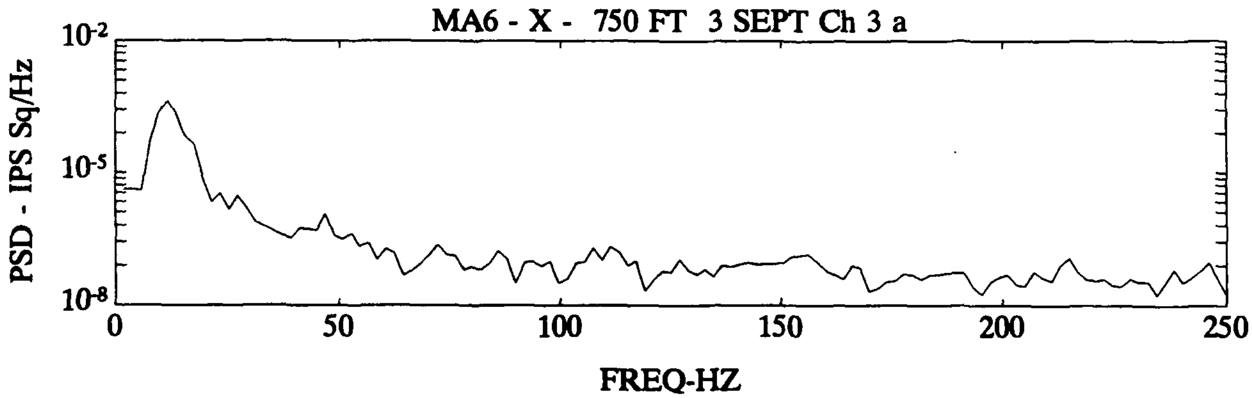
MA6 - X - 750 FT 3 SEPT Ch 3 a
PSD - IPS Sq/Hz
10^{-2}
10^{-5}
10^{-8}
0
50
100
150
200
250
FREQ-HZ

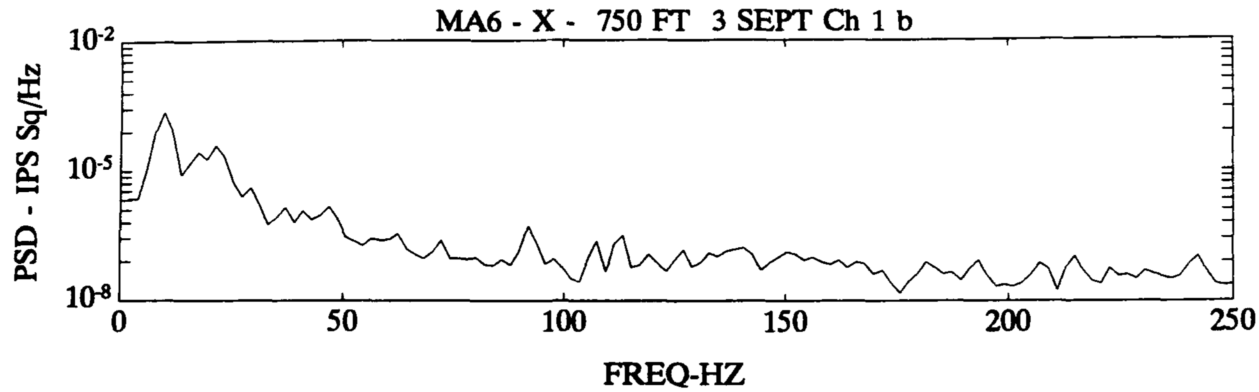
MA6 - X - 750 FT 3 SEPT Ch 1 b
PSD - IPS Sq/Hz
FREQ-HZ

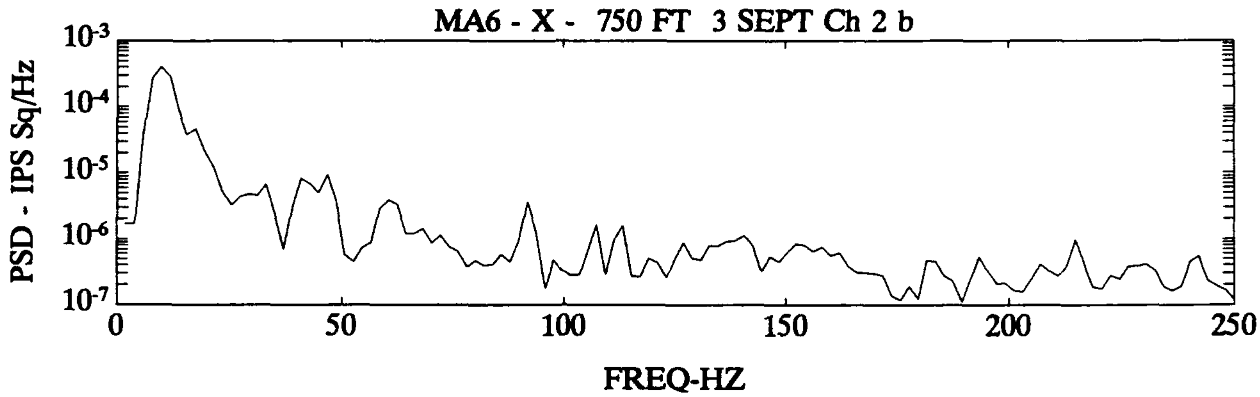
MA6 - X - 750 FT 3 SEPT Ch 2 b
PSD - IPS Sq/Hz
FREQ-HZ

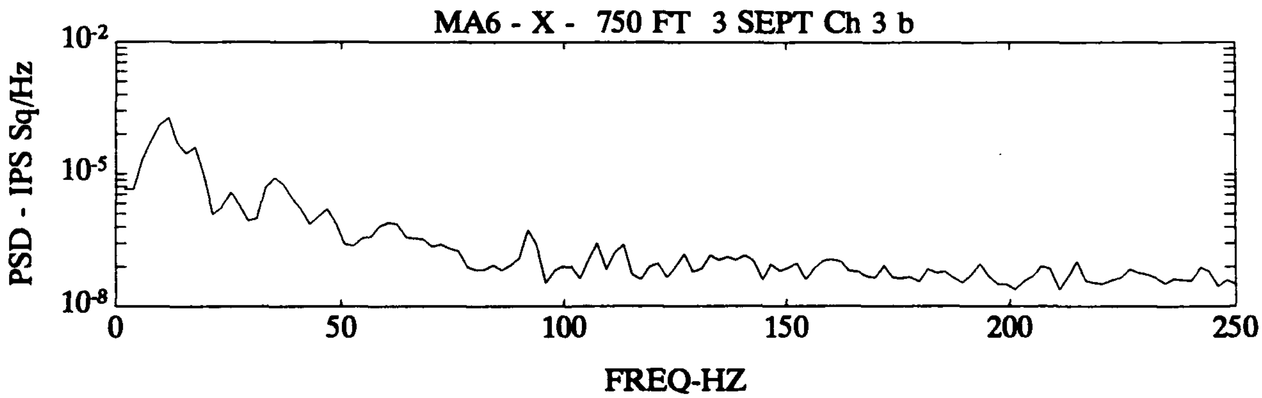
MA6 - X - 750 FT 3 SEPT Ch 3 b
PSD - IPS Sq/Hz
FREQ-HZ

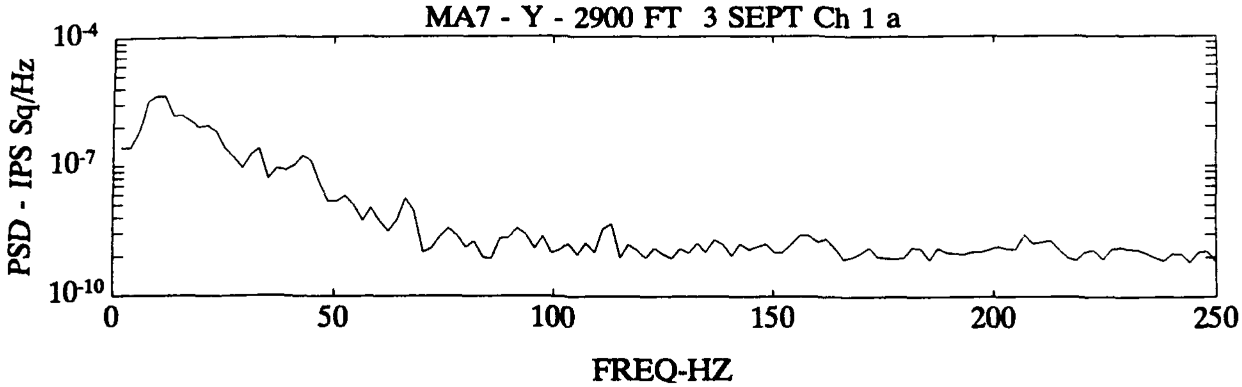

MA7 - Y - 2900 FT 3 SEPT Ch 1 a
PSD - IPS Sq/Hz
FREQ-HZ

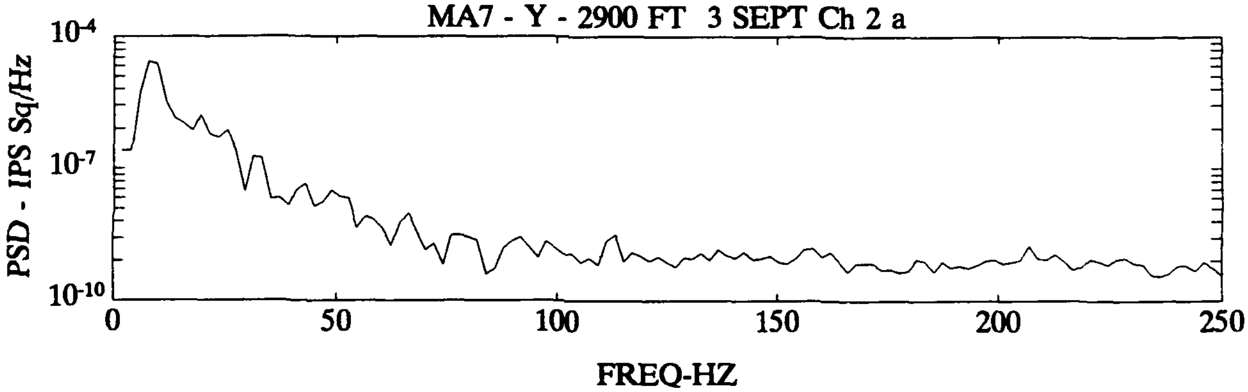

MA7 - Y - 2900 FT 3 SEPT Ch 2 a
PSD - IPS Sq/Hz
FREQ-HZ

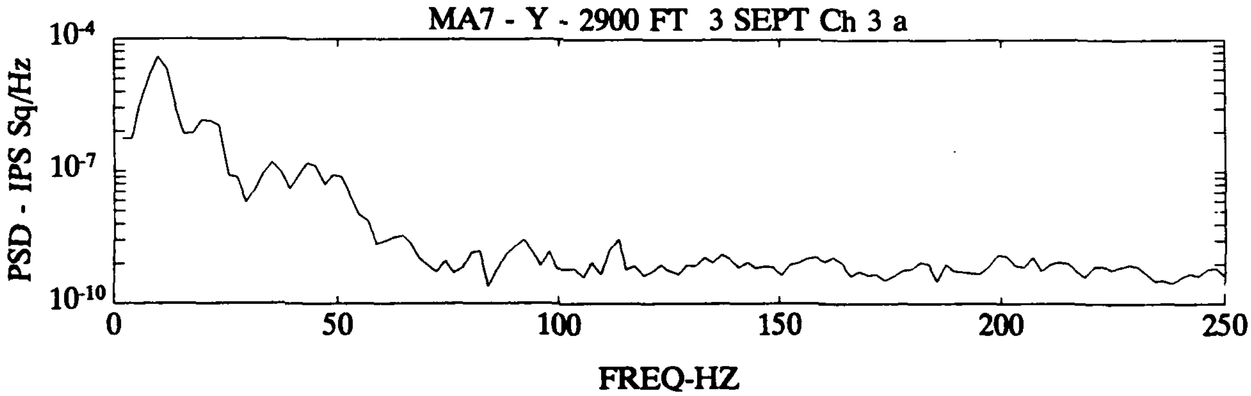

MA7 - Y - 2900 FT 3 SEPT Ch 3 a
PSD - IPS Sq/Hz
FREQ-HZ

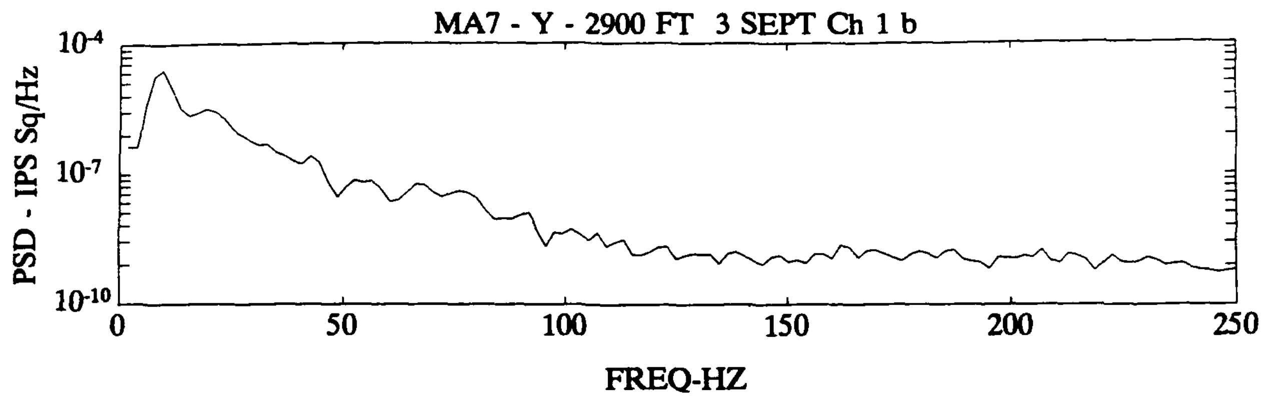
MA7 - Y - 2900 FT 3 SEPT Ch 1 b
PSD - IPS Sq/Hz
FREQ-HZ

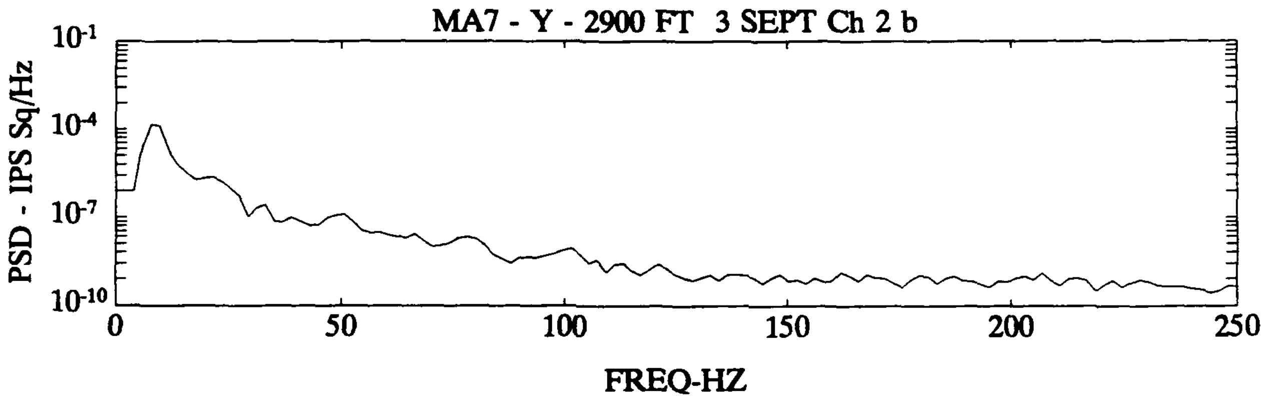
MA7 - Y - 2900 FT 3 SEPT Ch 2 b
PSD - IPS Sq/Hz
FREQ-HZ

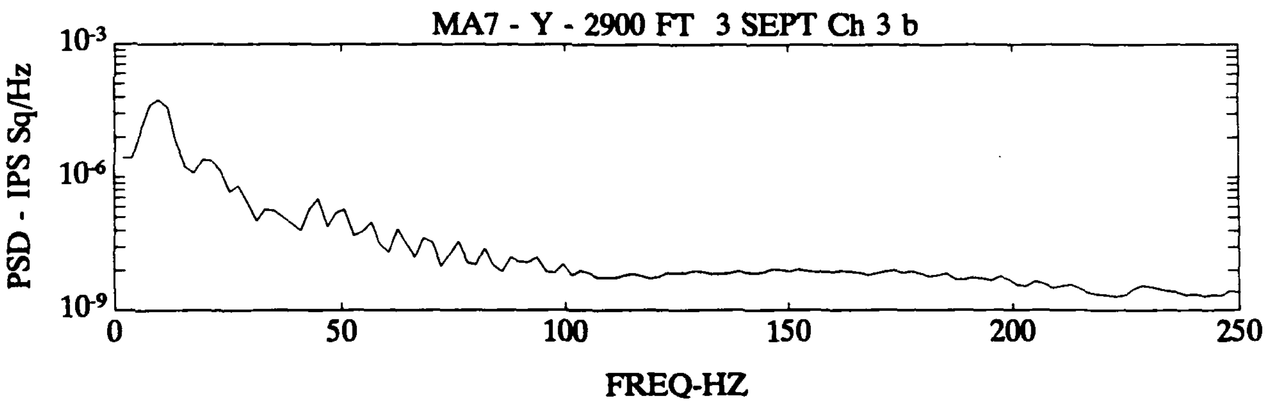
MA7 - Y - 2900 FT 3 SEPT Ch 3 b
PSD - IPS Sq/Hz
FREQ-HZ

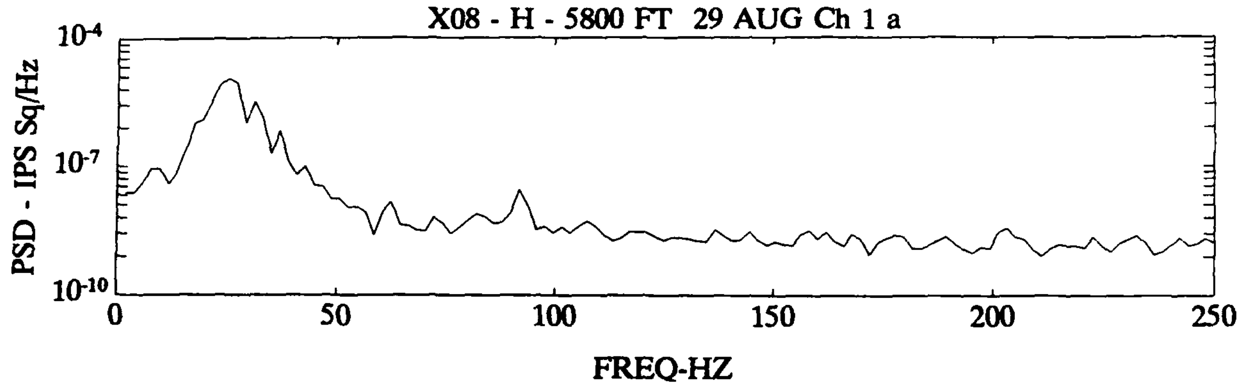
X08 - H - 5800 FT 29 AUG Ch 1 a
PSD - IPS Sq/Hz
10-4
10-7
10-10
0
50
100
150
200
250
FREQ-HZ

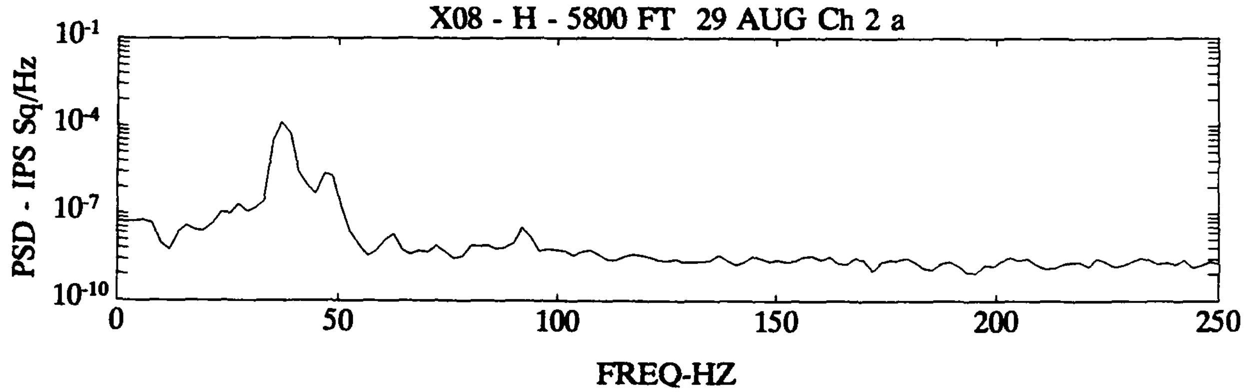
X08 - H - 5800 FT 29 AUG Ch 2 a
PSD - IPS Sq/Hz
10-1
10-4
10-7
10-10
0
50
100
150
200
250
FREQ-HZ

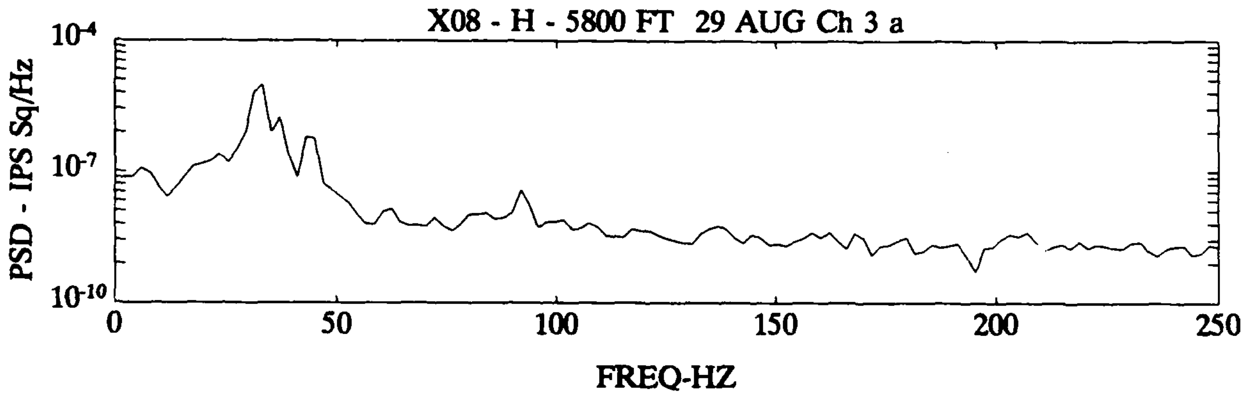
X08 - H - 5800 FT 29 AUG Ch 3 a
PSD - IPS Sq/Hz
10-4
10-7
10-10
0
50
100
150
200
250
FREQ-HZ

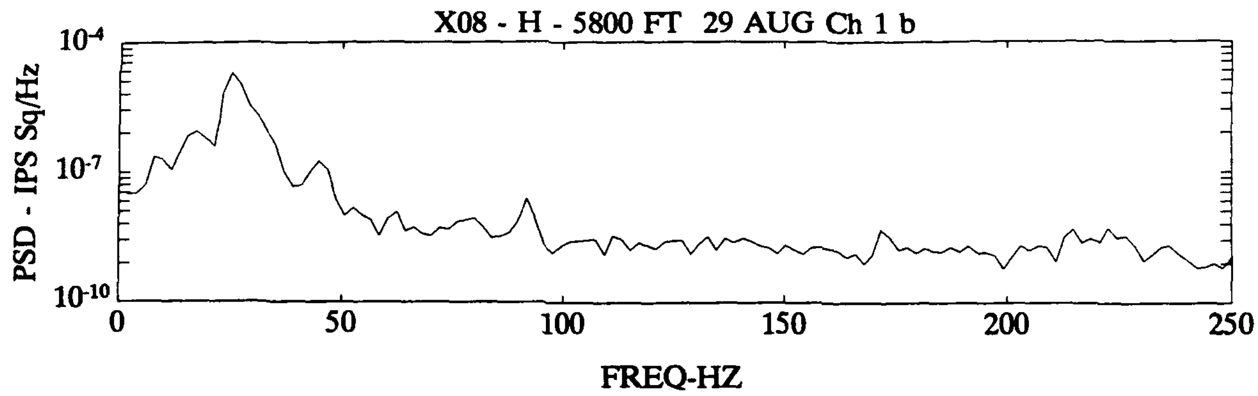

X08 - H - 5800 FT 29 AUG Ch 1 b
PSD - IPS Sq/Hz
10-4
10-7
10-10
0
50
100
150
200
250
FREQ-HZ

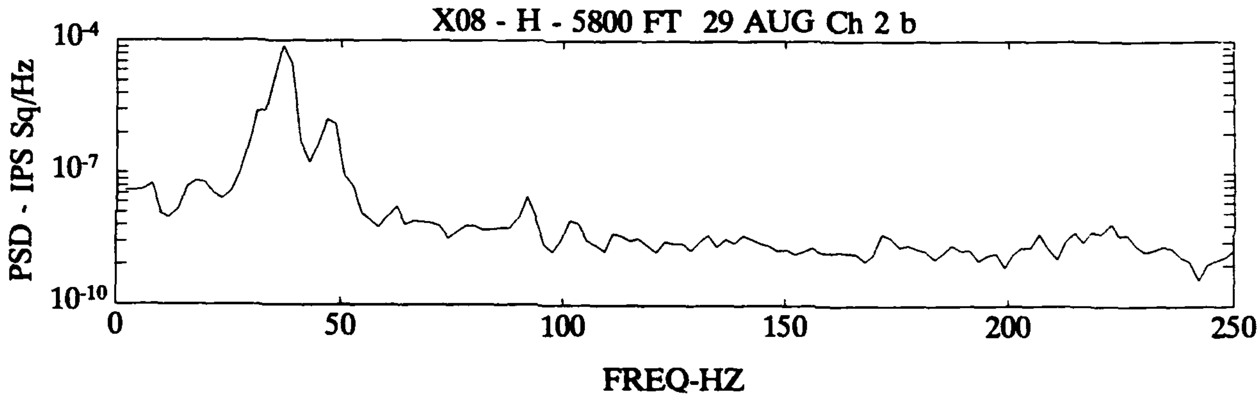

X08 - H - 5800 FT 29 AUG Ch 2 b
PSD - IPS Sq/Hz
10-4
10-7
10-10
0
50
100
150
200
250
FREQ-HZ

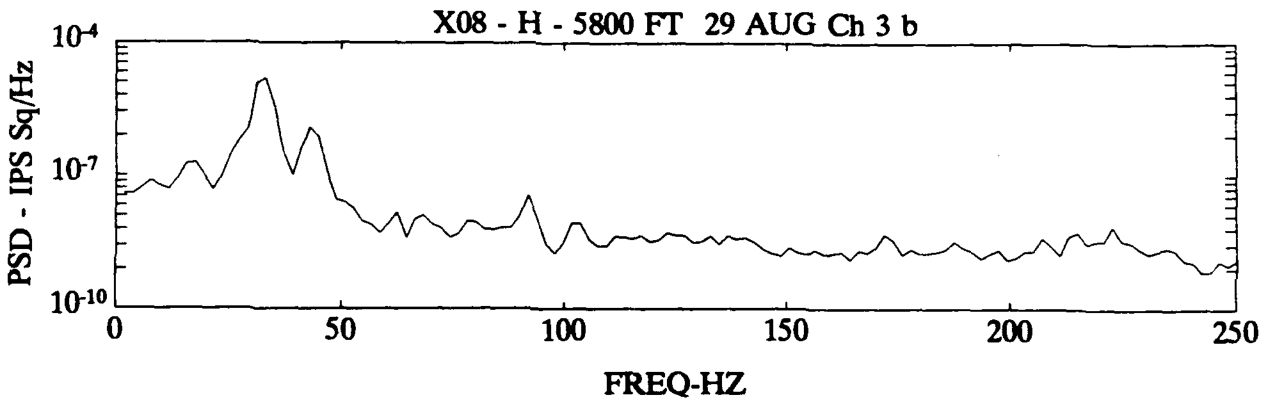

X08 - H - 5800 FT 29 AUG Ch 3 b
PSD - IPS Sq/Hz
10-4
10-7
10-10
0
50
100
150
200
250
FREQ-HZ

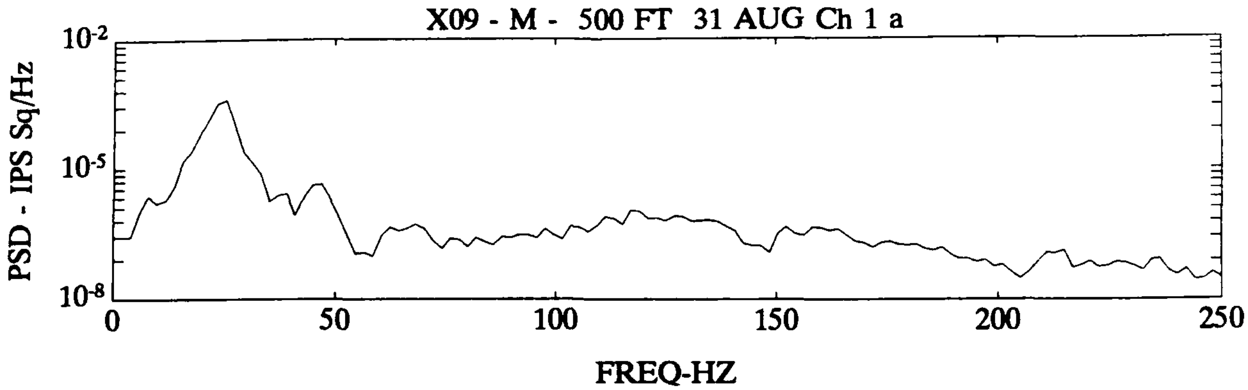
X09 - M - 500 FT 31 AUG Ch 1 a
PSD - IPS Sq/Hz
10-2
10-5
10-8
0
50
100
150
200
250
FREQ-HZ

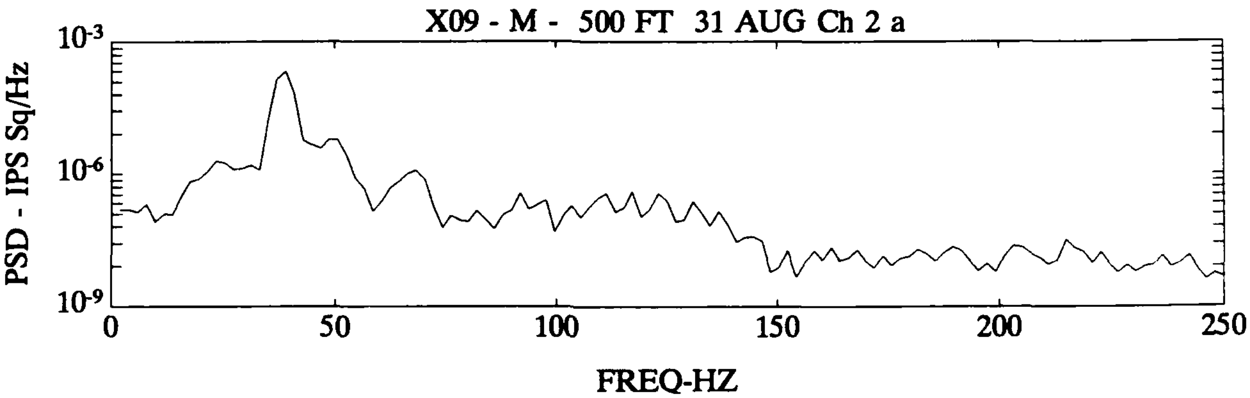
X09 - M - 500 FT 31 AUG Ch 2 a
PSD - IPS Sq/Hz
10-3
10-6
10-9
0
50
100
150
200
250
FREQ-HZ

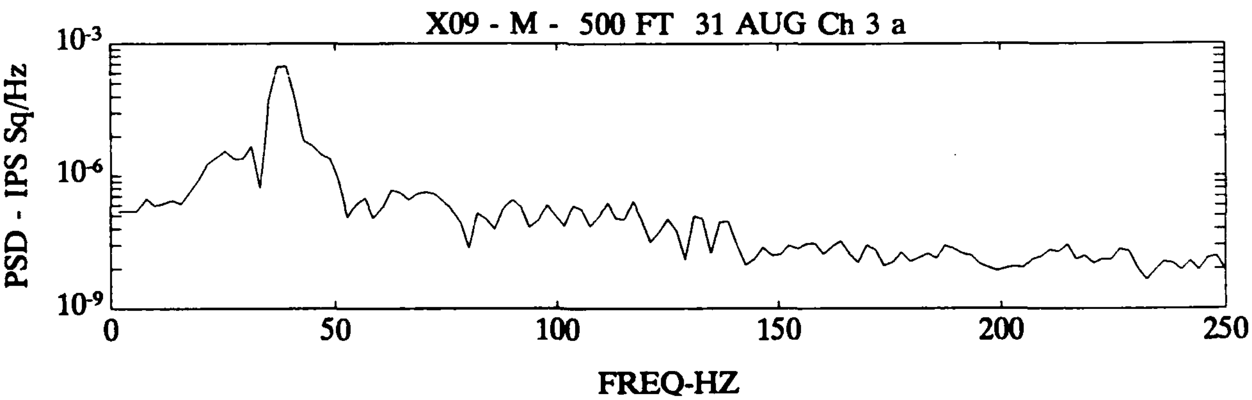
X09 - M - 500 FT 31 AUG Ch 3 a
PSD - IPS Sq/Hz
10-3
10-6
10-9
0
50
100
150
200
250
FREQ-HZ

X09 - M - 500 FT 31 AUG Ch 1 b

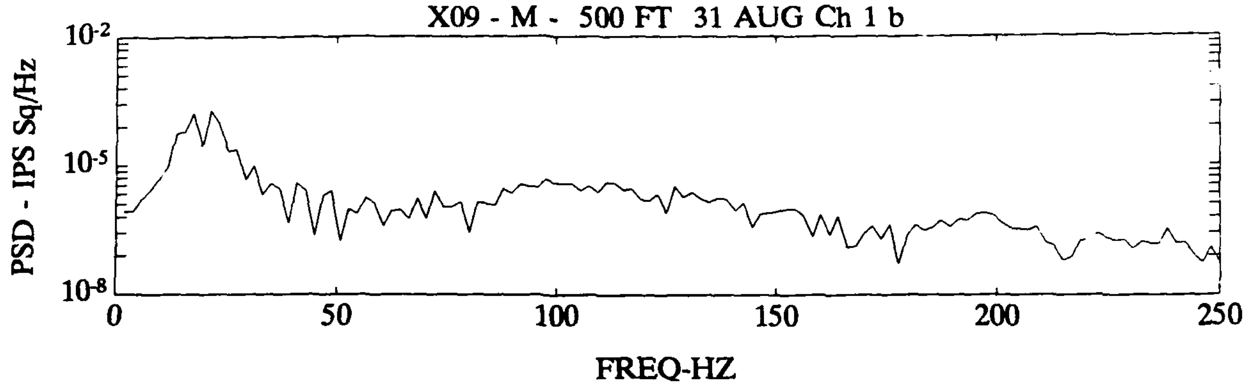

X09 - M - 500 FT 31 AUG Ch 2 b

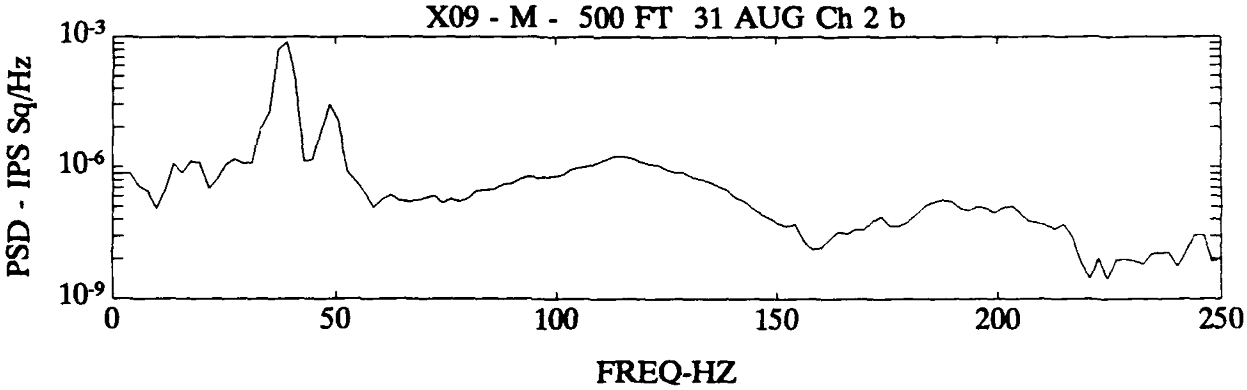

X09 - M - 500 FT 31 AUG Ch 3 b

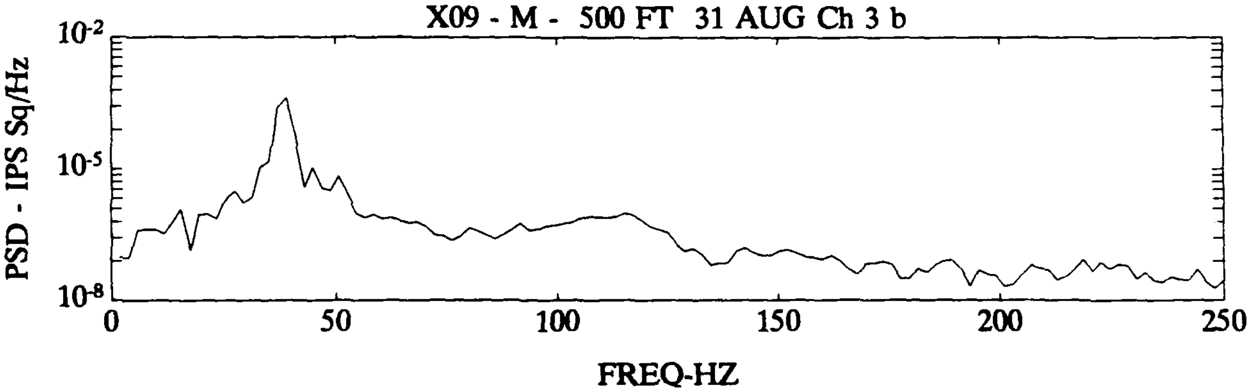

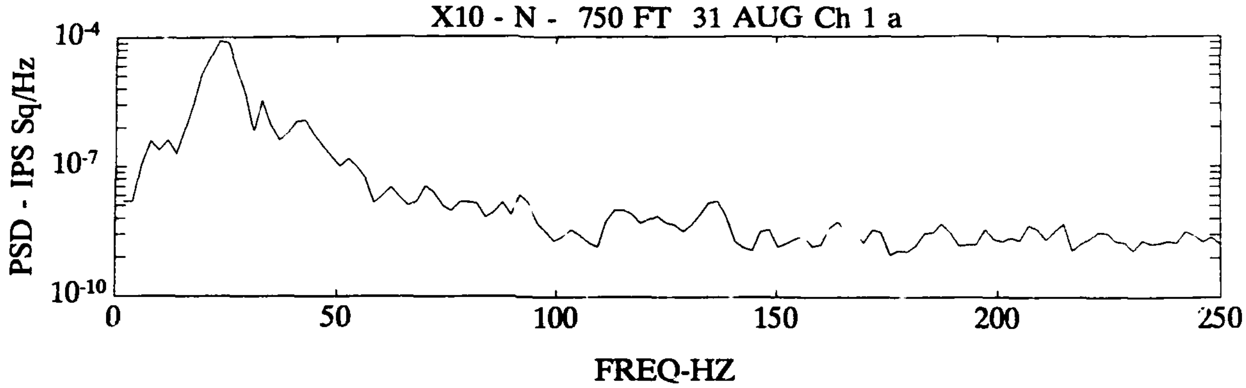

X10 - N - 750 FT 31 AUG Ch 1 a
PSD - IPS Sq/Hz
10^{-4}
10^{-7}
10^{-10}
0
50
100
150
200
250
FREQ-HZ

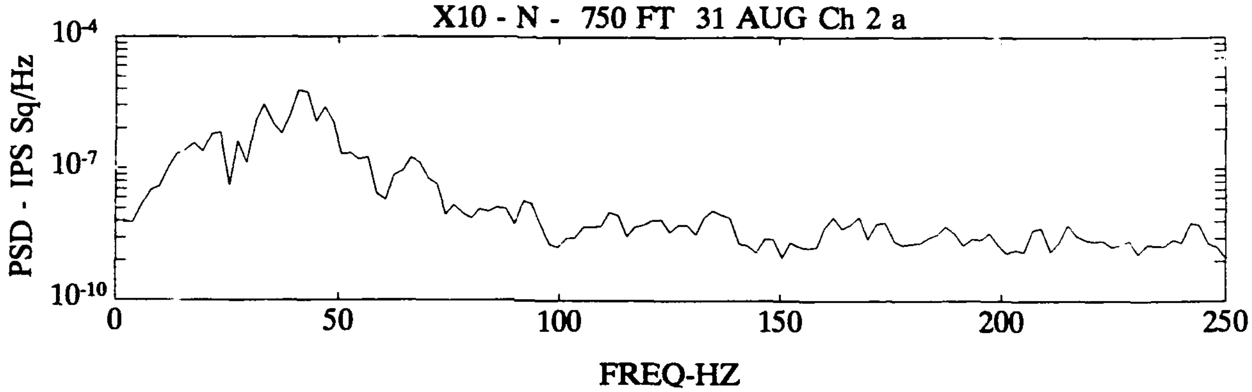

X10 - N - 750 FT 31 AUG Ch 2 a
PSD - IPS Sq/Hz
10^{-4}
10^{-7}
10^{-10}
0
50
100
150
200
250
FREQ-HZ

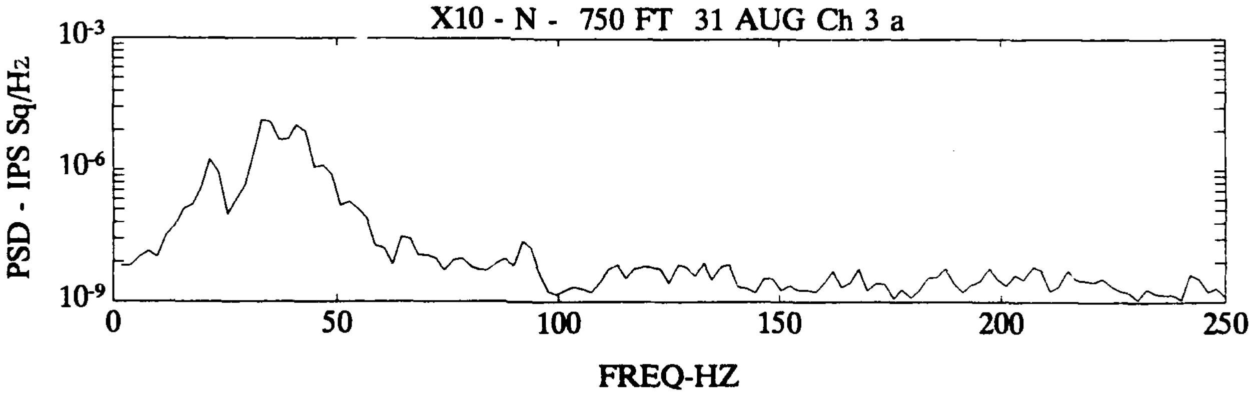

X10 - N - 750 FT 31 AUG Ch 3 a
PSD - IPS Sq/Hz
10^{-3}
10^{-6}
10^{-9}
0
50
100
150
200
250
FREQ-HZ

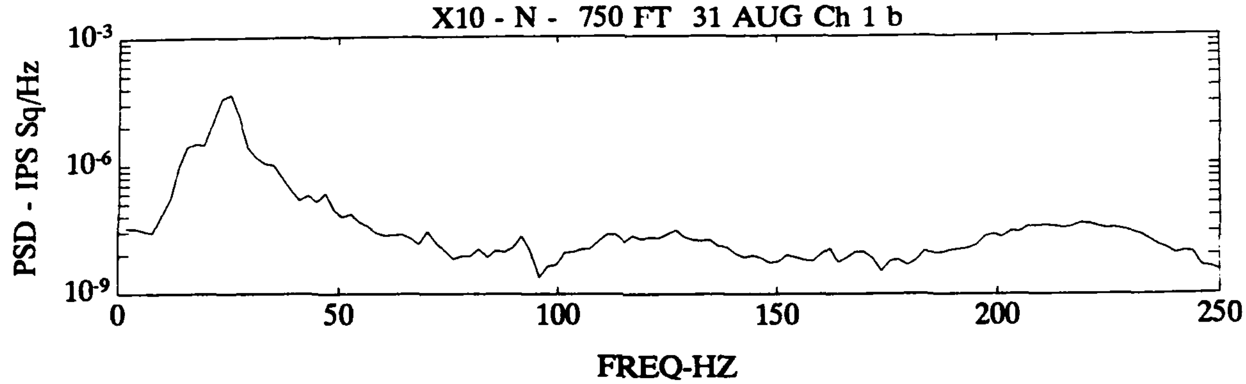
X10 - N - 750 FT 31 AUG Ch 1 b
PSD - IPS Sq/Hz
10^{-3}
10^{-6}
10^{-9}
0
50
100
150
200
250
FREQ-HZ

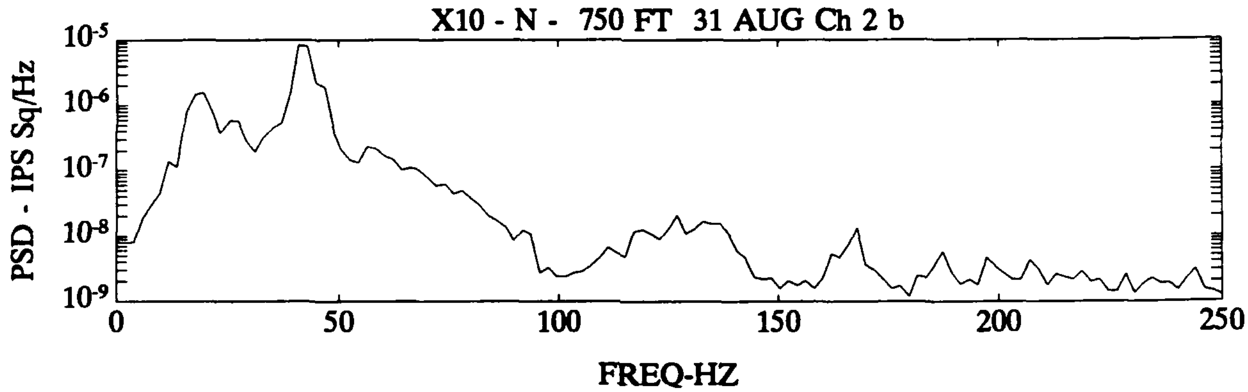
X10 - N - 750 FT 31 AUG Ch 2 b
PSD - IPS Sq/Hz
10^{-5}
10^{-6}
10^{-7}
10^{-8}
10^{-9}
0
50
100
150
200
250
FREQ-HZ

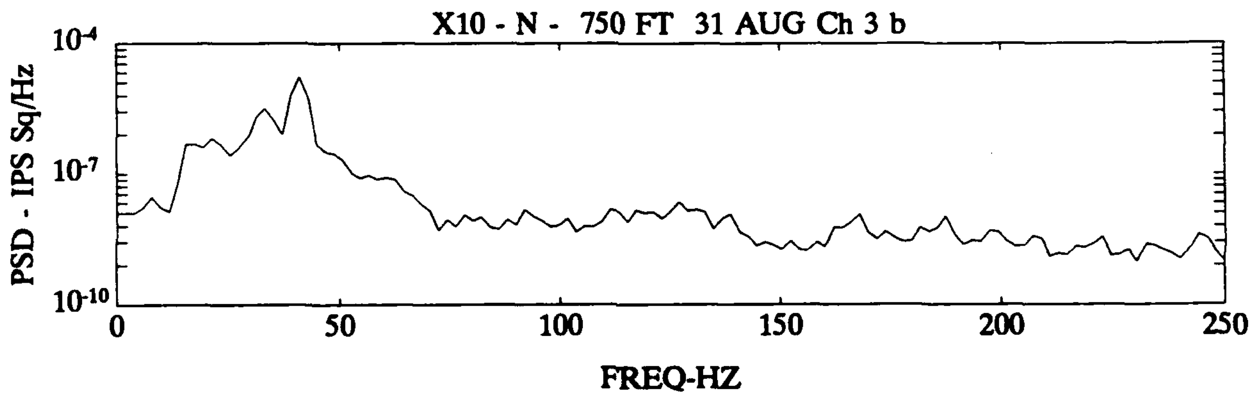
X10 - N - 750 FT 31 AUG Ch 3 b
PSD - IPS Sq/Hz
10^{-4}
10^{-7}
10^{-10}
0
50
100
150
200
250
FREQ-HZ

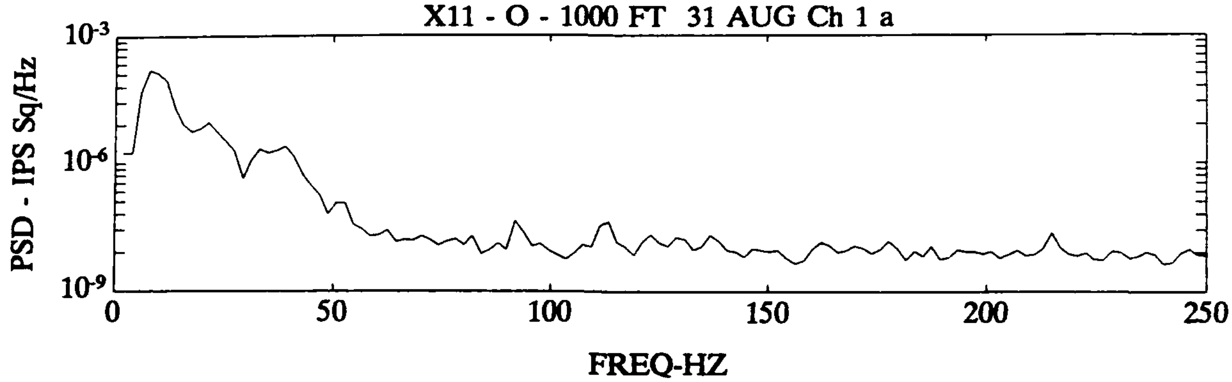
X11 - O - 1000 FT 31 AUG Ch 1 a
PSD - IPS Sq/Hz
10^{-3}
10^{-6}
10^{-9}
0
50
100
150
200
250
FREQ-HZ

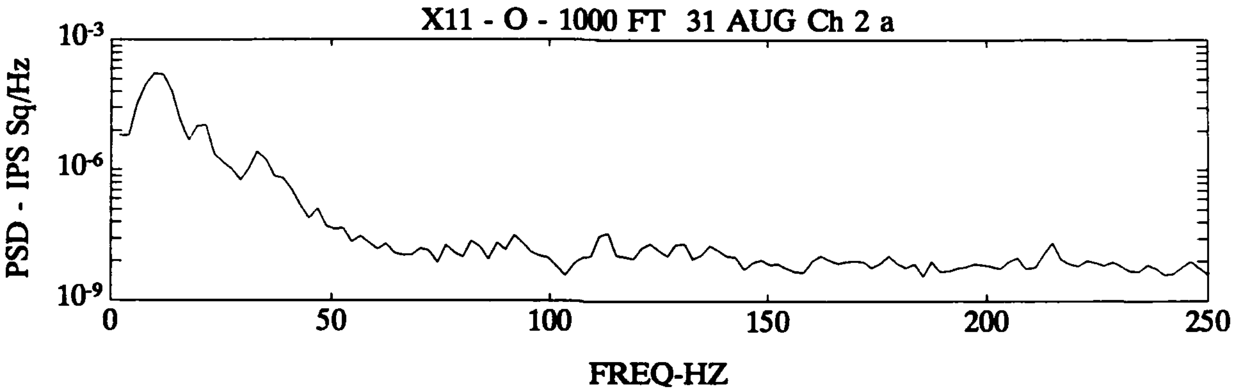
X11 - O - 1000 FT 31 AUG Ch 2 a
PSD - IPS Sq/Hz
10^{-3}
10^{-6}
10^{-9}
0
50
100
150
200
250
FREQ-HZ

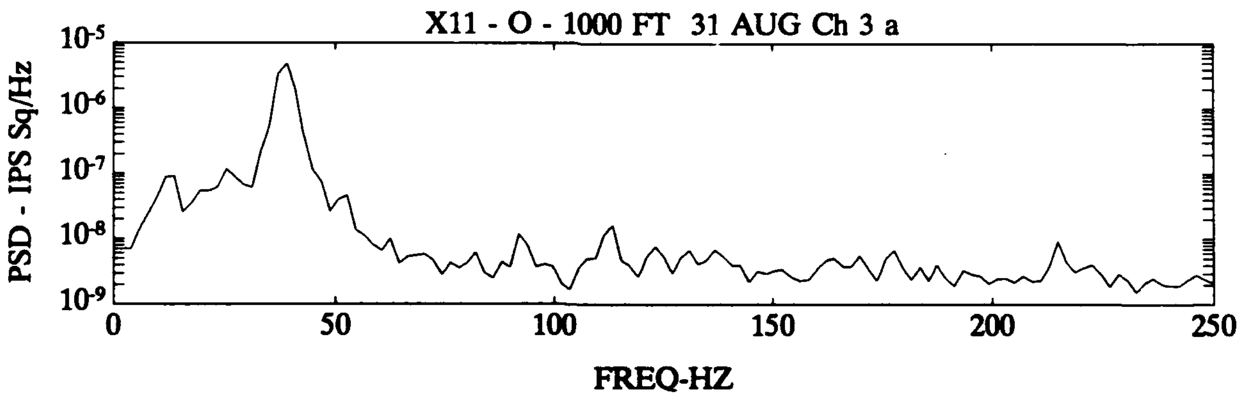
X11 - O - 1000 FT 31 AUG Ch 3 a
PSD - IPS Sq/Hz
10^{-5}
10^{-6}
10^{-7}
10^{-8}
10^{-9}
0
50
100
150
200
250
FREQ-HZ

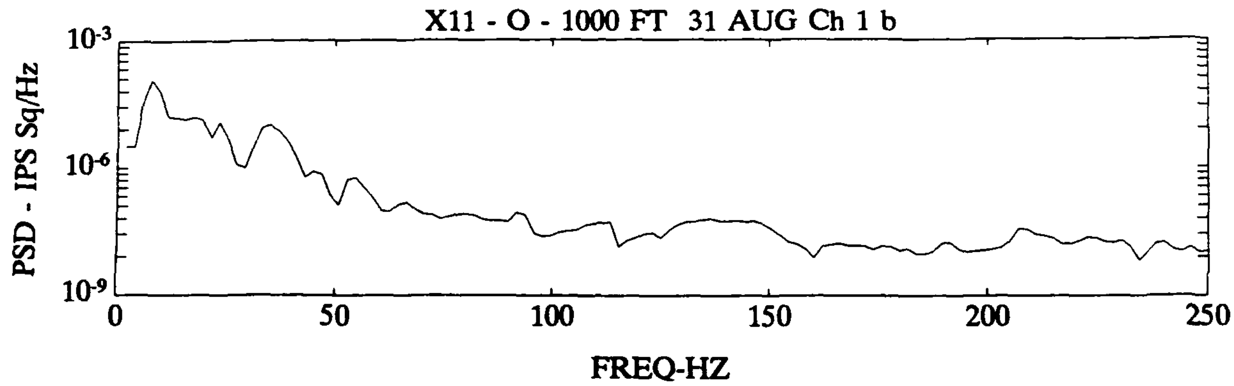
X11 - O - 1000 FT 31 AUG Ch 1 b
PSD - IPS Sq/Hz
10^{-3}
10^{-6}
10^{-9}
0
50
100
150
200
250
FREQ-HZ

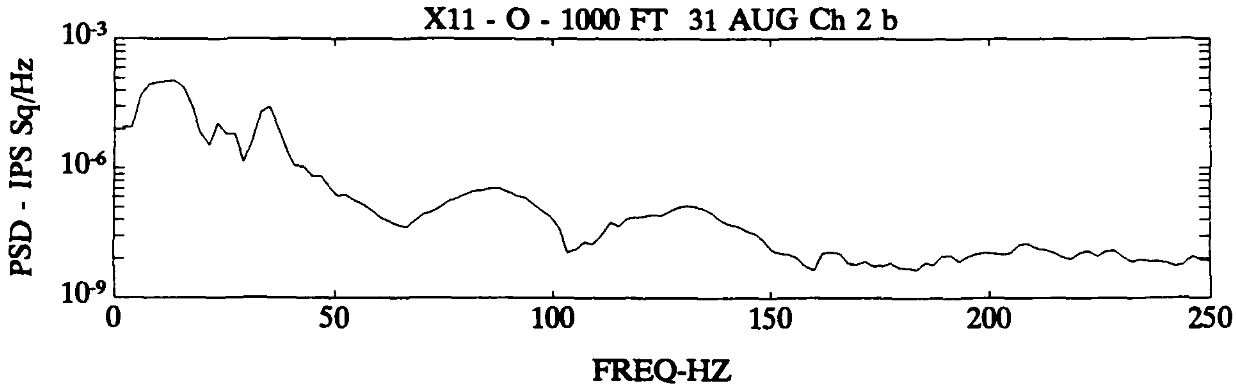
X11 - O - 1000 FT 31 AUG Ch 2 b
PSD - IPS Sq/Hz
10^{-3}
10^{-6}
10^{-9}
0
50
100
150
200
250
FREQ-HZ

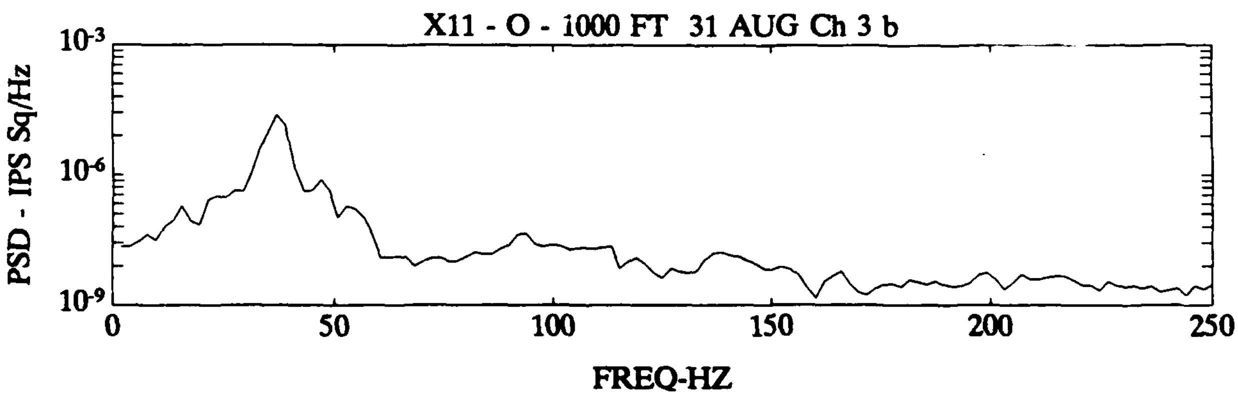
X11 - O - 1000 FT 31 AUG Ch 3 b
PSD - IPS Sq/Hz
10^{-3}
10^{-6}
10^{-9}
0
50
100
150
200
250
FREQ-HZ

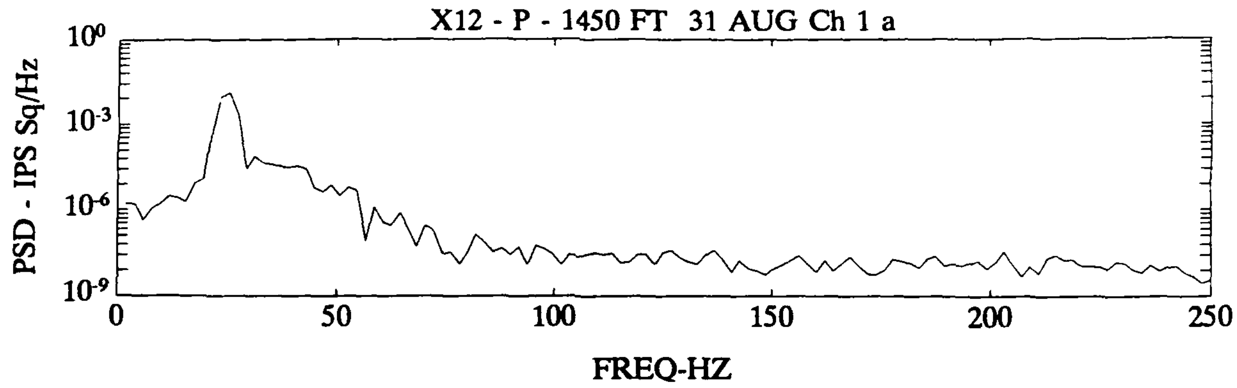
X12 - P - 1450 FT 31 AUG Ch 1 a
PSD - IPS Sq/Hz
10^{0}
10^{-3}
10^{-6}
10^{-9}
0
50
100
150
200
250
FREQ-HZ

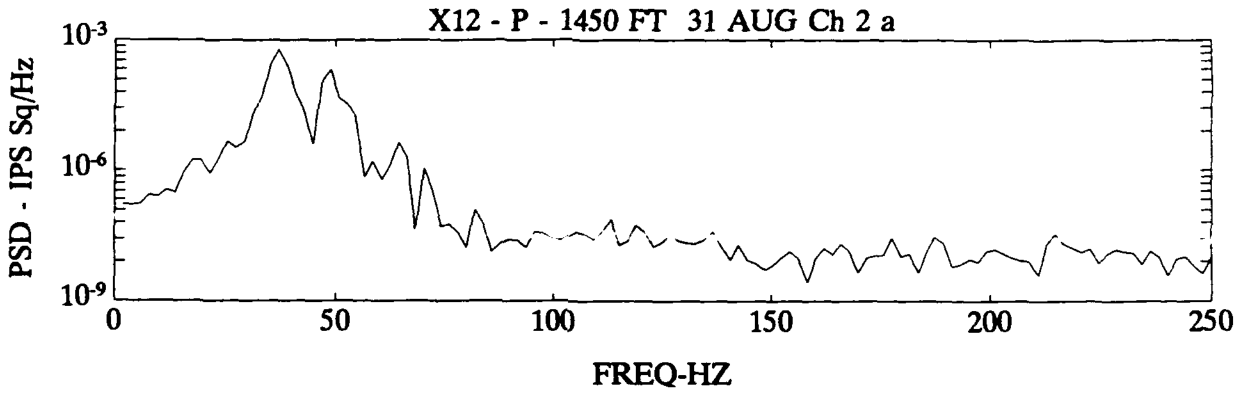
X12 - P - 1450 FT 31 AUG Ch 2 a
PSD - IPS Sq/Hz
10^{-3}
10^{-6}
10^{-9}
0
50
100
150
200
250
FREQ-HZ

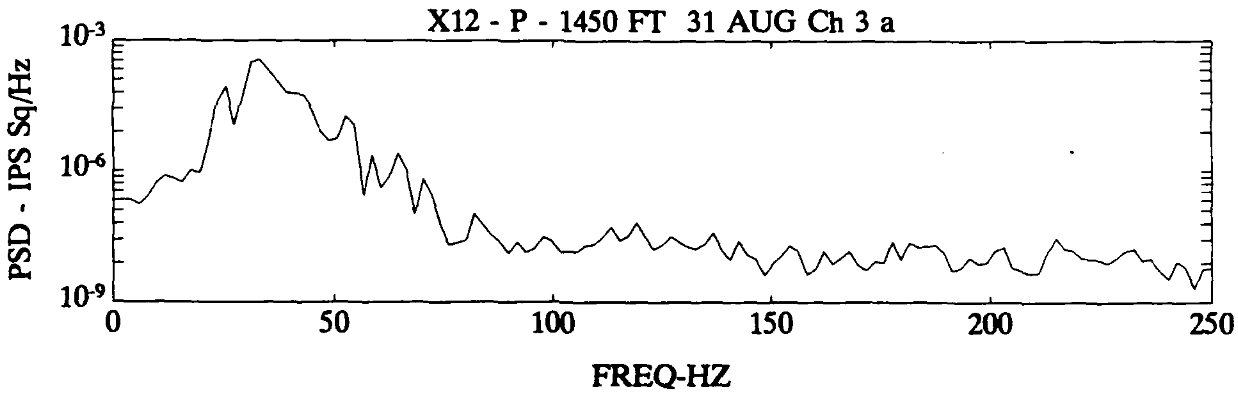
X12 - P - 1450 FT 31 AUG Ch 3 a
PSD - IPS Sq/Hz
10^{-3}
10^{-6}
10^{-9}
0
50
100
150
200
250
FREQ-HZ

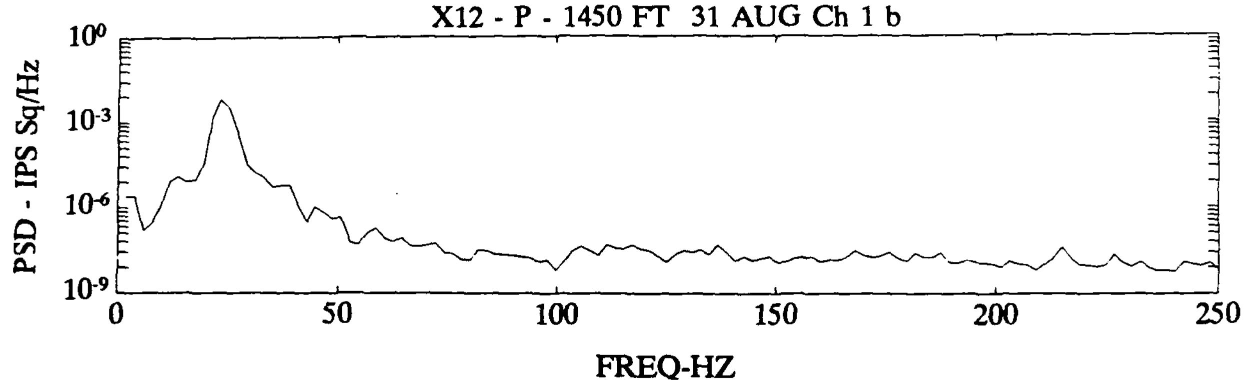
X12 - P - 1450 FT 31 AUG Ch 1 b
PSD - IPS Sq/Hz
10^{0}
10^{-3}
10^{-6}
10^{-9}
0
50
100
150
200
250
FREQ-HZ

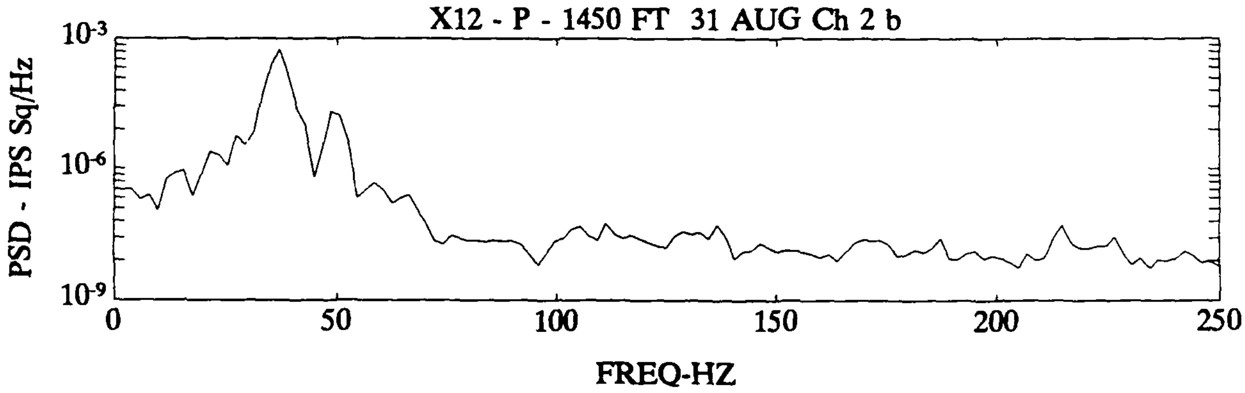
X12 - P - 1450 FT 31 AUG Ch 2 b
PSD - IPS Sq/Hz
10^{-3}
10^{-6}
10^{-9}
0
50
100
150
200
250
FREQ-HZ

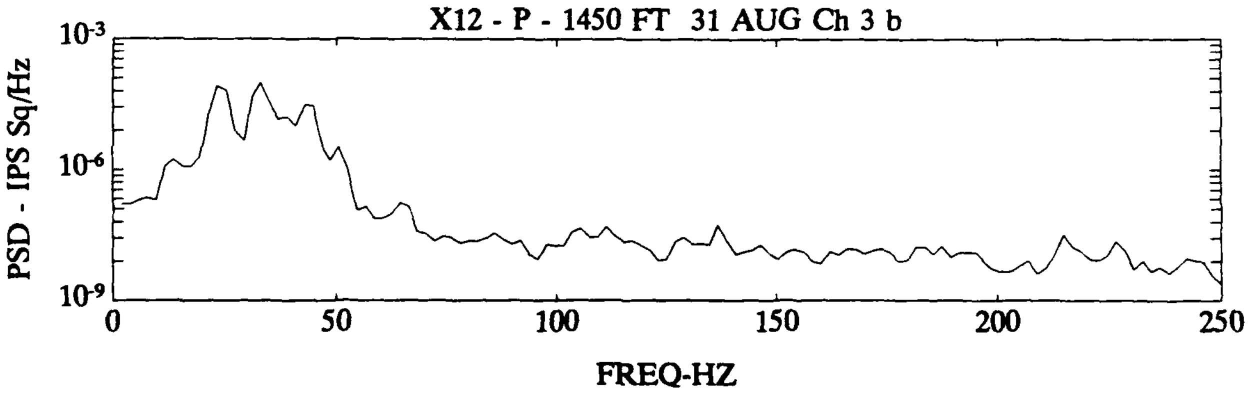
X12 - P - 1450 FT 31 AUG Ch 3 b
PSD - IPS Sq/Hz
10^{-3}
10^{-6}
10^{-9}
0
50
100
150
200
250
FREQ-HZ

REPORT DOCUMENTATION PAGE

Form Approved
OMB No. 0704-0188

1. AGENCY USE ONLY *(Leave blank)*

2. REPORT DATE
July 1993

3. REPORT TYPE AND DATES COVERED
Final report

4. TITLE AND SUBTITLE
Ground Motion and Air Overpressure Study at the Naval Surface Warfare Center, Crane, Indiana

5. FUNDING NUMBERS
MIPR Number
RMB 92-749

6. AUTHOR(S)
Michael K. Sharp, Janet Simms,
Cary Cox, Jim Pickens

7. PERFORMING ORGANIZATION NAME(S) AND ADDRESS(ES)
U.S. Army Engineer Waterways Experiment Station, Geotechnical Laboratory and Instrumentation Services Division, 3909 Halls Ferry Road, Vicksburg, MS 39180-6199

8. PERFORMING ORGANIZATION REPORT NUMBER
Miscellaneous Paper
GL-93-7

9. SPONSORING/MONITORING AGENCY NAME(S) AND ADDRESS(ES)
Crane Army Ammunition Activity, Naval Surface Warfare Center, Crane, IN 47522-5099

10. SPONSORING/MONITORING AGENCY REPORT NUMBER

11. SUPPLEMENTARY NOTES
This report is available from the National Technical Information Service, 5285 Port Royal Road, Springfield, VA 22161.

12a. DISTRIBUTION/AVAILABILITY STATEMENT
Approved for public release; distribution is unlimited.

12b. DISTRIBUTION CODE

13. ABSTRACT *(Maximum 200 words)*

This report provides documentation for and presents an analysis of a seismic attenuation and air overpressure study at the Naval Surface Warfare Center, Crane, Indiana. The investigation consisted of measuring peak particle velocities and peak air overpressures along two radials (N40°E and S40°W). Each radial consisted of four to five monitoring stations recording vertical, radial, and transverse ground motions in addition to air overpressures. Data were recorded from 24 August through 5 September 1992, with 3084 time histories being recorded. From the data, ground motion and air overpressure attenuation curves were developed from which predictions could be made given the size of the explosion and the distance from the explosion.

Based on the results obtained, the following attenuation curves are proposed.

(Continued)

14. SUBJECT TERMS
Air overpressure
Ground motions
Peak particle velocity
Regression

15. NUMBER OF PAGES
195

16. PRICE CODE

17. SECURITY CLASSIFICATION OF REPORT	18. SECURITY CLASSIFICATION OF THIS PAGE	19. SECURITY CLASSIFICATION OF ABSTRACT	20. LIMITATION OF ABSTRACT
Unclassified	Unclassified		

NSN 7540-01-280-5500

Standard Form 298 (Rev. 2-89)
Prescribed by ANSI Std Z39-18
298-102

13. Continued.

Ground motion predictions

$$y_{95\%} = 28.69 \ (x^{-1.43})$$

y = peak particle velocity, ips
x = scaled range, ft
distance from shot divided by square root of shot weight

Air overpressure predictions

$$y_{95\%} = 65.74 \ (x^{-1.51})$$

y = peak particle velocity, psi
x = scaled range, ft
distance from shot divided by cubic root of shot weight